

**Studies on potential co-operativity between different
types of tumour virus**

A thesis submitted to the University of Manchester for the degree of
Doctor of Philosophy
in the Faculty of Medical and Human Sciences

2015

Bandar Abdulmohsen Alosaimi

School of Medicine

Table of contents

Table of contents2

List of figures6

List of tables8

List of diagrams.....8

Abstract9

Declaration10

Copyright statement10

Acknowledgements11

List of abbreviations.....12

1. Introduction15

1.1 Human cancer viruses.....15

 1.1.1 Discovery of human cancer viruses15

 1.1.2 History of tumour viruses.....15

 1.1.3 Classification of human cancer viruses15

 1.1.3.1 DNA tumour viruses16

 1.1.3.2 RNA tumour viruses19

 1.1.4 Aspects of viral carcinogenesis19

 1.1.5 Co-operativity between oncogenic viruses20

1.2 Human polyomaviruses.....22

 1.2.1 History of human polyomaviruses22

 1.2.2 Classification and phylogeny of polyomaviruses23

 1.2.3 Polyomavirus genome structure24

 1.2.4 Polyomavirus life cycle and replication25

 1.2.4.1 Attachment and receptors26

 1.2.4.2 Virion entry and uncoating27

 1.2.4.3 Viral early gene expression27

 1.2.4.4 Replication of viral DNA27

 1.2.4.5 Viral late gene expression28

 1.2.4.6 Virion assembly and release28

 1.2.5 Proteins of polyomaviruses28

 1.2.5.1 Early viral protein29

 1.2.5.2 Late viral protein30

 1.2.5.3 The agnoprotein31

 1.2.6 Pathogenesis of polyomaviruses31

 1.2.7 Mechanisms by which polyomaviruses may act as a co-factor in virus-induced malignancies.....34

 1.2.8 Members of the human polyomavirus family35

 1.2.8.1 Simian Virus 40 (SV40).....35

 1.2.8.2 JCV.....36

 1.2.8.3 BKV37

 1.2.8.4 KIV38

 1.2.8.5 WUV39

 1.2.8.6 MCV.....39

 1.2.8.7 HPyV6 and HPyV741

 1.2.8.8 Trichodysplasia spinulosa-associated polyomavirus (TSV)41

 1.2.8.9 HPyV9.....42

 1.2.8.10 MWPvV and (HPyV10, MXPvV)43

 1.2.8.11 STLPvV and HPyV12.....44

1.2.9 Detection of polyomaviruses	44
1.2.9.1 Cytology	45
1.2.9.2 Immunological techniques	46
1.3 Functions of the polyomavirus LT antigen.....	48
1.3.1 Epithelial to Mesenchymal Transition (EMT)	49
1.4 Treatments for JC virus.....	52
1.4.1 Mefloquine cytotoxicity	52
1.5 Overall summary.....	52
1.6 Project aims and objectives	53
2. Materials and Methods.....	56
2.1 PCR screening of polyomaviruses in cervical cancer.....	56
2.1.1 Sample collection, design and population.....	56
2.1.2 DNA preparation	57
2.1.3 PCR primer design	57
2.1.4 Positive controls	58
2.1.5 Polymerase Chain Reaction (PCR)	59
2.1.5.1 Multiplex PCR	59
2.1.5.2 Singleplex PCR	60
2.1.5.3 Nested PCR	61
2.1.6 PCR products analysis	62
2.1.7 PCR optimisation and considerations	62
2.1.8 Positive controls optimisation and sensitivity test	63
2.1.9 Verification of DNA integrity by GAPDH	63
2.1.10 Screening of cervical smears and ICCs for polyomaviruses.....	64
2.1.11 Statistical analysis	64
2.1.12 DNA sequencing	65
2.2 WHO collaborative study.....	66
2.2.1 Sample collection, design and population.....	66
2.2.2 Ethics statement and consecrations	67
2.2.3 DNA preparation	67
2.2.4 Study protocol	68
2.2.4.1 Quantitative assays.....	68
2.2.4.2 Qualitative assays:.....	69
2.2.5 PCR results analyses	69
2.3 Cloning of JCV LT ORF for ectopic expression studies	70
2.3.1 DNA sequencing and PCR validation of LT gene in pCITE-4a.....	70
2.3.2 Mismatch PCR	70
2.3.3 PCR purification	72
2.3.4 TOPO cloning	73
2.3.5 Transformation of XL1-blue competent cells.....	73
2.3.6 'Picking' bacterial colonies.....	74
2.3.7 Plasmid mini-prep	74
2.3.8 Plasmid maxi-prep	75
2.3.9 Digestion of the LT-Topo construct and target pcDNA TM 4 vector	76
2.3.10 Post-digestion gel purification	77
2.3.11 Ligation of LT insert and pcDNA TM 4 vector.....	77
2.3.12 LT construct and pcDNA TM 4 vector linearisation	78
2.3.13 Cell Culture	79

2.3.13.1 Cell Line.....	79
2.3.13.2 Cell line thawing	79
2.3.13.3 Routine passaging	80
2.3.13.4 Freezing cultured cells	80
2.3.14 Validation of E6/E7 expression in E6/E7 immortalised keratinocytes	81
2.3.15 Determination of the selective marker concentration by kill curve	83
2.3.16 Analysis of the transient transfection efficiency of E6/E7 keratinocytes	83
2.3.17 Stable transfection of E6/E7 immortalised keratinocytes with JCV LT	84
2.3.18 Analysis of JCV LT protein expression	86
2.3.18.1 Western blot analyses.....	86
2.3.18.2 Immunohistochemistry staining	89
2.3.19 Cell Proliferation Assay (AQ-96 Assay).....	90
2.3.20 Trypan blue viability test of mefloquine cytotoxicity.....	91
2.3.21 Toluidine Blue stain of transformed colony forming assay	92
2.3.22 Microarray analysis of the effects of JCV LT on full transcriptome	92
2.3.22.1 RNA extraction	92
2.3.22.2 Array processing	93
2.3.22.3 Affymetrix expression console (AEC).....	94
2.3.22.4 Statistical analysis and data filtration.....	94
2.3.22.5 Pathway analysis	94
3. Results	96
3.1 <i>PCR screening of Polyomaviruses in cervical cancer</i>	96
3.1.1 Verification of sample's DNA integrity by GAPDH.....	96
3.1.2 Optimisation of primers involved in the study.....	97
3.1.3 Optimisation of positive controls	98
3.1.4 Optimising PCR annealing temperatures in the presence of genomic DNA	99
3.1.5 Sensitivity of polyomavirus detection by PCR	100
3.1.6 Sample Population	101
3.1.7 Screening of cervical samples for MCV	102
3.1.7.1 Screening of cervical smears by multiplex PCR.....	103
3.1.7.2 Screening of ICCs for MCV by singleplex PCR	104
3.1.8 Screening of samples for SV40.....	104
3.1.8.1 Screening of cervical smears for SV40.....	105
3.1.8.2 Screening of ICCs for SV40	105
3.1.9 PCR screening for BKV and JCV	106
3.1.9.1 Screening of cervical smears for JCV and BKV	107
3.1.9.2 Screening of ICC samples for BKV and JCV	108
3.1.9.3 Reamplification of JCV/BKV positives and distinction between nested JCV and BKV amplification products	109
3.1.9.4 Analysis of potential association between JCV and HPV16/18 infection	112
3.1.9.5 The association between JCV and HIV Infection	113
3.2 <i>WHO collaborative study results</i>	116
3.2.1 Verification of sample DNA integrity and sensitivity by GAPDH PCR	116
3.2.2 Determination of JC/BK viral load	116
3.2.3 Detection of JC/BK virus consensus amplicon	117
3.2.4 Detection of JC virus by Nested PCR.....	118
3.2.5 Detection of BK virus by Nested PCR.....	119
3.3 <i>Cloning of JCV LT ORF for ectopic expression studies</i>	120
3.3.1 Sequencing of pCITE-4a recombinant plasmid	121
3.3.2 Mismatch PCR	122

3.3.2.1 Nested PCR confirmation of mismatch amplification	123
3.3.3 TOPO cloning	123
3.3.3.1 Sequencing of the LT-TOPO clone.....	124
3.3.4 Digestion of the LT-Topo construct and target pcDNA TM 4 vector	125
3.3.5 Ligation of LT gene to pcDNA TM 4 vector	125
3.4 LT Transfection	128
3.4.1 Validation of E6/E7 expression in E6/E7 immortalised keratinocytes	128
3.4.2 Zeocin kill curve for E6/E7 immortalised keratinocytes	129
3.4.3 Analysis of the transient transfection efficiency of E6/E7 keratinocytes	130
3.4.4 Stable transfection of E6/E7 immortalised keratinocytes with JCV LT	131
3.4.5 Analysis of JCV LT Protein Expression	135
3.5 Molecular, biological and therapeutic tests on LT cell lines	138
3.5.1 Cell Doubling Time (CDT).....	139
3.5.2 Transformed colony forming assay using Toluidine Blue stain	140
3.5.3 Morphological characteristics of the transfected cells	141
3.5.4 EMT	143
3.5.4.1 Epithelial layers (β -catenin)	143
3.5.4.2 Loss of tight junctions (Claudin)	144
3.5.4.3 Loss of adherens junctions & desmosomes (E-cadherin)	146
3.5.4.4 Increased motility & migration (N-cadherin)	147
3.5.4.5 Cytoskeletal changes (Vimentin)	148
3.5.4.6 Transcriptional shift (Snail)	149
3.5.4.7 Concluding remarks of EMT on LT gene	150
3.5.5 Analysis of the effects of JCV targeting compounds.....	150
3.5.5.1 Mefloquine AQ-96 colorimetric cell proliferation assay	150
3.5.5.2 Mefloquine cytotoxicity by Trypan Blue exclusion assay	152
3.5.6 Use of microarrays to analyse the effects of JCV LT on full transcriptome.....	154
3.5.6.1 RNA extraction and data filtration	154
3.5.6.2 Array data filtration.....	154
3.5.6.3 JCV LT integration two group analysis	156
3.5.6.4 Two group analysis of polyclonal Vs monoclonal cells	159
4. Discussion.....	163
4.1 General discussion.....	163
4.2 Conclusion	178
4.3 Novel Findings	180
4.4 Future work.....	181
4.4.1 Business potential	181
4.4.2 Further research.....	182
Annotated References	184
5. Appendices	195
5.1 Appendix of the introduction chapter.....	195
5.2 Appendix of the Materials & Methods chapter	196
5.3 Appendix of the Results chapter.....	204
5.4 JCV paper & WHO correspondence.....	231

List of figures

Introduction	
1.1 genome map showing viral transcript expression of polyomavirus.....	24
1.2 Electron micrograph of polyomavirus (SV40).....	25
1.3 The JCV life cycle as an example of polyomaviruses life cycle.....	26
1.4 The structure of LT antigen.....	30
1.5 Clinical pictures of MCC.....	40
1.6 Clinical appearance of a TS patient	42
1.7 Urine cytology specimen showing an enlarged nucleus.....	46
1.8 Electron microscopical image of polyomavirus.....	47
1.9 Immunofluorescence microscopy of an abnormal transitional cell.....	48
1.10 Key events during EMT.....	50
Materials and Methods	
2.1 Multiple sequence alignment of BK and JC sequences.....	58
Results	
3.1 Agarose gel electrophoresis of GAPDH	97
3.2 Agarose gel electrophoresis of positive controls.....	98
3.3 Agarose gel electrophoresis of annealing temperatures optimisation.....	99
3.4 Agarose gel electrophoresis of PCR sensitivity.....	101
3.5 Agarose gel electrophoresis of PCR products from MCV amplification.....	102
3.6 Agarose gel electrophoresis of MCV multiplex PCR.....	103
3.7 Agarose gel electrophoresis of ICCs for MCV.....	104
3.8 Agarose gel electrophoresis of cervical smears for SV40.....	105
3.9 Agarose gel electrophoresis of ICCs for SV40.....	106
3.10 Agarose gel electrophoresis of JCV/BKV with consensus primers.....	107
3.11 Agarose gel electrophoresis of JCV/BKV with HIV positive ICCs.....	108
3.12 Agarose gel electrophoresis of JCV/BKV with HIV negative ICCs.....	109
3.13 Agarose gel electrophoresis of re-amplification of JCV/BKV.....	109
3.14 Agarose gel electrophoresis of nested PCR of JCV/BKV.....	110
3.15 Analysis of the overall percentage of JCV DNA in cervical specimens.....	111
3.16 Analysis of the association between JCV and HIV infection.....	114
3.17 Agarose gel electrophoresis of GAPDH on the WHO samples.....	116
3.18 Agarose gel electrophoresis of JCV viral load on the WHO samples.....	117
3.19 Agarose gel electrophoresis of JCV/BKV consensus primers.....	118

3.20 Agarose gel electrophoresis of JCV by nested PCR.....	118
3.21 Agarose gel electrophoresis of BKV by nested PCR.....	119
3.22 DNA sequencing of pCITE-4a recombinant plasmid.....	121
3.23 Agarose gel electrophoresis of LT ORF mismatch PCR products.....	122
3.24 Agarose gel analysis of nested PCR products from mismatch.....	123
3.25 Sanger sequencing results of LT-TOPO clone	124
3.26 Agarose gel electrophoresis of colony PCR products	126
3.27 Agarose gel electrophoresis of digested JCV LT pcDNA ^{TM4} construct.....	127
3.28 Agarose gel electrophoresis of HPV16 E6/E7 amplicon.....	129
3.29 Phase contract images of transient transfection efficiency of E6/E7.....	131
3.30 Agarose gel electrophoresis of mRNA of JCV LT and vector.....	132
3.31 Agarose gel electrophoresis of mRNA from poly and mono cells.....	134
3.32 Relative expression of mRNA from poly and mono cells.....	135
3.33 Western blot analysis of LT antibody.....	136
3.34 Immunostaining with Anti JCV LT antibody.....	137
3.35 Cell line population doubling times.....	139
3.36 Colony-forming assay.....	141
3.37 Morphological features of cells after 7 days in culture.....	142
3.38 Expression patterns of β -catenin in LT transfected and control cells.....	144
3.39 Expression patterns of claudin in LT transfected and control cells.....	145
3.40 Expression patterns of E-cadherin in LT transfected and control cells.....	146
3.41 Expression patterns of N-cadherin in LT transfected and control cells.....	147
3.42 Expression patterns of vimentin in LT transfected and control cells.....	148
3.43 Expression patterns of snail in LT transfected and control cells.....	149
3.44 IC ₅₀ value of Mefloquine treatment for 24 hrs using AQ-96.....	151
3.45 Mefloquine cytotoxicity post 24 hours treatment.....	153
3.46 Two-way ANOVA was conducted in QOE with JCV LT integration.....	155
3.47 Two-way ANOVA was conducted in QOE with vimentin clonality.....	156
3.48 Overlap charts of IPA Core Analysis on JCV LT	157
3.49 Overlap charts of IPA core analysis obtained on clonality	160

List of tables**Introduction**

1.1 List of the seven known oncoviruses.....	16
1.2 Polyomavirus proteins.....	29
1.3 Human polyomaviruses and associated pathologies	33
1.3 Human polyomaviruses and associated pathologies (continued).....	34
1.4 The contribution of various biological processes during EMT.....	51

Materials and Methods

2.1 A summary of the components used in Multiplex PCR reactions	59
2.2 A summary of the components used in Singleplex PCR reactions.....	60
2.3 A summary of the components used in Nested PCR reactions	61
2.4 List of volume and quantities of study samples	66
2.5 Mismatch PCR reaction mixture	71
2.6 Summary of thermal cycling conditions of mismatch PCR	71

Results

3.1 The overall prevalence of JCV DNA in cervical specimens.....	111
3.2 Analyses of the association between JCV and HPV16/18 infections.....	112
3.3 Analyses of the association between JCV and HIV infections	113
3.4 Summary of the potential association between JCV, HIV and HPV16/18.....	115
3.5 Zeocin concentration required to produce 100% cell death in 10-14 days.....	130
3.6 JCV LT Canonical Pathways	158
3.7 JCV LT Upstream Regulators	159
3.8 Ingenuity canonical pathways modulated by clonality.....	161

List of diagrams

3.1 A summary polyomaviruses PCR screening in cervical cancer.....	96
3.2 A summary of the JCV LT ORF cloning procedure	120
3.3 A summary of JCV LT gene transfection	128
3.4 A summary of the molecular, biological and therapeutic tests on LT cell lines.	138
4.1 A summary of the transitioning into the molecular diagnostics market	181

Word Count (excluding appendices): 36,403

Abstract

The University of Manchester

Bandar Alosaimi, March 2015

Degree of Doctor of Philosophy in the Faculty of Medical and Human Sciences

Studies on potential co-operativity between different types of tumour virus

Background: Although subclinical persistent infections with the human polyomaviruses are ubiquitous worldwide, they are known to vary in relation to geographical location, diseases present and may associate with different human tumours, especially in immunocompromised patients. The current study hypothesised that there may be co-operativity between HPV and polyomaviruses, particularly in HIV positive women, that could influence the rate of progression to invasive cervical carcinoma.

Patients and Methods: Novel PCR methods were developed for the detection of SV40, MCV, JCV and BKV polyomavirus DNA. These were used to test DNAs extracted from 220 cervical smears and 77 invasive cervical carcinomas (ICCs) from HIV positive and negative Kenyan women of known HPV status. An expression plasmid was constructed containing JCV Large T (LT) antigen and this, in addition to empty vector control, used to stably transfect HPV16 E6/E7 immortalised human keratinocytes. Expression of LT was analysed in transfected cell lines by PCR, immunocytology and Western blotting. These cells were then used to test for changes in Cell contact growth inhibition; Growth rate and Epithelial to Mesenchymal Transition (EMT). Screening of full transcriptome microarrays was carried out on vector and LT transfected cells and their sensitivity to the drug mefloquine tested by comparison of growth rates and live/dead cell assays.

Results: PCR accurately detected ~18 copies of SV40, MCV, JCV and BKV DNA in addition to simultaneous detection of JCV and BKV. None of the clinical samples tested were positive for SV40, MCV, or BKV DNA. However, JCV DNA was detected in 24/297 (8%) of cervical specimens. Comparison of the incidence of JCV in cervical smears and ICCs showed a ~3-fold increase in samples from HIV positive women with ICC ($P=0.025$) whereas no significant difference was found between smears and ICCs from HIV negative women ($P=0.553$). Analysis of the consequences of ectopic expression of JCV LT in E6/E7 immortalised human keratinocytes showed no difference in either growth rates or contact inhibition and changes in the EMT marker vimentin were found to be related to cellular clonality. Microarray analysis showed LT related alterations in gene expression which could have bearing on its carcinogenic potential in addition to changes related to clonality. JCV LT expressing monoclonal cell were the most sensitive to mefloquine treatment.

Conclusion: The simultaneous JCV/BKV detection method, described herein, is unique and has been evaluated by the WHO for this purpose. The results indicate the prevalence JCV and BKV with respect to the African geographical location and suggest that JCV may combine with high-risk HPV in a sub-set of HIV positive women to influence the rate of progression to invasive cervical carcinoma. *In vitro* JCV LT was found not to be an overt oncogene in the cell system used although cell cloning procedures clearly affected the assays. LT induced changes in total gene expression were consistent with neoplastic progression although a high proportion of genes with unknown function were dysregulated with respect to clonality. The anti JCV drug mefloquine showed some selectivity for LT expressing cells and further investigation of this indication is warranted.

Declaration

No portion of this work has been submitted in support of an application for another degree or qualification of this or any other university or other institute of learning.

Copyright statement

- i. The author of this thesis (including any appendices and/or schedules to this thesis) owns certain copyright or related rights in it (the “Copyright”) AND s/he has given The University of Manchester certain rights to use such Copyright, including for administrative purposes.
- ii. Copies of this thesis, either in full or in extracts and whether in hard or electronic copy, may be made only in accordance with the Copyright, Designs and Patents Act 1988 (as amended) and regulations issued under it or, where appropriate, in accordance with licensing agreements which the University has from time to time. This page must form part of any such copies made.
- iii. The ownership of certain Copyright, patents, designs, trade marks and other intellectual property (the “Intellectual Property”) and any reproductions of copyright works in the thesis, for example graphs and tables (“Reproductions”), which may be described in this thesis, may not be owned by the author and may be owned by third parties. Such Intellectual Property and Reproductions cannot and must not be made available for use without the prior written permission of the owner(s) of the relevant Intellectual Property and/or Reproductions.
- iv. Further information on the conditions under which disclosure, publication and commercialisation of this thesis, the Copyright and any Intellectual Property and/or Reproductions described in it may take place is available in the University IP Policy (see <http://www.campus.manchester.ac.uk/medialibrary/policies/intellectual-property.pdf>), in any relevant Thesis restriction declarations deposited in the University Library, The University Library’s regulations (see <http://www.manchester.ac.uk/library/aboutus/regulations>) and in The University’s policy on presentation of Theses.

Acknowledgements

I would firstly like to thank my supervisors, Dr Ian Hampson and Dr Lynne Hampson, for all of their guidance, expertise and support they have given me throughout the years of my PhD. This project was funded by King Fahad Medical City, Riyadh, Saudi Arabia, and I wish to acknowledge and thank them for their support.

I would also like to thank all the lab members, past and present, in particular, Dr Anthony Oliver, Dr Xiaotong He and Dr Thomas Walker for all their technical guidance and support. Finally I would like to give special thanks to my parents, my brothers & sisters, my wife Montaha & daughter Areen, and all my friends in Saudi Arabia and in The UK for all of their support and encouragement.

About the author

MSc from the school of Medicine at Manchester University, majoring in Medical & Molecular Microbiology and Masters dissertation on Characterisation of the agent produced by *Enterococcus faecium* strain TE1.

Bachelor Degree in Medical Microbiology, GPA: 3.85 out of 5 from Qassim University, College of Applied Medical Sciences. Followed by an iternship-training period at King Fahad Medical laboratories for one year.

List of abbreviations

AEC	Affymetrix expression console
AIDS	Acquired Immuno-Deficiency Syndrome
ART	acute respiratory tract
BKV	BK polyomavirus
CLL	chronic lymphocytic leukaemia
CNS	central nervous system
DMSO	dimethylsulphoxide
dNTP	deoxyribonucleotide triphosphate
dsDNA	double stranded deoxyribonucleic acid
EBV	Epstein-Barr virus
ECBS	Expert Committee on Biological Standardisation
EDTA	ethylenediaminetetraacetic acid
ELISA	Enzyme Linked Immunoassay
EMT	Epithelial to Mesenchymal Transition
GAPDH	Glyceraldehyde- 3-phosphate dehydrogenase
HAI	Haemagglutination Inhibition
HBV	Hepatitis B virus
HCC	Hepatocellular carcinoma
HCV	Hepatitis C virus
HSV-2	herpes simplex virus type 2
HHV-8	Human Herpes Virus 8
HIV	Human Immunodeficiency Virus
HPA	Health Protection Agency
HPV	Human Papillomavirus
HTA	Human Transcriptome Array
HTLV	Human T-cell Leukaemia virus type 1
ICC	Invasive Cervical Carcinomas
ICTV	International Committee on the Taxonomy of Viruses
IKB	Ingenuity Knowledge Base
IPA	Ingenuity Pathway Analysis
JCV	John Cunningham polyomavirus
Kb	kilo base pairs
kDa	kilo Daltons

KIV	Karolinska Institute polyomavirus
K-SFM	keratinocyte serum free medium
LBC	Liquid Based Cytology
MCC	Merkel cell carcinomas
MCV	Merkel cell polyomavirus
MKL-1	Merkel cell polyomavirus cell line
MWPyV	Malawi Polyomavirus
MXPyV	Mexico polyomavirus
NIBSC	National Institute of Biological Standardisation and control
p53	tumour suppressor protein p53
PAGE	polyacrylamide gel electrophoresis
PBS	phosphate buffered saline
PCR	polymerase chain reaction
PML	Progressive multifocal leukoencephalopathy
QOE	Qlucore Omics Explorer
RT-PCR	reverse transcription polymerase chain reaction
STLPyV	Saint Louis polyomavirus
SV40	Simian vacuolating virus 40 polyomavirus
TE	Tris-EDTA
TEMEDa	a – N, N, NI, NI-Tetramethylethylenediamine
T_m	Melting Temperatures
TS	Trichodysplasia spinulosa
TSV	Trichodysplasiaspinulosa-associated polyomavirus
V	volts
WGA	Whole Genome Amplification
WUV	Washington University polyomavirus

CHAPTER 1

INTRODUCTION

1. Introduction

1.1 Human cancer viruses

1.1.1 Discovery of human cancer viruses

Based on The Global Cancer Statistics of 2011, it is estimated that, with 14 million new cancer cases and 8.2 million cancer deaths every year, the world cancer burden will become the leading cause of death within the next 2 decades [1]. Viruses play a major role in human diseases including cancer and significantly they have been linked to the aetiology of between 15% and 20% of the current global burden of human cancers [2, 3] There are seven viruses (Table 1.1) known to be causally associated with over ten differing types of cancer.[4-9].

1.1.2 History of tumour viruses

In 1911, Peyton Rous identified a transmissible infectious agent that caused sarcoma in chickens [10] and this is accepted as the first recorded tumour virus. Over the course of the next fifty years, other animal tumour viruses were discovered [11] and attention soon turned towards the search for human equivalents [12]. The idea of virus-induced cancers was confirmed in 1964 by Anthony Epstein [13] who identified a new herpes virus associated with Burkitt's lymphoma which was later called the Epstein–Barr Virus (EBV) [6].

1.1.3 Classification of human cancer viruses

Tumour viruses are classified according to their genetic material as either DNA viruses which include EBV, HHV-8, HPV, HBV and Merkel cell Polyomaviruses (MCV) or RNA viruses such as HCV and HTLV-1 (Table 1.1). Although the seven viruses listed

below are all considered as tumour viruses, they have a wide variety of tissue tropisms, forms, genome sizes and life-cycles [14].

Table 1.1 List of the seven known oncoviruses, from [15].

Types	Virus	Associated cancer types	% cancer causing infections
DNA tumour viruses	EBV	Burkitt's lymphoma and Hodgkin's lymphoma	1%
	HHV-8	Kaposi's sarcoma	0.9%
	HPV	Cervical cancer	5.2%
	MCV	Merkel cell carcinoma	-
	HBV	Hepatocellular carcinoma	4.9%
RNA tumour viruses	HCV		
	HTLV-1	Adult T-cell leukaemia	0.3%

1.1.3.1 DNA tumour viruses

EBV is a human pathogen and a member of one of the most complex families of animal viruses - the herpes virus family with a genome size of around 170 kb [13]. Most people become infected with EBV as children, with an infection rate of more than 90% of the human population [8]. During adolescence or teenage years EBV is the cause of infectious mononucleosis [13]. Although EBV is one of the most common human double-stranded DNA viruses, it is also one of the few known viruses which has a proven causative role in human cancer [16]. EBV-associated cancers include Burkitt's Lymphoma, Hodgkin's Lymphoma, and nasopharyngeal and gastric carcinoma [17].

Another carcinogenic virus of the herpesvirus family is Kaposi's Sarcoma-Associated Herpesvirus or HHV-8, a large double-stranded DNA virus up to 170 kb in size which plays a critical role in the development of Kaposi's Sarcomas (KS) [18]. KS is a localised cancer that presents multifocal vascular tumours of mixed cellular composition [6]. It

commonly occurs in Acquired Immune Deficiency Syndrome (AIDS) patients and is most often seen as a cutaneous lesion predominantly in bisexual men and less commonly in intravenous drug users [8]. More than 95% of KS lesions are positive for HHV-8 viral DNA, demonstrating an aetiological association between the virus and KS [5].

HPV which is an epitheliotropic, small, double stranded, circular DNA genome approximately 8 kb in size virus was first identified in 1949 [19]. There are over 200 different HPV types, classified according to the genetic sequence of the outer capsid protein L1, more than 15 of which are considered more oncogenic when infecting the genital tract, leading to cervical cancer as well as anal cancer, vulvar cancer, vaginal cancer, and penile cancer [19, 20]. HPV enters the body through the mucosal membranes and infects basal cells either mucosal or epithelial. It does not spread systemically but is localized and highly restricted to the affected site [21]. HPV infections fall into two categories according to their potential to cause cervical cancer: high-risk and low-risk HPV. High-risk types such as HPV-16, 18, 31, 33, and 35 have been associated with cervical cancer and other mucosal anogenital and head and neck cancers [21]. Furthermore, High-risk HPV types are associated with 99% of cervical cancers and type 16 in particular is the foremost common type detected in 50% of cervical cancer world-wide, whilst types 16 and 18 together are the cause of approximately 70% of cervical cancers [21]. Low-risk HPV types (e.g. 6 & 11) have been shown to play a role in the development of benign or low-grade cervical tissue changes and anogenital warts in men and women. However, in children they cause wart-like growths on the vocal cords (juvenile or recurrent respiratory papillomatosis) which requires frequent surgical intervention [22].

Cervical cancer is one of the most common cancers, accounting for 5% to 10% of the world's cancers affecting half a million women every year with most of these residing in

developing countries [22]. The E6 and E7 oncoproteins from HPV interfere with the tumour suppressive functions of p53 and the retinoblastoma (Rb) proteins which are the two key regulators of the cell cycle. E6 and E7 oncoproteins act synergistically to overcome p53/Rb-dependent control of cell cycle progression and apoptosis. The E7 protein binds to and hyperphosphorylates Rb thereby releasing bound E2F to initiate transcription of proteins necessary for entry into the cell cycle [23]. In addition, the HPV E6 protein targets p53 for proteasomal-mediated degradation which inhibits p53 dependent induction of apoptosis which would result in deregulated cell growth produced by E7 induced release of E2F from Rb [21].

MCV was discovered in 2008 [24] and has been detected in approximately 80% of Merkel cell carcinoma (MCC) tumours [24-27]. Out of all the polyomaviruses only MCV has demonstrated a strong causative link with human cancer [28-30]. The pathology and virology of MCV will be discussed in more details in section (1.2.8.6).

HBV is the smallest of all animal DNA viruses with a genome size of approximately 3 kb, and over 400 million people are chronically infected [31]. Although HBV infects the liver and causes liver inflammation in acute illness, 15–20% of infected individuals will develop chronic infection which can in turn lead to cirrhosis, liver failure, or HCC [32]. Viral hepatocarcinogenesis is attributable to the integration of the HBV genome and subsequent expression of viral proteins in the host leading to transformation of hepatocytes accompanied by chromosomal deletions, epigenetic alterations and activation of proto-oncogenes [32, 33].

1.1.3.2 RNA tumour viruses

Two RNA viruses are known to cause cancer: HCV and HTLV-1. HCV is a small, enveloped, positive-single-stranded RNA virus of about 9.4 Kb length which infects 170 million people world-wide and is a major cause of chronic liver disease in humans [31]. After long-term inflammation of the liver, chronic HCV infection enhances cirrhosis and subsequent development of HCC [34]. HCV-related carcinogenesis is primarily the result of liver damage caused by chronic infection although the HCV core protein has been reported to inactivate expression of p53 [6, 8].

HTLV-1 is a single-stranded RNA retrovirus with genome size of 9 kb in length that establishes life-long chronic infection and causes adult T-cell leukaemia/lymphoma and HTLV-associated myelopathy. It may also be involved in other pathologies such as ‘Strongyloides Stercoralis’ [8]. It is assumed that transformation of T Lymphocytes by HTLV-I results from the expression of multiple viral gene products [35]. Amongst all of the regulatory proteins encoded by HTLV-1, the Tax oncoprotein appears to be the major oncogenic determinant playing a significant role in viral pathogenesis [17, 36].

1.1.4 Aspects of viral carcinogenesis

In humans, the response to a viral infection involves activation of both innate and adaptive immunity in order to eliminate the infection often provoking an acute inflammatory reaction [37]. If the infection is not eradicated during the acute phase, a sub-acute inflammation can become established [37, 38] whereby the infection persists producing chronic inflammation [37]. This persistence over long periods, or even the lifetime of the host, can lead to an increased chances of interference with the growth regulatory mechanisms of infected cells [39]. Furthermore, virally induced inflammation

causes the release of cytokines, chemokines and nitric oxide which can augment DNA damage thus promoting conditions for neoplastic transformation [40].

Virally encoded oncogenes also play an essential role in the formation of neoplasia either during its initiation or subsequent progression. The ‘Hit-and-Run’ hypothesis has been proposed to explain how some viruses cause persistent damage to cells which can lead to tumour formation and yet the virus is lost in the later stages of tumour development [41]. This mechanism draws attention to the fact that most tumour viruses are not complete carcinogens requiring other cofactors to induce cellular transformation [42]. These cofactors may themselves be other viruses, the identity of which will depend on tissue tropism. In this regard, it is also known that some viruses play a ‘bystander’ role infecting neighbouring cells as seen for a single tumour type such as hepatitis B virus (HBV) or multiple tumour types such as EBV [43, 44].

Tumour viruses can integrate into the host genome compromising cellular tumour suppressor pathways in order to facilitate their replication [7]. The balance between proliferation and apoptosis is thus altered and the cell carries on proliferating passing on the viral genome to future generations [40]. Furthermore, such viruses successfully evade the host immune surveillance by various strategies. For example, they can assimilate phospho-lipoproteins derived from the host cell nuclear envelope as in the case of DNA viruses and from the cell membrane as seen with RNA viruses which helps them evade the host immune system [45].

1.1.5 Co-operativity between oncogenic viruses

The contribution of oncogenic viruses to carcinogenesis can be anywhere from as little as 15% up to a complete 100% causative agent [6]. Co-operativity is a complicated

phenomenon involving identical or non-identical cancer-causing factors each often acting in a different way to contribute to the onset or the progression of a cancer [46]. In the case of viruses, this may occur following co-infection when two or more different pathogens infect an individual and non-independently facilitate one another [47].

Direct co-operativity is best exemplified in the case of HIV infection. The HIV-1 Tat protein is known to bind to the John Cunningham polyomavirus (JCV) non-coding region to stimulate JCV transcription and replication [48]. Moreover, HIV is also known to increase the risk of cancers associated with other viruses due to the ability of the Tat protein to promote the growth of human herpes virus-8 (HHV-8) associated Kaposi's sarcoma [49, 50]. Although not as a consequence of a direct interaction with HIV, it is known that hepatitis C virus (HCV) is the most common co-infection in HIV patients and presents as an HIV-related opportunistic infection [47]. This is not strict co-operativity but does result from one virus capitalising on the immunosuppressive effects of the other and as such could be considered an example of indirect cooperation. The result is a greater risk of developing severe liver damage has been attributed to HIV/HCV co-infection [47].

Co-infection of the same cell can also occur as is the case with human T-cell leukaemia virus type 1 (HTLV-1) and HIV. Many studies have demonstrated possible interactions between these two viruses, suggesting shortened survival of co-infected patients along with a more severe clinical course [51]. Human Papillomavirus (HPV) infections lead to an increased burden of HPV-induced dysplasia and cancer due to the progressive immune suppression caused by HIV. As such they represent another example of indirect co-operation with the opportunistic infection exploiting HIV driven immunosuppression [52].

Co-infection with polyomaviruses has also been proposed as a driver for HPV-related neoplasia. Interestingly several studies have documented urinary excretion of JCV and BKV in HIV positive patients, suggesting that polyomavirus reactivation is a feature of HIV infection [53, 54]. Furthermore, the BK polyomavirus (BKV) is known to establish latency near cervical tissue in the urogenital tract, especially in immunosuppressed patients and has been shown to act additively or synergistically with HPV to promote malignant transformation by altering cell-cycle control and inhibiting apoptosis [55]. Comar et al. (2011) reported that 44% (41/93) of HPV16 positive high-grade cervical intraepithelial neoplasias (HSILs) were also positive for BKV in Italian women. JCV is also associated with chromosomal instability in peripheral blood lymphocytes of EBV positive Hodgkin's and non-Hodgkin's lymphoma patients and was identified in 31% circulating lymphocytes of Hodgkin's lymphoma patients versus 7% in non- Hodgkin's patients [56].

1.2 Human polyomaviruses

1.2.1 History of human polyomaviruses

The first polyomavirus was discovered by Gross in 1953 when it was observed that mice injected with cell-free extracts of leukemic tissues developed salivary gland carcinomas and a range of other solid tumours. The name *polyoma* was used because of their ability to induce tumours at multiple sites [57]. Simian virus 40 (SV40) is one of the best known non-human polyomaviruses due to it being a contaminant in the early batches of polio vaccine in 1960 [58].

Two further human polyomaviruses were identified as pathogens in the 1970s, namely JCV, which causes Progressive Multifocal Leukoencephalopathy (PML), and BKV which causes BKV Associated Nephropathy (BKVAN) [28]. Furthermore, both of these were

shown to be oncogenic when inoculated into newborn rodents and found to be closely related to SV40. Between 2008 and 2011, three more novel putative human polyomaviruses were identified KI, WU and, more importantly, MCV [25]. Recently, the HPyV6, HPyV7, TSV, HPyV9, HPyV10, MWPyV, MXPpyV, STLPyV and HPyV12 human polyomaviruses have been identified [59]. Polyomaviruses subtypes have been shown to infect humans, and the importance of these viruses is derived from the fact that they are highly tumourigenic in cell culture and animal model systems [5].

1.2.2 Classification and phylogeny of polyomaviruses

Polyomaviruses are members of the non-enveloped *Polyomaviridae* family that are double-stranded small circular DNA viruses with a genome of around 5 Kb in size and an icosahedral shape [42, 60]. Although polyomaviruses affect 80% of the human population with no symptoms, they often persist as latent infections [28]. The *Polyomaviridae* family are widespread in nature and have capsids with a diameter of about 45 nm consisting of 88% protein and 12% DNA [60, 61].

Polyomaviruses were historically classified as a genus of the family *Papovaviridae*, with the papillomaviruses based on their sequence rearrangement in the regulatory region until their separation into two distinct families, *Polyomaviridae* and *Papillomaviridae* [28, 62, 63] which was formally recognized in 2000 by the International Committee on the Taxonomy of Viruses (ICTV). The current classification by the ICTV comprises only twelve members of the genus polyomavirus with the genotype being based on the intergenic region which includes the 3' ends of Viral Protein 1 (VP1) and Large T antigen (LT) gene sequence [63].

1.2.3 Polyomavirus genome structure

As shown in Figure 1.1 the genome codes for six structural proteins labelled according to their expression in polyoma-induced tumours. There are three structural capsid T-antigen proteins (Large, Small-ST, Middle-MT) which play an essential role in viral DNA replication, virion assembly, cellular transformation and early gene expression [57]. The other three structural-coating capsid proteins are named VP 1, 2, and 3 which are transcribed in late gene expression [57, 64]

The molecular biology of these viral genomes is functionally organised into three different regions: (i) a non-coding control region (NCCR) which encompasses the origin of DNA replication; (ii) an early coding region which encodes the tumour antigens: LT, MT and ST; and (iii) a late coding region which codes for viral capsid proteins VP1, VP2, and VP3 and the agnoprotein [28, 60] as in Figure 1.1.

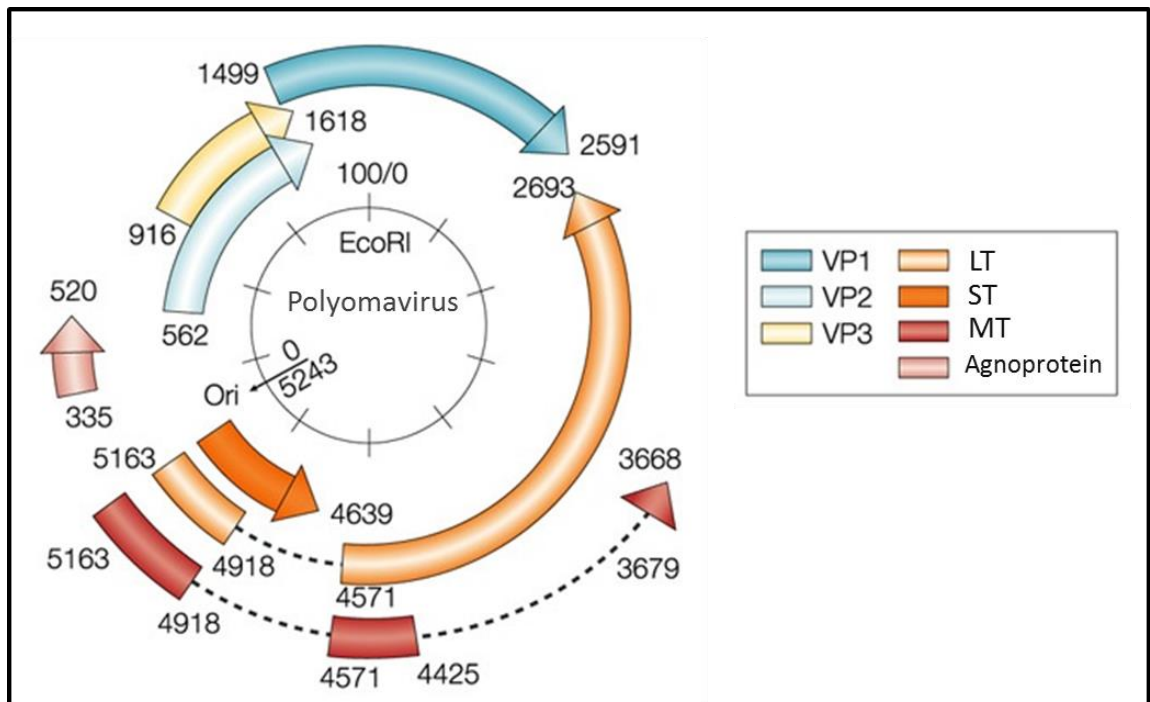


Figure 1.1 A genome map showing viral transcript expression from the polyomavirus genome. Adapted from [65].

The expression of both early and late gene transcription is directed by control factors in the NCCR. The early coding region genes and the late coding region genes are transcribed before and after DNA replication respectively. The outer shell of new virions has 72 capsomeres (Figure 1.2 B) with a barrel-shaped morphology. Each pentamer consists of two interior units of capsid proteins (VP2, VP3) attached to the exterior major capsid protein (VP1) [28, 66]. A schematic diagram of the virion of polyomavirus is shown in Figure 5.1.1 (appendix 5.1).

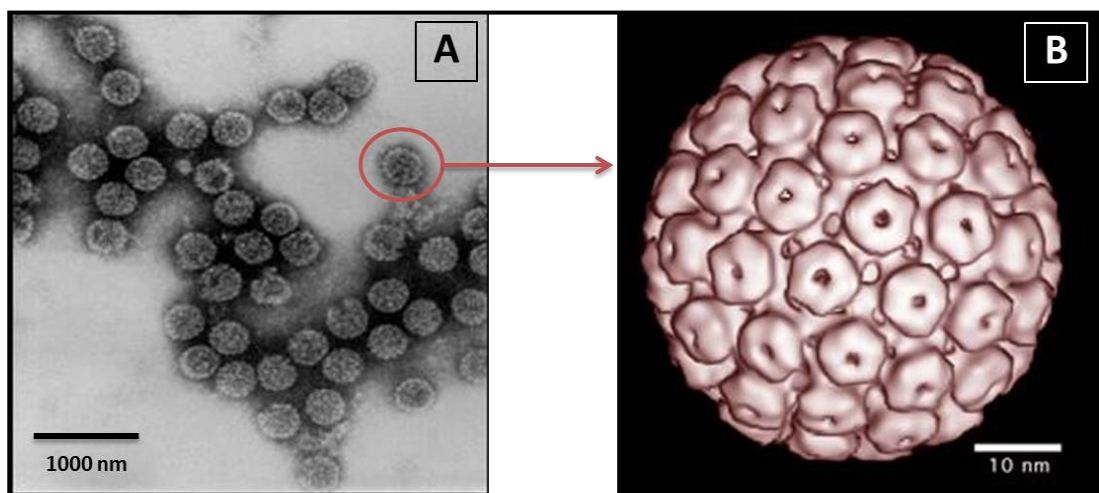


Figure 1.2 (A) Electron micrograph of polyomavirus (SV40) (B) is a shaded view of polyomavirus virion adapted from [67].

1.2.4 Polyomavirus life cycle and replication

The life-cycle of polyomaviruses begins by attachment of the virion to cellular glycoprotein receptors on the outer cell membrane (Figure 1.3 below). The virus is then internalized into the cytoplasm by endocytosis and travels through early endosomes and caveosomes to the nucleus for replication. In the nucleus, viral DNA replication occurs after viral early-gene transcription and before late-gene transcription, during which the structural proteins VP1, VP2 and VP3 are produced. Viral genomic DNA is then packaged

into virions which are assembled in the nucleus and eventually released by lysis of the cell [68, 69].

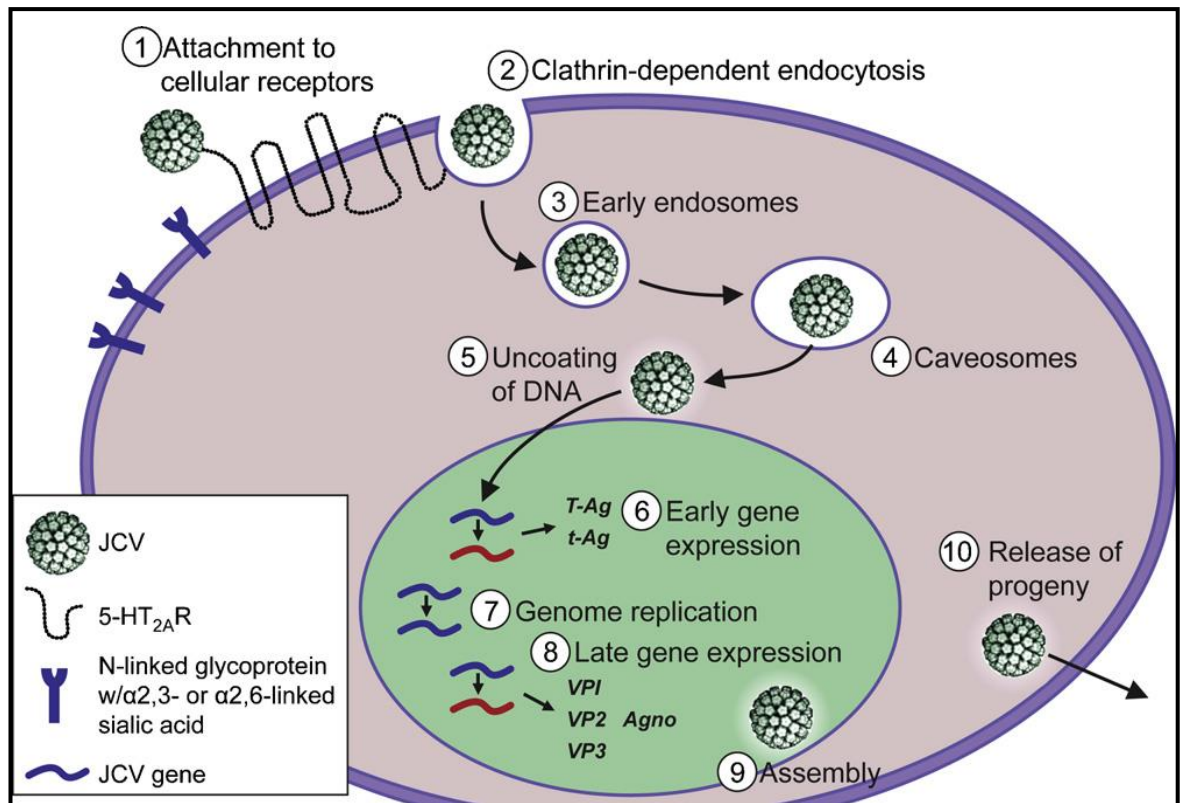


Figure 1.3 The JCV life cycle as an example of polyomaviruses life cycle. Adapted from [68].

1.2.4.1 Attachment and receptors

Polyomavirus cellular tropism is exemplified by the observation that JCV can bind to glial cells, tonsillar stromal cells, and B but not T lymphocytes [70]. In most mammalian cell types, JCV binds to oligosaccharides ubiquitously existing on the cell membrane's glycoprotein and glycolipids. The uptake of JCV through human glial cells is aided by the involvement of 2, 6-linked sialic acids and the serotonin receptor 5HT2AR [71].

1.2.4.2 Virion entry and uncoating

After binding to the cell membrane of the host, virus particles penetrate into the cytoplasm by inducing caveolae-mediated endocytosis as in BKV [72] or clathrin-dependent endocytosis that is blocked by tyrosine-specific protein kinase inhibition as in JCV [73]. Once the virus is internalized into the cell, the virus then traffics through early endosomes and caveosomes to the nucleus. Uncoating of the virus occurs after penetration of the virus particles through the nuclear pore complex [68].

1.2.4.3 Viral early gene expression

Having been transported to the nucleus, early mRNA for LT and ST antigens is transcribed by cellular RNA polymerase. LT antigen contributes to chromosomal instability that may affect cell cycle control causing genetic abnormality and malignant transformation of the target cells [74]. The ST antigen's role in viral early gene expression is not fully understood. However, Shuda et al., 2011 showed that MCV ST antigen is an oncoprotein targeting the 4E-BP1 translation regulator and expressed in most MCC, where it is required for tumour cell growth. MT antigen is not thought to be an important antigen in human disease and its possible role in human malignancies remains to be fully addressed [75].

1.2.4.4 Replication of viral DNA

During replication, viral DNA utilises the host's machinery by association with host cell histones H2A, H2B, H3, and H4 to form mini viral chromosomes which are structurally indistinguishable from host cell chromatin due to the homologous genomic structure between them. As a result, the duplicated viral genome is synthesised and processed as if it were cellular DNA [60].

1.2.4.5 Viral late gene expression

After viral DNA synthesis, transcription of the late genes occurs from the late promoter and results in the synthesis of VP1, VP2 and VP3. VP1 is a major capsid protein (1.1 kb) which forms the viral icosahedron, enables entry, and mediates haemagglutination. VP2 (0.9 kb) and VP3 (0.6 kb) are minor capsid proteins making up the structural mass of the virion [68] (See Figure 5.1.1 in appendix 5.1).

1.2.4.6 Virion assembly and release

Assembly and maturation of the particle are simultaneous. Maturation of the virions occurs in the nucleus. Viral proteins are synthesized in the cytoplasm and then transported back into the nucleus for assembly which is led by nuclear localisation signals. Virus particles are then exported to the cell surface and released by lytic rupture of the host cell with the complete replication cycle taking 48-72 hours [76].

1.2.5 Proteins of polyomaviruses

The life-cycle of polyomaviruses can be divided into early and late stages with characteristic expression of early and late viral proteins (summarised in Table 1.2).

Table 1.2 Polyomavirus proteins. Modified from reference [60].

Region	Protein	No. of amino acid JCV/BKV	Function
Early coding	LT	688/695	Initiates viral replication; stimulates host DNA synthesis; modulates early and late transcription; establishes and maintains host transformation.
	ST	172/172	Facilitates viral DNA replication
Late coding	VP 1	354/362	Major capsid protein; forms viral icosahedron, enables entry, mediates hemagglutination.
	VP 2	344/351	Minor capsid protein.
	VP 3	225/232	Minor capsid protein.
	Agnoprotein	71/66	Facilitates capsid assembly.

1.2.5.1 Early viral protein

As mentioned previously, the LT antigen is also an oncogenic protein that contributes to chromosomal instability, which may affect cell cycle control causing genetic abnormality and malignant transformation of target cells. In particular, it initiates viral replication; stimulates host DNA synthesis; modulates early and late transcription; and establishes and maintains host transformation [57, 60, 74]. Four well-folded domains and motifs make up the LT antigen: J domain (J), origin-binding domain (OBD), zinc (Zn)-binding domain and an ATPase domain (AAA+). See Fig 1.4 [77].

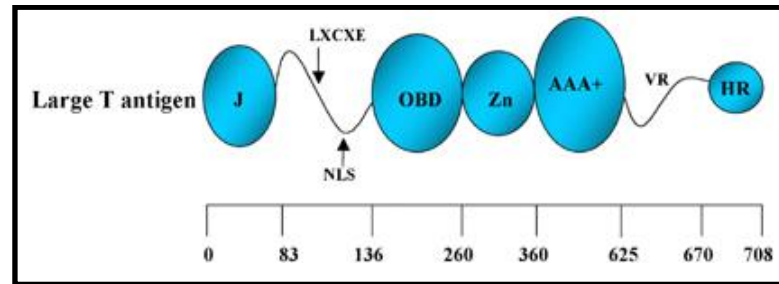


Figure 1.4 The structure of the LT antigen: (J) J domain, (LXCXE) Rb-protein-binding motif, (NLS) nuclear localization signal, (OBD) origin-binding domain, (Zn) zinc domain, (AAA+) ATPase domain, (VR) variable region, and (HR) host-range domain. Amino acid residue numbers are indicated below the domain structure Adapted from [77].

ST antigen is expressed by all polyomaviruses and is found in both the nucleus and the cytoplasm [78]. The unique functions of ST antigen are mainly mediated by interactions and integration with the multifunctional cellular phosphatase PP2A. The enzymatic activity of PP2A is inhibited which causes the cell to lose the ability to initiate transcription, thereby regulating multiple pathways including Akt, the mitogen-activated protein kinase (MAPK) pathway, and the stress-activated protein kinase (SAPK) pathway [29, 75]. Although ST can redirect PP2A to dephosphorylate new targets that may alter signalling pathways, the ST and PP2A interactions remain to be fully defined [78].

1.2.5.2 Late viral protein

VP1, the major capsid protein, accounts for almost three-quarters of the total virion protein content and makes the outer layer of the capsid (see Figure 1.2). VP2 and VP3 are the minor structural proteins and are translated in the same reading frame. Although the assumption is that VP2 and VP3 are completely hidden inside the capsid, both minor

proteins are essential for packaging of the virus [28, 29, 66] (See Figure 5.1.1 in appendix 5.1).

1.2.5.3 The agnoprotein

The agnoprotein is also a polyomavirus late protein which is multifunctional having multiple binding partners. Agnoprotein is known to interact with p53 influencing cell cycle progression [79]. It has been demonstrated that agnoprotein also acts as a viroporin and may be involved in virion assembly [49].

1.2.6 Pathogenesis of polyomaviruses

Primary infections caused by polyomaviruses are typically sub-clinical or linked to mild respiratory illness and often occur early in childhood. This can be followed by viral dissemination to sites of lifelong persistent latent infection giving rise to lifelong persistent infection [54]. Respiratory inhalation is considered the primary and most likely route of infection [49, 54].

Although it is not known which factors control the balance between latency and reactivation, polyomaviruses establish a latent infection in their hosts and can be reactivated by immunosuppression (e.g. in transplant recipients and HIV-infected individuals). This can take the form of a persistent sub-clinical state or alternatively a lytic infection which can lead to severe or fatal diseases [53]. For example, AIDS is the most common underlying cause of immunosuppression leading to JCV reactivation. BKV is associated with haemorrhagic cystitis in hematopoietic stem cell transplantation (HSCT) recipients and interstitial nephropathy in kidney transplant recipients. Both procedures

require patients to receive anti-rejection drugs resulting in their being immunocompromised [80].

Although polyomaviruses have been proved to have a direct causal role in human malignancies, there is no definitive proof of an association between polyomaviruses and the development of tumours except for MCV [81]. However, various reports have indicated the presence of viral genomic sequences in multiple human cancers (listed in Table 1.3). Indeed, the oncogenic potential of polyomaviruses suggests that intensive studies should be made on human tumours focusing on substantiating any link between these viruses and cancers [4].

Table 1.3 Human polyomaviruses and associated pathologies

Virus	Discovery	Associated diseases	Associated cancer	Reference
SV40*	1960 by Sweet	Oligodendrocytes, Interstitial pneumonia, Renal tubular necrosis, and Neurological lesions.	Osteosarcoma, Mesotheliomas, Brain and bone tumours, Non-Hodgkin's lymphoma, leukaemias, urotheliomas, breast cancer, and colorectal carcinomas.	[6] [82] [12] [83] [84]
JCV	1971 by Padgett	Oligodendrocytes and PML.	Astrocytomas, Brain tumours, Lymphoma, Leukemias, Colorectal carcinoma, Gastric cancer, Lung cancer, Oesophageal carcinomas, Prostate cancer, and Tongue carcinoma.	[68] [83] [12] [85] [7] [86]
BKV	1971 by Gardner	ART, Meningoencephalitis, Urethral stenosis, Ulceration, and Tubulointerstitial nephritis.	Cerebral tumours, osteosarcomas, Urinary tract tumours, Bladder tumour, Adrenal adenoma, Genital tumours, Renal carcinoma, Prostate cancer.	[83] [12]
KI	2007 by Allander	ART.	Lung cancer.	[87] [25]
WU	2007 by Gaynor	ART and PML.	Not known.	[25, 88]

* SV40 is now endemic in the human population.

Table 1.3 Human polyomaviruses and associated pathologies (continued)

Virus	Discovery	Associated diseases	Associated cancer	Reference
MCV	2008 by Feng	Not known.	MCC.	[24]
HPyV6 and HPyV7	2010 by Schowalter	Not known.	Not known.	[89]
TSV	2010 by Meijden	Trichodysplasia spinulosa.	EBV-positive large B-cell lymphoma.	[90]
HPyV9	2011 by Scuda	Infects kidneys of transplant patient.	MCC.	[91]
HPyV10 MWPyV MXPpyV	2012 by Buck, Siebrasse, Yu	Hypogammaglobulinemi, infections and myelokathexis (WHIM) syndrome.	Not known.	[92] [93] [94]
STLPyV HPyV12	2013 by Lim and Korup	Isolated from a stool sample of a healthy boy and a metastatic liver tissue from a colon cancer patient.	Not known.	[95] [96]

1.2.7 Mechanisms by which polyomaviruses may act as a co-factor in virus-induced malignancies.

All viruses in Table 1.1 are capable of forming virions and become transmissible sometime during their natural life-cycles, but they are normally latent within tumours so that productive virus replication is either diminished or absent [97]. Cancer viruses persist as a naked nucleic acid and rely on tumour cell machinery for their continued presence [45]. Viral latency plays a fundamental part in the evasion of innate immunity by switching off unnecessary viral proteins that might be recognised by cell-mediated immune responses [45]. The evasion of innate immunity is one of the direct mechanisms of oncovirus-induced carcinogenesis and plays a fundamental part in viral tumourigenesis [45]. For example, the polyomaviruses MCV and BKV inhibit the innate immune response by down-regulation of

Toll-like receptors expression (especially TLR9) which is one of the pattern-recognition receptors that senses viral infection [98].

Transactivation of oncovirus promoters by polyomavirus proteins is another mechanism by which polyomaviruses may act as a co-factor in oncovirus-induced malignancy. Polyomavirus LT antigen is known to possess a TBP-associated factor II 250 (TAF_{II}250 or TAF1)-like function, allowing transactivation of oncovirus promoters. For example, HBV pX protein, the HCV NS5A and core proteins, and the Tax protein of HTLV-1 can stimulate the transcriptional activity of the SV40 promoter so that, in cells co-infected with these viruses, increased polyomavirus promoter activity can occur [35, 99, 100]. Polyomaviruses' LT and ST antigens were shown to trans-activate the HPV E6 and E7 of HPV16 and HPV18 in human keratinocytes which suggests that double infection may potentiate the malignant process [101].

1.2.8 Members of the human polyomavirus family

As previously mentioned there are 12 polyomaviruses which have been identified in humans (Table 1.3) namely: SV40, BKV, JCV, KIV, WUV, MCV, HPyV6, HPyV7, TSV, HPyV9, HPyV10 (and isolates MW and MX), STLPyV, and HPyV12.

1.2.8.1 Simian Virus 40 (SV40)

SV40 was an unknown contaminant in early batches of polio vaccine and was accidentally inoculated into >100 million people in the U.S in the 1950s. Initial investigations showed that it caused multiple tumours in hamsters, although it replicated in the kidneys of Rhesus monkey without causing disease [102]. Although it has been challenging to demonstrate an association of SV40 with human tumours, the strongest

association between SV40 and human malignancies was demonstrated for malignant mesothelioma, brain tumours, and non-Hodgkin's lymphoma [36, 103, 104].

Co-expression of SV40 LT, telomerase activity, and oncogenic hRAS can initiate and maintain malignant transformation of human cells *in vitro* [104]. However, molecular studies of neoplastic transformation have shown no clear evidence for the presence of SV40 antibodies in human sera [39, 105]. Furthermore, two studies by Engels and co-workers examined seroprevalence for SV40 and found no significant difference in SV40 seropositivity amongst cancer patients [106, 107].

Although some data have proven the presence of SV40 DNA in some human tumours, suggesting the probability of the virus playing a causative role, more studies are necessary to build definitive proof of an association between tumourogenesis and SV40 [6, 28, 58].

1.2.8.2 JCV

In 1971, Padgett found JCV in the brain of a patient with a sub-acute fatal demyelinating disease (PML) [108]. Viral particles which were structurally identical to the polyoma virion were subsequently detected in the nucleus of infected oligodendrocytes from PML tissue [60]. PML is a rare disorder that damages the material (myelin) that covers and protects nerves in the white matter of the brain and is by multiple symptoms characteristic of neurological dysfunction in immunosuppressed patients [79, 109-111]. Several studies have detected JCV DNA sequences in the respiratory system, kidneys, brain, liver, lung, spleen, lymph nodes, and colorectal epithelium with viral proteins also being detectable in serum from 80% of adults [72, 81, 85, 86, 110].

In addition to its important role in PML development, JCV has been shown to be associated with several human malignancies such as colorectal carcinoma, central nervous system (CNS) lymphoma, glioblastomas and paediatric medulloblastoma, [7, 39, 85, 86, 109, 112]. In animal models, the oncogenic potential of JCV was shown when JCV is inoculated into hamsters and rats CNS, it effectively induces undifferentiated neuroectodermal tumours [113, 114]. While these findings are compelling, there is not a clear correlation of JCV with a particular type of tumour [68]. Taken together as previously discussed JCV may serve as a co-factor in tumourigenesis [115] especially in a cell that is already undergoing cell cycle disruption by other genetic or environmental effects [116].

1.2.8.3 BKV

BKV was identified in the urine of a renal transplant recipient after inoculation of the infected urine into African green monkey kidney cells [117]. In addition to its previously mentioned associations with stem cell and BKVAN in renal transplantation recipients, it is less commonly found in pneumonitis, retinitis, liver disease and meningoencephalitis [118-120]. More specifically, it affects the epithelial lining of the collecting ducts and tubular epithelium of the renal pelvis [69, 119]. BKV is known to establish persistent infections in individuals and to be excreted in the urine by asymptomatic people with 63% seropositivity in the adult population [81]. Following renal transplantation, reactivation of the latent virus is commonly observed in 30-50% of transplant recipients with 80% of these having BK viraemia and 5-10% of these going on to develop BKVAN [80, 119].

Evidence regarding the potential role of BKV in human cancer is due to the virus's ability to transform embryonic fibroblasts and cells cultured from the kidneys and brains of

hamsters, mice, rats, rabbits, and monkeys [121]. Further evidence supporting a possible role for BKV in the development of human cancer is that BKV sequences have been consistently identified in human tumours such as in ependymoma, astrocytomas, oligodendrogliomas, meningiomas and schwannomas [28, 39, 66, 122]. However, other reports have detected BKV in the urine of normal asymptomatic healthy individuals which casts doubt on its potential role in the aetiology of human cancers [121, 123].

1.2.8.4 KIV

In 2007, Allander and co-workers discovered the Karolinska Institute polyomavirus (KIV). The virus was isolated from the respiratory secretions of patients with acute respiratory tract (ART) infection in the Karolinska Institute, Stockholm, Sweden and was named after the place it was discovered [87]. Another Australian group reported finding KIV. By retrospective examination of 951 respiratory samples they found that twenty-four of the samples (2.5%) were KIV positive, indicating that the virus has a global presence, particularly in children [124]. Several studies investigated the presence of KIV at sites other than respiratory, and it has now been detected in tonsils, lymphoid tissue, urine, and plasma from HIV-1 positive patients, reviewed in [125]. Taken together, these studies do not provide a direct link between KIV and any human disease. However, a recent study has reported evidence of KIV in 9/20 lung cancer cases although, in two of the lung tissues, only the C-terminal domain of the early region was identified [125]. The implications of this finding [62] remain unclear and yet a role for KIV in tumorigenesis is still a possibility as its LT antigen has putative binding sites for both the p53 and the Rb family of tumour suppressor proteins [87].

1.2.8.5 WUV

Washington University polyomavirus (WUV) was isolated from a nasopharyngeal aspirate of a 3-year-old Australian child with ART infection, and named after the University which first reported it [88]. In patients with ART infections WUV was detected in 3% (37/1245) in Australia, 0.7% (6/ 890), in the USA and 7% (34/486) in South Korea [4, 25, 88]. WUV was also found to have an ART prevalence of 4.9% (62/1326) in Germany [125]. Detection of WUV among very young children with ART implies that the virus may have an aetiological role in childhood respiratory diseases worldwide [88, 124].

In another study, WUV DNA was detected in the brains of HIV positive individuals with PML where the virus was localised in all regions of the CNS such as cerebral hemispheres, cerebellum, pons, and medulla oblongata [126]. However, the presence of WUV DNA does not necessarily mean that the virus is associated with PML or other signs of CNS injury [126]. In one study, WUV-positive patients were co-infected with other respiratory pathogens which suggests two possibilities : WUV may act as an opportunistic pathogen taking advantage of immunosuppression or presence of other pathogens in the individual, or it may act as part of the endogenous viral flora that colonize the respiratory tract without causing any disease [127]. Clearly, the role of WUV in the aetiology of human disease needs to be further investigated [28].

1.2.8.6 MCV

Since the surprising discovery of MCV in 2008 by Feng and colleagues using the digital transcriptome subtraction technique, a number of studies have detected MCV in approximately 80% of MCC tumours. Indeed, MCV is the only human polyomavirus to have a demonstrated strong correlation with the pathogenesis of human cancer [24-27].

MCCs are dermally-based, rare, but aggressive, tumours which frequently cause fatalities. They are usually present as intraepidermal small round blue lesions (Figure 1.5). MCC patients frequently have very high antibody titres to MCV and a life expectancy of less than 9 months is seen in 50% of advanced MCC patients [24, 30]. This type of skin carcinoma is likely to be found in elderly white/fair-skinned men and mostly occurs in sun-exposed areas of the skin, particularly the neck, head, and extremities [128]. Over the past two decades in the United States it is estimated that there are 1500 new diagnosed cases of MCC annually [27].

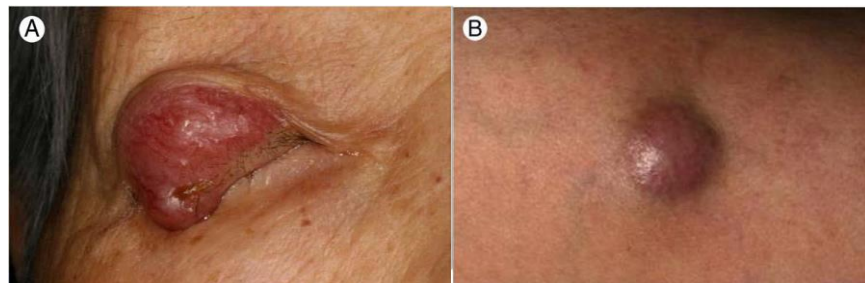


Figure 1.5 Clinical pictures of MCC arising in the right upper eyelid (A) and in the thigh (B). Adapted from [30].

MCV DNA has been detected in other tumours, particularly in non-melanoma skin cancer such as squamous cell carcinoma, basal cell carcinoma, and extracutaneous melanomas [28-30]. The risk of developing MCC is increased in patients who have HIV, chronic lymphocytic leukaemia (CLL) or are immunocompromised transplant recipients [27, 62, 63]. Other than a direct role in MCC, there is no evidence that MCV can function in a Hit-and-Run mode of action to promote other tumour types [41]. Indeed, no evidence of MCV DNA has been found in tumours from the brain, lung, prostate uterus, cervix, large bowel, ovary, breast, bone, and soft tissue in a total of 1241 tumours analysed by PCR [44].

Studies of the interactions of MCV LT antigen with dermal cell proteins such as pRB, Hsc70, and PP2A, have demonstrated that it specifically targets these tumour suppressor proteins [63, 105]. The MCV LT antigen has domain homologies similar to those described for other polyomaviruses with a DnaJ, pRb binding sequence, viral origin binding and helicase, suggesting ATPase-p53 binding domains [44]. Truncations of the protein product of the LT antigen were observed within the second exon as a result of viral mutations (integration and truncation of LT). Furthermore, these mutations appear to be necessary for the development of MCC as they prevent the autoactivation of viral DNA replication that would negatively affect cell survival [25, 36, 105].

1.2.8.7 HPyV6 and HPyV7

The discovery of MCV prompted Schowalter and colleagues to capture full-length MCV clones, using the improved random-primed Rolling Circle Amplification (RCA) method combined with modern high-throughput sequencing methods. This resulted in the detection of MCV in 14/35 (40%) of swabs from healthy volunteers and also identified HPyV6 and HPyV7 on human skin and mucosal surfaces [89].

A pilot study in 95 serum samples proved that infections with HPyV6 and HPyV7 are very common and demonstrated seropositivity of 69% against HPyV6 and 35% against HPyV7 [89]. Further investigation concluded that there was no evidence of a correlation between HPyV6 or HPyV7 and disease within 108 analysed skin cancer samples [129].

1.2.8.8 Trichodysplasia spinulosa-associated polyomavirus (TSV)

TSV was identified in August 2010 in plucked facial spines of a heart transplant patient. Trichodysplasia spinulosa (TS) is a rare skin disease exclusively found in

proliferative skin lesions characterised by the development of papules, spines and alopecia in the face of immunosuppressed patients [90]. In the same study, a prevalence of 4% TSV was found in the plucked eyebrows of 3/69 patients not suffering from TS.

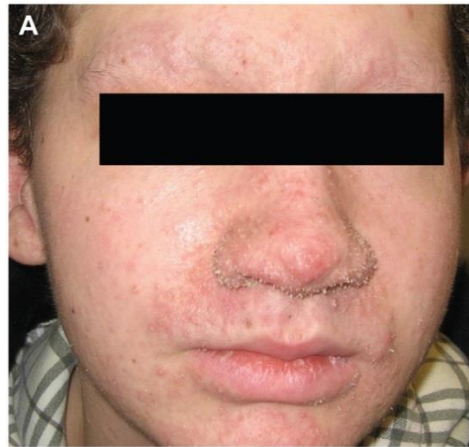


Figure 1.6 Clinical appearance of a TS patient with thickened skin, particularly on the nose and in the eyebrow area accompanied by central alopecia. Adapted from [90].

Later, Van der Meijden and co-workers in 2011 showed that the overall TSV seroprevalence in 528 healthy persons in the Netherlands was 70% [130]. TSV high seroprevalence in clinically healthy persons suggests that the virus is circulating in the human population, causing subclinical and probably latent infections [90]. TSV is potentially the cause of TS although whether it is involved in other diseases or tumours remains to be investigated.

1.2.8.9 HPyV9

HPyV9 was discovered in March, 2011 in a kidney transplant immunosuppressed patient. The goal of the Scuda et al, study was to identify possible new polyomaviruses associated with opportunistic infections in the serum of renal transplant patients. DNA from 597 clinical samples, (e.g. serum, plasma, urine or whole blood) was extracted, and

HPyV9 was detected in 84 of 597 samples [91]. A seroprevalence of 21–53% was determined in healthy adults and adolescents and 20% in children [131].

It has been shown that HPyV9 also resides in the skin and was detected in cutaneous samples of a patient with an MCC [132]. Nevertheless, HPyV9 infection may not remain restricted to a specific site in the body, and additional studies are required to identify other possible sites and any potential role in human disease [91].

1.2.8.10 MWPyV and (HPyV10, MXPyV)

In 2012, Malawi polyomavirus (MWPyV), HPyV10 and Mexico polyomavirus (MXPyV) were identified [92-94]. MWPyV was identified by shotgun pyrosequencing of DNA extracted from a stool sample collected from a healthy 15-month-old girl from Malawi. In the USA, 12/514 stool samples of children with diarrhoea were positive for MWPyV DNA [93].

HPyV10 was isolated from warts from condyloma specimens from a patient suffering from a rare genetic disorder known as Warts Hypogammaglobulinemia Infections, and Myelokathexis (WHIM) syndrome. Since the sample also contained HPV type 6, it has not been determined whether HPyV10 was causally related to the wart although this seems unlikely [92].

MXPyV is a closely related variant of MWPyV which was identified in stool samples from children suffering from diarrhoea in Mexico [94]. This study confirmed that MXPyV can frequently be found in stools, but whether the virus causes a gastrointestinal infection or is responsible for any disease in humans has yet to be investigated. The genomes

reported for MXPpyV and HPyV10 show that they are 95% to 99% identical to MWPpyV and very likely to be the same virus [44].

1.2.8.11 STLPyV and HPyV12

In 2013, Saint Louis polyomavirus (STLPyV) was isolated by Lim and co-workers from the faeces of a healthy 15-month-old boy from Malawi. Viral DNA from STLPyV was also detected in faecal specimens collected in the United States and the Gambia although it is unclear whether STLPyV is a genuine human polyomavirus species or is instead derived from a dietary source [95].

2013 saw the isolation of HPyV12 using PCR with degenerate VP1 primers. It was detected in the organs of the digestive tract most specifically in metastatic liver tissue from a colon cancer patient. Approximately 10–20% of the population appears to be sub-clinically infected with this virus [96].

1.2.9 Detection of polyomaviruses

Unfortunately, the gold standard diagnostic test for BK virus related BKVN and JC virus related PML is biopsy, which is invasive and costly. In recent years, it has been of increasing interest to find alternative ways of simultaneously measuring both BK and JCV due to the difficulty and risk involved in obtaining brain or renal tissue [133]. These have mainly been PCR-based protocols. Problems ensue however if viral DNA is no longer present in the sample or the concentration is less than the detectable limit leading to false negatives. Quantitative real time PCR assay for detection of polyomavirus was developed to help improve detection limits. Elfaitouri et al. in 2006 examined 41 clinical samples to compare real time and conventional PCR and found that 24 (58.5%) were positive by

conventional PCR, while 31 (75%) were positive with Quantitative PCR which suggested higher sensitivity of the latter technique [134]. Urinary PCR has also proved very useful. Indeed, it is considered that if this is negative then one can exclude BK/JC viruses as a cause of disease since urine viral load is generally 1000-fold higher than found in the plasma [135].

Several non-invasive assays of blood and urine have been developed although none have been validated prospectively using PCR as a comparator [136]. The following sections summarises current literature concerning diagnostic approaches used to detect polyomaviruses other than the already discussed PCR.

1.2.9.1 Cytology

In 1971 Gardner et al, used cytological examination of urine from renal transplant recipients to detect BKV. Cells with enlarged deeply-stained basophilic nuclei containing a single inclusion surrounded by an irregular halo were observed (Figure 1.7). However, cytology is not a reliable method to detect polyomaviruses since only 44% of clinical specimens from renal allograft recipients showed positivity by cytology in comparison to 75% by DNA hybridisation.

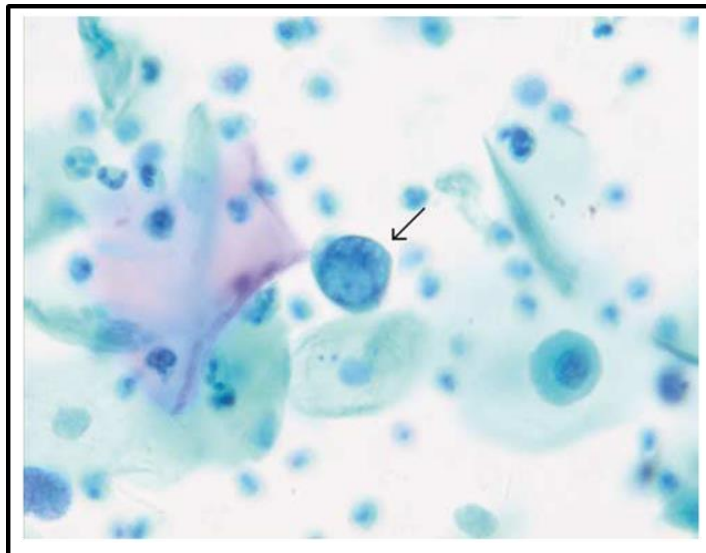


Figure 1.7 A urine cytology specimen showing an enlarged nucleus with a single large basophilic intranuclear inclusion (arrowed). Adapted from [137].

1.2.9.2 Immunological techniques

With specific antisera, immune-electron microscopy (IEM) allows visualisation of JCV virions during examination of brain tissues. JCV particles were seen as spherical, non-enveloped virions 40-45 nm in diameter. Ultrathin sections of brain material fixed in formalin or glutaraldehyde can be examined to show the particles arranged in crystalloid arrays with distinctive enlarged nuclei [60] (Figure 1.8).



Figure 1.8 An electron microscopical image of densely packed viral particles (arrows) with a diameter of approximately 40 nanometers of the enlarged nuclei. Adapted from [138].

Haemagglutination Inhibition (HAI) and Enzyme Linked Immunoassay (ELISA) methods were compared in terms of their sensitivity for the detection of the BK virus antibody in patients' serum. Although HAI has been the standard method for measurement of antibody titres to BKV and JCV [139], ELISA detected IgG antibodies to BKV/JCV with greater sensitivity and precision, compared with HAI [140].

Indirect immunofluorescence has also been developed for the rapid and sensitive detection and identification of urinary excretion of abnormal transitional cells infected with JCV and BKV [141] (Figure 1.9).

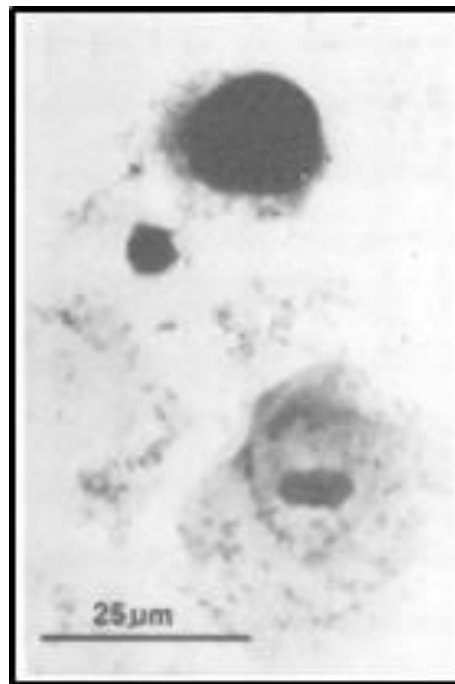


Figure 1.9 Immunofluorescence microscopy of an abnormal transitional cell in urine sediments with thickened nuclear membrane (top) and normal squamous cell (below) shown for comparison. Adapted from [142].

1.3 Functions of the polyomavirus LT antigen

All multicellular organisms need to maintain a balance between cell proliferation and death and perturbation of this by environmental, hereditary and exogenous factors like viruses can lead to cancer. For this reason, viruses have often been used as agents to aid in studying the neoplastic process. The polyomavirus most used for this has been SV40 and, in particular, its LT product [143]. When measuring the transforming ability of a protein like LT, there is a need to consider what the main steps of transformation and subsequent neoplasia are. In 2011 Hanahan and Weinberg published a work which delineated 6 hallmarks of cancer, namely sustaining proliferation, evading growth suppressors (like p53 and pRB), enabling replicative immortality, inducing angiogenesis and activating metastasis and invasion [144].

Examples of assays, which have been used to study the effects of SV40 LT on these processes, have indicated that it is involved in all of these areas [77]. For instance saturation density assays have shown that SV40 LT expressing cells do not undergo contact inhibition and can grow to higher densities as a result (sustaining proliferation), LT has been demonstrated by various methods to interact with p53 and pRb (evading growth suppressors) and mouse embryonic fibroblasts over-expressing LT are immortal (enablement of replicative immortality), However it is worth noting that some LT expressing cell lines also need an active telomerase. Transformation and angiogenesis has been seen in the thymus of transgenic mice expressing SV40 LT (angiogenesis) [145] and non-invasive serous borderline ovarian tumours transiently expressing SV40 LT produced morphological EMT and associated invasion (metastasis and invasion) [146].

1.3.1 Epithelial to Mesenchymal Transition (EMT)

EMT describes a process by which cells lose their epithelial characteristics and acquire more motile migratory mesenchymal properties, contributing pathologically to cancer progression [147]. This transient and reversible process is classified into six stages (Figure 1.10 and Table 1.4). It has also been demonstrated by others in ovarian tissue. For instance, human surface epithelial cells of the ovary were immortalised with LT SV40 and a proportion of the cells underwent senescence and/or apoptosis while others exhibited a dual EMT phenotype, with absence of E-cadherin expression and consistent expression of vimentin, cytokeratins and type III collagen [148]. In another study, SV40 LT caused loss of epithelial differentiation in Madin-Darby canine kidney epithelial cells and the cells exhibited a fibroblast-like morphology, showed a strong down-regulation of the vHNF1 transcription factor and acquired invasive properties [149]. EMT was also observed in human mammary epithelial cells immortalised with SV40 LT antigen and overexpression of TGF- β , Snail, or Twist was observed when exposed to exogenous TGF- β protein alone

without any additional factors [150]. No reports to date have demonstrated EMT in cells expressing JCV LT.

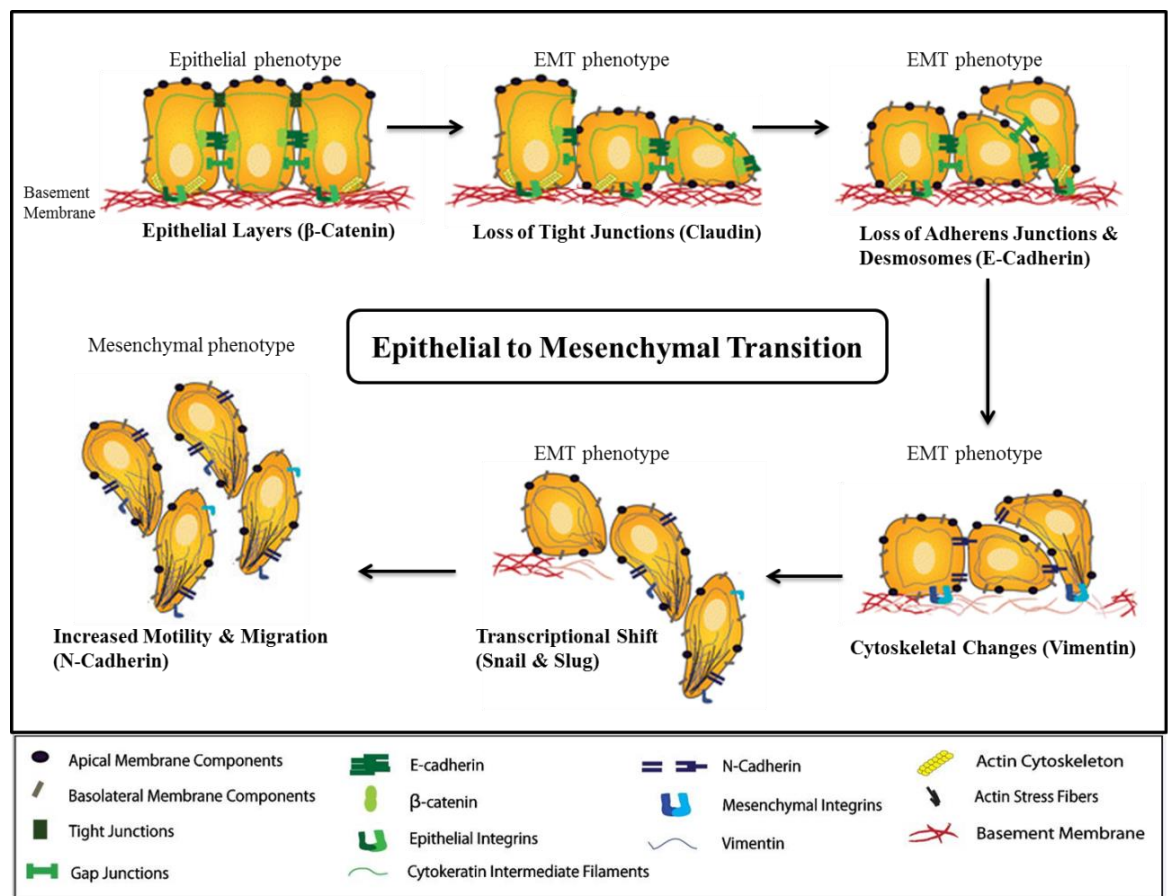


Figure 1.10 Key events during EMT. The diagram shows six key steps that are essential for the completion of the entire EMT course and the most commonly used epithelial and mesenchymal markers. (Diagram designed by the author and drawings adapted from [151]).

Table 1.4 The contribution of various biological processes during the progressive stages of EMT.

Stage	EMT Marker	Biological processes	References
Epithelial layers	β -catenin	Tight, gap and adherens junctions closely connect the layers to each other. They express high levels of β -catenin that primarily connect cadherins to actin filaments. When there is no room for more cells in the area, β -catenin signals cells to stop proliferating.	[152].
Loss of tight junctions	Claudin	Epithelial cells lose their apical and basal polarity indicated by high expression of Claudin. Tight junctions are composed of Claudin, which joins them to the cytoskeleton. During EMT, maintenance of cell polarity by tight junctions is blocked.	[153]
Loss of adherens junctions and desmosomes	E-cadherin	Cells are now at the latter stage of their epithelial phenotype. Adherens junctions and desmosomes are disassembled and cell surface proteins such as E-cadherin are down-regulated. E-cadherin is considered an active suppressor of invasion and down-regulation decreases the strength of cellular adhesion within a tissue, resulting in an increase in cellular motility, a fundamental event in EMT.	[154, 155]
Cytoskeletal changes	Vimentin	Following loss of junctional complexes, cells are at the earliest mesenchymal stage. The underlying basement membrane is degraded and the cell invades and moves into the surrounding tissue. Vimentin, a cytoskeletal protein, is responsible for maintaining cell shape, integrity of the cytoplasm, stabilizing cytoskeletal interactions, and is expressed only in mesenchymal cells.	[156]
Transcriptional shift	Snail	E-cadherin transcriptional repressors such as Snail have been implicated in promoting EMT when they bind to the E-cadherin promoter region to repress transcription during development. Snail suppresses epithelial markers and activates mesenchymal genes.	[157]
Increased motility and migration	N-cadherin	Up-regulation of N-cadherin increases cell motility, facilitates cell migration. Up-regulation of N-cadherin in addition to loss of E-cadherin is called the 'cadherin switch' and means that the cells have become mesenchymal cells.	[154, 155]

1.4 Treatments for JC virus

1.4.1 Mefloquine cytotoxicity

Mefloquine is an antimalarial medication with efficacy against JC virus [111] although the exact mechanism of action is uncertain. Previous studies have shown that mefloquine exerts anti-cancer activity in prostate cancer cells [158] and it has been reported to show sufficiently high penetration into the CNS such that it could be predicted to achieve efficacious concentrations in the brain. This may act against JC infection as found in the condition of PML [159-163]. In support of this, Gofton et al. in 2013 reported the successful treatment of PML with mefloquine in a 54-year-old woman. In 2014, Rodrigues et al. evaluated mefloquine activity against four cancer cell lines and concluded that mefloquine–oxazolidine derivatives are useful leads for the rational design of new anti-tumour agents [163]. Based on these findings, it was planned to investigate whether mefloquine possessed an anti-cancer effect against LT antigen.

1.5 Overall summary

The association of polyomaviruses with cancer is rare despite the fact that they are ubiquitous in nature. Even if a cancer were to develop there would usually be a long period following the infection before there were any clinical signs of the disease. This is as some polyomaviruses employ the ‘hit and run’ mechanism. Studies of human polyomaviruses in animal models are often complicated by the fact that many are strictly human pathogens e.g. JCV and BKV and also the carcinogenic process may be modulated by various environmental cofactors (e.g., carcinogens) or host factors (e.g., immune status) [74].

Zur Hausen has established four criteria for defining the role for a virus in cancer [39]. Evidence has been presented that JCV, BKV, and SV40 fulfil at least three of these criteria

[74]. Quoting from [74], the criteria are “(1) epidemiological plausibility and evidence that a virus infection represents a risk factor for the development of a specific tumour; (2) regular presence and persistence of the nucleic acid of the respective agent in cells of the specific tumour; (3) stimulation of cell proliferation upon transfection of the respective genome or parts thereof in corresponding tissue culture cells; (4) demonstration that the induction of proliferation and the malignant phenotype of specific tumour cells depend on functions exerted by the persisting nucleic acid of the respective agent”.

In a review of the literature it is clear polyomaviruses are linked to some human malignancies. In first place is MCV which is accepted to be an aetiological factor in about 80% of MCC. SV40 comes second in the importance hierarchy, as it has been linked to the aetiology of multiple human malignancies [103, 104]. JCV and BKV come third as they have been strongly linked to the pathogenesis of PML and BKVAN. More studies are needed to examine further this emerging family of viruses.

1.6 Project aims and objectives

The first aim of this project is: “To examine cervical smears and invasive cervical carcinomas for the presence of polyomavirus infections and to identify co-operativity that might exist between HPV and polyomavirus present in the presence or absence of HIV infection”. Cervical cancer is a very useful model with which to study the aetiology of virally induced malignant disease and the hypotheses being tested is that there is co-operativity between HPV and the polyomavirus family members SV40, JCV, BKV and MCV in women with cervical carcinomas influenced by HIV infection. Use will be made of material from a cohort of Kenyan women with cervical dysplasia, both with and without HIV co-infection. (i.e. genomic DNA isolated from 220 cervical smears samples and 77

advanced carcinoma biopsies) This aim is robust because: 1) the patients' HIV status is known and varied; 2) previous analyses carried out on HPV positivity and subtype within the Viral Oncology Group headed by Dr Ian Hampson has yielded valuable genotype data; 3) the results of this investigation can be linked to previous analyses.

A secondary aim is to develop an independently validated PCR approach for detection and diagnosis of polyomavirus infection, especially those caused by BKV and JCV. Improving diagnosis promises to lead to an increased understanding of the pathogenesis of this infection and thereby aid in contributing to the development of new treatment strategies.

The third aim is to establish a cell culture system that can address the potential for synergistic interactions between polyoma and other viruses to transform cells and also assess the ability of various antiviral compounds to interfere with this process. In view of our PCR findings, it is planned to investigate the potential of the JCV LT antigen (2067 bp ORF) to synergise with HPV in transforming human keratinocytes. In order to do this, the JCV LT ORF will initially be cloned into a mammalian expression vector for subsequent transfection into the prototype E6/E7 immortalised cell lines (Keratinocytes) of Professor Ingeborg Zehbe, reported in [164].

CHAPTER 2

MATERIALS & METHODS

2. Materials and Methods

The following methods were performed to address the thesis objective: “To examine invasive human cervical carcinomas and normal cervical smears for the presence of polyomavirus infections and to identify any potential co-operativity that exists between HPV and polyomavirus present in the presence or absence of HIV infection”.

2.1 PCR screening of polyomaviruses in cervical cancer

2.1.1 Sample collection, design and population

The study design is a retrospective case-control study, conducted by Dr. Maranga and colleagues at Kenyatta National Hospital (KNH), Nairobi Kenya. Specimen analysis was carried out at the Gynaecological Oncology Laboratories, the University of Manchester, UK. The study samples were 220 cervical smears and 77 ICCs. The women ranged in age between 21 and 52 years (median age: 35 years) and those who had prior destructive procedures for cervical disease and hysterectomies were excluded. A structured questionnaire was administered and blood samples taken, followed by an HIV test using the Determine® test kit (Abbot Pharmaceuticals, Chicago, USA), and if positive, was confirmed by Uni-Gold® (Trinity Biotech Plc, Ireland). Sampling of cervical smears was done in Liquid Based Cytology (LBC). All patients were examined with a speculum and cervical samples collected using a Cervex brush which was stirred into a vial of PreservCyt transport solution (ThinPrep Pap Test, Hologic Inc, USA). Cytospins thereof were stained with Papanicolaou (pap) stain and were independently examined by two pathologists. The 2001 Bethesda classification [165] was used for slide interpretation. More details on sample collection, design and ethical approval could be found in [166, 167].

2.1.2 DNA preparation

500 μ l of PreserveCyt material was used for extraction of DNA from clinical specimens using BioRobot® M48 (Qiagen, Sussex, UK) as described by the manufacturer. Approximately 4 x 10 μ l (FFPE) invasive cervical carcinomas sections were cut using single-use disposable microtome blades and disposable forceps for section handling. DNA isolation was carried out using the Qiagen Qiacube FFPE kits (Qiagen, Sussex, UK) as described by the manufacturer by Jay Brown at Manchester BRC Biobank. To preserve the original sample and increase stock, sample DNA was then amplified using a Whole Genome Amplification (WGA) Kit (Sigma) according to the manufacturer's instructions by Dr. Xiaotong He.

2.1.3 PCR primer design

Table 5.2.1 in appendix 5.2 lists all primers used in PCR amplification of polyomaviruses in cervical cancer. Figures 5.2.1 - 3 in appendix 5.2 illustrate the primer binding sites on MCV, SV40, and JCV LT ORF respectively. As illustrated in Figure 2.1, nested PCR primer design of BKV and JCV was designed to amplify a conserved 181 bp long fragment from both BKV and JCV. The inner primer sets amplify a 77 bp long fragment of BKV and 75 bp of JCV respectively.

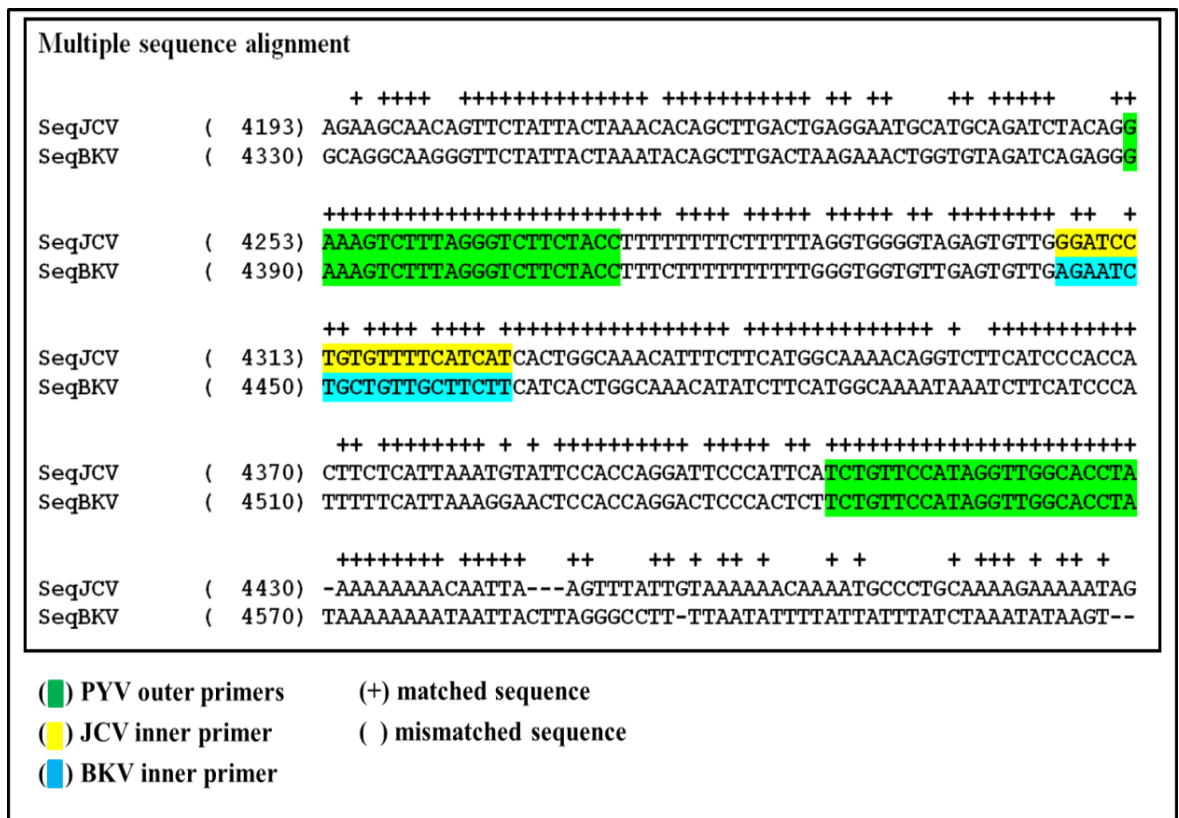


Figure 2.1 multiple sequence alignment of BK and JC sequences. Alignment was performed using EMBL-EBI software (<http://www.ebi.ac.uk/Tools/msa/clustalo/>).

Only 1,003 mismatches were detected of 4,871 aligned bases. Matching up the nucleotides of BK and JC sequences achieved a percentage of identity 77% (3736/4871) which helped to assess the degree of similarity and the possibility of homology. Therefore, BK and JC viruses are structurally similar since they have identical nucleotides over their whole length when aligned. This feature was exploited to design the nested assay of detecting the two polyomaviruses at once.

2.1.4 Positive controls

For the detection of MCV, MKL-1 (5 µg) positive control was purchased from Health Protection Agency, Salisbury, UK. MKL-1 cells contain MCV integrated into the genome

[24]. All the other viral positive controls used in PCR amplification were provided by Dr. Xiaotong He. An amount of an equivalent of 20 copies of each virus was used.

2.1.5 Polymerase Chain Reaction (PCR)

Technical training on PCR screening was kindly provided by Dr Xiaotong He. PCR master-mix reactions were prepared in UV-sterilised PCR workstations (Ultra-Violet Products, Cambridge, UK). All preparation was conducted on ice. Thermocycling was carried out on a Viriti 96-Well Fast Thermal Cycler (Applied Biosystems, California, USA). All PCR primers (Table 5.2.1 in appendix 5.2) were purchased from Eurofins Genetic Services Ltd (Ebersberg, Germany). Three PCR approaches were performed during the course of screening the cervical specimens:

2.1.5.1 Multiplex PCR

Multiplex PCR facilitates amplification of two or more targets within the same reaction format simultaneously in a single run of the assay. To enable multiplex detection, a multiplex PCR assay involves two sets of primers. Multiplex PCR was performed using Qiagen Multiplex PCR kit according to the manufacturer's instructions (Qiagen, West Sussex, UK).

Table 2.1 A summary of the components used in multiplex PCR reactions.

Component	Volume (μ l)
Qiagen Multiplex Master Mix	12.5
Primer 1 F	1
Primer 1 R	1
Primer 2 F	1
Primer 2 R	1
d H ₂ O	6.5
Sample	2
Final Volume (μ l)	25

PCR reaction was prepared and thermocycling conditions started with a single denaturation step of 95°C for 2 mins to activate the HotStart enzyme. Two amplification stages were carried out: the first involved eight amplification cycles each consisting of a denaturation step at 94°C for 30 secs, an annealing step at 59°C for 30 secs and extension step at 72°C for 5 mins. the second stage of amplification involved 38 amplification cycles each consisting of a denaturation step at 94°C for 30 secs, an annealing step at 58°C for 30 secs and extension step at 72°C for 5 mins. A final cooling cycle at 72°C for 7 mins was carried out and the PRC products were then held on 4°C until used in agarose gel electrophoresis.

2.1.5.2 Singleplex PCR

A singleplex PCR is a type of assay that facilitates amplification of one target at a time. Singleplex PCR was performed using Taq DNA Polymerase 1000 units according to the manufacturer's instructions (Qiagen, West Sussex, UK).

Table 2.2 A summary of the components used in singleplex PCR reactions.

Component	Volume (µl)
10xCl ₂	5
MgCl ₂	2
dNTPs	0.4
Primer F	1
Primer R	1
Taq DNA polymerase	0.5
d H ₂ O	38.1
sample	2
Final Volume (µl)	50

PCR reaction was prepared and thermocycling conditions started with a single denaturation step of 95°C for 2 mins to activate the HotStart enzyme. Forty amplification

cycles were carried out each consisting of a denaturation step at 94°C for 30 secs, an annealing step at 58°C for 30 secs and extension step at 72°C for 5 mins. A final cooling cycle at 72°C for 7 mins was carried out and the PCR products were then held on 4°C until used in agarose gel electrophoresis.

2.1.5.3 Nested PCR

Nested PCR involves two sets of primers, used in two separate runs; the second set intended to amplify an internal target within the first run product. It is a confirmatory test as the target sequence undergoes the first run of PCR with the first set of primers (outer). The product from the first reaction then undergoes a second run with the second set of primers (inner).

Table 2.3 A summary of the components used in Nested PCR reactions.

Component	Volume (µl)
5× GoTaq Green buffer	10
MgCl ₂	2
dNTPs	0.2
Primer F	1
Primer R	1
Platinum Taq DNA polymerase	0.5
d H ₂ O	38.1
sample	2
Final Volume (µl)	50

PCR reaction was prepared and thermocycling conditions were 95°C for 2 mins HotStart activation followed by 40 cycles for primary (outer) amplification and 30 cycles for the secondary nested virus specific amplification (Table 5.2.1). Thermocycling conditions started with a single denaturation step of 95°C for 2 mins to activate the HotStart enzyme. Forty amplification cycles were carried out each consisting of a

denaturation step at 94°C for 30 secs, an annealing step at 58°C for 30 ssec and extension step at 72°C for 5 mins. A final cooling cycle at 72°C for 7 mins was carried out and the PRC products were then held on 4°C until used in agarose gel electrophoresis. In the second run, 2 µl of outer product were diluted in 100 µl dH₂O and used as template for the secondary internal nested PCR using the same thermocycling conditions [166].

2.1.6 PCR products analysis

20 µl of amplification products in 30 % Ficoll loading buffer were separated by agarose gel electrophoresis. Agarose gels were prepared in 1 x tris-acetate-EDTA (1 x TAE) buffer and stained using 4 µl ethidium bromide added per 100 ml agarose gel solution. 100 bp and 1 kb DNA ladders (New England Biolabs, Hertfordshire, UK) were separated alongside the samples by electrophoresis. A Clarit-E Maxi EL 1660 (Alpha Laboratories Ltd, Eastleigh, UK) tank with 1x TAE buffer (see Appendix 5.2.2) was used to run the gel for 45-60 mins at 90-100 volts. The UV transilluminator UVP GDS 7500 Gel documentation system (Ultra-violet Products Ltd., Cambridge, UK) was used to visualise and analyse products by molecular weight marker comparative analysis.

2.1.7 PCR optimisation and considerations

Optimisation of PCR was carried out in order to ensure sensitivity, specificity and reproducibility of PCR assay. Multiplex and singleplex PCR were subsequently optimised and repeated to create relatively reliable amplification profiles. A number of approaches were implemented as an attempt to improve PCR amplification. Reaction components which may be used to ameliorate PCR amplification such as magnesium chloride (MgCl₂), dNTPs, primer, template concentration and adjuvant addition and polymerases selection were also investigated.

2.1.8 Positive controls optimisation and sensitivity test

Positive control concentration is another parameter that must be considered to minimise the risk of amplification artefacts. Therefore, positive control optimisation in this study was performed with serial dilutions of DNA. A number of concentrations of positive control were serially diluted which can then be used to estimate the concentration of DNA in samples using a Nanodrop 1000 spectrophotometer (Thermo Fisher Scientific Inc, Loughborough, UK). After PCR amplification, the lowest concentration that resulted in a visible band was chosen in order to minimise the risk of contamination.

Determining the number of copies of a template is based on the assumption that the average weight of a base pair is 650 Daltons. For example, the length of JCV LT antigen is 2067 bp and the amount of DNA calculated by spectrophotometer was 10^{-7} ng. Using Avogadro's number (6.022×10^{23}) the formula used was: number of copies = (amount (ng) * 6.022×10^{23}) / (length (bp) * 1×10^9 * 650). The sensitivity limit of the assay was shown to be 10^{-7} ng of input plasmid DNA which is equivalent to an input of 18 copies of the JC/BK ORF per reaction.

2.1.9 Verification of DNA integrity by GAPDH

Glyceraldehyde-3-phosphate dehydrogenase (GAPDH) is a housekeeping gene (NCBI accession number: NM 002046) that is used to verify the integrity of DNA because of its stable and constitutive expression at high levels in most human tissues and cells [168]. For this reason, GAPDH primers (listed in the table 5.2.1) were used to perform this test using singleplex PCR.

2.1.10 Screening of cervical smears and ICCs for polyomaviruses

A screening was carried out for MCV in the 220 cervical smears and the 77 tissue samples. The first screening was conducted using singleplex primers with an amplicon size of 139 bp (Table 5.2.1). The second screening was conducted using multiplex primers with amplicons of 309 bp and 139 bp respectively (Table 5.2.1).

PCR amplification of SV40 in the cervical specimens was carried out in duplicate using two sets of primers. The size of the product using SV1 primers was 325 bp (Table 5.2.1). Additional screening with different primers (SV2) resulted in a band size of 308 bp (Table 5.2.1).

A nested primer set was used for PCR amplification of BKV and JCV DNA. The outer primer set amplified an 181 bp long fragment of BKV and JCV with no differentiation (Table 5.2.1). The inner primer set amplified a 77 bp long fragment of BKV and 75 bp of JCV (Table 5.2.1). 2 µl of outer product were diluted in 100 µl dH₂O and used as template for the secondary internal nested PCR.

2.1.11 Statistical analysis

Statistical analyses were performed using the Chi-square test for comparative statistical analysis between group frequencies, using IBM SPSS statistics 20 version. In order to assess the significance levels between the categorical variables, values $p < 0.05$ were regarded statistically significant. One-Way ANOVA statistical analysis was also performed in IBM SPSS 20 to determine if significant differences exist between two or more groups. Average intensities, standard deviations, errors, and mean values calculated using Microsoft Excel 2010.

2.1.12 DNA sequencing

Initially, DNA extraction of excised gel fragments was performed using ISOLATE DNA kit (Bioline, London, UK) for the purification of post-PCR products. The technique uses spin columns and collection tubes for silica-membrane-based purification that allow elution of volume as little as 10 μ l. The protocol was performed according to the manufacturer's instructions.

Sequencing was carried out using a Big Dye Terminator Cycle sequencing kit (ABI, Warrington, UK) according to the manufacturer's instructions. Briefly, Sequencing reaction mixture of 500 ng/ μ l DNA, 4 μ l of Big Dye, 1 μ l (5 pmol) of the relevant sequencing primer and 13 μ l H₂O to a total volume of 20 μ l were thermally cycled 35 times.

A salt precipitation step then was applied to the subsequent PCR product by addition of 2 μ l of sodium acetate salt (3 M), 44 μ l of 100% Ethanol, and 1 μ l of Blue Dye (Ambion, Warrington, The UK). The content was left at room temperature for 15 mins; it was then spun at 15,183 x g for 10 mins (SIGMA 1-14 centrifuge). The supernatant was aspirated gently and washed with 80% Ethanol and left 5 mins at room temperature. It was spun again for 2 mins, then left to dry for 10 mins and the DNA sequencing carried out on a 48 capillary ABI 3730 Genetic analyser for Sanger sequencing at the DNA Sequencing facility, the University of Manchester, UK.

2.2 WHO collaborative study

Based on our recent publication on JCV and cervical carcinoma [166], we were contacted by the World Health Organisation (WHO) to participate in a collaborative study with 23 participants from clinical and research laboratories as well as kit manufacturers (see appendix 5.4 for WHO correspondence). The study aimed to evaluate suitable candidate material for the 1st WHO International Standard (IS) for JCV and BKV NAT-based assays (nucleic amplification), as part of the IS development process.

2.2.1 Sample collection, design and population

It was requested to test dilutions of 4 urine samples of the test panel, on three separate occasions in duplicate. In addition, we were also supplied with relevant clinical samples for testing alongside the candidate IS material. Study samples were received and found to be coded: samples A-F. As requested, sample E was stored at -20°C and Samples A-D and F were stored at -70°C . Samples A, B, C, D and F comprise of frozen liquid preparations. Sample E is a lyophilized preparation in a 5ml screw cap glass vial. The volume and quantities of each sample are stated in the table below.

Table 2.4 List of volume and quantities of study samples.

sample A	sample B	sample C	sample D	sample E	sample F
0.25 ml	0.25 ml	1.0 ml	1.0 ml	1.0 ml	1.0 ml
6 vials	6 vials	6 vials	6 vials	6 vials	6 vials

2.2.2 Ethics statement and consecrations

The WHO stated *“The study samples have been prepared from material provided by donors, and must be treated as proprietary. They must not be used for any other purpose other than for the performance of this study. Study samples contain infectious JCV and should be handled only in appropriate containment facilities by fully trained and competent staff in accordance with national safety guidelines. These preparations contain material of human origin, which have been tested and found negative for HBsAg, HIV antibody, and HCV RNA by PCR”*.

2.2.3 DNA preparation

Samples were received and stored appropriately. DNA preparation was performed using QIAamp MinElute Virus Spin Kit according to the manufacturer’s instructions (Qiagen, West Sussex, UK). The kit is suitable for purification of viral DNA and RNA from plasma, serum, and cell-free body fluids. Purified viral nucleic acids are free of proteins, nucleases, and other impurities. Briefly, all centrifugation steps were carried out at room temperature (15–25°C). 25 µl of QIAGEN Protease were pipetted into a 1.5 ml microcentrifuge tube prior to adding 200 µl Buffer AL and mixing by pulse-vortexing for 15 secs in order to ensure efficient lysis. Once a homogeneous solution was observed, the tubes were incubated at 56°C for 15 mins in a heating block and then centrifuged to remove drops from the inside of the lid. The lysates were applied onto the QIAamp MinElute column and centrifuged at 6000 x g for 1 min. The columns were then placed in a clean 2 ml collection tube, and 500 µl of Buffer AW1 was added followed by centrifugation at 6000 x g for 1 min. AW2 Buffer was then added and the samples were centrifuged again and the columns were placed in a clean 2 ml collection tube. To dry the membranes completely, firstly the tubes were centrifuged at full speed (20,000 x g ; 14,000

rpm) for 3 mins and then incubated at 56°C for 3 mins in a heating block. Fifty microliters of RNase-free water were applied to the centre of the membrane, incubated at room temperature for 1 min and then centrifuged at full speed (20,000 x g; 14,000 rpm) for 1 min. All tubes were stored at -20°C ready for use in amplification reactions. This was followed by GAPDH tests using end-point PCR-based method which was constructed to detect genomic DNA isolated from these samples (section 2.1.11).

2.2.4 Study protocol

All samples were extracted prior to amplification. Two independent assays were performed on separate days, using a fresh vial of each sample (A-F). One vial of sample A and B and two vials of sample C, D and F were used per assay. A routine JCV amplification assay (procedure in section 2.1.5.3 with primers in table 5.2.1 in appendix 5.2) was carried out to determine the viral load. Sample E is a lyophilised preparation and was reconstituted in 1 ml of deionized, nuclease-free molecular grade water and left for 20 mins with occasional agitation before use and a proportion was saved to be tested undiluted. The rest were used for a serial dilution into a sample matrix using dH₂O as a diluent. Amplification reactions of all samples A-F for each assay were performed in one run.

2.2.4.1 Quantitative assays

For the first assay, sample E was tested, neat and at a minimum of two serial ten-fold dilutions in the sample matrix at dilutions of 1/10 and 1/100 as suggested. For the remaining assays, a minimum of two serial dilutions of sample E, that fall within the linear range of the assay were tested. If the dilutions tested in the first assay did not fall within

the linear range, samples were adjusted so that each dilution is within the range for subsequent assays. A fresh vial of each sample was used for each independent assay.

2.2.4.2 Qualitative assays:

For the first assay, ten-fold serial dilutions of Sample E were tested in order to determine the end point from 10^{-1} to 10^{-7} ng. Sample E in the sample matrix was diluted. For the remaining assays, the dilution at the assay end point was tested, and a minimum of two half-log serial dilutions either side of the pre-determined end point (five dilutions in total) were tested too.

2.2.5 PCR results analyses

All PCR preparations and thermocycling conditions were previously described in section 2.1.5. The results and methodology used were recorded and then reported to the National Institute of Biological Standardisation and control (NIBSC) for analysis. The analysis will assess the concentration of each sample, relative to each other, and the sensitivities of the different assay methods. The formal establishment of the standard by the WHO Expert Committee on Biological Standardisation (ECBS) will be published by the NIBSC study organiser.

2.3 Cloning of JCV LT ORF for ectopic expression studies

In view of the PCR findings it was decided to investigate the potential of the JCV LT protein (2067 bp ORF) to synergise with HPV in transforming human keratinocytes *in vitro*. In order to accomplish this, it was firstly necessary to clone the JCV LT ORF into a suitable expression vector. Technical training on cloning was kindly provided by Dr Anthony Oliver.

2.3.1 DNA sequencing and PCR validation of LT gene in pCITE-4a

The complete ORF of the JCV LT gene was available in the vector pCITE-4a (see vector map in Figure 5.3.14, Appendix 5.3, provided by Dr Chengang Li). pCITE-4a is a 3703 bp plasmid, consisting of multiple cloning sites. For example, EcoR I cuts at 630 and Xho I cuts at 664 of the restriction sites. The CITE region of the pCITE-4a contains single-stranded DNA that corresponds to the T7 RNA polymerase coding strand (see pCITE-4a cloning/expression region in Figure 5.3.15 in Appendix 5.3). Therefore, DNA sequencing and PCR amplification were performed using the T7 promoter and terminator primers in Table 2.5 and the PCR reaction conditions (see Table 2.4). PCR was conducted following the procedure described in 2.1.5.2 singleplex End-Point PCR and DNA sequencing was conducted following the procedure described in 2.1.17.

2.3.2 Mismatch PCR

Mismatch PCR is primarily performed for recognizing and repairing erroneous insertion, deletion, and mis-incorporation of bases generated during DNA replication and recombination. Reinsertion of the missing stop codon was incorporated during the design of the mismatch primers. The mismatch primer should consist of: clamp, codon, restriction site and the LT gene sequence (see Table 5.3.1 in Appendix 5.3). Note that a high fidelity

proofreading Taq DNA Polymerase (Roche Ltd, UK) was used in all reactions. The reaction mixture is outlined in the tables below.

Table 2.5 Mismatch PCR reaction mixture

No.	Reaction Mix Component	Volume (μ l)
1	Forward Primer	1
2	Reverse Primer	1
3	Template (<10 ng/ μ l)	1
4	10X PCR Buffer (inc MgCl ₂)	10
5	5mM dNTP Mix	1
6	Taq Polymerase (Hi-Fi Roche)	1
7	dH ₂ O	85
	Final Volume (μ l)	100

The use of a low annealing temperature is recommended in order to significantly reduce preferential amplification while maintaining the specificity of PCR. Variable annealing temperatures were expected to show indications of the optimum temperature for mismatch PCR amplification as outlined in the tables below.

Table 2.6 Summary of thermal cycling conditions of mismatch PCR

Stage	Hot start	Mismatch step			PCR step			Storing step	
No. Of Cycles	1	2			25			1	
PCR Condition	Denatu.	Denatu.	Anneal.	Elong.	Denatu.	Anneal.	Elong.	cool	store
Temperature	94°C	94°C	variable	72°C	94°C	61°C	72°C	72°C	4°C
Time	2:00	0:45	0:30	2:30	1:00	0:45	2:30	7:00	∞

Key: Denatu: denaturation ; Anneal: Annealing ; Elong: Elongation.

Modifications to the standard cycling conditions were subsequently applied. These included pausing the program after the Hot Start to add the Taq polymerase. Another helpful variation in the PCR cycle is to “ramp” the annealing to extension steps during the cycle. A gradual ‘ramp-up’ step between denaturation and annealing was introduced in order to decrease speed of temperature change by 10%, thus allowing the Taq polymerase time to lock the primer to the template.

Nested PCR was performed using internal primers of LT gene (see Figure 5.2.3 in Appendix 5.2). Subsequent amplification of mismatch PCR products with specific internal primer pairs (Table 5.2.2) was carried out in order to confirm LT gene integrity.

2.3.3 PCR purification

The PCR product was then purified using a QIAquick PCR Purification Kit according to the manufacturer protocol (Qiagen, West Sussex, UK). Five volumes of PB buffer were added to one volume of PCR reaction and mixed by pipetting. The entire mixture was transferred to a QIAquick spin column after being placed in 2 ml collection tube. To bind DNA, the sample was applied to a QIAquick spin column, and spun at full speed (15183 x g) for 5 mins. The flow-through was discarded and the QIAquick spin column was placed back in the same collection tube. The column was washed twice by adding 750 µl Buffer PE and centrifuged for 5 mins. The flow-through was discarded and the QIAquick column was placed back in the same collection tube. The column was then centrifuged once more to remove residual wash buffer. The QIAquick column was placed in a clean 1.5 ml microcentrifuge tube and 30 µl of elution buffer EB was added to the centre of QIAquick column membrane and centrifuged for 1 min at 13,000 g. Following a final spin, the PCR product was stored at -20°C until required for TOPO cloning.

2.3.4 TOPO cloning

TOPO TA Cloning Kit for sequencing™ (Life Technologies Ltd, UK) was used to for the purpose of shuttling the PCR product into an expression vector. The manufacturer's instructions were followed, briefly: 4 µL of the PCR product was added to 1 µL salt solution and 1 µL TOPO TA vector. A total volume of 6 µL was attained by adding dH₂O. The reaction was gently mixed and incubated for 5 mins at room temperature (22–23°C). The reaction was then placed on ice in preparation for bacterial transformation using XL1-Blue competent cells (Agilent Technologies LDA UK Limited, Stockport, UK). Cloning was performed using the manufacturers' instructions (see section 2.3.5). Kanamycin was used as a selective agent. For PCR amplification, M13 forward and reverse primers were used (Table 5.2.2).

2.3.5 Transformation of XL1-blue competent cells

Competent cells were thawed on ice and incubated with 50-100 ng of plasmid DNA on ice for 30 mins. The cells were then heat shocked at 42°C for 45 secs using a water bath, and then returned to ice for a further 2 mins. Following this, Luria Broth (LB) medium (Invitrogen, Paisley, UK) was prepared (see 5.2.2 in appendix 5.2). Following this, 1 ml of pre-warmed LB media with 100 µg/ml of kanamycin was then added and the mixture incubated at 37°C for 30 mins with shaking (200 rpm) and grown to an optical density of between OD₆₀₀ 0.4 - 0.6. During this incubation, LB agar plates were prepared by adding 1.5% agar to 25 ml of kanamycin selective (LB) medium. LB agar plates were prepared with a negative control plate containing 100 µg/ml of kanamycin antibiotic. Following the incubation period, 100 µl of the transformation mix was then streaked onto one LB selective agar plate. The remaining mix was then pelleted by centrifugation at 1646 x g for 5 mins at 4°C, and the supernatant aspirated and the cells resuspended in 100 µl

fresh LB media which was then plated onto a separate LB selective agar plate. Two control plates without kanamycin were prepared; one contained XL1-Blue competent cells only acted as a negative control for the assay and positive control plate contained neat plasmid (pcDNA™4) was used to confirm competency. All plates were incubated at 37°C overnight.

2.3.6 ‘Picking’ bacterial colonies

For subsequent PCR analysis (see Figure 5.3.18 in appendix 5.3.), eighteen bacterial colonies were picked from selection plates into 150 µl of Phosphate Buffered Saline (PBS). 5 µl of each colony suspension was added to each PCR reaction (see 2.5.1).

2.3.7 Plasmid mini-prep

After successful plasmid amplification in combatant bacteria, midi-prep plasmid purification was used according to the manufacturer's instructions (Qiagen, Crawley, UK). Bacterial colonies numbers 2 and 3 were inoculated into 10 ml of LB broth for overnight incubation. From 10 ml of overnight cultures, freezer stocks were stored at -80 (400 µl of 80% glycerol + 600 µl for LB broth). After centrifugation at 6000 xg for 30 mins at 4°C, the supernatant was poured off and the bacterial pellets were resuspended in 300 µl of ice-cold solution I before being transferred to a 1.5 ml microfuge tube. The mixture was then lysed with 300 µl of freshly prepared solution II by inverting the tube rapidly 20 times. After storing at room temperature for 5 mins, 300 µl of ice-cold solution III was added, the samples mixed by inversion and stored on ice for a further 20 mins. After centrifuging at maximum speed for 10 mins at 4°C, the supernatant (without any excess material) was applied to the column and was allowed to empty by gravity flow. The QIAGEN-tip 20 was washed with 2 ml QC buffer twice and the DNA was eluted with 0.8 ml QF buffer. The

eluted product was precipitated by the addition of 700 μ l isopropanol followed by centrifugation at 10258 x g for 30 mins. The supernatant was discarded carefully and the pellet was air-dried at room temperature for 5-10 mins before being redissolved in 40 μ L TE buffer or dH₂O and stored at -20°C for further analysis such as DNA sequencing (2.1.17).

2.3.8 Plasmid maxi-prep

The large scale plasmid purification protocol of (Qiagen, Crawley, UK) was used for plasmid purification according to the manufacturer's instructions. A bacterial colony was selected and used to inoculate 10 ml of kanamycin-containing LB media (100 μ g/ml) to an OD 0.1. This was then incubated at 37°C for 6 hrs with shaking at 150 rpm and then made up to a total volume of 250 ml with fresh LB media containing kanamycin (100 μ g/ml), and incubated at 37°C overnight (N Biotek NB-205) with shaking at 150 rpm until reaching an OD₆₀₀ of 0.7. On the following day glycerol (40%) stocks were stored at -80°C and the remaining culture was decanted into 50 ml falcon tubes and centrifuged at 6000 x g for 30 mins at 4°C. Pellets were resuspended completely in 10 ml resuspension buffer P1 to which an equal volume of lysis buffer P2 was added and the tube mixed by inversion until the contents became a clear viscous and homogenous solution and incubated for 15 mins at room temperature. Following this, 15 ml of neutralisation solution-3 was added to the falcon, and the tube gently inverted for several minutes before placing on ice for 40 min. The mixture was then pelleted by centrifugation at 6155 x g for 30 mins at 4°C and the supernatant (containing plasmid) was transferred to a new tube. A second centrifugation step was performed and the supernatant was passed through layers of gauze into a fresh falcon tube. Qiagen resin filter tips were equilibrated with equilibration buffer QBT and plasmid samples were loaded to bind DNA to the resin (an aliquot of flow-through was retained for subsequent analysis of the DNA binding affinity). Bound plasmid

DNA was subjected to two washes of 30 ml wash buffer QC (aliquots of each wash flow-through was retained for subsequent analysis of DNA wash). Plasmid DNA was eluted with 15 ml of elution buffer QF (an aliquot of elution was retained for subsequent analysis) into a fresh falcon tube. DNA was precipitated with 0.7 volumes of isopropanol and centrifuged at 4°C 6155 x g for 30 mins. DNA pellets were washed with 2 ml 70% ethanol and centrifuged again. Pellets were air dried for 10 mins and dissolved in 300 µl 1x tris-Ethylenediaminetetraacetic acid (TE) buffer. Spectrophotometric assessment was then performed using a Nanodrop and the DNA was then stored at -20°C.

2.3.9 Digestion of the LT-Topo construct and target pcDNA^{TM4} vector

All restriction endonuclease digests were carried out by incubating the sample DNA along with the appropriate enzyme using buffers and conditions recommended by the supplier (New England Biolabs Ltd UK and Roche Ltd UK). A double restriction digest was carried out with EcoR I and Xho I to create 'sticky ends'. Digestion was conducted using LT-Topo construct and the target pcDNA^{TM4} vector with EcoR I and Xho I restriction enzymes (see pcDNA^{TM4} map in Figure 5.3.22 in Appendix 5.3). In two separate Eppendorf tube one containing 20 µg of the LT-Topo construct and the other one 20 µg of the target vector (pcDNA^{TM4}), 10 µl of digestion buffer was added, along with 1 µl EcoR I and Xho I restriction enzymes which was then made up to 100 µl total volume using dH₂O. The resulting mix was then placed in an *AccuBlock* Digital Dry Bath (Labnet International, Inc., New Jersey, USA) at 37°C for 3 hrs, after which an agarose gel electrophoresis was carried out to confirm a successful digestion. Following visualisation under UV light, the desired band was cut from the agarose gel with a sharp scalpel and the resulting segment of gel containing DNA was placed into an Eppendorf tube. Sufficient dH₂O to cover the gel slice was added to the tube and the tube was then placed in -20°C for storage.

2.3.10 Post-digestion gel purification

Gel purification was carried out using Qiagen's QIAquick Gel Extraction Kit according to the manufacturer's instructions (Qiagen, West Sussex, UK). The size of the gel slice was determined by weight and twice the total Eppendorf volume of Buffer QG were added to one volume of gel (100 mg ~ 100 µl). The tube was incubated at 50°C in a water bath until the gel slice had dissolved completely. To help dissolve the gel, the tube was mixed by inversion several times during the incubation. After the gel slice had dissolved, 200 µl of isopropanol (100%) was added to the sample and mixed. To bind DNA, the sample was applied to a QIAquick spin column, and spun at full speed (15183 x g) for 5 mins. The flow-through was discarded and 500 µl Buffer QG was added to the column and centrifuged again to remove all traces of agarose and the flow-through was discarded again. The column was washed twice by adding 750 µl Buffer PE and centrifuged for 5 mins after being incubated at room temperature for 15 mins. The flow-through was discarded and the QIAprep spin column was placed in a clean 1.5 ml microcentrifuge tube. The DNA was eluted by adding 30 µl Buffer EB to the centre of the membrane before it was centrifuged for the last time. Following the final spin, this stock solution was measured by Nanodrop and agarose gel electrophoresis (Figure 5.3.23 in appendix 5.3.) and stored at -20°C until future use.

2.3.11 Ligation of LT insert and pcDNATM4 vector

The ligation reactions were carried by incubating the products of the restriction reaction with the T4 DNA Ligase enzyme (Promega, Southampton, UK) in which the enzyme catalyzes the joining of two strands of the insert and the vector. For ligation, the insert and the vector were mixed in the ratio determined by the following equation: Amount of insert [ng] = 3 x amount of vector [ng] x (size of insert [bp] / size of vector

[bp]). In a microfuge tube, the previously calculated amount was added to 1 µl of 10 x ligation buffer, 1 µl of T4 DNA ligase and sterile water to a total volume of 10 µl. To do a self-ligation test, a control reaction containing all the reagents listed above except the DNA insert was set up. The ligation mixture was set to incubation overnight at 12-16 °C. Ligation of LT gene into pcDNATM4 vector was checked for the presence of the full length of the LT construct by PCR agarose gel analysis (Figure 5.3.24 in appendix 5.3.). The product now is a LT construct.

2.3.12 LT construct and pcDNATM4 vector linearisation

Having confirmed that LT construct confers full-length of pcDNATM4 vector and LT gene at the anticipated sizes, it was recommended to linearise the construct before transfection in order to increase the chances of productive integration of large plasmids into the cell line. To linearise the construct, a non-essential plasmid region, such as the bacterial marker gene, was chosen to increase the likelihood that the breakage point would occur at this region. Prior to linearisation the LT gene sequence was checked for the absence of Sca I restriction site of the ampicillin resistant gene using NEBcutter software (<http://tools.neb.com/NEBcutter2/help/cite.html>) (see Figure 5.3.16 and the NEBcutter result in Appendix 5.3). Sca I (New England Biolabs, Hitchin, UK) digestion reaction conditions were determined from the manufacturer's guidelines. A concentration of 20 µg of LT construct and pcDNATM4 control vector were linearised in a reaction comprising 10 µl 10x H Buffer, 3 µl Sca I enzyme; made up to 100 µl with dH₂O. This was incubated at 37°C for 3 hrs in an AccuBlock Digital Dry Bath (Labnet International, Inc., New Jersey, USA) followed by heat inactivation at 65°C for 20 mins. The products were resolved on a 1% agarose gel for 70 mins to confirm linearisation and the linearised products were purified using the QIAquick PCR Purification Kit as per the manufacturer's instructions (see section 2.3.3). This stock was stored at -20°C until required for stable transfection.

2.3.13 Cell Culture

All cell culture was carried out in a sterile environment using a class II microbiological safety cabinet (ESCO Class II BSC). All cell types were cultured in humidified air incubator with 5% CO₂ at 37°C (Forma Scientific, Loughborough, UK). Details of all solutions used throughout cell culture are detailed in Appendix (5.2.2.1). All reagents, unless otherwise stated were purchased from Sigma-Aldrich (Dorset, UK) or Invitrogen (Paisley, UK). All PCR primers were purchased from Eurofins Genetic Services Ltd (Ebersberg, Germany). Technical training on cell culture was kindly provided by Dr Gavin Batman.

2.3.13.1 Cell Line

In collaboration with Professor Ingeborg Zehbe (Lakehead University, Thunder Bay, Canada) the stable E6/E7 immortalised primary human foreskin keratinocytes (PHFKs) cell line was provided with kind permission (See [169]). E6/E7 cells were cultured in keratinocyte serum free medium (K-SFM) (Invitrogen, Paisley, UK) supplemented with 100 ng epidermal growth factor (Invitrogen, Paisley, UK), 25 µg/ml bovine pituitary extract (Invitrogen, Paisley, UK), 0.3 M calcium chloride dissolved and filter sterilised (Sigma-Aldrich, Dorset, UK).

2.3.13.2 Cell line thawing

An aliquot of the E6/E7 cell line was removed from liquid nitrogen and rapidly but gently thawed in a water bath at 37°C. Once thawed, the cells were transferred by sterile disposable pasteur pipette to a 50 ml sterile disposable falcon tube. Ten millilitres of warmed K-SFM were then introduced to the cell suspension slowly while mixing, whilst gently mixing the cells after which these were pelleted by centrifugation at 1000 x g for 5

mins. Following centrifugation the supernatant was aspirated and the pellet thoroughly resuspended in 10 ml complete K-SFM by sterile pipette before being split equally between two T-75 flasks (75cm²). Culture flasks were made up to a total volume of 20 ml with complete medium and cells were then maintained at 37°C in a humidified incubator containing 5% CO₂.

2.3.13.3 Routine passaging

During routine passage, E6/E7 cells were sub-cultured when they reached 80% confluency. The growth medium was aspirated and the cells washed once with 5 ml of sterile 1 x PBS. Cells were trypsinised with 800 µl Trypsin, and returned to the incubator for 3-4 mins to ensure complete cell detachment. To neutralise Trypsin, the cells were resuspended in 10 ml neutralising medium, composed of Ham F-12 nutrient mix (Invitrogen, Paisley, UK) supplemented with 10% bovine serum (Sigma Aldrich Co. Ltd, UK), before being centrifuged at 1000 x g for 5 mins. To harvest the cells, the supernatant was aspirated and the cell pellet resuspended in 10 ml complete K-SFM medium. Cells were then counted with the use of a haemocytometer and new flasks reseeded at 0.5 x 10⁶ cells/T-75 flask in a total volume of 20 ml and maintained at 37°C with 5% CO₂.

2.3.13.4 Freezing cultured cells

When cells had reached no more than 80% confluency, cells were harvested and counted as detailed above before being pelleted by centrifugation 1000 x g for 5 min and the supernatant aspirated. The cells were resuspended in an appropriate volume of freezing medium. E6/E7 cells were frozen in freezing medium consisting of a 40% of K-SFM and 40% of Ham F-12 nutrient mixture, supplemented with 10% DMSO and 10% bovine serum. The cell pellet was then resuspended in 1 ml of freezing medium and transferred to

a 1 ml freezing vial (Nunc, Roskilde, Denmark) to provide a cell suspension at 0.5×10^6 cells/ml. Vials were then placed in an isopropanol freezer gradient pot, designed to lower the temperature gradually (Nalgene, Roskilde, Denmark) and stored at -80°C overnight before transferring to a liquid nitrogen tank for longer term storage.

2.3.14 Validation of E6/E7 expression in E6/E7 immortalised keratinocytes

mRNA was extracted from the prototype E6/E7 immortalised keratinocytes by the use of TRIzol extraction method and this then used to test for expression of E6/E7 gene of HPV by RT-PCR (primers are listed in Table 5.2.2 in appendix 5.2). The same method was used for RT-PCR expressions of JCV LT gene and control vector (primers in Table 5.2.2 in appendix 5.2). It was also used with EMT markers (primers in Table 5.2.3 in appendix 5.2).

Homogenisation: Culture media was aspirated from T-75 flask of cells grown to 70% confluency. Cells were harvested as detailed (2.3.13.3) and pelleted by centrifugation at $2100 \times g$ for 5 mins and culture media was aspirated. Cells were washed in sterile PBS, pelleted again by centrifugation and the PBS was aspirated. Cells were counted and suspended in PBS at a density of 1×10^6 cells/ml. In a fume hood, cells were lysed by addition of 1 ml TRIzol Reagent (Life Technologies, Paisley, UK) and incubated at room temperature for 5 mins.

Phase separation: After a room temperature incubation for 5 mins $200 \mu\text{l}$ of 100% chloroform was added. Samples were mixed by inversion, incubated at room temperature for 3 mins followed by centrifugation at $12,800 \times g$ for 10 mins and the aqueous phase containing RNA was then transferred carefully to a new 1.5 ml Eppendorf tube.

RNA precipitation: the aqueous phase was precipitated with 500 μ l of 100% isopropyl alcohol (2-propanol) and the sample was incubated at room temperature for 10 mins followed by centrifugation at 12,800 x g for 10 mins. The supernatant was discarded and the pellet was air dried for 10 mins prior to re-dissolving in 30 μ l dH₂O. Nucleotide quantity and purity were determined by NanoDrop and stored at -20°C.

DNase I treatment: Reactions were prepared on ice in a UV-sterilised PCR workstation (Ultra-Violet Products, Cambridge, UK). RNA samples were treated with 2.5 μ l 10 x DNase I (RNase-free) buffer (New England Biolabs, Hitchin, UK), 6 μ l DNase I (RNase-free) (New England Biolabs, Hitchin, UK), and a maximum of 1000 μ g RNA sample were prepared in 25 μ l volumes (adjusted with dH₂O). Samples were incubated at 37°C for 90 mins in a Virci 96-Well Fast PCR Thermal Cycler (Applied Biosystems, California, USA).

RNA denaturation: 3 μ l 50 μ M Random Decamers (Bioline, London, UK) and 2 μ l 10mM dNTP mix (Bioline, London, UK) were added to each sample and incubated at 70°C for 6 mins. Prior to the RT step, 5 μ l of this sample was transferred to a new PCR tube and mixed with 5 μ l dH₂O and at -20°C for future use as an RT negative control.

First-strand cDNA synthesis: A 10 μ l volume was added to each 25 μ l RNA sample which comprised: 7 μ l 5 X First-Strand Buffer (Life Technologies, Paisley, UK), 0.5 μ l bioScript, 0.5 μ l RNase inhibitor, 2 μ l dH₂O. All RT reagents were purchased from Bioline, London, UK. The RT step was carried out by heating to 42°C for 60 mins. The final cDNA sample volume of 35 μ l was then stored at -20°C for PCR amplification.

2.3.15 Determination of the selective marker concentration by kill curve

Zeocin (Invitrogen, Paisley, UK) was the eukaryotic selectable marker used in the pcDNATM4 vector. Prior to stable transfection, the minimal zeocin concentration required to kill 100% of the parent cells was determined. Untransfected E6/E7 parent cell lines were seeded at 1×10^6 cells in 9 x T-25 cell culture flasks in complete K-SFM growth medium. 48 hrs later (80% confluence), the growth medium was aspirated and replaced with growth medium supplemented with a series of zeocin concentrations from 0 to 800 $\mu\text{g/ml}$ for a minimum of ten days at $37^\circ\text{C} / 5\% \text{CO}_2$, during which time microscopic inspection of the cultures was carried out. Following this, cells were washed, resuspended in medium without zeocin and returned to the incubator for a further period to monitor for signs of recovery or growth of surviving cells. The zeocin concentration that resulted in 100% cell death in approximately 10-14 days was chosen for the selection of stable transfectants.

2.3.16 Analysis of the transient transfection efficiency of E6/E7 immortalised keratinocytes

Transient transfection with LacZ plasmid: Preparation of the transfection mixture was carried out in a sterile environment using a class II microbiological safety cabinet. 2 x T-25 flasks of E6/E7 cells were grown as described (section 2.2.15.3) to 80% confluency whereupon cells were transfected using the lipofectamine-2000 method (Invitrogen, Paisley, UK) according to the manufacturer's instructions. A lacZ reporter plasmid pcDNA 3.1 V5/his was used to check transfection efficiency. LacZ positive mixture contained 15 μl of lipofectamine-2000 and 116.7 μl OptiMem (Invitrogen, Paisley, UK), and in a separate vial, LacZ negative mixture contained 7.96 μl LacZ and 116.7 μl OptiMem and both vials were incubated for 15 mins at room temperature. The contents of both tubes were then combined, incubated at room temperature for a further 20-35 mins and added

drop-wise to the cell culture flasks, containing no medium with gentle agitation making sure that the mixture covered the entire flask by rotation. This was then incubated for 30 mins at 37°C / 5% CO₂ before being gently rocked and returned to the incubator for another 30 mins. After this final incubation, a fresh complete K-SFM was added and the flasks were incubated overnight.

β-galactosidase staining: 24 hrs post-transfection, the medium containing the transfection mixture was aspirated, the cells were washed with sterile 1x PBS and fixed with 2 ml 2% paraformaldehyde for 10 mins at room temperature. During this incubation, β-galactosidase staining solution was prepared (for 1ml of stain: 10 µl 200 mM magnesium chloride, 10 µl 400 mM potassium ferricyanide, 10 µl 400 mM potassium ferrocyanide, 50 µl 20 mg/ml X-Gal in 920 µl PBS) to make up a total volume of 1000 µl. After fixation, cells were gently washed twice in sterile 1x PBS and 2 ml/T25 of staining solution was added and flasks incubated at 37°C for 15-120 mins and checked under microscope to observe the development of blue cells. Once staining was complete, the staining solution was aspirated and the reaction quenched using PBS and sealed with parafilm and stored at 4°C. Images at 20x magnification were captured with a Hirocam 1.3 megapixel MA88-130 microscope camera and TS View software (Science Company, Denver, USA). Within 5 random fields of view, one hundred cells were counted in a vertical line and the number of blue transfected cells was expressed as a percentage of transfection efficiency.

2.3.17 Stable transfection of E6/E7 immortalised keratinocytes with JCV LT

Stable co-transfection was carried out on E6/E7 parent cells using Lipofectamine-2000 method. Co-transfection was performed using the linearised LT construct and pcDNATM4 vector. E6/E7 cell line was seeded at 0.5 x 10⁶ cells in 2 x T-25 cell culture flasks in 20 ml complete K-SFM growth medium to achieve 90% confluency as described

in (2.3.14). In brief, for one T-25 a 12.5 μ l aliquot of lipofectamine-2000 was mixed with 626 μ l OptiMem (Invitrogen, Paisley, UK), and in a separate vial, 30 μ g linearised LT construct was mixed with 626 μ l OptiMem and both vials were incubated for 5 mins at room temperature. Another set of reactions was performed with 30 μ g linearised pcDNATM4 vector only. The contents of both tubes were then combined, incubated at room temperature for a further 20-35 mins and added drop wise to the cell culture flasks, containing no medium with gentle agitation making sure that the mixture covered the entire flask. This was then incubated for 30 mins at 37°C / 5%CO₂ before being gently rocked and returned to the incubator for another 30 mins. After this final incubation, a fresh complete K-SFM was added and the flasks were incubated overnight. Twenty-four hours post-transfection the growth medium was replaced with 10 ml fresh medium supplemented with 50 μ g/ml zeocin. Cells were monitored over a period of several weeks under zeocin selection. The medium was changed every 2-3 days.

Dishes were monitored daily for the development of single celled colonies. zeocin resistant colonies were visualized after 21 days, the flasks were washed, trypsinised, expanded in a T-75 flasks and labelled as (Con 1, Con 2, and Con 3) for LT construct and (Vec 1 and Vec 2) for the empty vector. Only 5-10 cells were transferred to Petri dishes in preparation for the generation of monoclonal cell lines. Once single celled colonies had expanded to contain approximately 20-30 cells, they were transferred to a 24-well plate. For colony picking, sterile cloning rings were prepared by cutting the lower rim of a yellow tip and autoclaving. The lower rim of a sterile hoop was coated in sterile Vaseline and gently placed over the colony, a process which was repeated for each colony to be picked. Briefly, 30 μ l of trypsin was transferred to each ring and Petri dishes were maintained at 37°C / 5% CO₂ incubator for 5 mins or until complete cell rounding had occurred microscopically. Once cells had fully detached they were resuspended in 1 ml K-

SFM, transferred to a 24-well plate, and made up to a total volume of 2 ml and maintained at 37°C 5% CO₂ and grown to 80% confluency. Subsequently, cell growth was then monitored and expanded from 24-well plate followed by 6-well plates and then to T-25 culture flasks and the selection medium was changed every 2-3 days. Cells were eventually transferred to T-75 culture flasks and grown to 80% confluency whereupon stocks of cells were frozen as described in section (2.3.13.4). In total, 8 colonies were successfully picked and labelled (M 1 to M 8) monoclones.

2.3.18 Analysis of JCV LT protein expression

Prior to studying the ability of LT gene to influence the protein expression profile in E6/E7 cell lines, mRNAs from the 3 polys and 8 monos were extracted by the use of TRIzol extraction method (2.3.14) and this then used to test for RT-PCR expressions.

2.3.18.1 Western blot analyses

Details of all solutions used throughout western blotting are detailed in appendix (5.2.2). All reagents, unless otherwise stated were purchased from Sigma-Aldrich (Dorset, UK). Technical training on Western blot was kindly provided by Dr Gavin batman and Dr Sultan Alqahtani.

Preparation of protein lysates: Cells grown in T-75 flasks were harvested and counted as detailed in section 2.2.1.3. The cells were then pelleted by centrifugation for 5 mins at 1000 x g and the supernatant aspirated. One million cells were then resuspended in 500 µl PBS and transferred to a 1.5 ml Eppendorf, before being centrifuged at 2100 x g for 5 mins and the supernatant aspirated. Cells were then resuspended in a volume of PBS and an equal volume of 2x Laemmle sample buffer to provide a final concentration of 1.0x10⁶

cells / 20 μ l [170]. Samples were then subjected to three cycles of heating to 95°C for 10 mins followed by snap freezing in liquid nitrogen and were stored at -20°C.

Gel Electrophoresis: Protein transfer was carried out using one-dimensional sodium dodecyl sulphate polyacrylamide gel electrophoresis (SDS-PAGE) with a Whatman minigel twin system (Whatman Biometra, Goettingen, Germany). Plates were assembled as per manufacturer's instructions. A 6% separating gel was prepared (5 ml dH₂O, 6 ml 30% acrylamide mix, 3.8 ml 1.5 M Tris-HCL (pH 8.8), 150 μ l 10% SDS solution, 150 μ l 10% ammonium persulphate (APS) solution and 6 μ l N, N, N', N'-tetramethylethylenediamine (TEMED), mixed to ensure a uniform and contiguous interface upon polymerisation. Once the separating gel polymerised a stacking gel was prepared (2.7 ml dH₂O, 670 μ l 30% acrylamide mix, 500 μ l 1 Molar Tris-HCL (pH 6.8), 40 μ l 10% SDS, 40 μ l 10% APS and 4 μ l TEMED) to allow a 1.5 cm depth between the bottom of the sample well and the separating gel. A sample well comb was inserted into the stacking gel liquid before being allowed to completely polymerise. Protein samples underwent incubation at 95°C for 10 mins before being loaded alongside 10 μ l HiMark High Molecular Weight Protein Standard (Life Technologies, Paisley, UK) and were separated in 1 x Laemmle running buffer at 30 mA.

Western Blot: The protein transfer and western blotting was carried out using the method described by Towbin et al, (1979). **Transfer:** proteins were transferred from PAGE gels onto Hybond-C nitrocellulose membrane (Amersham Biosciences, Bucks, UK) soaked in 1 x transfer buffer containing methanol using a Titanium Whatman Biometra semidry blotter (Whatman Biometra, Goettingen, Germany) for 50 min at 10 V. **Blocking:** The membrane was air dried prior to blocking in PBS 5% non-fat milk powder and 0.1% Tween-20 (Sigma Aldrich, Dorset, UK) at room temperature for 2 hrs with gentle shaking

followed by a single 4 mins wash in PBS. **Primary antibody incubation:** membranes were incubated with primary PAb 2000 and 2003 monoclonal antibodies, that are specific for JCV T antigen and kindly provided by Dr. Richard Frisque, at a concentration of 1/1000 in PBS with gentle rotation for 3 hrs followed by three 5 mins T-PBS washes in PBS with gentle shaking. **Secondary antibody incubation:** membranes were incubated for 2 hrs at room temperature with goat anti-rabbit IgG, HRP-linked secondary antibody at a concentration of 1/2000 in PBS containing 2% non-fat milk powder with gentle rotation followed by three further 5 mins PBS washes. **Detection:** proteins were detected using ECL Plus (Amersham Biosciences, Bucks, UK) and exposure to hyperfilm (Amersham Biosciences, Bucks, UK) according to the manufacturer's recommendations. Following different exposure times, films were visualised using developer and fixative reagents (Sigma Aldrich Co. Ltd, UK) in a dark room. **Control detections:** Membranes were re-probed with GAPDH protein antibody to confirm genuine signals. Following a brief PBS wash, membranes were re-blocked for 1 hr at room temperature in 5% non-fat milk powder in PBS with gentle rotation. Membranes were incubated for 2 hrs at room temperature with primary mouse anti-GAPDH (ab9484, Abcam, Cambridge, UK) at a concentration of 1/1500 with gentle rotation. Following three 7 mins PBS washes membranes were then incubated for 1 hr at room temperature with rabbit antimouse HRP conjugated secondary antibody (Dako, Cambridge, UK) at a concentration of 1/2000 in PBS containing 2% non-fat milk powder followed by three 7 mins PBS washes. Proteins were visualised using ECL and exposure to hyperfilm (as described above) according to the manufacturers' instructions.

Western blot of EMT markers was performed similarly. Details of all solutions used throughout western blotting are detailed in (table 5.2.4 in appendix 5.2). All primary

antibodies were purchased as an Antibody Sampler Kit from Cell Signalling Technology (MA, USA).

2.3.18.2 Immunohistochemistry staining

To investigate whether LT antigen was functioning correctly in stable transfected E6/E7 cell lines by immunohistochemistry Dako EnVision detection systems was used (Dako, Copenhagen, Denmark). Technical training on Western blot was kindly provided by Suzannah Lant. Cell lines were harvested and collected at 0.5×10^6 cells per Eppendorf tube in a total volume of 500 μ l complete K-SFM and cells were mounted onto slides using Cyto-Spin at 60 x g for 4 mins. The slides were air-dried for 2 mins before being fixed for 10 mins with 500 μ l 2% paraformaldehyde. Cells were washed twice in 500 μ l PBS for 5 mins at 50 rpm shaking. Pre-heated antigen retrieval buffer EDTA (pH 8) was used to unmask the cells for 10 mins at 95°C in water bath; and then allowed to stand and cool for 25 mins at room temperature. Cells were washed twice in 500 μ l PBS for 5 mins at 50 rpm shaking before wiping off excess water from the back of the slide and area around the section. The slides were then incubated with 200 μ l blocking solution (3% BSA in 1 x PBS) at room temperature for 45 mins to block endogenous peroxidase activity. Cells were washed twice in 500 μ l PBS for 5 mins at 50 rpm shaking before wiping off excess water from back of slide and area around section. Excess water from back of slide and area around section was wiped off before being applied to 200 μ l primary antibodies at a concentration of 1:200 in 0.5% BSA in PBS (0.1 g in 20 mls of PBS) and incubated for 1 hr using PAb 2000 and 2003 are monoclonal antibodies that are specific for JCV T antigen and kindly provided by Dr. Richard Frisque. Goat anti-mouse secondary antibody (HRP) was applied for 30 mins after similar washing routine just once. Twenty microliters of DAB Chromagen per 1ml of Substrate Buffer were applied to each slide in an aliquot of 150 μ l. The reaction was quenched with PBS and the Nuclei were counterstained in

Haematoxylin at a concentration of 1:5 for 30 secs made up using d H₂O. The reaction was quenched with PBS and the cells dehydrated through an ethanol gradient (30% , 50%, 70% , 95% , 95% , Xylene 1, Xylene 2) prior to two 5 mins Xylene incubations and mounting in DPX. Images at 60x magnification were captured using Nikon's NIS-Elements imaging software with Hologic's ThinPrep integrated imager viewing 67.5 microns (Hologic, MA, USA).

2.3.19 Cell Proliferation Assay (AQ-96 Assay)

Cell proliferation was assessed using the AQ-96 reagent assay (Promega, Southampton, UK). Clones and controls cell lines were each grown to 80% confluency in a T75 flask and recovered into a 50 ml falcon tube of culture medium by previously described methods (2.3.13.3). Cell densities were calculated with a haemocytometer inspecting nine fields of view and aliquots were prepared to provide 2000 cells per well in a 96-well assay plate (Corning Ltd, US) in triplicate per cell type and the manufacturer's instructions were followed. 24 hrs post-seeding, an aliquot of CellTiter 96® AQueous One Solution® reagent was thawed for 10 mins in a water bath at 37°C and 20 µl of reagent was added to the first three wells of each row in order to provide a time zero data point, and the plates returned to the incubator. This was then incubated for 2 hrs at 37 °C, 5% CO₂ in the dark, after which time the absorbance at 490 nm was recorded for each triplicate using a Dynex MRX plate reader (Dynex Technologies, West Sussex, UK). This procedure was repeated every 12 hrs for a time course of 72 hrs. The plates were then returned to the incubator (37°C 5% CO₂) and assessment of cell proliferation using AQ-96 reagent was repeated at 24, 48 and 72 hrs. Cell growth was calculated as percentage growth change from the 24 hrs time point and optical densities of the growth were recorded.

Similarly, for mefloquine cytotoxicity, cells were seeded onto 96-well plates at a density of 2000 cells per well and incubated for 1 day. Twenty-four hours post-seeding, the growth medium was aspirated and replaced with 200 μ l K-SFM supplemented with mefloquine at concentrations of 5 μ M, 10 μ M and 20 μ M, with DMSO volumes adjusted to remain constant. One full row of the 96-well plate was used for each drug concentration in triplicate. DMSO-only treated cells were included as controls and the plates were then returned to the incubator.

2.3.20 Trypan blue viability test of mefloquine cytotoxicity

The effects of an escalating dose of mefloquine on the growth of LT transfected cells were assessed using the Trypan Blue exclusion (Sigma Aldrich, Dorset, UK). Cells were seeded onto 6-well plates at a density of 0.3×10^6 cells per well and grown to 80% confluency. The growth medium was aspirated and replaced with 3 ml Keratinocyte-SFM supplemented with mefloquine at concentrations of 5 μ M, 10 μ M and 20 μ M alongside a negative control DMSO only. 24 hrs post-treatment, the growth medium containing free floating cells was removed from the culture flasks and transferred to a 50 ml falcon tube. Cell monolayers were washed with PBS and 100 μ l of pre-warmed Trypsin and the flasks returned to the incubator for 3 mins until complete cell detachment had occurred. The Trypsin was then neutralised by adding the complete growth medium previously removed from each specific flask, thoroughly re-suspending the cells. A Haemocytometer live/dead cell count was then performed by preparing a 1:1 dilution of the cell suspension using a 0.4% Trypan Blue solution and incubated for 1 – 2 mins at room temperature before the beginning of counting. The number of unstained (live) cells expressed as a percentage of the total number of cells was counted. Triplicate cell counts were performed for each well (Non-viable cells were blue, viable cells were unstained). For an accurate determination,

cells were counted under the microscope in four 1 x 1 mm squares of one chamber and the average number of cells per square was determined (all nine of 1 mm² squares).

2.3.21 Toluidine Blue stain of transformed colony forming assay

Transformed colony forming assay was assessed by a visual observation of the formation of transformed colonies obtained by Toluidine Blue staining (Sigma Aldrich, Dorset, UK). The four cell lines were optimised for the optimal seeding density that would result in a visible colony forming in two to three weeks in triplicate at 0.6×10^6 , 0.3×10^6 and 0.15×10^6 cells per well of the 6-well plate. The lowest seeding density was chosen to inoculate a triplicate of the 4 cell lines in T25 flasks for two time points (2 and 3 weeks). Flasks were maintained as described in (2.3.13.3) for two weeks. Two weeks post-inoculation, the growth medium was aspirated from the two-week flasks and the cells gently washed once in PBS and stained with 10 mins incubation with 200 μ l 0.5% Toluidine Blue. The staining solution was then aspirated and the cells washed with 100 % Methanol (Fisher Scientific Ltd, UK) for a period of 10 mins. The cells were then gently washed twice in dH₂O and the plates inverted and allowed to air dry then photographed using a cold light illuminator (Kodak, London, UK) and a camera. A similar procedure was applied to the three-week flasks.

2.3.22 Microarray analysis of the effects of JCV LT on full transcriptome

2.3.22.1 RNA extraction

Total RNA was purified from the 4-cell lines in preparation for a gene expression profiling experiment to study the effects of LT expression in E6/E7 immortalised cell lines. Purification of samples was performed using the RNeasy Mini Kit according to the manufacturer's instructions (Qiagen, West Sussex, UK). At 80% confluency, cells were

harvested, counted and cell pellets of 1.5×10^6 cells used to extract RNA. Cells were disrupted and lysed with 350 μ l buffer containing guanidinium-isothiocyanate (RLT) the mixture centrifuged at maximum speed (20,000 x g; 14,000 rpm) and the supernatant decanted. One volume of 70% ethanol was added to the supernatant, and this mixed thoroughly before applying to the RNeasy mini spin column. Columns were centrifuged for 20 secs at 9000 x g and the flow through discarded. Wash buffer, RW1, (700 μ l) was then applied to the column, centrifuged and the flow through discarded. The column was then washed twice with RPE buffer (500 μ l), the flow through discarded and the column then dried by centrifugation for 1 min. Total RNA was eluted in 300 μ l RNase free water and centrifuged at 9000 x g for 1 min followed by quantification by spectrophotometry (Nanodrop RNA-40 program). The RNA was then stored at -80°C until further use. The following processing of the arrays was carried out by Dr. Xiaotong He and Dr. Thomas Walker.

2.3.22.2 Array processing

Affymetrix GeneChip® Human Transcriptome Array 2.0 (HTA) microarrays were processed with RNA samples of sufficient purity and yield according to the manufacturer's protocol (Affymetrix, Santa Clara, CA, USA). Briefly, arrays were hybridised in a GeneChip® Hybridization Oven 645, washed and stained on GeneChip® Fluidics Station 450 then scanned with a GeneChip® Scanner 3000 7G. Six arrays were probed with RNA extracted from: Parent; Vector 1; Vector 2; M3; M6; LT1.

2.3.22.3 Affymetrix expression console (AEC)

Array .CEL files were subject to quality assurance in AEC (Affymetrix, Santa Clara, CA, USA). Robust Multi-array Average- sketch (RMA-sketch) gene normalisation and signal summarization method was used to generate .CHP files for the six arrays and these were assessed by standard means. Additional quality control was assessed within Qlucore Omics Explorer (QOE) 3.1 64 bit (Qlucore, Lund, Sweden).

2.3.22.4 Statistical analysis and data filtration

Gene expression analysis was conducted by a principal component analysis (PCA) approach in QOE 3.1 64 bit (Qlucore, Lund, Sweden). The array data were imported and normalised by RMA-sketch. Variable annotations were downloaded within QOE and parsed onto variables. Sample annotations were applied for JCV LT integration (negative for Parent; Vector 1; Vector 2, positive for M3; M6; LT1); and vimentin clonality (negative for parent, LT1; positive for M3; M6; Vector 1; Vector 2). Variables were collapsed by max value of Entrez ID and these were selected for the Variables Identifier.

2.3.22.5 Pathway analysis

Variable lists exported from QOE were transposed and uploaded into Ingenuity Pathway Analysis (IPA) (Qiagen, Limburg, Netherlands) using Affymetrix probe code as “ID” and corresponding ratio, p value, and q values. Linear ratio values were transposed into symmetrical log values (e.g 2=2; 0.5 =-2). Core Analyses were conducted on variable lists with a parsing confidence set at ‘Experimentally observed’; remaining analytical preferences were standard. Statistically significant changes for pathways, upstream regulators, and IPA networks were assessed by p value overlap of array data with the Ingenuity Knowledge Base (IKB) and activation Z scores.

CHAPTER 3

RESULTS

3. Results

3.1 PCR screening of Polyomaviruses in cervical cancer

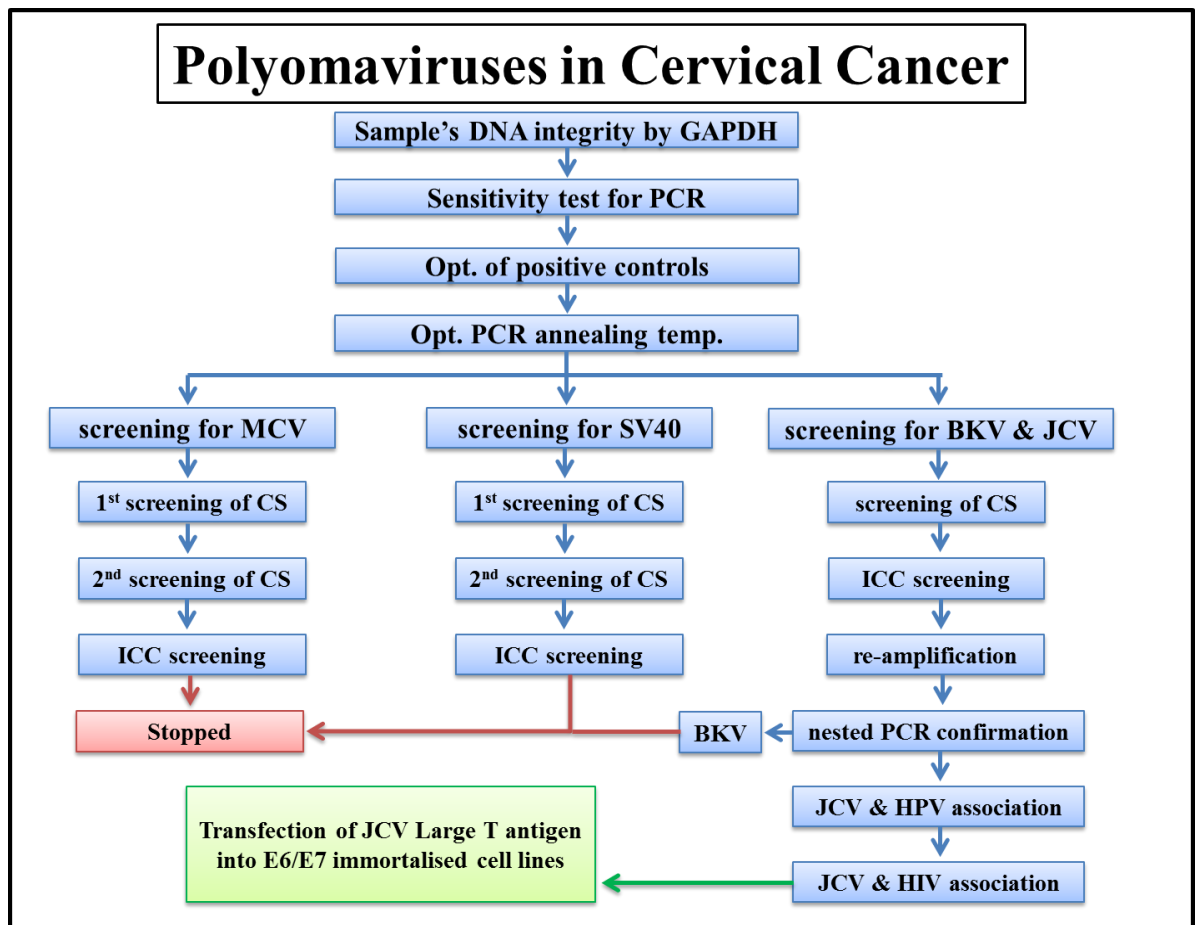


Diagram 3.1 A summary of PCR screening of 220 cervical smear samples and 77 cervical cancer tissue samples for MCV, SV40, and BKV. Only JCV was detected and was further investigated.

3.1.1 Verification of sample's DNA integrity by GAPDH

All samples were PCR amplified with housekeeping gene primers (GAPDH) in order to confirm DNA integrity using singleplex end point PCR (See table 2.2 for PCR conditions).

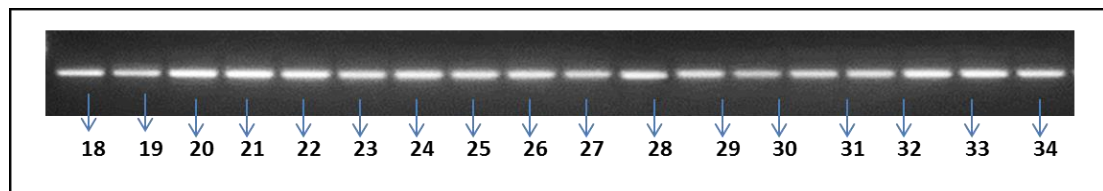


Figure 3.1 Agarose gel (1.5%) electrophoresis of the 130 bp GAPDH housekeeping gene PCR products.

Figure 3.1 illustrates a representative GAPDH housekeeping gene analyses performed on DNA extracted from 220 cervical smears and 77 cervical carcinoma (see Figure 5.3.1, 5.3.2 and 5.3.3 in Appendix 5.3.1) showing a 130 bp amplicon product which was consistent with the expected GAPDH product size (see Table 5.2.1). The signal intensities observed were used to evaluate template quality and to balance template input.

3.1.2 Optimisation of primers involved in the study

More than 14 primer combinations (listed in Table 5.2.5 in appendix 5.2) were designed to amplify the LT gene in all tested polyomaviruses. Critical parameters which may affect efficiency and/or specificity of PCR amplification such as the optimal length of PCR primer, GC content, and the optimal melting temperature were considered during primer design (section 2.1.9). The possibility of designing consensus primers was also considered. Two out of the 14 primers were consensus primers, SVBKJC primer was designed to allow amplification of SV40, BKV, and JCV together and PYV was designed to amplify BKV and JCV (primers are listed in Table 5.2.1 in appendix 5.2).

PCR optimisation and considerations were carried out in order to choose primer combinations of the highest sensitivity, specificity and reproducibility (described in the following sections). Post amplification, several attempts were made to identify any other reaction conditions that may have affected the reaction. All primer combinations that failed

to avoid mis-priming and non-specific amplification caused by primer dimer were excluded from the study.

3.1.3 Optimisation of positive controls

The aim of this experiment was to carry out test amplifications for (JCV/BKV, SV40, MCV) positive controls using a singleplex PCR. All positive controls were tested alongside a negative control (dH₂O).

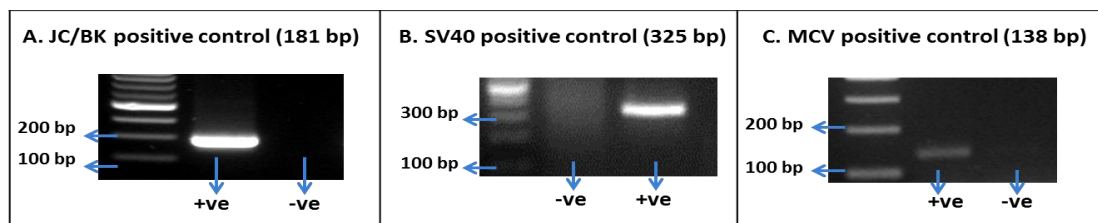


Figure 3.2 Agarose gel (1.5%) electrophoresis of PCR products from (A): JCV positive control (181 bp). (B): SV40 positive control (325 bp). (C) MCV (138 bp). dH₂O was the negative control used.

Optimisation was carried out in order to determine the sizes of expected amplicon of DNA from positive controls for all viruses tested. The common JCV/BKV target produced a strong signal of the correct amplicon size of 181 bp. Analysis of the SV40 positive control showed a strong signal of the correct amplicon size of 325 bp whereas the MCV positive control produced a weaker signal at the expected size of 138 bp. These results confirmed the qualitative nature of the signals but did not provide any measure of sensitivity or selectivity since genomic DNA template was not present.

3.1.4 Optimising PCR annealing temperatures in the presence of genomic DNA

The aim of this experiment was to optimise the annealing temperatures used to amplify MCV, SV40, and BKV/JCV PCR products and to evaluate selectivity when genomic DNA was included in the PCR reaction. Amplification was carried out at four different annealing temperatures in order to optimise performance and plasmid containing positive controls were tested alongside genomic DNA from three randomly selected patient samples (labelled as 1, 2, and 3). In all tests, dH₂O was used as a negative control.

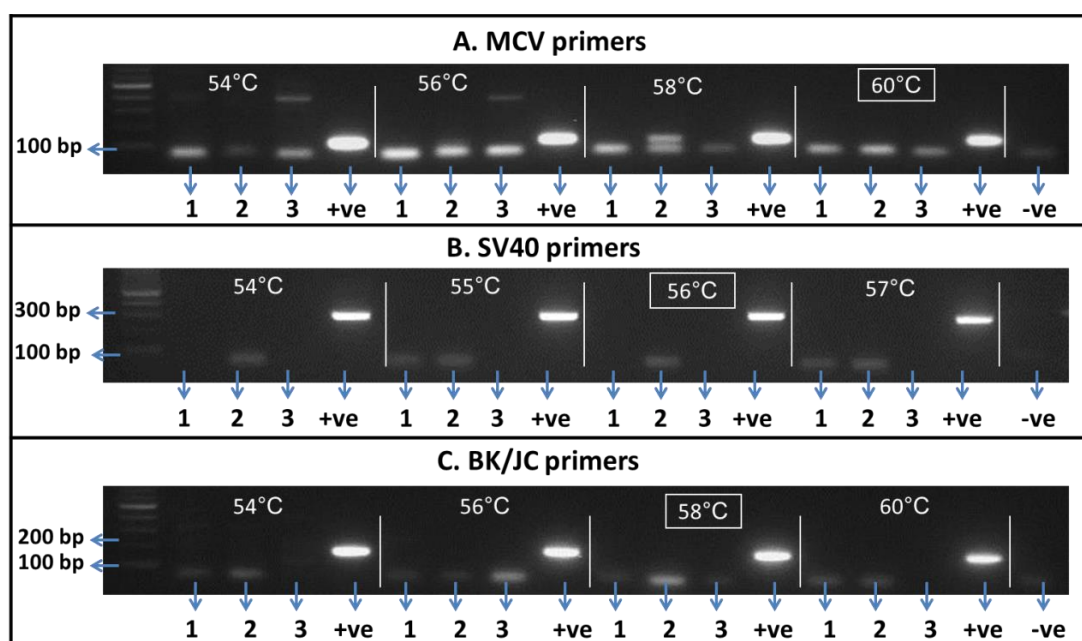


Figure 3.3 Agarose gel (1.5%) electrophoresis of PCR products from (A): MCV conducted at annealing temperatures of 54°C, 56°C, 58°C & 60°C (138 bp Amplicon). (B): SV40 conducted at annealing temperatures of 54°C, 55°C, 56°C & 57°C (325 bp Amplicon) (C): BK/JC conducted at annealing temperatures of 54°C, 56°C, 58°C, & 60°C (181 bp Amplicon). dH₂O was used as a negative control.

For the MCV amplification, non-specific signals could be seen in some genomic DNAs when annealing was carried out at 54°C and 56°C which indicated that the optimum annealing temperature was 58°C or higher. Just by chance, sample 2 showed a potentially

positive signal of the correct amplicon size at 58°C although this was later shown not to be genuine. In view of the identified selectivity issues, a temperature of 60°C was eventually used since formation of primer dimers appeared to be less pronounced.

For SV40 amplification, although there was evidence of some limited primer dimer formation, the range of annealing temperatures tested did not appear to influence the selectivity therefore 56°C was chosen as the optimum annealing temperature for subsequent analysis.

For BK/JC amplification a gradual improvement in selectivity was observed with increasing temperature. At 54°C there was some evidence of non-specific amplification products which disappeared at 56°C and above, therefore that latter was chosen for subsequent analysis.

3.1.5 Sensitivity of polyomavirus detection by PCR

In order to determine the sensitivity of the previously described PCR methods, serial dilutions were used in order to determine the lowest input copy number of a plasmid encoded template which was detectable using this method.

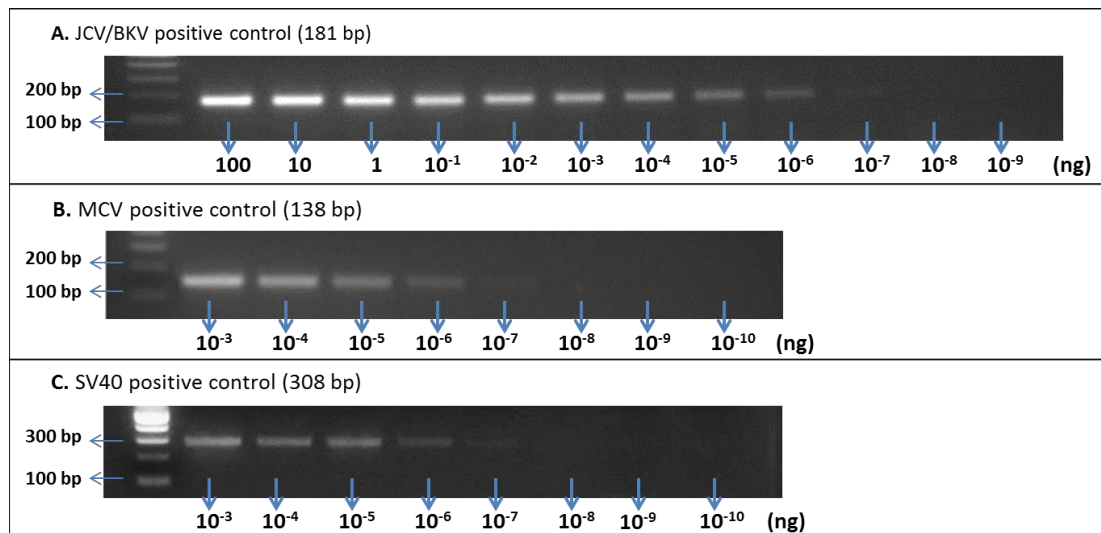


Figure 3.4 Agarose gel electrophoresis (1.5%) of PCR products produced from serial dilutions of input plasmid templates from: (A) JCV/BKV (B) MCV (C) SV40.

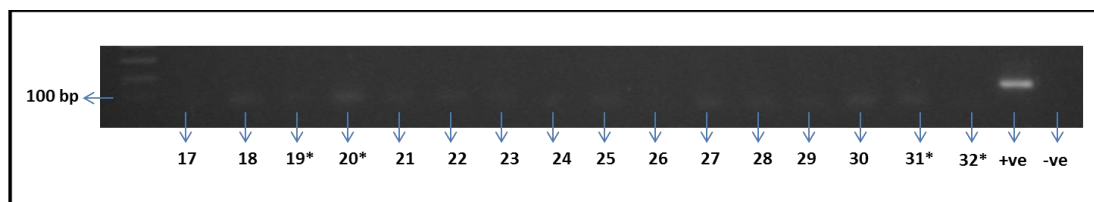
Figure 3.4 shows that the limit of detection was 10^{-7} ng of plasmid DNA for all three of the virus amplimers tested, and the negative control (dH_2O) showed no signal establishing absence of contamination. The 10^{-7} ng sensitivity limit of the assay was calculated to be equivalent to an input of 18 copies of the JC/BK LT ORF (2067 bp) per reaction, 16 copies of the SV40 LT ORF (2124 bp) per reaction, and 11 copies of the MCV LT ORF (2458 bp) per reaction.

3.1.6 Sample Population

The study population used was a sample bank of 220 cervical smears consisting of 105 HIV positive and 115 HIV negative Kenyan women. A total of 77 tissue biopsies were also available from 77 women with ICC of which 37 were from HIV positive and 40 from HIV negative patients.

3.1.7 Screening of cervical samples for MCV

Screening for MCV was carried out on genomic DNA extracted from the 220 cervical smears and 77 ICC's and each assay was performed in duplicate (Figure 5.2.1, Appendix 5.2, illustrates the primer binding sites on the Merkel cell polyomavirus LT sequence). Reduction in the formation of primer dimers was accomplished by using HotStarTaq PCR and an equivalent of 20 copies of MCV LT encoding plasmid was used as a positive control.



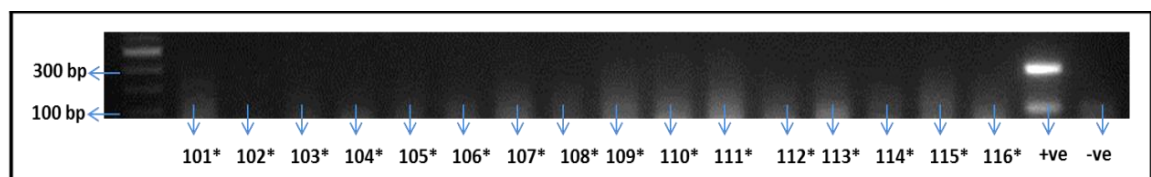
Note: HIV positive samples are marked with (*).

Figure 3.5 A representative example of agarose gel (1.5%) electrophoresis of PCR products from MCV amplification. All 220 cervical smear samples tested were negative for the MCV 139 bp amplicon. MCV LT plasmid was used as the positive control and dH₂O was used as a negative control.

Figure 3.5 is a representative example of the MCV detection analyses performed on 220 cervical smears' samples (Figure 5.3.4 & 5.3.5, Appendix 5.3). Potential positive signals were observed for samples 86, 124 and 139 which showed very faint signals (Figure 5.3.4, Appendix 5.3) although these could not be amplified from gel purified products indicating they were false positives. Since no evidence of MCV detection using singleplex PCR was observed, additional primers located on the MCV LT were designed for use in multiplex PCR analysis (Figure 5.2.1).

3.1.7.1 Screening of cervical smears by multiplex PCR.

DNA extracted from 220 cervical smears was tested for the presence of MCV LT by multiplex PCR. The second set of PCR primers (MCV2 primers) produced an amplicon product of 309 bp which was clearly distinguishable from that produced by the first set of MCV primers (139 bp) which were included in the one multiplex reaction.



Note: HIV positive samples are marked with (*).

Figure 3.6 A representative example of agarose gel (1.5%) electrophoresis of MCV multiplex PCR products produced from genomic DNA extracted from cervical smears obtained from HIV positive women. The predicted amplicons of 309 bp and 139 bp were clearly visible in the positive control (20 copies of template). All samples screened were negative for MCV irrespective of HIV status (Figures 5.3.6 & 5.3.7, Appendix 5.3) dH₂O was used as a negative control.

Figure 3.6 is a representative example of the multiplex PCR method which was developed to detect two separate loci on the MCV LT gene. The analyses on all 220 cervical smears can be seen in Figures 5.3.6 & 5.3.7, Appendix 5.3. Where there was evidence of potential positive signals (Samples 123, 126 & 150, Appendix 5.3) these were gel purified and the PCR repeated. However, no reproducible MCV signals were detected for each of the amplicons in any of the cervical smear samples tested.

3.1.7.2 Screening of ICCs for MCV by singleplex PCR

DNA extracted from 77 ICC samples (40 HIV-positive, 37 HIV-negative) were screened for the presence of MCV using singleplex amplification of the 309bp amplicon (The full data set is shown in Figure 5.3.8, Appendix 5.3).

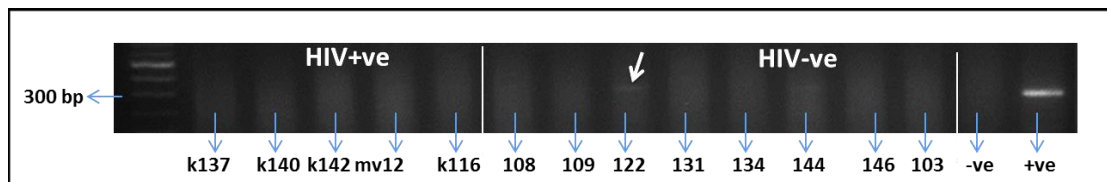


Figure 3.7 A representative example of agarose gel (1.5%) electrophoresis of PCR products obtained for MCV LT in genomic DNAs obtained from ICC's from HIV positive and HIV negative women. The very faint arrowed signal in sample 122 is an example of a potential positive which could not be re-amplified. Twenty copies of plasmid template MCV LT was used as a positive control and dH₂O was used as a negative control.

The full data set of MCV detection in all 77 ICC samples is shown in Figure 5.3.8, Appendix 5.3. Potential positive signals were observed in samples 122 & 156 although neither of these could be re-amplified (Illustrated in Figure 5.3.8 in Appendix 5.3). Therefore, it was concluded that MCV was not present in any of the 77 ICCs irrespective of HIV status.

3.1.8 Screening of samples for SV40

DNA from the 220 cervical smears was screened for detection of the SV40 LT gene by PCR. Figure 5.2.2 in the appendix 5.2 illustrates the primer binding sites on the SV40 LT gene.

3.1.8.1 Screening of cervical smears for SV40

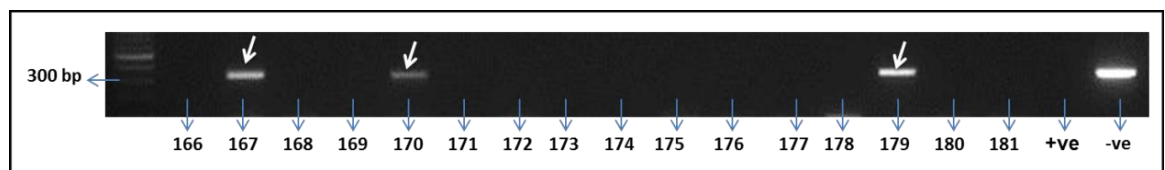


Figure 3.8 A representative example of agarose gel (1.5%) electrophoresis of PCR products obtained from singleplex amplification of an SV40 LT amplimer from genomic DNA extracted from cervical smears. The predicted size of the amplimer was 325 bp. Most of the samples were negative for SV40 except for samples 7, 49, 167, 170 & 179 (see Figure 5.3.9 and 5.3.10 in Appendix 5.3).

Figure 3.8 is representative of the first SV40 LT analyses performed on all 220 cervical smear samples (Figures 5.3.9 & 5.3.10, Appendix 5.3). Although the potential positives (7, 49, 167, 170 and 179) showed a strong signal, further attempts to re-amplify the signal proved unsuccessful. In light of this discrepancy, all samples were analysed again which confirmed no signal was present in any sample tested. A second screening with different primers (SV2) also concluded that SV40 was not present in any of the samples (The full data set is shown in Figure 5.3.11 & 5.3.12, Appendix 5.3).

3.1.8.2 Screening of ICCs for SV40

As previously described for MCV, DNA from 77 ICCs were screened for the presence of SV40 as shown in Figure 5.3.13, Appendix 5.3.

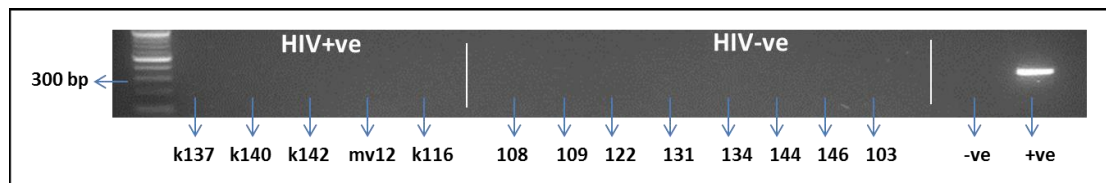


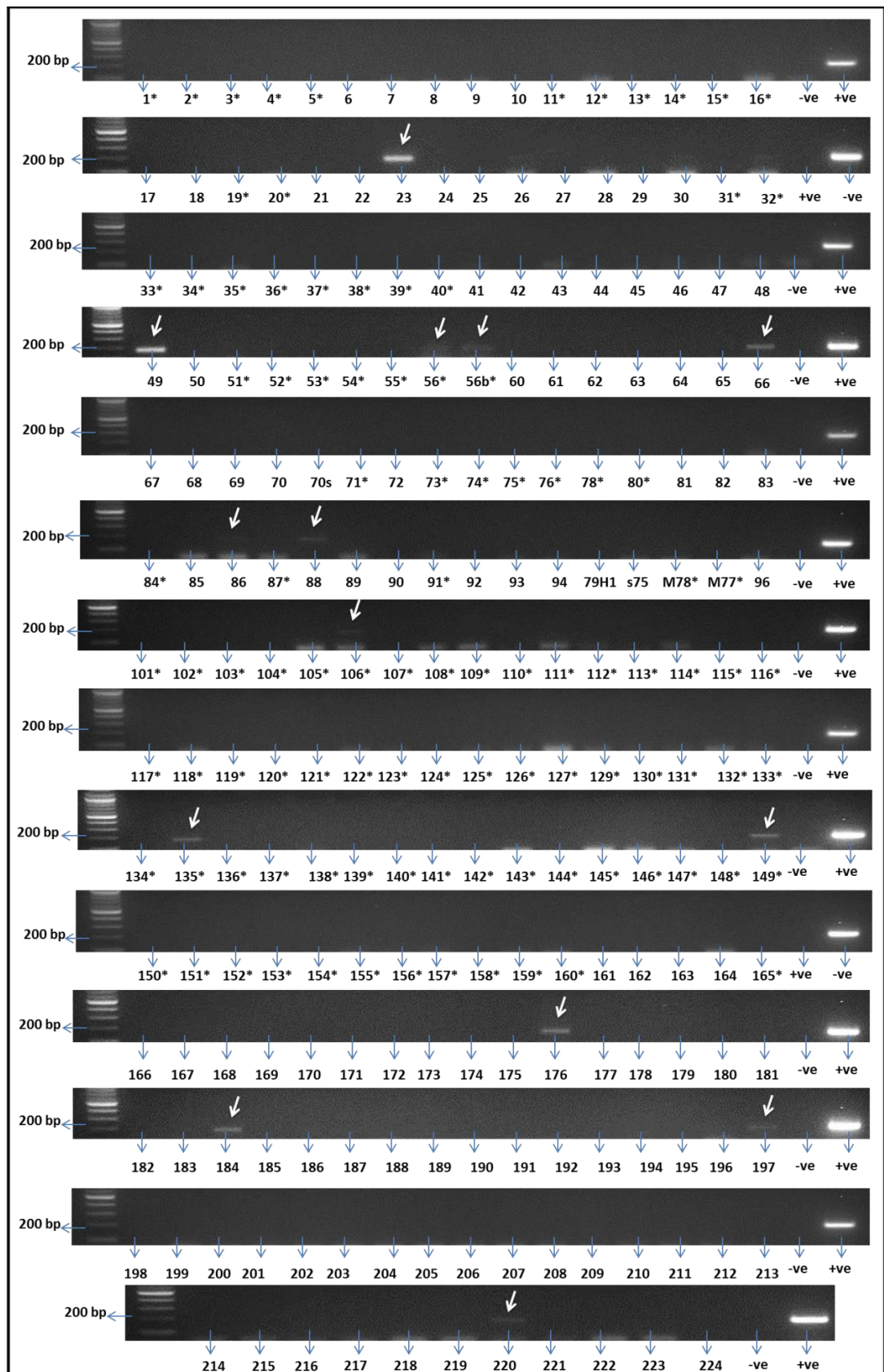
Figure 3.9 Representative example of agarose gel (1.5%) electrophoresis of PCR products obtained from singleplex amplification of an SV40 LT amplicon from genomic DNA extracted from HIV positive and HIV negative ICCs (Figure 5.3.13, Appendix 5.3.). The predicted size of the positive control (20 copies of plasmid) was 308 bp and dH₂O was used as the negative control.

Results of the SV40 analyses performed for all 77 cervical carcinoma samples are shown in Figure 5.3.13, Appendix 5.3. Since the positive controls showed the predicted amplicon size and the negative no signal, it was concluded that none of the ICCs had any evidence of infection with SV40 irrespective of HIV status.

3.1.9 PCR screening for BKV and JCV

Screening for BKV and JCV was carried using the same sample set used for MCV and SV40. Universal BKV/JCV consensus primers (Table 5.2.1 in appendix 5.2) were designed which amplify a common BK and JC virus amplicon. Any positive samples were subsequently reamplified using virus-specific (JCV or BKV) nested PCR. Sequence alignment of the BKV and JCV LT sequences in Figure 5.2.3 illustrates the primer binding sites. All work described in BKV/JCV sections has been published (see Appendix 5.4).

3.1.9.1 Screening of cervical smears for JCV and BKV



Note: HIV positive samples are marked with (*).

Figure 3.10 Agarose gel (1.5%) electrophoresis of PCR products amplified with JCV/BKV consensus primers (Table 5.2.1 in appendix 5.2) from DNA extracted from 116 cervical smears. Fourteen samples (arrowed): 23, 49, 56, 56b, 66, 86, 88, 106, 135, 149, 176, 184, 197 & 220 showed an amplicon of the correct size (181 bp) and the negative control was dH₂O.

Figure 3.10 shows that 14 samples were potentially positive for BKV or JCV. Further confirmation was carried out by reamplification and distinction between JCV and BKV was carried by the use of nested PCR (Section 3.1.7.3).

3.1.9.2 Screening of ICC samples for BKV and JCV

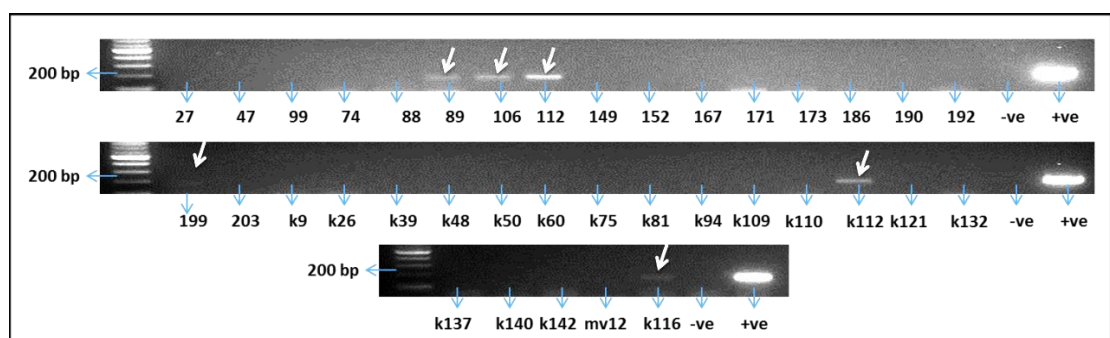


Figure 3.11 Agarose gel (1.5%) electrophoresis of PCR products amplified with JCV/BKV consensus primers (Table 5.2.1 in appendix 5.2) from DNA extracted from 40 HIV positive ICCs. Six samples: 89, 106, 112, 199, k112 & k116 were positive for an amplicon of the correct size (181 bp) and the negative control was dH₂O.

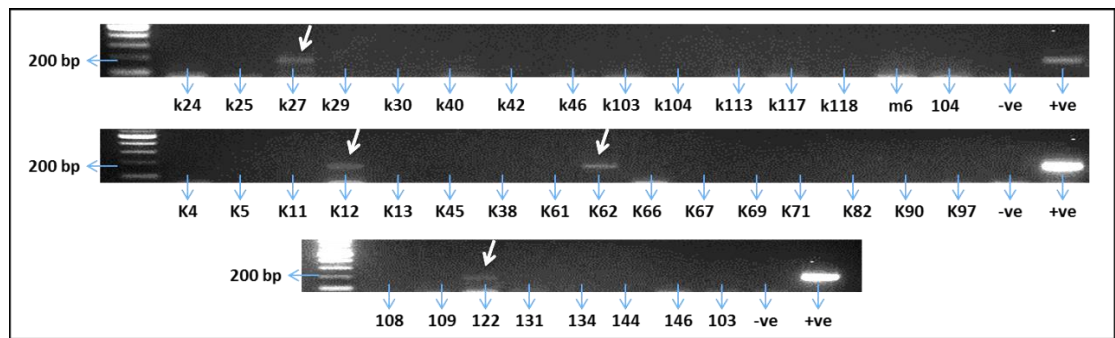
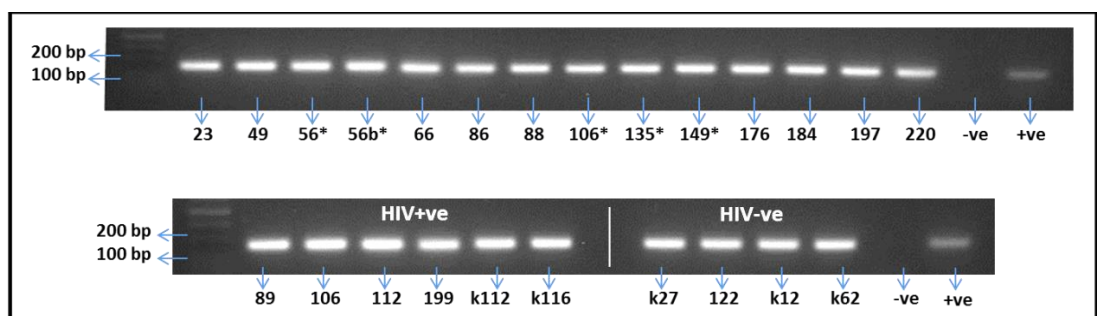


Figure 3.12 Agarose gel (1.5%) electrophoresis of PCR products amplified with JCV/BKV consensus primers (Table 5.2.1 in appendix 5.2) from DNA extracted from 37 HIV negative ICCs. Four samples: (k27, k12, k62 and 122) were positive for an amplicon of the correct size (181 bp) and the negative control was dH₂O.

Figure 3.11 & 3.12 show amplification of the BKV/JCV consensus amplicon in 10 samples. Further confirmation of these signals was carried out by re-amplification and distinction between JCV and BKV was carried out by nested PCR (Section 3.1.7.3).

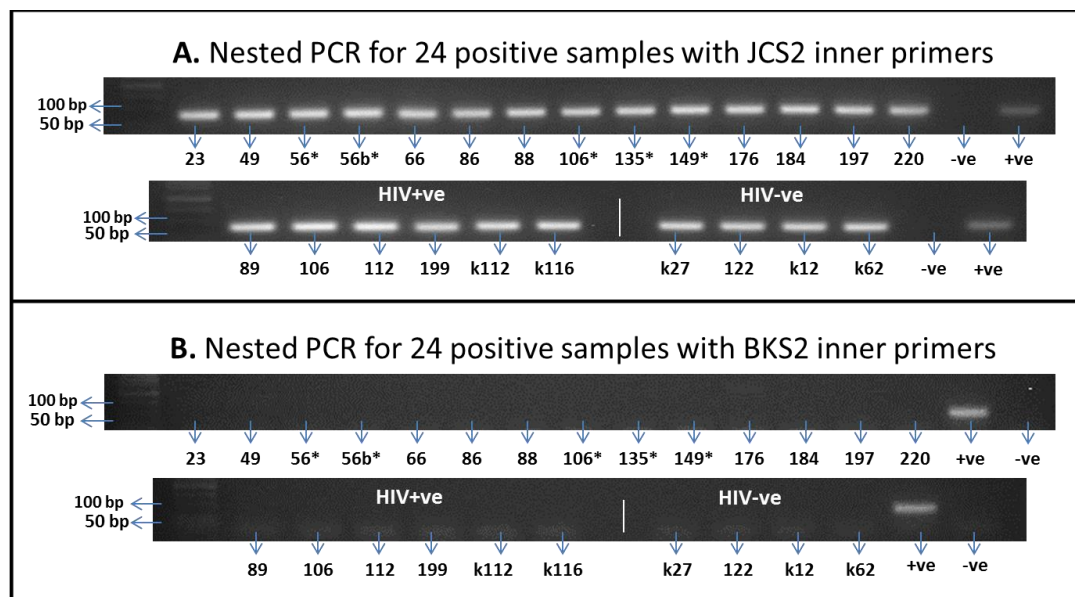
3.1.9.3 Reamplification of JCV/BKV positives and distinction between nested JCV and BKV amplification products



Note: HIV positive samples are marked with (*).

Figure 3.13 Agarose gel (1.5%) electrophoresis of re-amplification products obtained for all samples with a positive JCV/BKV amplicon signal (181 bp) from DNA isolated from cervical smears and carcinomas.

Figure 3.13 shows that 14 out of the 220 cervical smear samples and 10 out of the 77 ICCs demonstrated re-amplification of signals accounting for all 24 potential positives.



Note: HIV positive samples are marked with (*).

Figure 3.14 Agarose gel (1.5%) electrophoresis of nested PCR products amplified from JCV/BKV amplicon with (A): JCV-specific nested primers showing 24 positive for the predicted 77 bp JCV specific amplicon. (B): BKV-specific nested primers showing that all 24 were negative for the 75 bp BKV specific amplicon (See Figure 5.2.3, appendix 5.2 for primers binding sites).

These data indicate that JCV DNA was present in all 24 samples (Figure 3.15A), whereas none were positive for BKV (B).

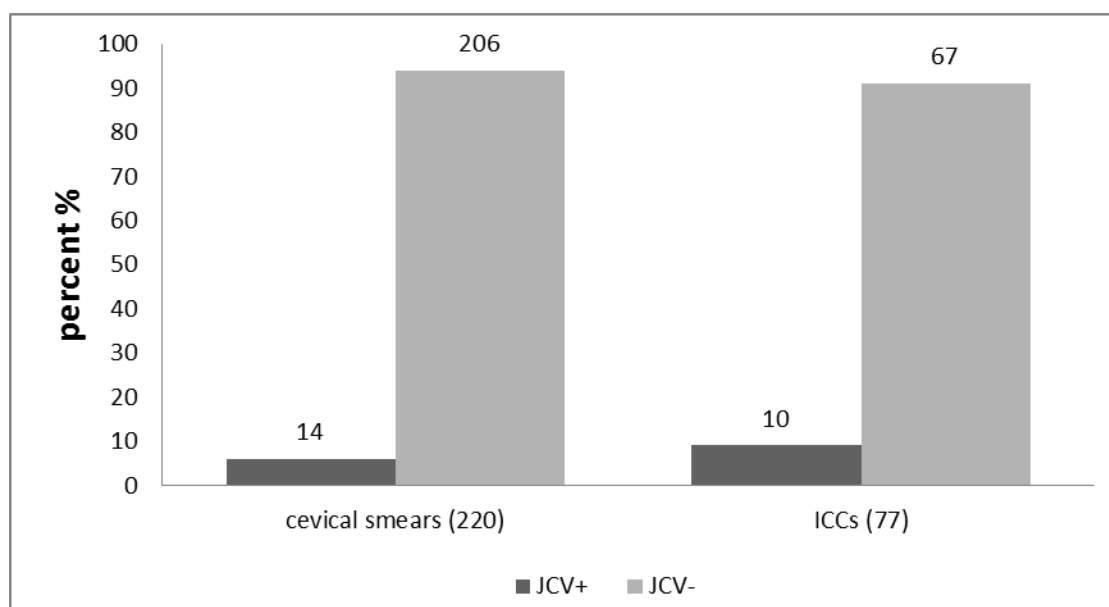


Figure 3.15 Analysis of the overall percentage of JCV DNA in cervical specimens. The frequency of JCV infection in cervical smears and carcinomas was not significantly different (p -value $0.3566 > 0.05$).

Figure 3.16 illustrates the overall prevalence of 8% (24/297) JCV/BKV DNA in cervical specimens which were all shown to be exclusively JCV. For cervical smears JCV DNA was found in 6% (14/220) whereas for carcinomas JCV was found in 12% (10/77) although this was not significantly different ($P > 0.05$) as illustrated in the table below.

Table 3.1. The overall prevalence of JCV DNA in cervical specimens

	JCV+	JCV-	Total
Cervical smears	14 (6%)	206 (94%)	220
Cervical Carcinomas	10 (12%)	67(88%)	77
Total	24	273	297

p -value $0.3566 > 0.05$ (statistically not significant)

3.1.9.4 Analysis of potential association between JCV and HPV16/18 infection

The cervical smears and cervical carcinoma samples used in this study have been previously analysed for the presence of various HPV types using Papillocheck HPV genotyping and dual locus multiplex PCRs respectively as described in Maranga et al. (2012). The data from this earlier study was used to stratify with respect to the current JCV prevalence and HPV16/18 positivity, and the results are shown in Table 3.2. Within the HPV16/18 positive subset, JCV DNA was detected in 3% (5/206) of the cervical smears, and in 6% (4/67) of the ICCs. By contrast, JCV DNA was amplified in 5% (9/206) of cervical smears, and 9% (6/67) of the ICCs within the HPV16/18 negative subset (Table 3.1).

Table 3.2 Analyses of the association between JCV and HPV16/18 infections

Infections	CS		<i>p</i> -value	ICC		<i>p</i> -value
	HPV16/18+	HPV16/18-		HPV16/18+	HPV16/18-	
JCV+	5	9	0.1253	4	6	0.2794
JCV-	117	89	> 0.05	39	28	> 0.05

CS, cervical smears; ICC, invasive cervical carcinomas. (Statistically not significant)

Although all cervical smears and ICCs which were positive for JCV were also positive for a “high-risk” oncogenic HPV type, analyses of these data showed that there was no significant association between JCV and HPV16/18 in any group ($p > 0.05$) either in cervical smears group ($p = 0.1253$) or ICC group ($p = 0.2794$).

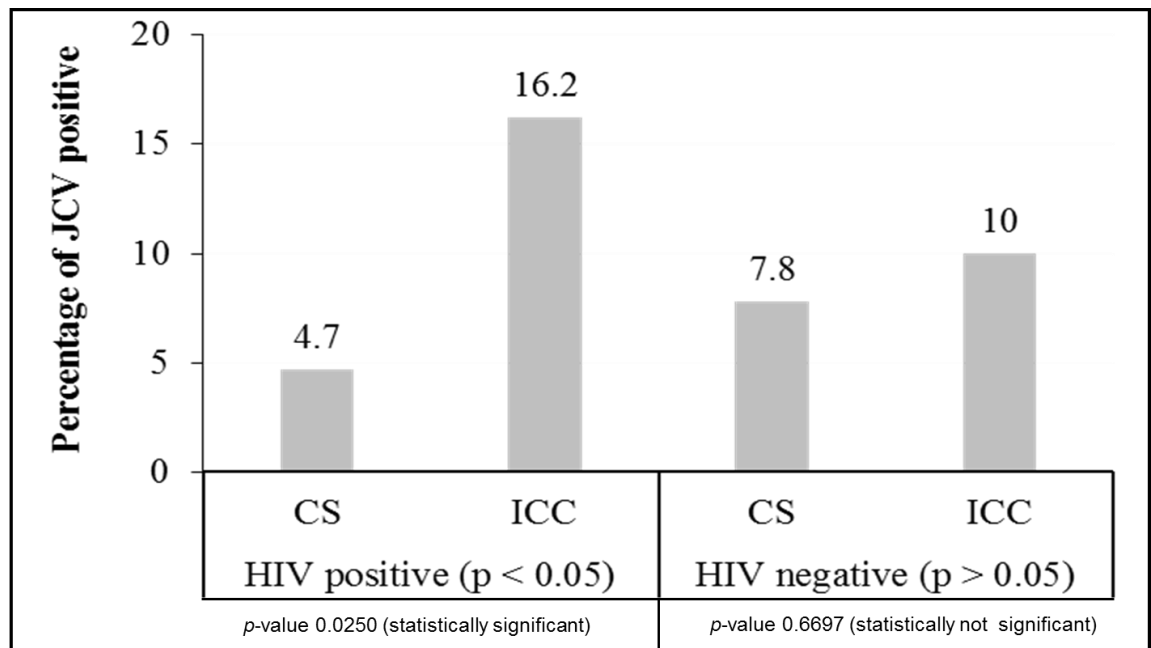
3.1.9.5 The association between JCV and HIV Infection

Since the HIV status of the women used in this study was also previously reported (Maranga et al., 2012) the samples were stratified by HIV status and the number of JCV positives was compared in cervical smears and carcinomas. Within the HIV positive group, JCV DNA was detected in 4.7% (5/105) of cervical smears and in 16.2% (6/37) of ICCs. By contrast, JCV DNA was amplified in 7.8% (9/115) of the cervical smears and in 10% (4/40) of ICCs within the HIV negative group as demonstrated in Table 3.3 and Figure 3.17.

Table 3.3 Analyses of the association between JCV and HIV infections

HIV+ve group	JCV+	JCV-	Total
Cervical smears	5 (4.7%) *	100 (95.3%)	105
ICC	6 (16.2%) *	31 (83.8%)	37
Total	11	131	142
<i>p</i> -value 0.0250 < 0.05 (statistically significant)			
HIV-ve group	JCV+	JCV-	Total
Cervical smears	9 (7.8%)	106 (92.2%)	115
ICC	4 (10%)	36 (90%)	40
Total	13	142	155
<i>p</i> -value 0.6697 > 0.05 (not statistically significant)			

(*): 3-fold increase in HIV+ve women with ICC compared to smears.



CS, cervical smears ; ICC, invasive cervical carcinomas.

Figure 3.16 Analysis of the association between JCV and HIV infection. The frequency of JCV infection in cervical carcinomas was significantly higher in HIV positive ICCs than that in any of the other groups tested irrespective of HIV status ($P < 0.05$).

These data show the potential association between JCV and HIV infection in ICCs. For HIV negative women, JCV DNA was detected in 7.8% of the cervical smears and in 10% of ICCs which was not statistically significant ($p > 0.05$). However, for HIV positive women, JCV DNA was detected in 4.7% of the cervical smears and in 16.2% of ICCs which is significant ($p = 0.025$) and suggests there may be an association between JCV and cervical carcinoma in HIV positive women.

Table 3.4 Summary of the potential association between JCV, HIV and HPV16/18

	ID	Type	JCV	HIV	HPV
1	23	Smear	+	-	18
2	49	Smear	+	-	-
3	56	Smear	+	+	-
4	56b	Smear	+	+	-
5	66	Smear	+	-	-
6	86	Smear	+	-	-
7	88	Smear	+	-	-
8	106	Smear	+	+	18, 16
9	135	Smear	+	+	-
10	149	Smear	+	+	18
11	176	Smear	+	-	18
12	184	Smear	+	-	-
13	197	Smear	+	-	18
14	220	Smear	+	-	-
15	89	Tissue	+	+	-
16	106	Tissue	+	+	16
17	112	Tissue	+	+	-
18	199	Tissue	+	+	-
19	k112	Tissue	+	+	-
20	k116	Tissue	+	+	16, 18
21	k27	Tissue	+	-	16
22	122	Tissue	+	-	18
23	k12	Tissue	+	-	-
24	k62	Tissue	+	-	-

Table 3.4 shows that 4 samples out of 24 were positive for all three viruses, 12 samples were positive for at least two viruses, and 8 samples were positive to JCV only.

3.2 WHO collaborative study results

Clinical urine samples were provided, named A, B, C, D, E and F. Sample E was a known JCV positive and was serially diluted with an equivalent matrix prior to DNA extraction with the QIAamp MinElute Virus Spin Kit (See the Methods, 2.3.3). Two sets of each sample were provided and ten-fold serial dilutions of sample E were prepared prior to DNA extraction.

3.2.1 Verification of sample DNA integrity and sensitivity by GAPDH PCR

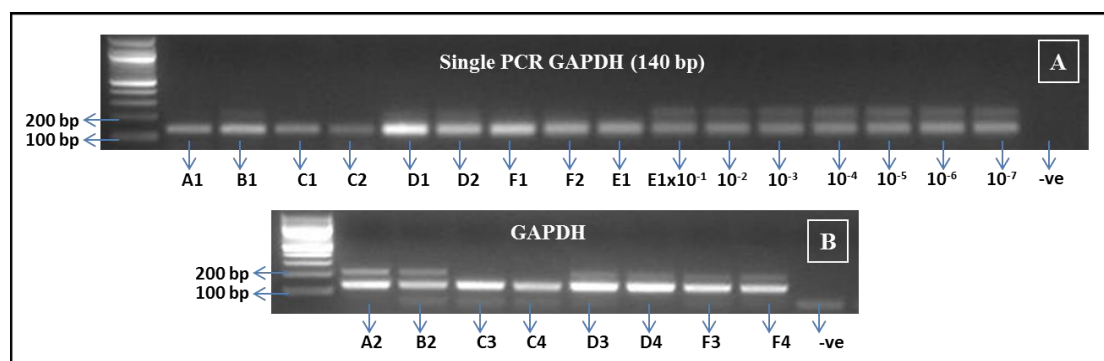


Figure 3.17 A and B Agarose gel (1.5%) electrophoresis of GAPDH PCR products using DNA were extracted from the WHO samples as a template. Sample E was the known JCV positive control and was serially diluted. dH₂O was used as the negative control.

The 140 bp signal obtained was consistent with the GAPDH amplicon product size (see Table 5.2.1 in appendix 5.2) and this was detectable in serial dilutions greater than 10⁷ ng which indicated the template quality was acceptable for subsequent analysis.

3.2.2 Determination of JC/BK viral load

In order to distinguish between JCV and BKV, the previous analysis of JCV/BKV in cervical samples (Figure 3.15 A) was carried out with nested PCR, using either JCV or

BKV specific primers and the JCV/BKV consensus amplicon product as a template. As an alternative approach, initially DNA extracted from the WHO samples was used directly as a template for the JCV specific primer set without first amplifying the JCV/BKV consensus product. Serial dilutions of sample E (down to 10^{-7} ng) were used in order to determine the lowest copy number of a JCV template detectable.

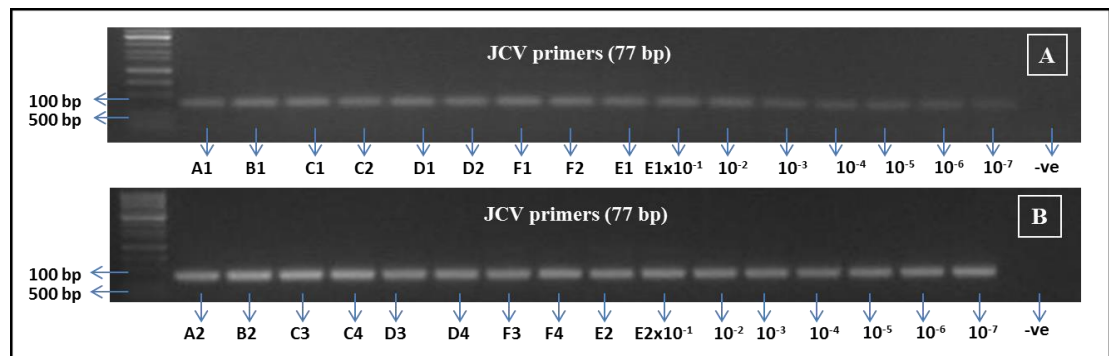


Figure 3.18 A and B Agarose gel (1.5%) electrophoresis of JCV amplification products obtained from direct amplification of the 77 bp JCV specific amplicon using WHO sample DNA as template .

Two independent assays were performed on separate days, using a fresh vial of each sample (A-F). One vial of sample A and B and two vials of sample C, D and F were used per assay. Sample E was diluted into a sample matrix (10^{-1} to 10^{-7} ng) using dH₂O as a diluent prior to DNA extraction. The results clearly show a reproducible JCV signal detection at 10^{-7} dilution.

3.2.3 Detection of JC/BK virus consensus amplicon

Amplification of the JCV/BKV consensus 181 bp amplicon from DNA extracted from the WHO samples was carried out as described previously for DNA extracted from cervical samples (see Methods, 2.2.3).

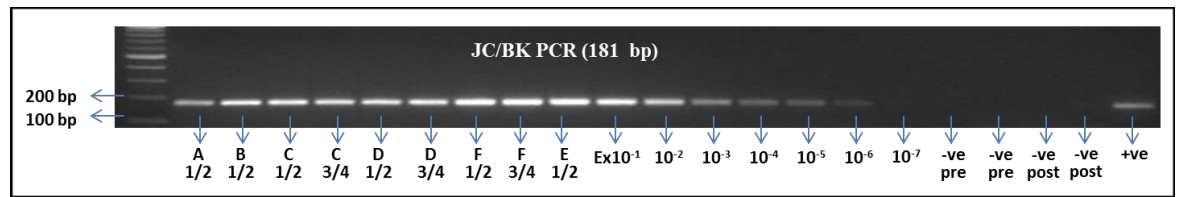


Figure 3.19 Agarose gel (1.5%) electrophoresis of PCR products amplified with JCV/BKV consensus primers (181 bp amplicon Table 5.2.1 in appendix 5.2) from WHO samples A-F. Sample E was diluted into a sample matrix (10^{-1} to 10^{-7} ng).

Figure 3.19 shows that the 181 bp JC/BK consensus amplicon was clearly detectable at dilutions down to 10^{-7} ng.

3.2.4 Detection of JC virus by Nested PCR

As previously described for the cervical DNA's, the JCV/BKV consensus product does not discriminate between these two viruses so the 181 bp amplicon product from Figure 3.20 was used for nested PCR with the JCV specific primer.

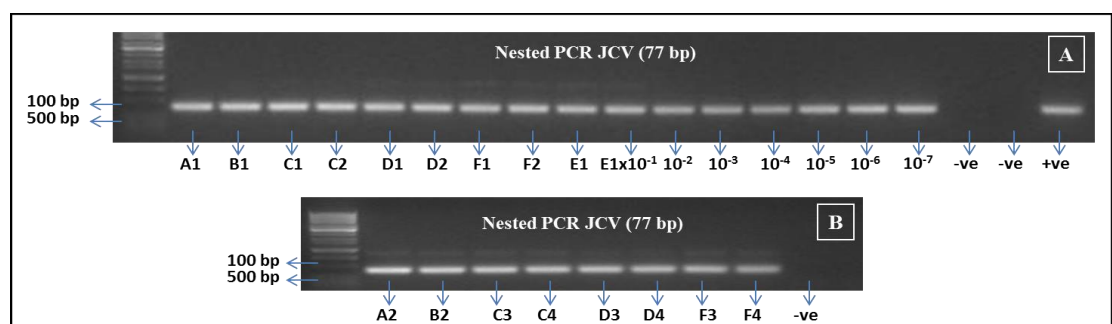


Figure 3.20 Agarose gel (1.5%) electrophoresis of PCR products produced by nested PCR with primers targeting the 77 bp JCV amplicon using the JCV/BKV consensus amplicon as template (A): one vial of sample A and B and two vials of sample C, D and F as well as sample E diluted into a sample matrix (10^{-1} to 10^{-7} ng). (B): the other vials of sample A and B and two extra vials of sample C, D and F.

These data clearly show that JCV DNA was present in all samples tested and that the lower limit of sensitivity was approximately 10^{-7} . Dilution, beyond this to 10^{-8} made the results unreliable since this will reduce the input template to <one copy per reaction.

3.2.5 Detection of BK virus by Nested PCR

The JCV/BKV consensus amplicon from Figure 3.20 was also used as a template for nested PCR with BKV specific primers which target a 75 bp amplicon.

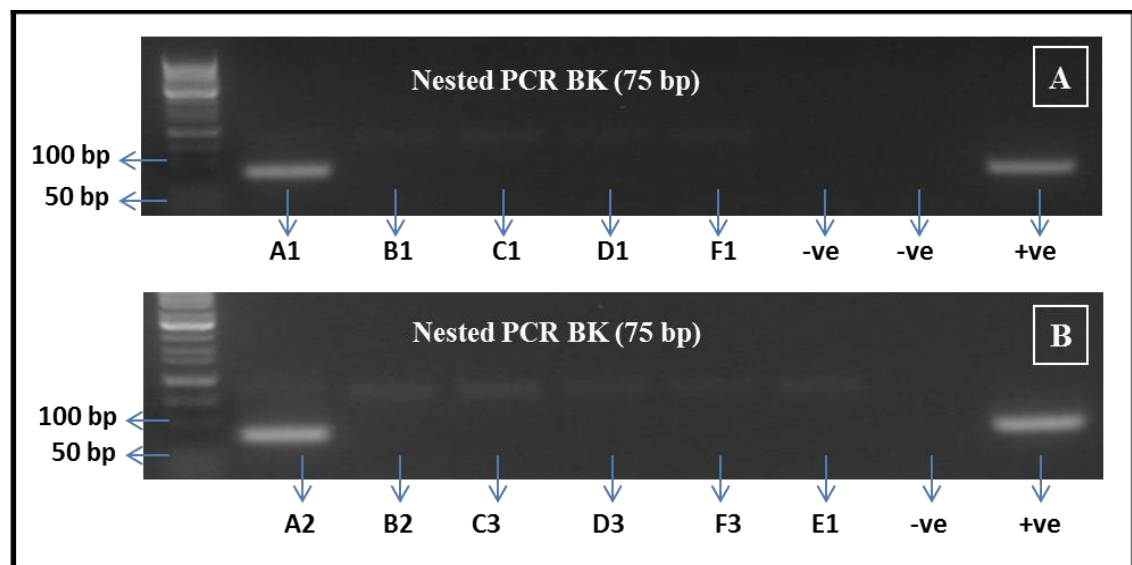


Figure 3.21 Agarose gel (1.5%) electrophoresis of nested PCR products produced by nested PCR with primers targeting the 75 bp BKV amplicon using the JCV/BKV consensus amplicon as template. (A): sample A1 and B1 and one vial of sample C1, D1 and F1 representing C2, D2, and F2. (B): the other vials of sample A, B and E as well as the other vial of sample C3, D3 and F3 representing C4, D4, and F4.

Previous results (Figures 3.19 & 3.20) indicated that JCV DNA was present in all WHO samples tested with a strong signal in both vials A1 and A2. The results shown in Figure 3.21 indicate that patient A is co-infected with both JCV and BKV. Furthermore, out of all the other laboratories who assessed these samples, the method presented herein was the only one which detected this co-infection.

3.3 Cloning of JCV LT ORF for ectopic expression studies

The observation of a statistically significantly higher prevalence of JCV DNA in HIV positive ICCs than was found in HIV positive cervical smears suggested that JCV could be participating in the development of some cases of ICC (Section 3.1.9.5). In view of these findings, it was decided to investigate the potential of the JCV LT protein (2067 bp ORF) to synergise with HPV to transform human keratinocytes *in vitro*. In order to accomplish this it was firstly necessary to clone the JCV LT ORF into a suitable expression vector.

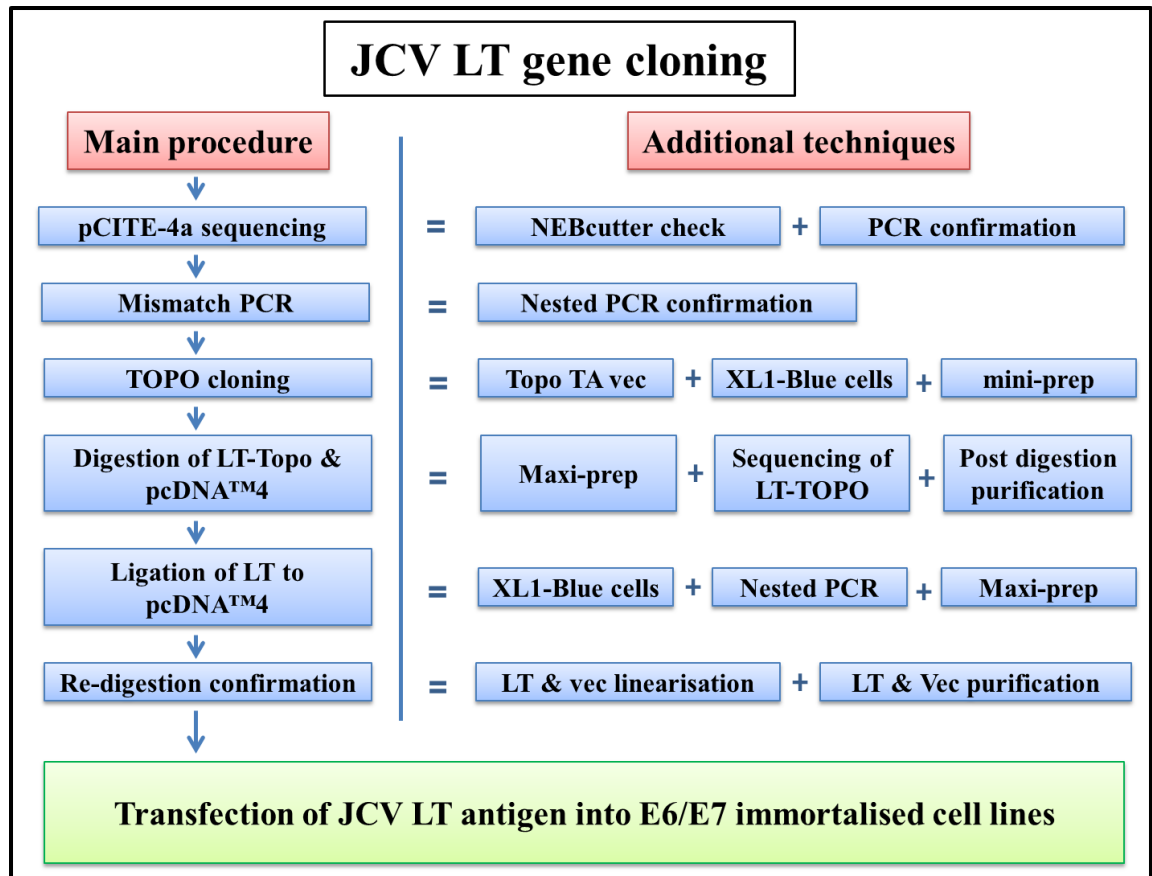


Diagram 3.2 A summary of the JCV LT ORF cloning procedure.

The aim of this sequencing was to confirm whether the JCV LT ORF had been cloned without a stop codon. Figure 3.22 shows DNA sequencing results of pCITE-4a recombinant plasmid. Nucleotide databases of NCBI software were used to compare the DNA sequencing results of the JCV LT ORF with the NCBI library using Basic Local Alignment Search Tool (BLAST). In order to use EcoR I and Xho I for excision and re-cloning, they should not be present within the JCV LT ORF (see NEBcutter in Figure 5.3.16 in Appendix 5.3). It was noted that the 3' stop codon in the pCITE-4a LT ORF had been deleted which necessitated this to be reinserted by the use of mismatch primer PCR.

3.3.2 Mismatch PCR

Mismatch PCR was carried out using the primers shown in Table 5.3.1 (Appendix 5.3) and PCR reaction conditions outlined in (2.3.2). It is noteworthy that a proofreading Taq DNA Polymerase (Roche Ltd, UK) was used to enhance fidelity.

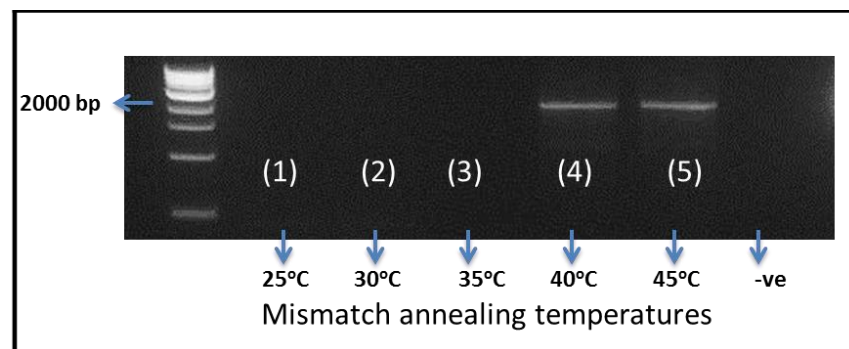


Figure 3.23 Agarose gel (1.5%) electrophoresis of LT ORF 2067 bp mismatch PCR products showing reactions conducted at different annealing temperatures (25°C, 30°C, 35°C, 40°C and 45°C).

Use of the correct annealing temperature is important in order to achieve a balance between product quantity and fidelity. Figure 3.17 shows a successful amplification of JCV

LT e in PCR tube numbers 4 and 5 at 40°C and 45°C respectively with a gradual ‘ramp-up’ step described in (2.3.2). The products were then carried forward for TOPO cloning.

3.3.2.1 Nested PCR confirmation of mismatch amplification

Nested PCR was performed using internal primers for the LT ORF (see Figure 5.2.3 in Appendix 5.2) in order to confirm the product identity and to optimise the PCR annealing temperature as shown.

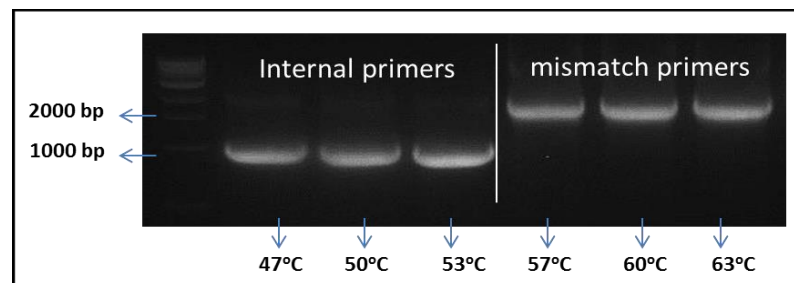


Figure 3.24 Agarose gel analysis of nested PCR products from mismatch PCR product. Internal primers were tested at three annealing temperatures 47°C, 50°C and 53°C while mismatch primers were tested at 57°C, 60°C and 63°C.

The results obtained from nested PCR showed signals at the appropriate sizes (1075 bp) for the internal primer binding sites and (2067 bp) for mismatch primers which confirmed the identity of the JCV LT ORF.

3.3.3 TOPO cloning

The stop codon modified LT ORF product was purified using a QIAquick PCR Purification Kit (see section 2.3.3) and cloned into the Topo TA vector (see vector map Figure 5.3.17 in Appendix 5.3). This was transformed into XL1-Blue competent cells (see section 2.3.5), a bacterial colony picked (see Section 2.3.6) and a mini-scale plasmid

preparation carried out (see Section 2.3.7). The cloning was successful and the results are shown in figure 5.3.19 in appendix 5.3. Eighteen colonies were picked and PCR amplification performed using vector flanking M13 Forward and reverse primers (see vector map Figure 5.3.17 in Appendix 5.3). Colonies 2 and 3 showed amplification of the modified LT ORF gene at the anticipated product size of 2067 bp (results are shown in 5.3.18 appendix 5.3). Colony number 3 was chosen for a Plasmid Mini-prep (2.3.7) and the predicted size of the LT-TOPO plasmid product was checked.

3.3.3.1 Sequencing of the LT-TOPO clone

The fidelity of the modified LT-TOPO clone was checked by Sanger sequencing in order to determine if the mismatch PCR process had reinserted the stop codon and/or introduced any mutations. The results shown in Figure 3.25 show successful reinsertion of the stop codon.

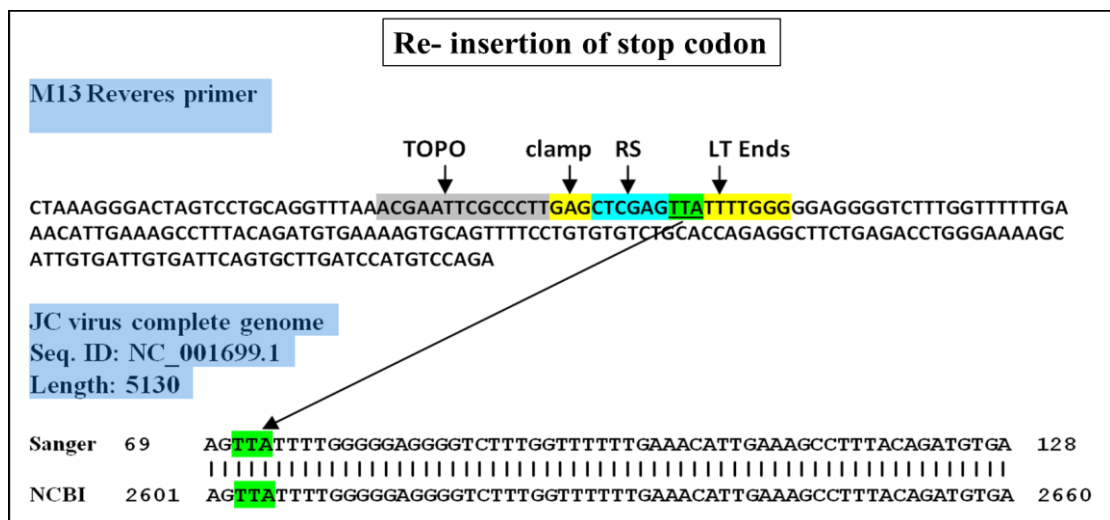


Figure 3.25 Sanger sequencing results of LT-TOPO clone showing re-insertion of stop codon that identified missing in Figure 3.17. Homology maps show the comparison of LT-TOPO clone sequence to JCV LT ORF sequence (NCBI Reference Sequence: NC_001699.1).

The fidelity of the LT-TOPO clone was confirmed, as shown in Figure 5.3.20 in appendix 5.3. Since re-insertion of the stop codon was confirmed, the LT-TOPO bacterial clone was carried forward for Plasmid Maxi-prep (2.3.8) as shown in 5.3.21 in appendix 5.3.

3.3.4 Digestion of the LT-Topo construct and target pcDNATM4 vector

Both the source LT-Topo TA and the target pcDNATM4 (Life Technologies Ltd, UK) vectors were double restriction digested with EcoR I and Xho I (see pcDNATM4 map in Figure 5.3.22 in Appendix 5.3). pcDNATM4 was chosen since it has compatible restriction sites for cloning the EcoR I and Xho I JCVLT digested product from the LT Topo construct. Furthermore, it carries the zeocin selectable marker which is suitable for use with the E6/E7 immortalised keratinocyte cell line (Zehbe et al. 2010) since these were already G418 resistant.

The results in Figure 5.3.23 in Appendix 5.3 confirm that the both plasmids had cut to completion. The restriction digest products of the LT ORF and pcDNATM4 vector were gel purified in preparation for the ligation step. The LT insert was found to be at the expected size (2067 bp) as was the digested amplicon of pcDNATM4 vector (5068 bp). The concentration of extracted DNA was deemed to be sufficient for subsequent ligation and transfection of these products.

3.3.5 Ligation of LT gene to pcDNATM4 vector

The gel purified EcoR I and Xho I digested products of LT ORF and pcDNATM4 vector were ligated and transformed into XL1-Blue competent cells (Figure 5.3.25 in

appendix 5.3). Fifteen colonies were picked and direct colony PCR was used as confirm the presence of LT insert in the target vector.

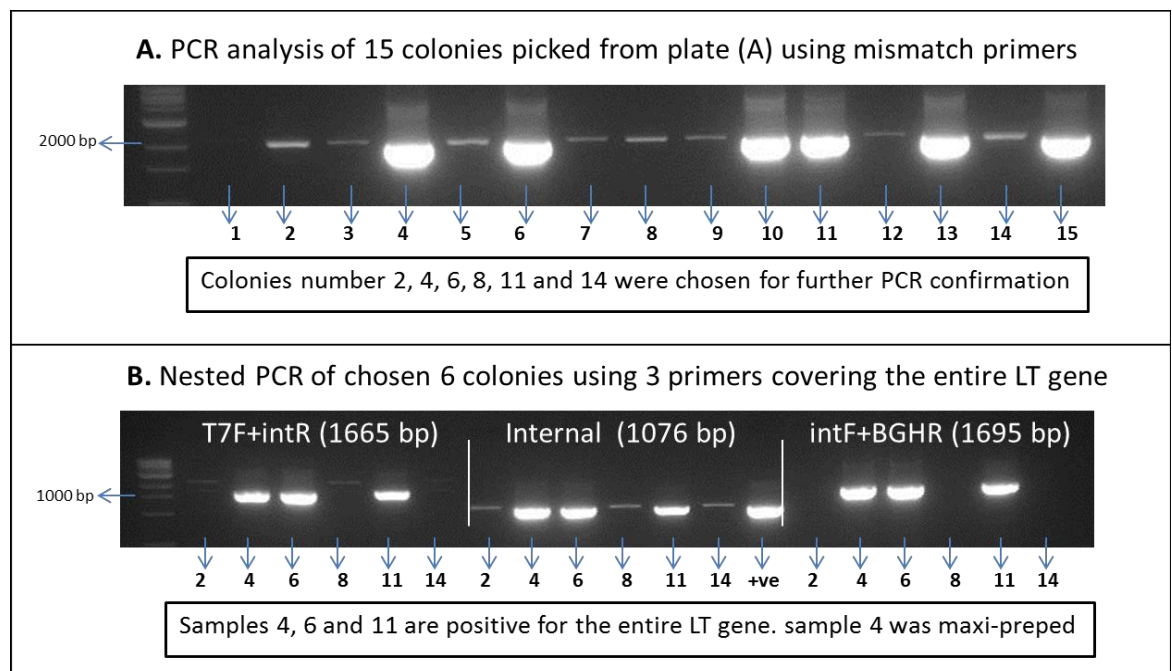


Figure 3.26 Agarose gel (1.5%) electrophoresis of colony PCR products from: (A) 16 colonies picked from the plate of bacterial transformation and the 2067 bp signal was amplified using the stop codon mismatch primers. (B) Nested PCR confirmation using three additional sets of primers.

Sample numbers 4, 6 and 11 were positive for the LT ORF and colony 4 was chosen for Plasmid Maxi-prep (Figure 5.3.26). This product digested with EcoR I and/or Xho I and Not I digestion was also used to linearise the vector.

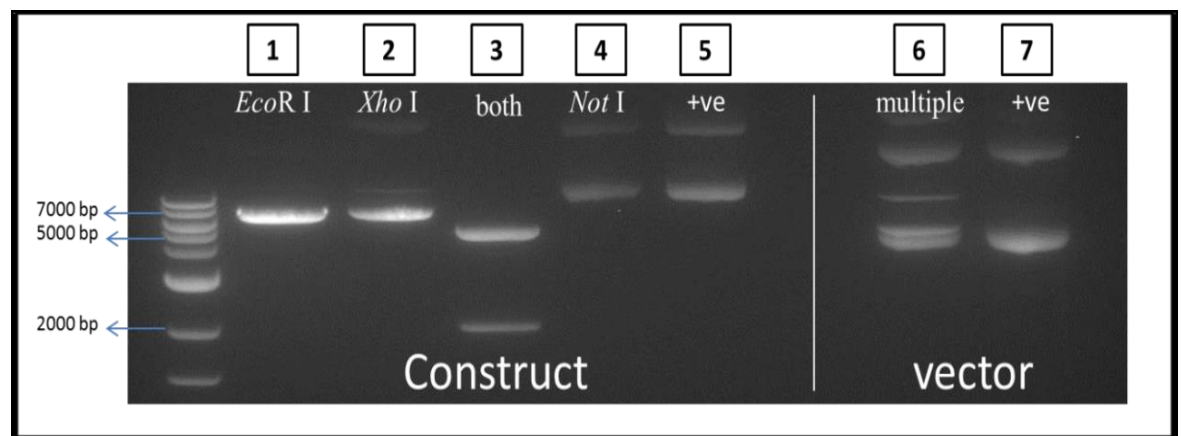


Figure 3.27 Agarose gel (1%) electrophoresis of digested JCV LT pcDNA^{TM4} construct. Single digest with either EcoR I, Xho I or Not I linearised the construct (7135 bp). Double digest with EcoR I, Xho I produced bands equivalent to the 5068 bp pcDNA^{TM4} vector and 2067 bp LT ORF. Digestion of empty pcDNA^{TM4} vector control with EcoR I, Xho I and Not I did not produce a 2067 bp insert.

Having confirmed that the JCV LT ORF had been successfully cloned into pcDNA^{TM4} vector, it was decided to linearise this at a selected restriction site prior to its use for transfection of cells. The rationale for this is that it increases the chances of successful integration into the host genome without disruption of the expression construct. The Sca I restriction site was chosen as this was absent from the JCV LT ORF and is located in the bacterial ampicillin resistance gene which is non-functional in eukaryotic gene expression studies (see Figure 5.3.16 and the NEBcutter result in Appendix 5.3). The results of linearisation of the construct and vector are shown in 5.3.27 in appendix 5.3 and these products were purified as shown in Figure 5.3.28.

3.4 LT Transfection

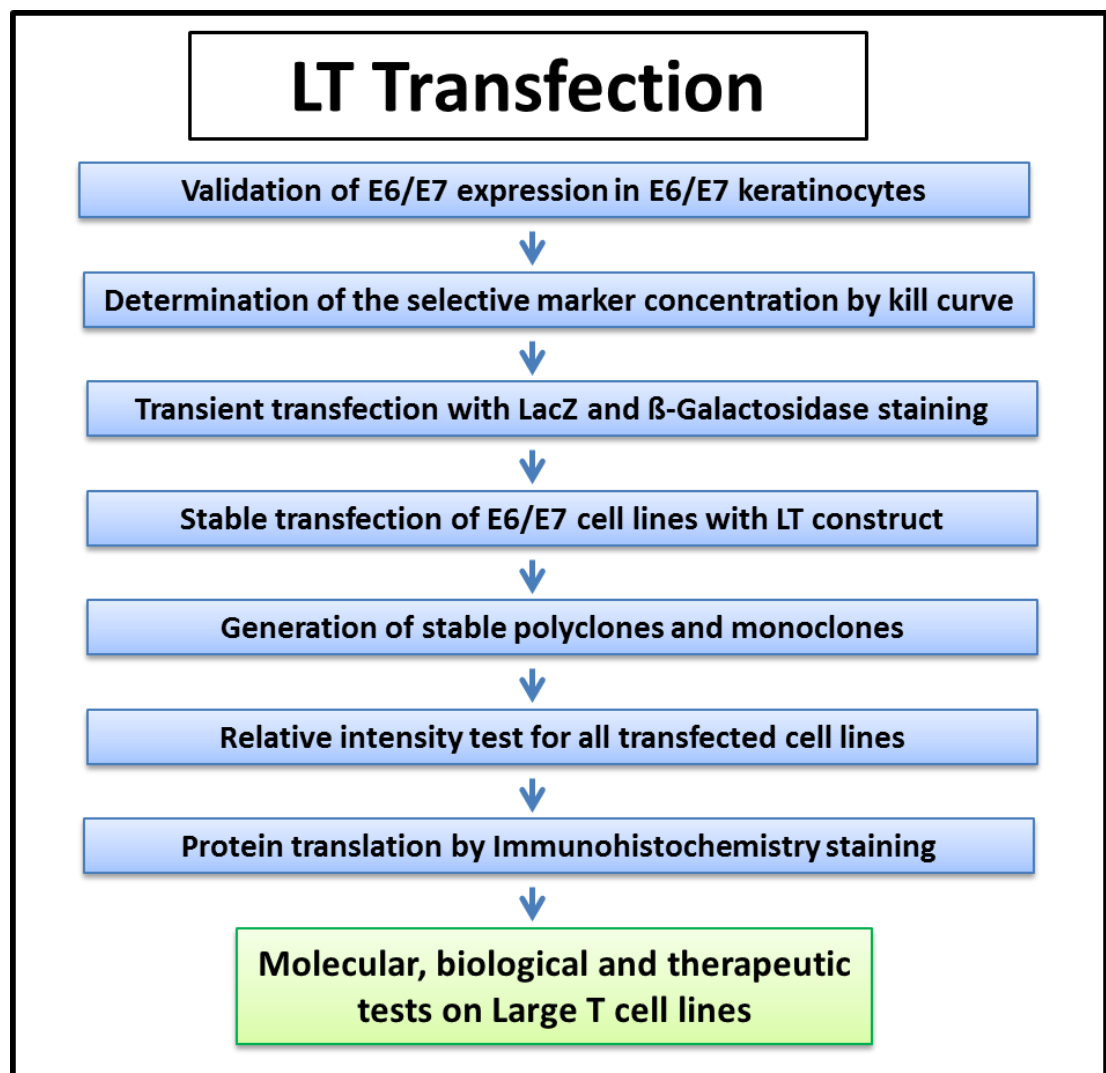


Diagram 3.3 A summary of JCV LT gene transfection.

3.4.1 Validation of E6/E7 expression in E6/E7 immortalised keratinocytes

mRNA was extracted from E6/E7 immortalised keratinocytes by the use of TRIzol and this then used to test for expression of E6/E7 by RT-PCR (see section 2.3.14, in the Methodology).

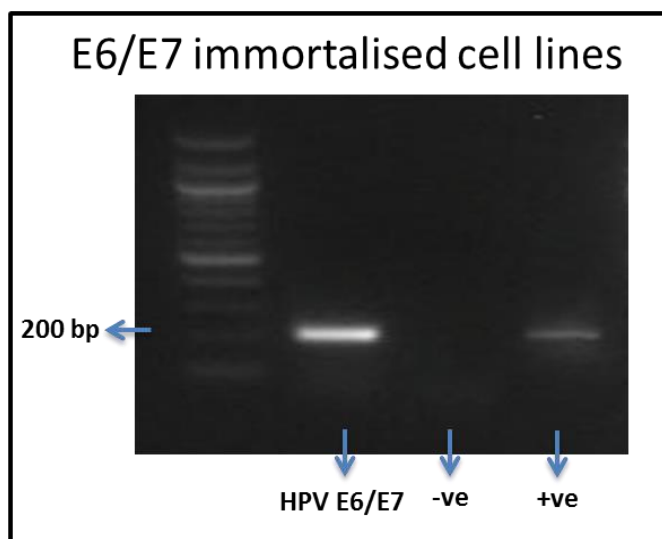


Figure 3.28 Agarose gel electrophoresis (1.5%) of RT-PCR products obtained from amplification of a 209 bp HPV16 E6/E7 amplicon from mRNA extracted from E6/E7 immortalised keratinocytes. The primers used are listed in (Table 5.2.2 in appendix 5.2) and the E6/E7 positive control was obtained from Dr Xiaotong He.

An amplicon of the correct size for E6/E7 (209 bp) was observed which confirmed the expression E6/E7 in these cells.

3.4.2 Zeocin kill curve for E6/E7 immortalised keratinocytes

Determining the optimal concentration of the selectable marker antibiotic is important in the generation of stable cell lines. The optimal concentration of zeocin needed to produce 100% cell death in parent non-transfected E6/E7 Keratinocytes in 10-14 days was found to be 50µg/ml, as illustrated in Table 3.5.

Table 3.5 Zeocin concentration required to produce 100% cell death in 10-14 days

Days\Conc.	0 µg	25 µg	50 µg	100 µg	200 µg	300 µg	400 µg	600 µg	800 µg
1	80%	80%	80%	80%	80%	80%	80%	80%	80%
2	90%	85%	85%	85%	75%	70%	70%	70%	70%
3	95%	75%	75%	70%	70%	60%	40%	50%	70%
4	100%	70%	60%	60%	65%	50%	30%	40%	50%
5	Over grow	60%	50%	50%	50%	40%	25%	30%	30%
6	-	50%	30%	30%	40%	20%	20%	15%	10%
7	-	40%	20%	20%	20%	10%	10%	Non Viable	Non Viable
8	-	30%	15%	10%	10%	Non Viable	Non Viable	-	-
9	-	20%	10%	Non Viable	Non Viable	-	-	-	-
10	-	15%	Non Viable	-	-	-	-	-	-
11	-	10%	-	-	-	-	-	-	-

A concentration of 50 µg/ml was chosen for selection of stable transfectants since cells at 25µg/ml continued to grow after 11 days, indicating that this concentration did not result in 100% cell death. Antibiotic was removed from the 50µg and 100µg treated cells which were then incubated for a further 3 days with no visible recovery.

3.4.3 Analysis of the transient transfection efficiency of E6/E7 immortalised keratinocytes

The aim of this experiment was to study the transfection efficiency of the prototype E6/E7 keratinocytes using the lacZ expressing (pcDNA 3.1 V5/his LacZ) reporter vector. Cells were transiently transfected as described in (2.3.16) then fixed and stained for β-galactosidase activity after 24 hrs. LacZ expressing cells turn blue when they stained for β-galactosidase activity.

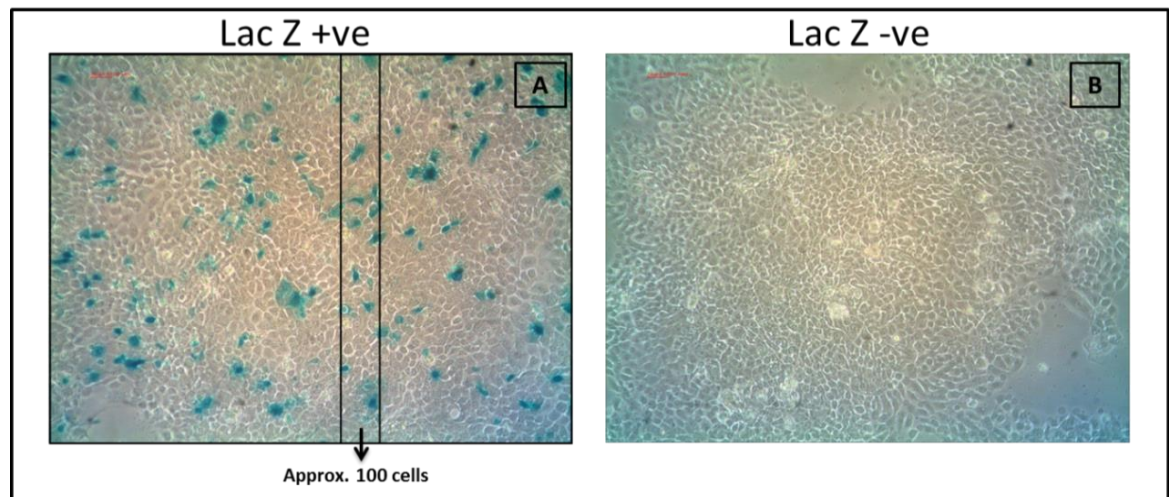


Figure 3.29 Phase contrast images of E6/E7 immortalised cells transiently transfected with pcDNA 3.1 V5/his LacZ: A. pcDNA 3.1 V5/his LacZ transfected cells; B. Utransfected negative control cells. 24 hrs post transfection, cells were fixed, stained and representative images taken from several fields of view using Nikon Eclipse TS100 light microscope. Approximately 100 cells were selected to calculate the percentage of the transfection efficiency, as shown in A.

A transient transfection efficiency of 15% was determined for the E6/E7 keratinocytes by assessing the number of blue cells in 5 representative fields of 100 cells.

3.4.4 Stable transfection of E6/E7 immortalised keratinocytes with JCV LT

E6/E7 cell lines were stably transfected with the JCVLT pcDNA^{TM4} construct as described in (2.3.17) and these cultured in 50 µg/ml zeocin 24 hrs post-transfection for 2 weeks. Considerable cell death was observed over this period since only cells which had stably integrated the construct would survive. Three stable polyclonal cell lines (LT1, 2 & 3) were generated from JCV LT pcDNA^{TM4} transfected cells and 2 stable polyclonal lines from pcDNA^{TM4} vector only transfected cells (Vec 1 & 2). mRNA was extracted from these cells and RT-PCR used to confirm expression of the JCV LT ORF using LT internal primers, T7/BGH primers from the vector and GAPDH primers as housekeeping control .

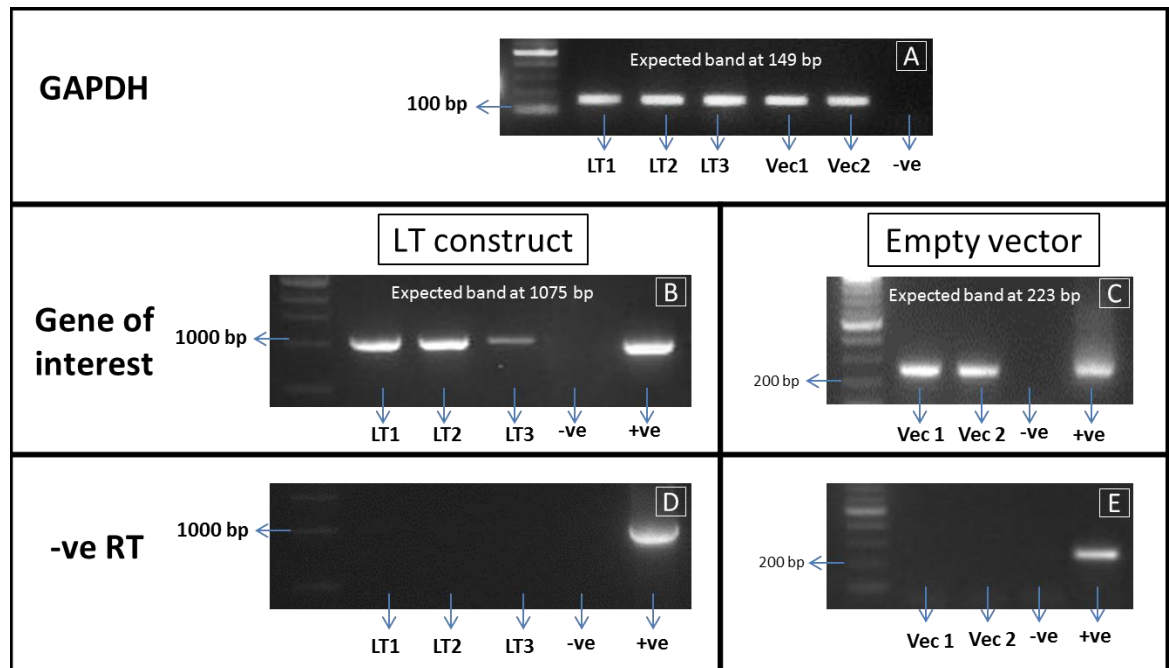


Figure 3.30 Agarose gel electrophoresis (1.5%) of RT-PCR products of mRNA extracted from JCV LT transfected and vector control transfected E6/E7 Keratinocytes. (A) GAPDH primers showed a uniform signal of the predicted amplicon (149 bp). (B) LT 1, LT 2, and LT 3 primers showed the predicted amplicon size (1075 bp). (C) Vec 1 and Vec 2 primers showed the predicted amplicon size of (223 bp). (D) & (E) Represent identical reaction conditions minus reverse transcriptase.

RT-PCR with GAPDH primers confirmed equal loading and quality of input mRNA template. LT primer RT-PCR on equivalent amounts of input mRNA produced from LT transfected cells showed a clear signal of the correct size in the three polyclonal populations tested although LT 3 had reduced levels compared to LT 1 and 2. These data confirmed expression of vector-encoded JCV LT mRNA in these cells. PCR was also carried out using vector specific T7/BGH primers on mRNA extracted from vector control transfected cells which confirmed the presence of mRNA transcript expressed from the T7/BGH multicloning site of the vector in these cells. In addition, PCR was carried out

using the same primers and equivalent amounts of mRNA but without reverse transcriptase which showed no evidence of signals. This clearly indicates that the previous post-RT positive results were derived from expressed mRNA and not from genomic DNA contamination.

In order to facilitate single colony isolation from these polyclonal cell populations LT 1 and Vec 1 cells were plated at a variety of cell densities and monitored over a period of several weeks in the presence of zeocin. Cultures which became over-dense were discarded, as single colonies could not be discriminated. Once single colonies had expanded to contain approximately 20-30 cells, they were transferred to a 24-well plate. Cells were expanded before being trypsinised and transferred from the 24-well plate to 6-well plates and eventually to T-25 with changes of selection medium every 2-3 days. Curiously, a number of colonies failed to expand during passage from 24 well plates through to T25 flask where some cells remained viable but appeared to senesce and attempts to expand these cells further proved unsuccessful. After approximately 90 days, 8 colonies had been successfully picked from JCV LT transfected cells and expanded to produce freezer stocks (Mono 1 – 8) together with vector control (Vec).

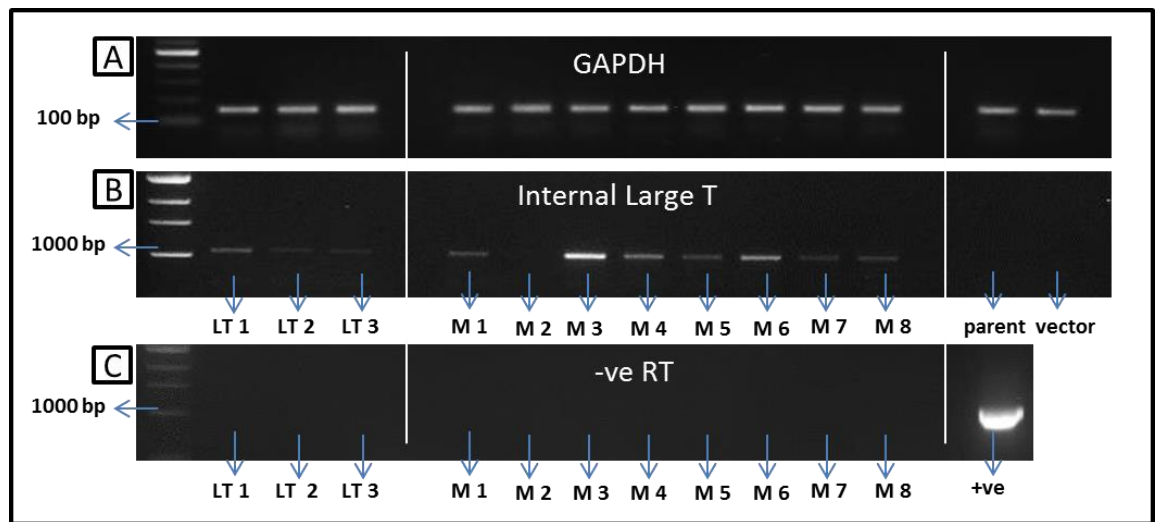


Figure 3.31 Agarose gel electrophoresis of RT-PCR products produced from mRNA extracted from polyclonal and monoclonal LT transfected cell (A) GAPDH primers gave a balanced signal of the predicted amplicon (149 bp). (B) JCV LT primers gave a range of different signal intensities of the predicted amplicon (1075 bp). (C) Identical reactions but lacking reverse transcriptase.

RT-PCR carried out using GAPDH primers confirmed both template quality and equivalent template loading as shown in Figure 3.36 (A). Image B shows that JCV LT amplicon was present in 7 out of 8 monoclonal cell lines indicating that the JCV LT pcDNA^{TM4} construct was stably integrated and producing JC LT mRNA. Variation in expression levels of LT mRNA were observed between the different monoclonal cell lines and no signal was observed when reverse transcriptase was omitted from equivalent PCR reactions (C) indicating that the signals observed in (B) were not derived from genomic DNA contamination.

Analysis of the image shown in Figure 3.31 was carried out with ImageJ software in order to compare relative JCV LT signal intensities from all the cell line tested normalised to their respective GAPDH signals.

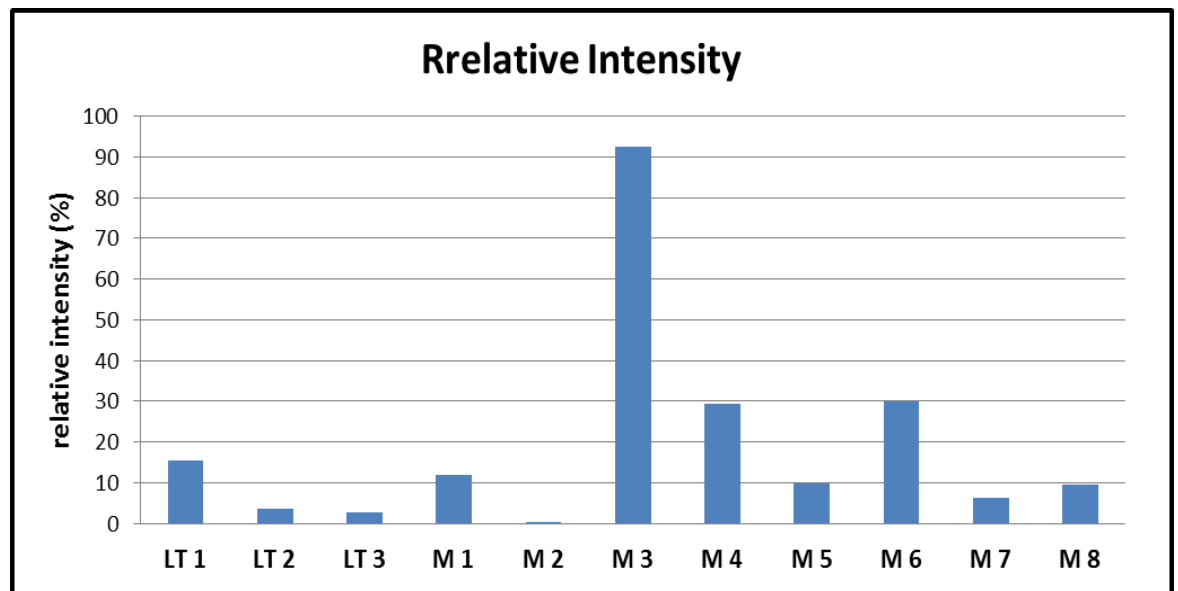


Figure 3.32 ImageJ analysis: Relative expression of JCV LT mRNA from polyclonal and monoclonal cell lines expressed as percentage expression after normalisation with GAPDH signals.

LT 1 polyclonal cells had an observed JCV LT signal of 15% which was the highest observed amongst the three polyclonals. M3 had the greatest signal strength (92%) of all the monoclonals tested with M2 showing no activity. Based on these results LT 1 and M3 were selected for further study.

3.4.5 Analysis of JCV LT Protein Expression

Having used RT-PCR to confirm stable expression of LT mRNA in transfected cells, it was necessary to confirm whether the LT protein was being expressed in these cell lines. Initially, confirmation of JCV LT protein expression was attempted by western blot.

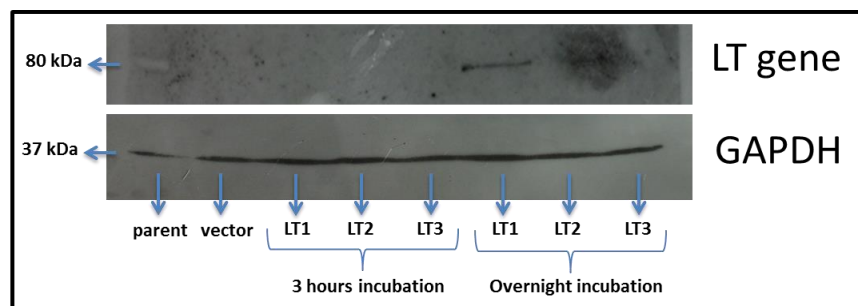


Figure 3.33 Western blot analysis of LT antibody on Parent, Vector, and the 3 polyclonal populations. Proteins were separated on a 12% SDS-PAGE, transferred to Hybond-C nitrocellulose membrane and visualised with ECL. The primary anti-JCV T-Ag was used at a concentration of 1:200 followed by goat anti-mouse secondary antibody (HRP). The predicted signal sizes were 80 kDa and 37 kDa for JCV T-ag and GAPDH respectively.

No expression of JCV LT protein was observed in parent and vector wells as anticipated and only the LT1 polyclonal cell line showed any LT signal after an overnight incubation with the primary antibody. Further attempts were made to detect JCV LT by western blotting in the monoclonal cell lines but this proved difficult to reproduce which prompted the use of immunocytochemistry. Figure 5.3.30 in Appendix 5.3 shows full images of western blot.

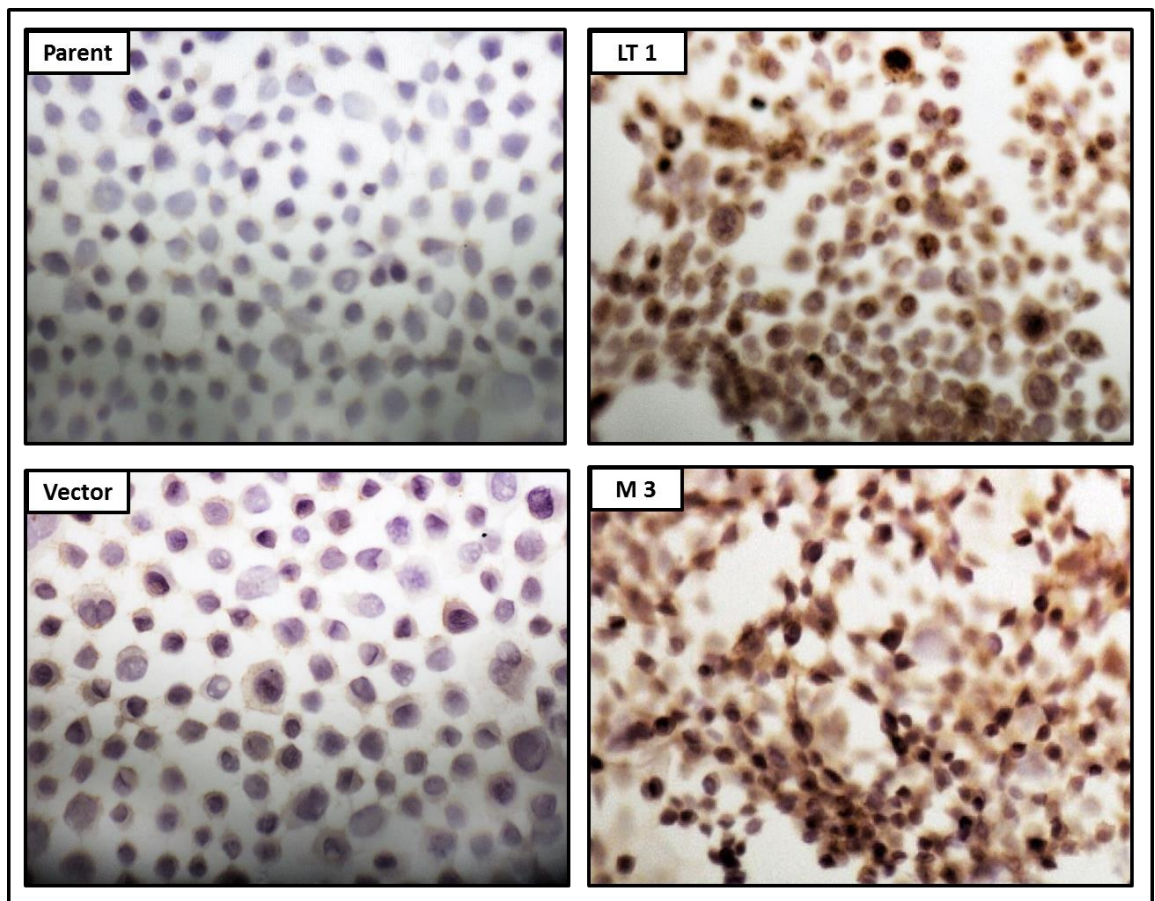


Figure 3.34 Immunostaining with Anti-JCV LT antibody. At 80% confluency, cells were harvested 0.5×10^6 cells were cytospun, fixed with 3% Formaldehyde and stained using a mouse monoclonal antibody mixture against JCV T-Ag (clones PAb2003 and PAb2000 kindly provided by Dr. Richard Frisque) at a concentration of 1:200, and goat anti-mouse secondary antibody (HRP). Signals were visualised using DAB staining and counterstained with haematoxylin. Pictures were taken at 60 x magnification viewing 67.5 microns. Both LT1 and M3 cells showed strong nuclear and cytoplasmic staining (brown colour) which was consistent with expression of the JCV LT protein whereas both parent and vector cells transfected cells showed no evidence of staining.

Immunocytology showed strong staining of LT1 and M3 cells with the anti-JCV T-Ag monoclonal antibody and clearly demonstrated that the JCV LT protein was expressed in the cytoplasm and nuclei of LT transfected cells whereas no signal was detected in either parent or vector-transfected cells. It was also noted that not all cells in both the polyclonal and monoclonal cell lines showed strong nuclear staining.

3.5 Molecular, biological and therapeutic tests on LT cell lines

Having confirmed the LT mRNA expression and protein translation in LT transfected cell lines, these were then used also to study the potential ability of this protein to induce transformation of the parental E6/E7 immortalised cell lines. In this regard it was decided to investigate markers of Epithelial to Mesenchymal Transition (EMT) in addition to assays for transformed colony formation, cell proliferation assays, drug cytotoxicity and gene expression microarrays.

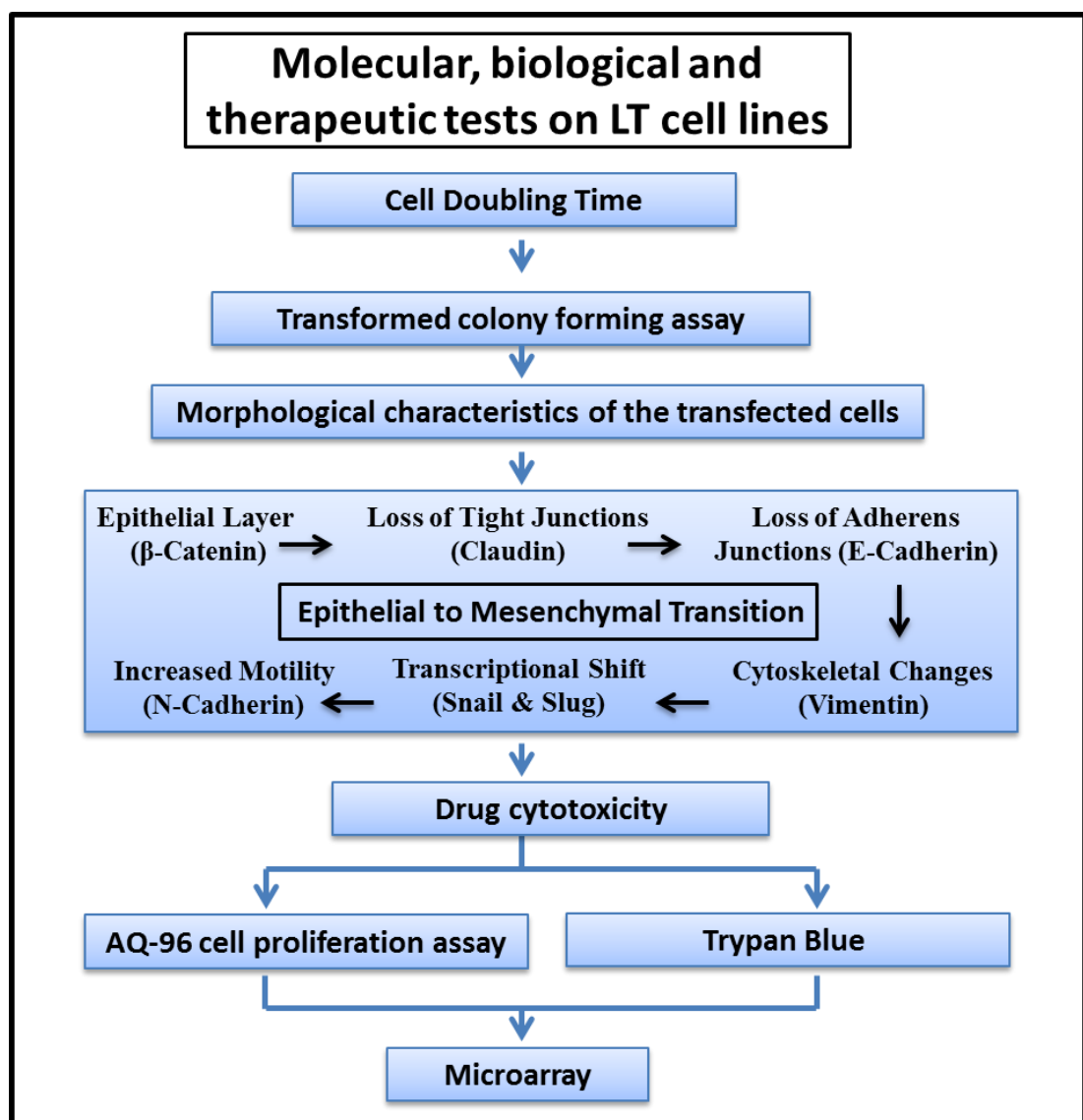


Diagram 3.4 A summary of the molecular, biological and therapeutic tests on LT cell lines.

3.5.1 Cell Doubling Time (CDT)

Cell growth was assessed at four time points (0, 24, 48 and 72 hrs) by means of the CellTiter 96® AQueous One Solution Cell Proliferation Assay (AQ-96 Assay) using the manufacturer's instructions (Promega, Southampton, UK). Cell proliferation assays are shown as percentages and calculated from triplicate wells for each time point.

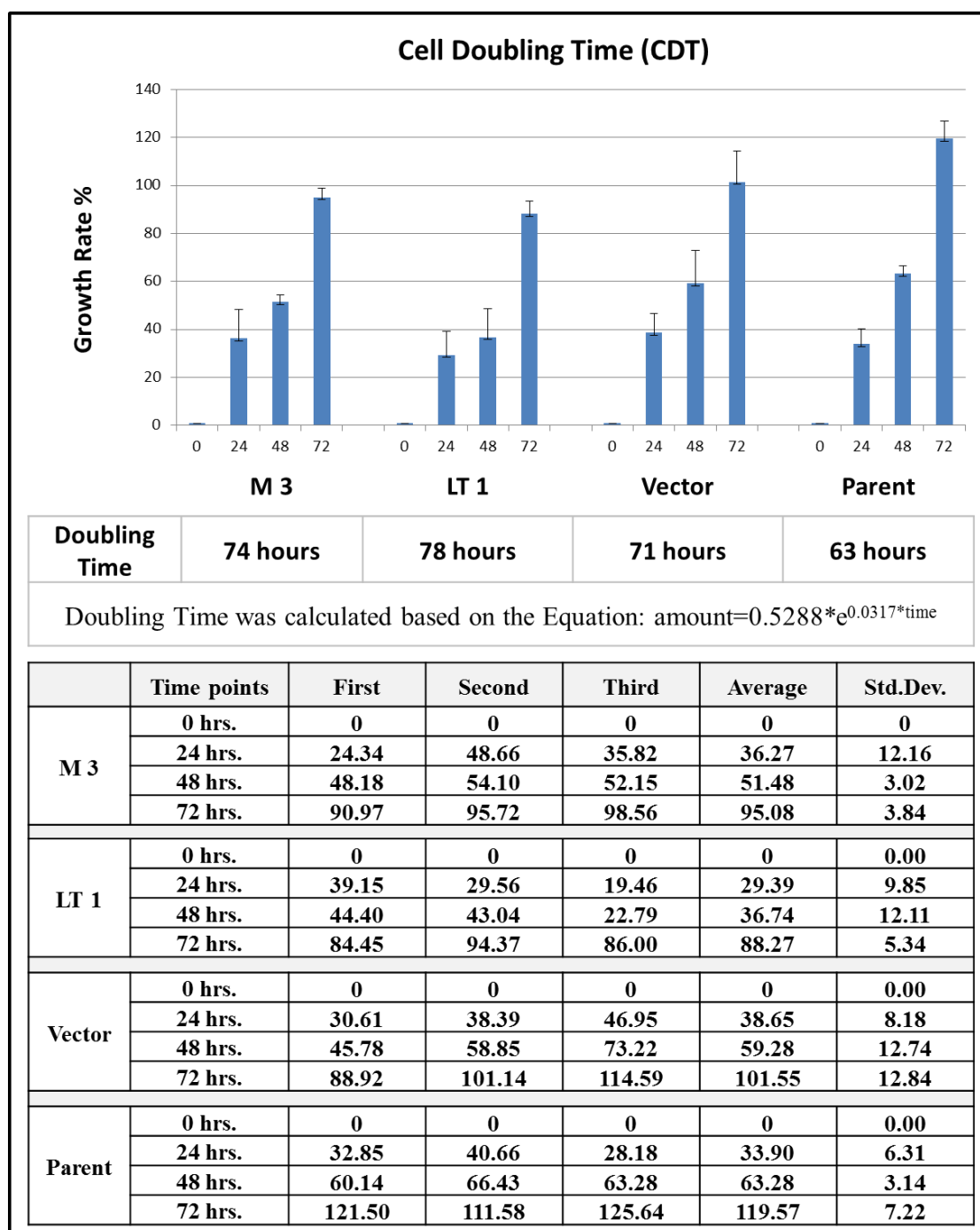


Figure 3.35 Cell line population doubling times (hrs). The table shows cell proliferation data of the AQ-96 Assay performed in triplicate wells for each time point.

The cell line population doubling times are shown as percentage growth change over three days and were carried out in triplicate for each time point of the LT expressing cells and controls. No statistically significant difference in growth rate was observed between any of the transfected cells and parental controls which had the following doubling times: M3 74 hrs; LT1 78 hrs; Vector 71 hrs; Parent 63 hrs.

For each triplicate consisting of control Vector and Parent cells and transfected Poly and Mono cells, a one-way ANOVA was performed, followed by Dunnett's post hoc test to find where, if any, significant differences occurred. Dunnett's post hoc test allows comparison of each experimental test sample. P values of 0.05 were considered significant. Statistical analysis of the data indicates that no correlations were apparent between cell growth rates of the clones and their controls, as one-way ANOVAs were not significant ($p = 0.766$). Although LT expressing cells showed no statistically significant difference in growth rates to the control cells (Std.Dev.) there was a trend which suggested that expression the LT protein reduced the growth rate.

3.5.2 Transformed colony forming assay using Toluidine Blue stain

Cells were seeded at a density of 0.15×10^6 cells in T25 flasks and colony formation examined after 2 and 3 weeks in culture.

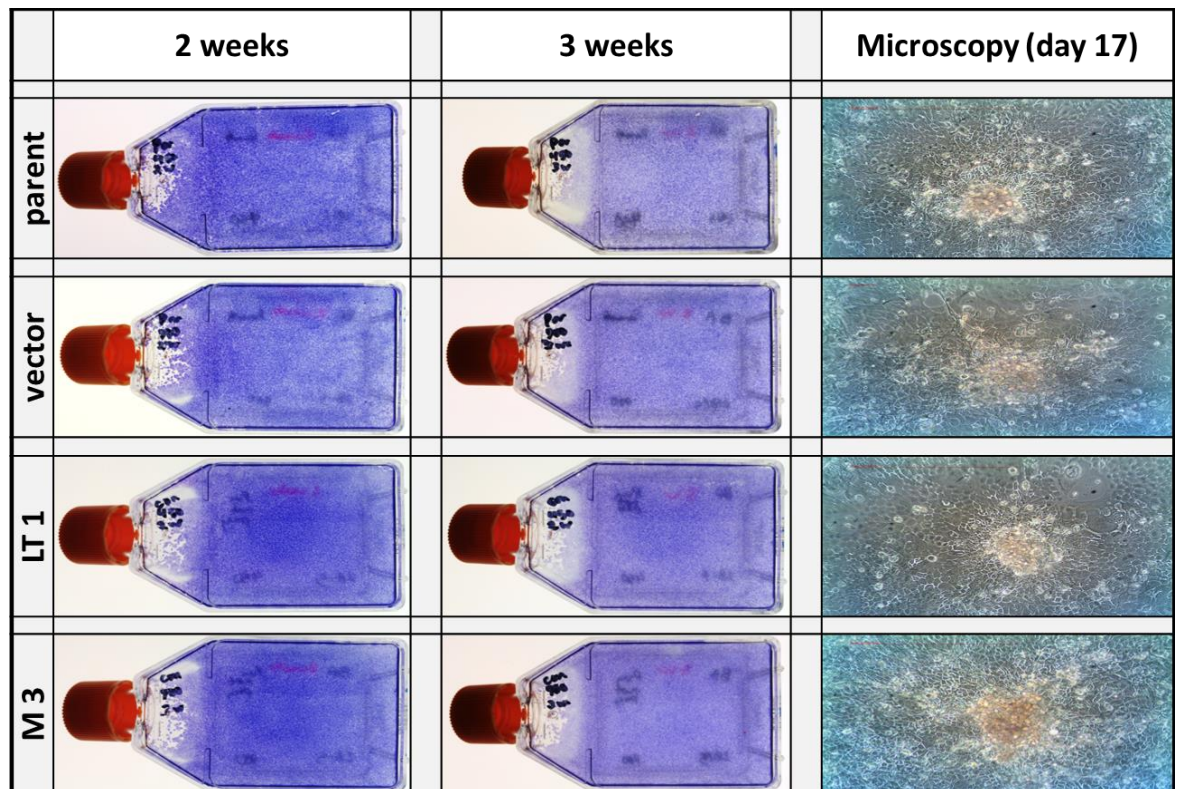


Figure 3.36 Colony-forming assay. The panel displays representative photographs of cells seeded, expanded, and stained by Toluidine Blue staining in T25 flasks at two time points of two and three weeks. Pictures of small foci were taken on the seventeenth day which were generally of smaller size.

After 2 and 3 weeks of continuous growth there was no significant difference in macroscopic or microscopic colony formation between any of the cell lines tested indicating that the JC LT protein was not able to induce the formation of transformed colonies in these cells.

3.5.3 Morphological characteristics of the transfected cells

Cell morphology and viability were assessed and images of live cells recorded by phase contrast microscopy.

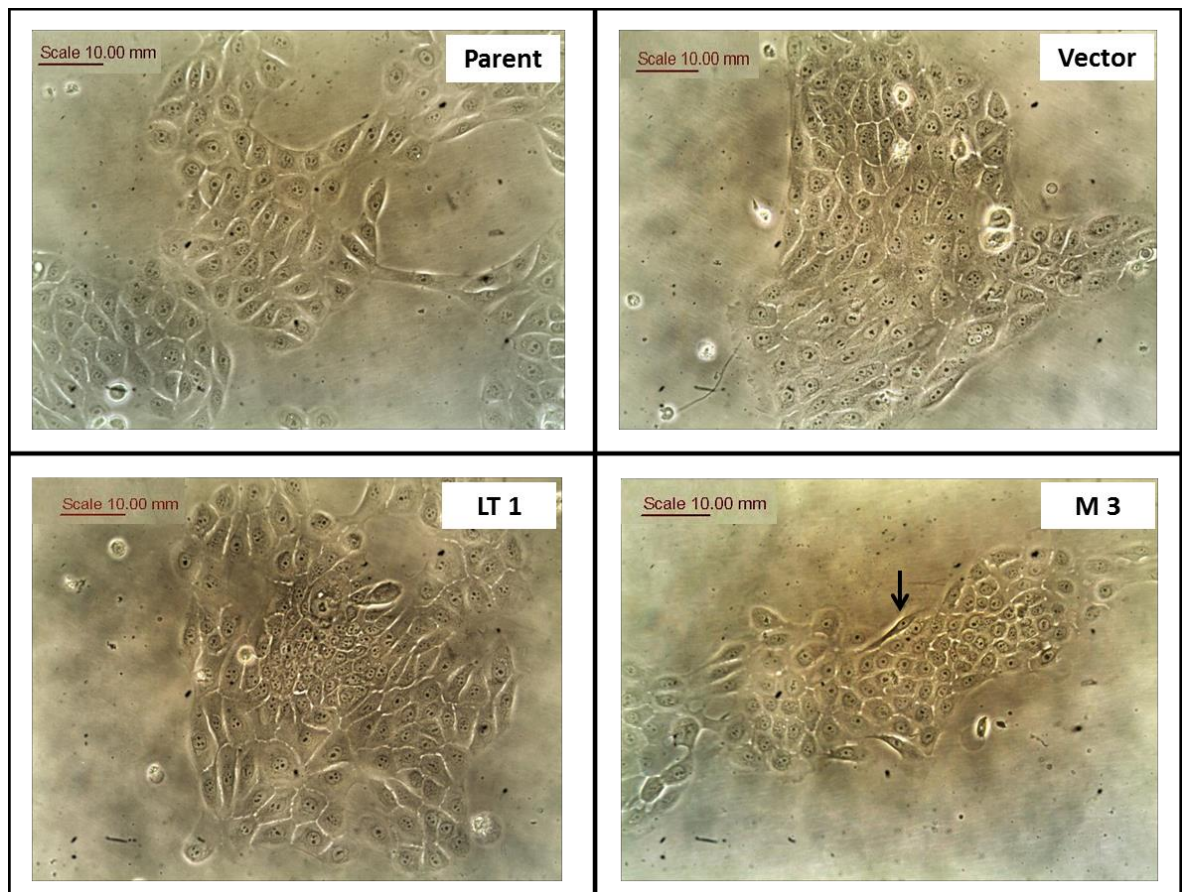


Figure 3.37 Morphological features of cells after 7 days in culture. Cells were reseeded at low densities and left to grow with medium replacement every two days and photographed under phase contrast.

Parental cells exhibited typical flat polygonal morphology with more regular dimensions and grew closely associated with each other in discrete patches with large cell-free areas clearly visible. Vector cells presented with regular compact monolayers very similar to the Parental cells. M3 monoclonal cells showed some spindle-shaped cells (arrowed) which are consistent with an EMT and they remained more rounded with less spreading unless adjacent to other cells. The LT1 polyclonal cells formed colonies of adherent and flattened cells at the edges with small rounded cells in the centre with some evidence of multi-layering which is indicative of loss of contact inhibition.

3.5.4 EMT

This process can be defined by changes in six cellular characteristics depending on the biological and functional setting in which these occur [151, 171]:

1. Formation of epithelial layers (β -Catenin)
2. Loss of tight junctions (Claudin)
3. Loss of adherens junctions & desmosomes (E-Cadherin)
4. Cytoskeletal changes (Vimentin)
5. Transcriptional shift (Snail)
6. Increased motility & migration (N-Cadherin)

The expression of these EMT markers was analysed by RT-PCR for transcript levels and western immunoblotting for protein levels. The expected signal sizes of GAPDH in PCR and western blot were 149 bp and 37 kDa respectively. Figure 5.3.29 in Appendix 5.3 shows full images of western blot. Relative intensity analysis of transcript and protein levels compared to match GAPDH signals are shown in Table 5.3.2 in Appendix 5.3 and the primers used are shown in Table 5.2.3 in Appendix 5.2.

3.5.4.1 Epithelial layers (β -catenin)

Epithelial cells express high levels of β -catenin. β -catenin primarily connects adhesion junctions of epithelial cells. When there is no room for more cells in the area, β -catenin tells the cell to stop proliferating (see Figure 1.10).

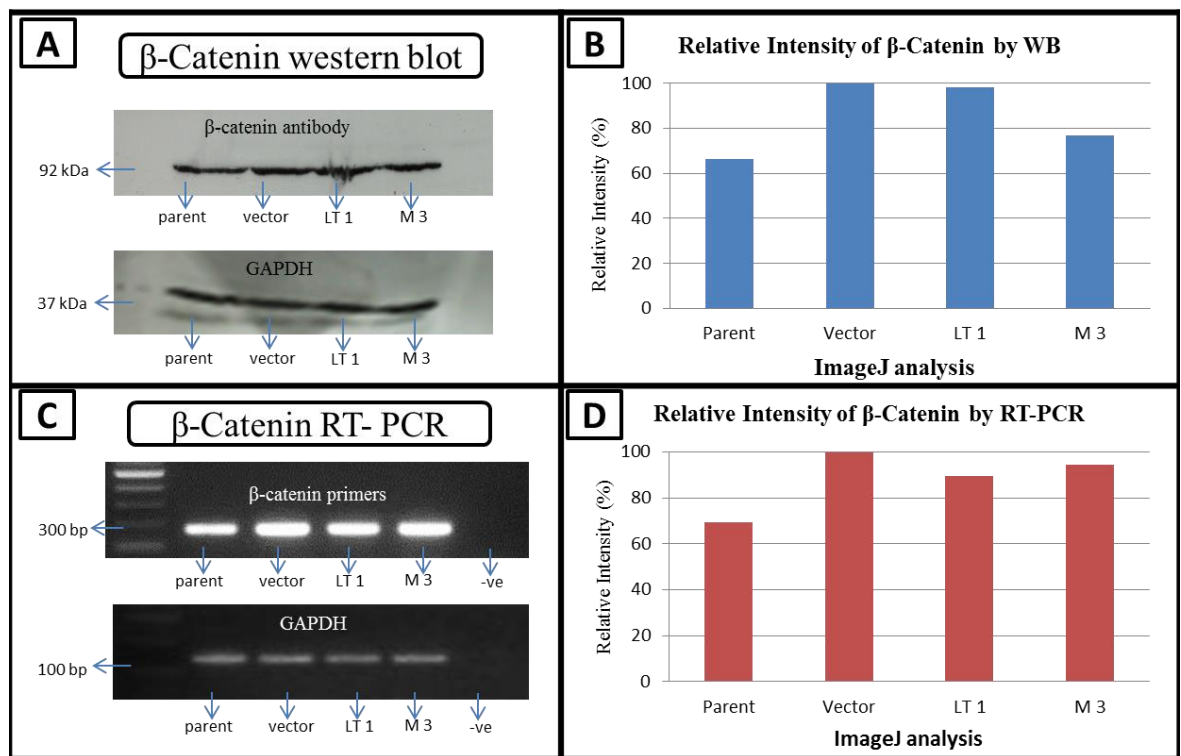


Figure 3.38 Expression patterns of β -catenin in LT transfected and control cells. (**A & B**) Western blot showing uniform expression of 92 kDa β -catenin protein in addition to quantitation by Image J; (**C & D**) Agarose gel electrophoresis of RT-PCR products obtained from β -catenin primers (250 bp) using mRNA template extracted from the same cells. Relative intensities were quantified by Image J.

Relatively high expression levels of β -catenin protein were detected by western blot which showed no difference between any of the cell lines tested. RT-PCR analysis of β -catenin mRNA levels showed that this was consistent with the levels of protein detected. These results indicate that all cell lines tested were at an equivalent stage in potentially moving towards EMT.

3.5.4.2 Loss of tight junctions (Claudin)

One of the earliest events during EMT is when epithelial cells start losing their apical and basal polarity which can be detected by increased expression of claudin [172, 173].

Tight junctions are composed of claudin protein which joins the junctions to the cytoskeleton (see Figure 1.10).

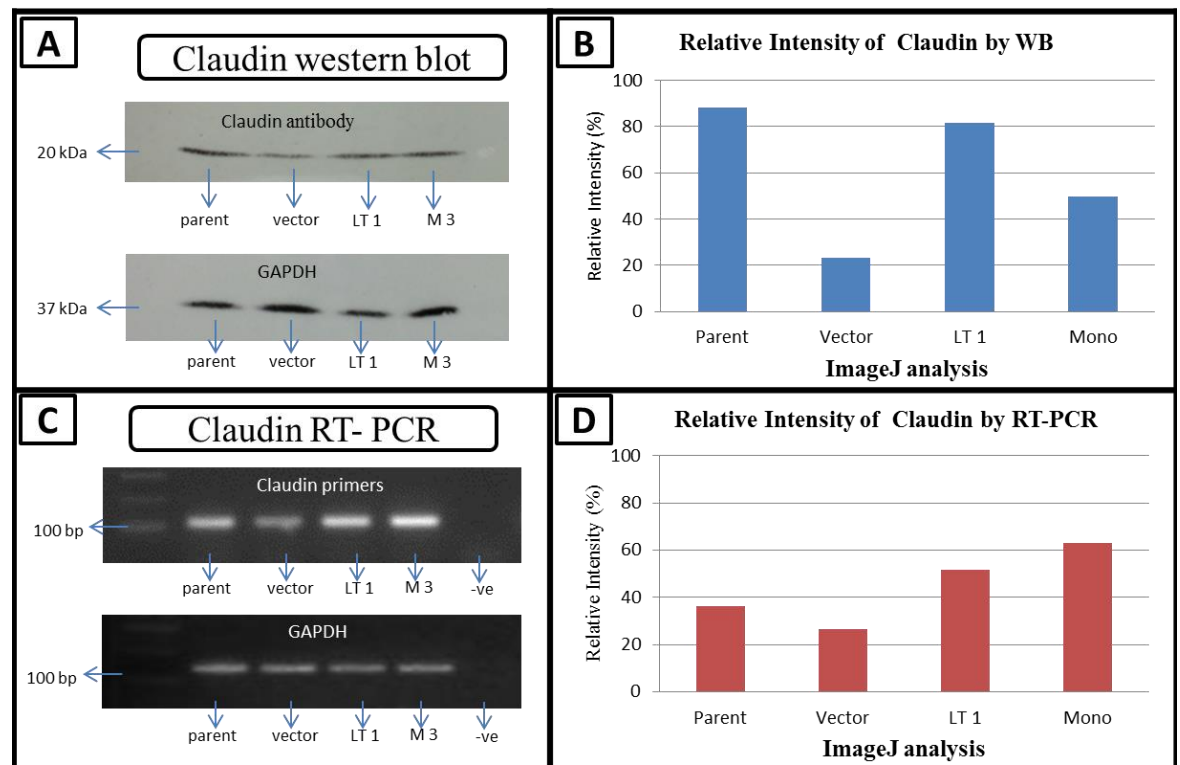


Figure 3.39 Expression patterns of claudin in LT transfected and control cells. (A & B) Western blot showing uniform expression of 20 kDa claudin protein in addition to quantitation by Image J; (C & D) Agarose gel electrophoresis of RT-PCR products obtained from claudin primers (110 bp) using mRNA template extracted from the same cells. Relative intensities were quantified by Image J.

Variable expressions of claudin protein were observed when this was compared to mRNA expression by RT-PCR although there was no consistent association of elevated claudin protein or mRNA levels with expression of JCV LT.

3.5.4.3 Loss of adherens junctions & desmosomes (E-cadherin)

E-cadherin plays important roles in cell adhesion, ensuring that cells within tissues are bound together. Up-regulation of E-cadherin increases the strength of cellular adhesion within a tissue, resulting in a decrease in cellular motility which is a fundamental event the regulation of EMT. In contrast, down-regulation indicates that cells are undergoing transition to the more motile mesenchymal phenotype (see Figure 1.10).

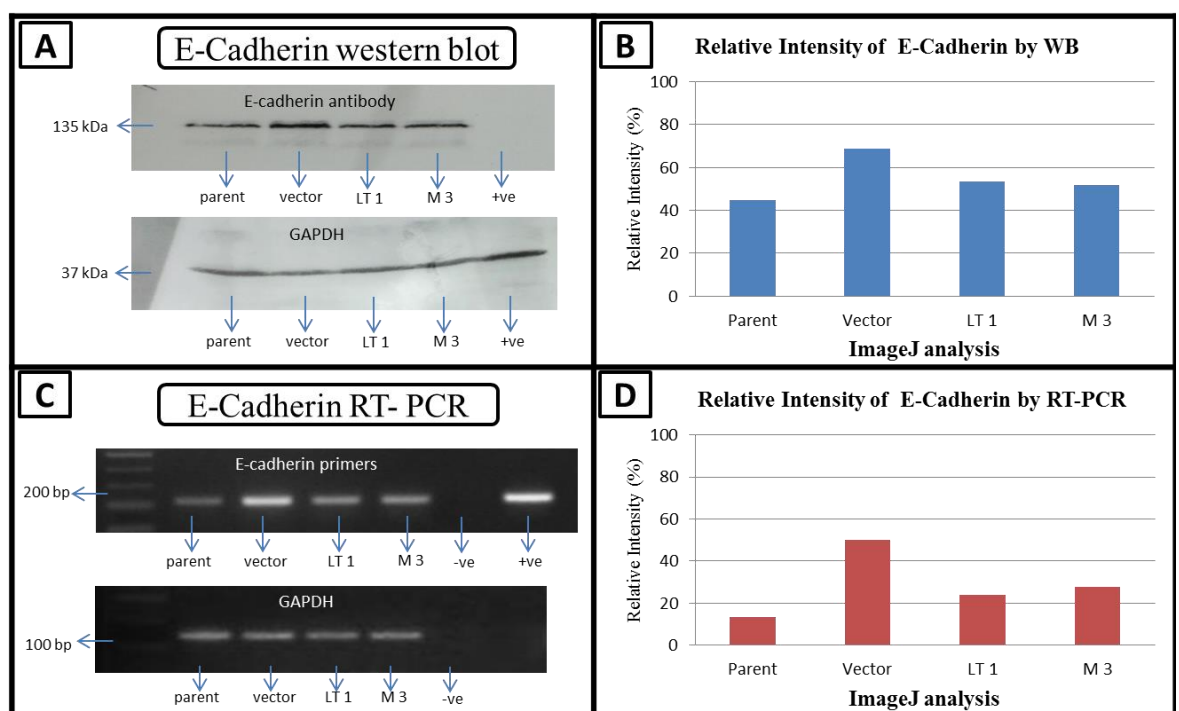


Figure 3.40 Expression patterns of E-cadherin in LT transfected and control cells. (A & B) Western blot showing uniform expression of 135 kDa E-cadherin protein in addition to quantitation by Image J; (C & D) Agarose gel electrophoresis of RT-PCR products obtained from E-cadherin primers (298 bp) using mRNA template extracted from the same cells. Relative intensities were quantified by Image J. The positive control was a transformed hepatocyte cell line provided by S Almatrouk.

These results show no convincing association between JCV LT expression and a change in E-cadherin expression.

3.5.4.4 Increased motility & migration (N-cadherin)

In the final stages of EMT, up-regulation of N-cadherin increases cell motility, and facilitates cell migration, Increased N-cadherin expression is associated with the mesenchymal phenotype whereby cells have a spindle-shaped morphology and interact with each other only through focal points (see Figure 1.10) [174].

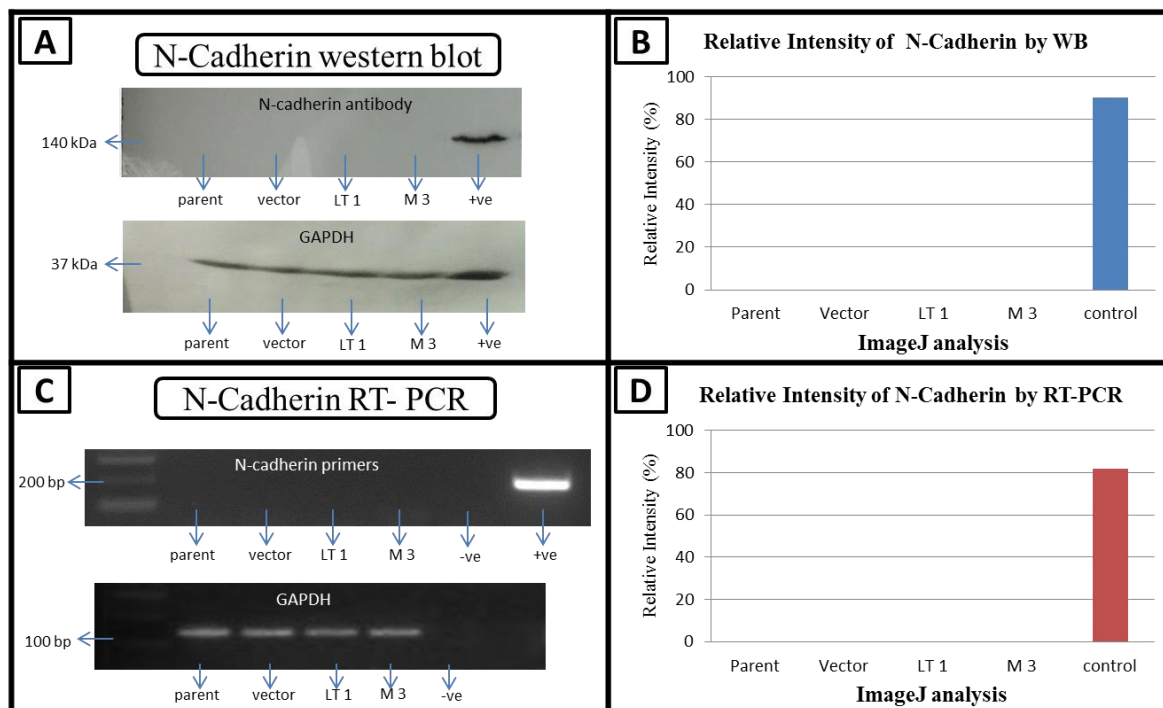


Figure 3.41 Expression patterns of N-cadherin in LT transfected and control cells. (**A** & **B**) Western blot showing uniform expression of 140 kDa N-cadherin protein in addition to quantitation by Image J; (**C** & **D**) Agarose gel electrophoresis of RT-PCR products obtained from N-cadherin primers (165 bp) using mRNA template extracted from the same cells. Relative intensities were quantified by Image J. The positive control was a transformed hepatocyte cell line provided by S Almatrouk.

No N-cadherin protein or mRNA was detected in any of the cell lines tested apart from the transformed hepatocyte positive control.

3.5.4.5 Cytoskeletal changes (Vimentin)

Vimentin is a cytoskeletal protein which is responsible for maintaining cell shape, integrity of the cytoplasm and stabilization of cytoskeletal interactions. It is expressed only in mesenchymal cells and is often used as a marker of mesenchymally-derived cells [175].

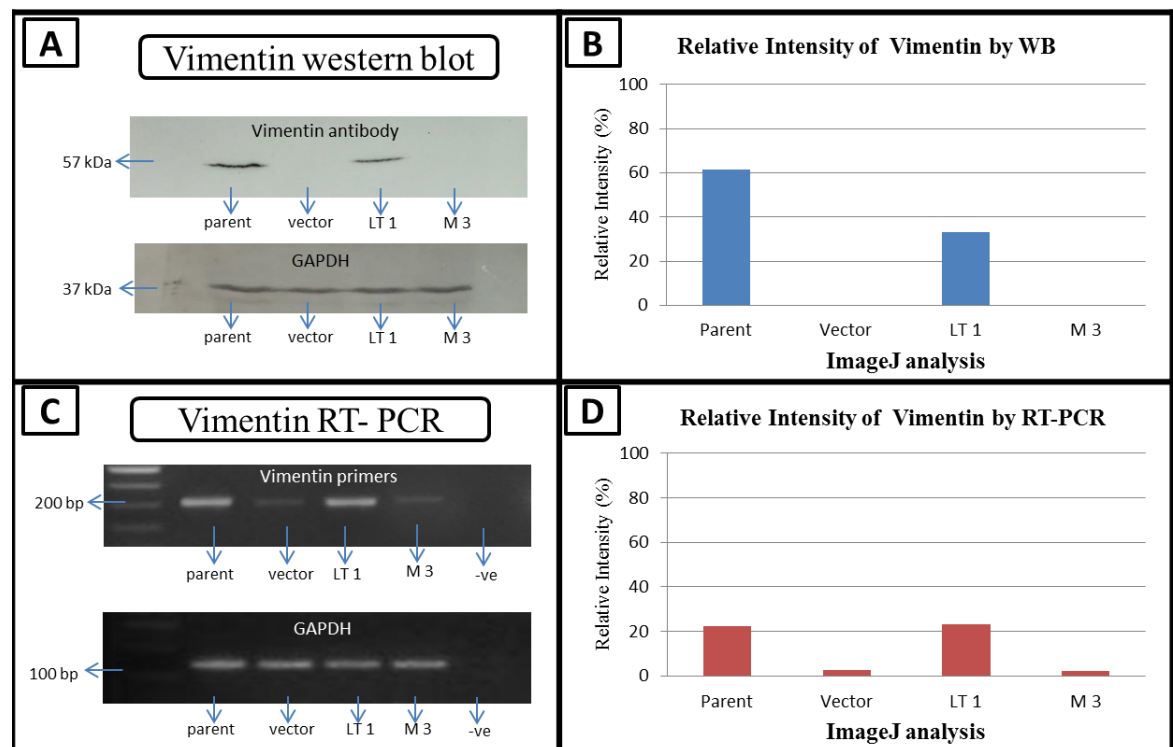


Figure 3.42 Expression patterns of vimentin in LT transfected and control cells. (A & B) Western blot showing uniform expression of 57 kDa vimentin protein in addition to quantitation by Image J; (C & D) Agarose gel electrophoresis of RT-PCR products obtained from vimentin primers (210 bp) using mRNA template extracted from the same cells. Relative intensities were quantified by Image J.

Expression levels of vimentin mRNA and protein showed a good correlation as determined by western blotting and RT-PCR. Curiously both vector and M3 monoclonal cells had undetectable levels of vimentin protein associated with very low levels mRNA and yet parent and LT1 polyclonal cells had elevated levels of both vimentin protein and

transcript. These results indicate there was no convincing association between JCV LT expression and vimentin although they have profound implications for the cloning process used.

3.5.4.6 Transcriptional shift (Snail)

Transcriptional repressors such as snail have been implicated in promoting EMT by binding to the E-cadherin promoter region in order to repress its transcription during development [157]. Thus snail is known to suppress epithelial markers and activate mesenchymal genes (see Figure 1.10).

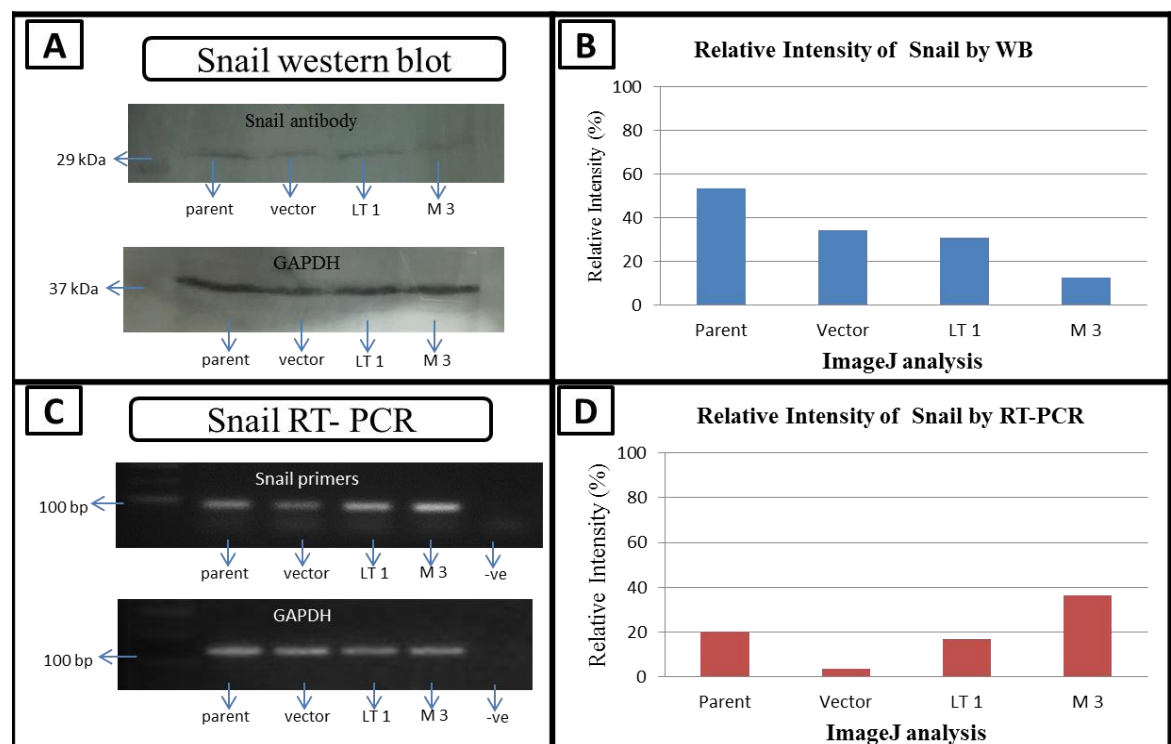


Figure 3.43 Expression patterns of snail in LT transfected and control cells. (**A & B**) Western blot showing uniform expression of 29 kDa snail protein in addition to quantitation by Image J; (**C & D**) Agarose gel electrophoresis of RT-PCR products obtained from snail primers (94 bp) using mRNA template extracted from the same cells. Relative intensities were quantified by Image J.

Although the signal was weak, the results suggest that a modest reduction in the expression of snail protein may have occurred in M3 monoclonal cells relative to all the other cell lines tested. Interestingly the snail mRNA was actually increased in M3 cells suggesting that snail protein expression is being translationally regulated.

3.5.4.7 Concluding remarks of EMT on LT gene

It is very clear that JCV LT does not induce EMT in E6/E7 immortalised keratinocytes since none of the markers tested showed any convincing LT-related alteration in either mRNA or protein. Indeed, the observation that vimentin expression was detected in polyclonal Parent and LT1 cells but was down-regulated in monoclonal Vector and M3 cells indicated that this result could have wider implications for the selection pressure introduced as a consequence of the cloning procedure.

3.5.5 Analysis of the effects of JCV targeting compounds

Mefloquine is an antimalarial medication with efficacy against JC virus [111]. Gofton et al. in 2013 reported the successful treatment of progressive multifocal leukoencephalopathy with Mefloquine in a 54-year-old woman [163]. In 2014, Rodrigues et al. evaluated Mefloquine activity against four cancer cell lines and concluded that Mefloquine–Oxazolidine derivatives are considered to be useful leads for the rational design of new anti-tumour agents [176].

3.5.5.1 Mefloquine AQ-96 colorimetric cell proliferation assay

The effects of an escalating dose of mefloquine on the growth rate of JCV LT transfected cells were assessed by colorimetric cell proliferation assays using the AQ-96 reagent. The results were compared using half maximal inhibitory concentration (IC₅₀).

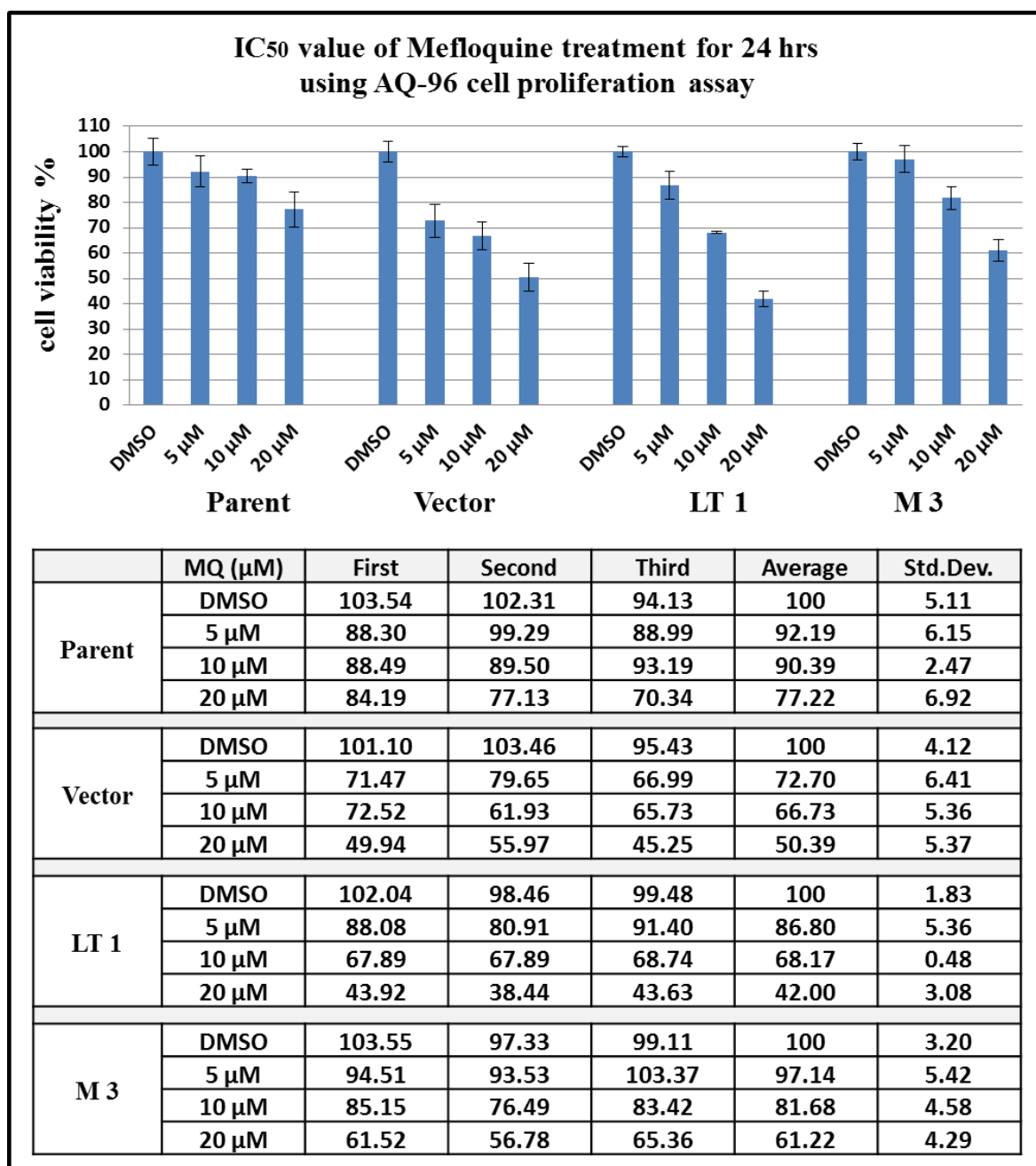


Figure 3.44 IC₅₀ value of Mefloquine treatment for 24 hrs using AQ-96 cell proliferation assay. Cell viability is expressed as the percentage of absorption of the treated cells relative to that of the DMSO-only treated cells. The table shows growth rate data of mefloquine treatment for 24 hrs using AQ-96 cell proliferation assay calculated from triplicate wells for each time point.

Growth inhibitory effects of mefloquine were examined at three concentrations of 5, 10, and 20 μM and the data is presented as the percentage change in growth relative to DMSO-treated control cells. Vector and LT1 polyclonal cells were shown to be more susceptible to mefloquine treatment at 20 μM inhibiting cell growth by half (IC₅₀ ~20 μM mefloquine) in comparison to the other cells tested. A concomitant growth inhibitory effect was observed with escalating doses of mefloquine in all tested cell lines although parent cells seemed to be the most resistant. Whilst the AQ-96 cell proliferation assay is a colorimetric method for determining the number of actively growing viable cells in a population, it does not measure cell death.

3.5.5.2 Mefloquine cytotoxicity by Trypan Blue exclusion assay

The effects of an escalating doses of mefloquine on cell death were assessed in JCV LT transfected cells using a Trypan Blue exclusion assay. The number of unstained (live) cells was expressed as a percentage of the total number of cells present.

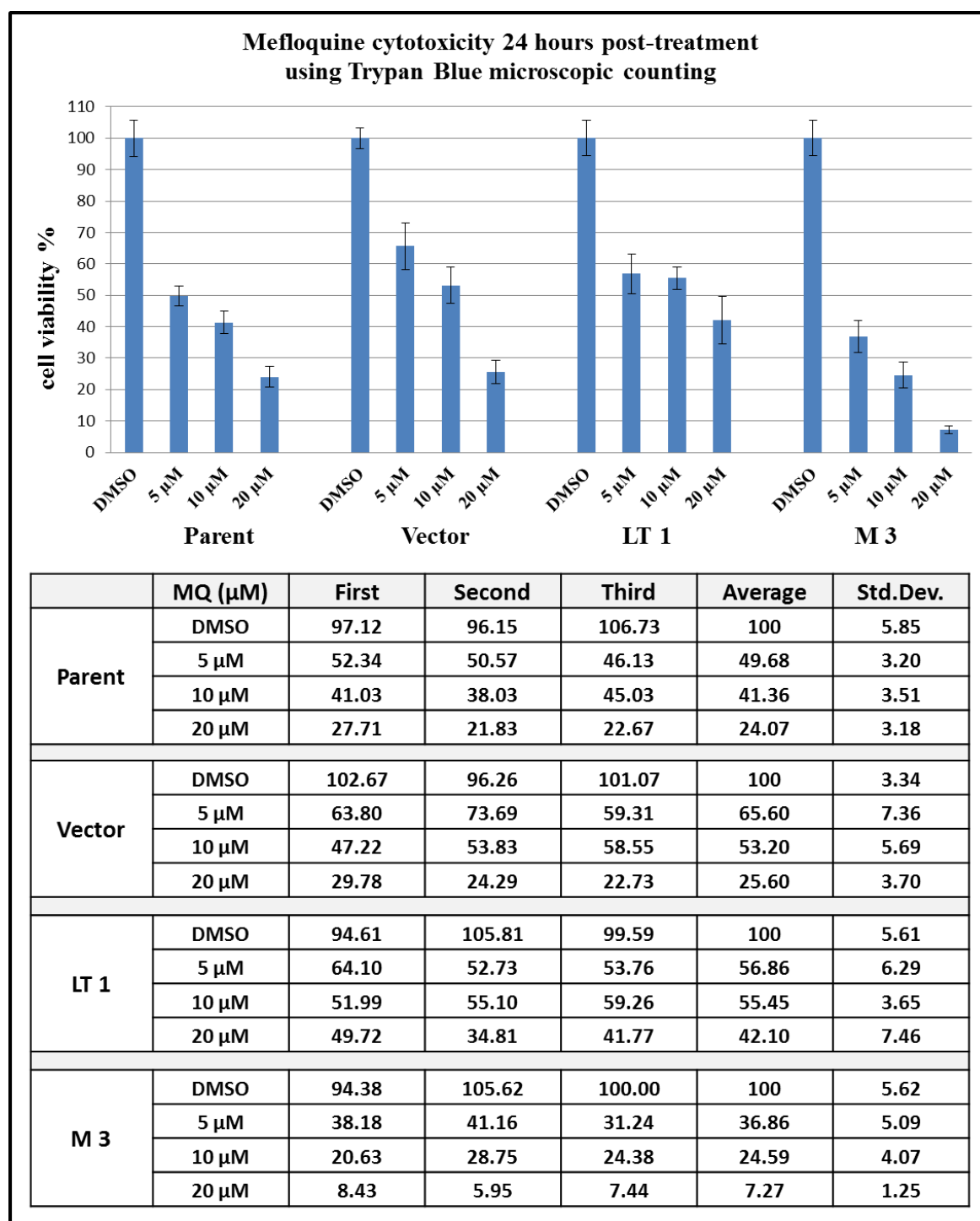


Figure 3.45 Mefloquine cytotoxicity post 24 hrs treatment. Data presented was based on triplicate counts from separate cultures. The table shows cytotoxicity data post-24 hrs treatment with mefloquine .

DMSO-only treated cells showed minimal cell death (Table 3.7) whereas escalating doses of mefloquine were toxic in all tested cell lines. However, JCV LT M3 monoclonal cells exhibited the greatest susceptibility to Mefloquine exposure compared with all the other cells tested. Indeed, >92% of M3 cells were killed by exposure to 20 μ M mefloquine compared to approximately 75% for the other cell lines tested. However, this was not statically significant (p-value $0.06 > 0.05$).

3.5.6 Use of microarrays to analyse the effects of JCV LT on full transcriptome

3.5.6.1 RNA extraction and data filtration

All samples (Figure 5.3.31 in appendix 5.3) had A260/A280 ratios between 1.8 to 2.00 and A260/A230 ratios between 2.00 to 2.20. Purified RNA concentrations were 396 ng/ μ l, 257 ng/ μ l, 385 ng/ μ l, 680 ng/ μ l, 408 ng/ μ l, and 263 ng/ μ l for Parent; LT1; Vector 1; Vector 2; M3; and M6 respectively. Quality control and assurance results are shown in Figure 5.3.32 in appendix 5.3.

3.5.6.2 Array data filtration

Two Group analyses were conducted for JCV LT expression and polyclonal vs monoclonal by t-test with a p value threshold of ≤ 0.05 and a fold change of ≥ 1.5 . Synchronised sample and variable PCA plots were used for cross-validation of AEC quality assurance and node clustering whilst variable heatmap plots were used for unsupervised dendrogram hierarchical clustering. Annotated variable lists which incorporated relevant statistical classes (p value, t statistic, r statistic, fold change) were extracted from the variable PCA plots or variable heatmap plots and these were exported for downstream interpretation. Statistical analysis and filtering JCV LT integration and clonality annotation are shown in Figure 3.46 and Figure 3.47 respectively.

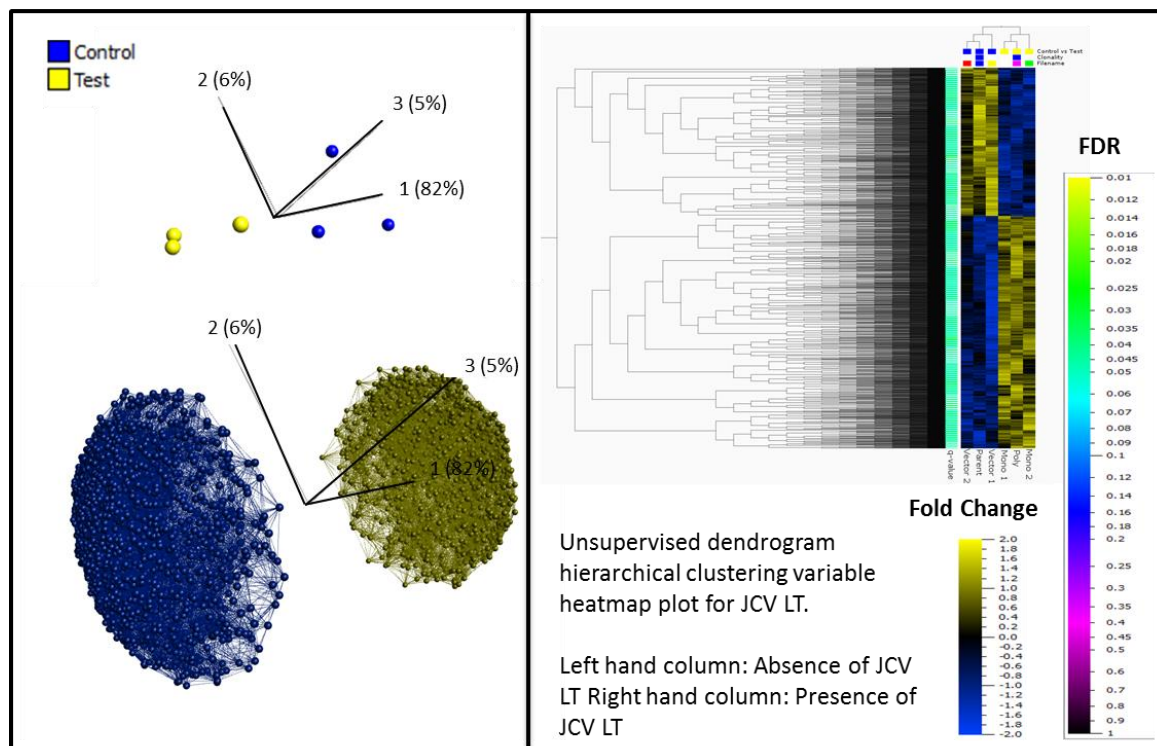


Figure 3.46 Two-way ANOVA was conducted in QOE with JCV LT integration as sample identifier and Entrez Max value as variable identifier. An alpha level of 0.05 provided 3698 variables with 93% PCA coverage at an $FDR \leq 0.05$.

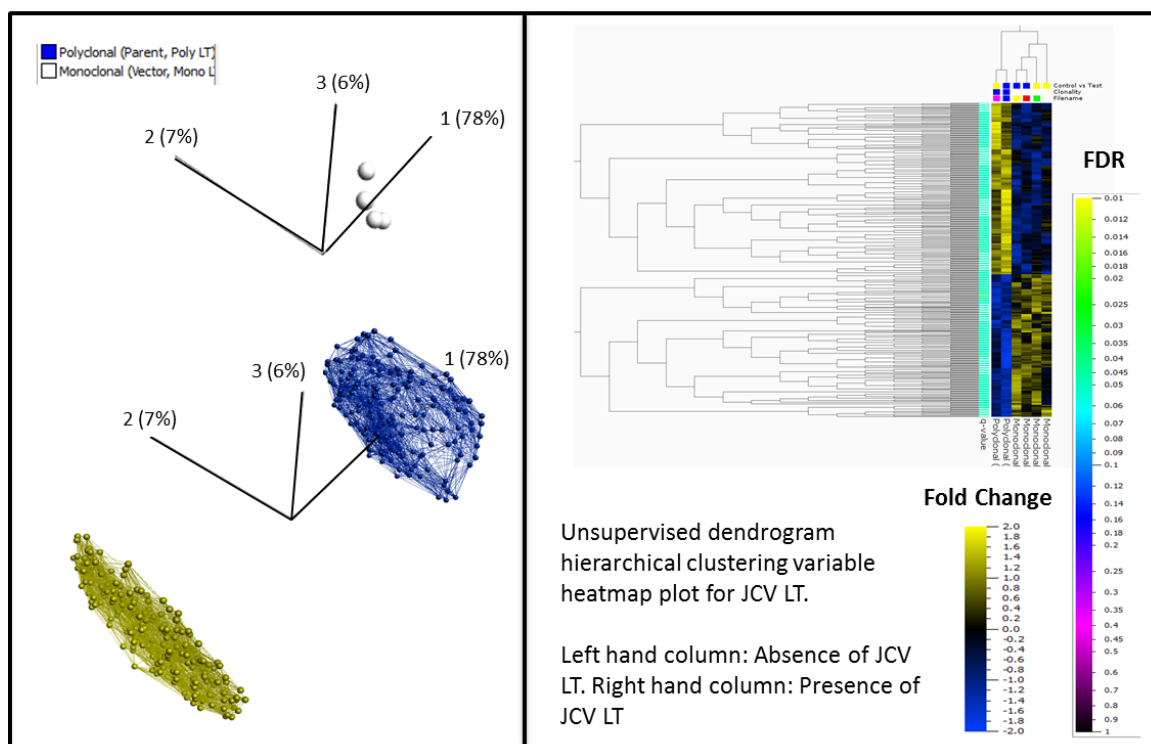


Figure 3.47 Two-way ANOVA was conducted in QOE with vimentin clonality as sample identifier and Entrez Max value as variable identifier. An alpha level of 0.05 provided 411 variables with 91% PCA coverage at an $FDR \leq 0.05$.

3.5.6.3 JCV LT integration two group analysis

Statistically significant changes for pathways, upstream regulators, and IPA networks were assessed by p value overlap of array data with the IKB and activation Z scores. The list from QOE of JCV LT was parsed into ingenuity pathway analysis and core analyses were conducted.

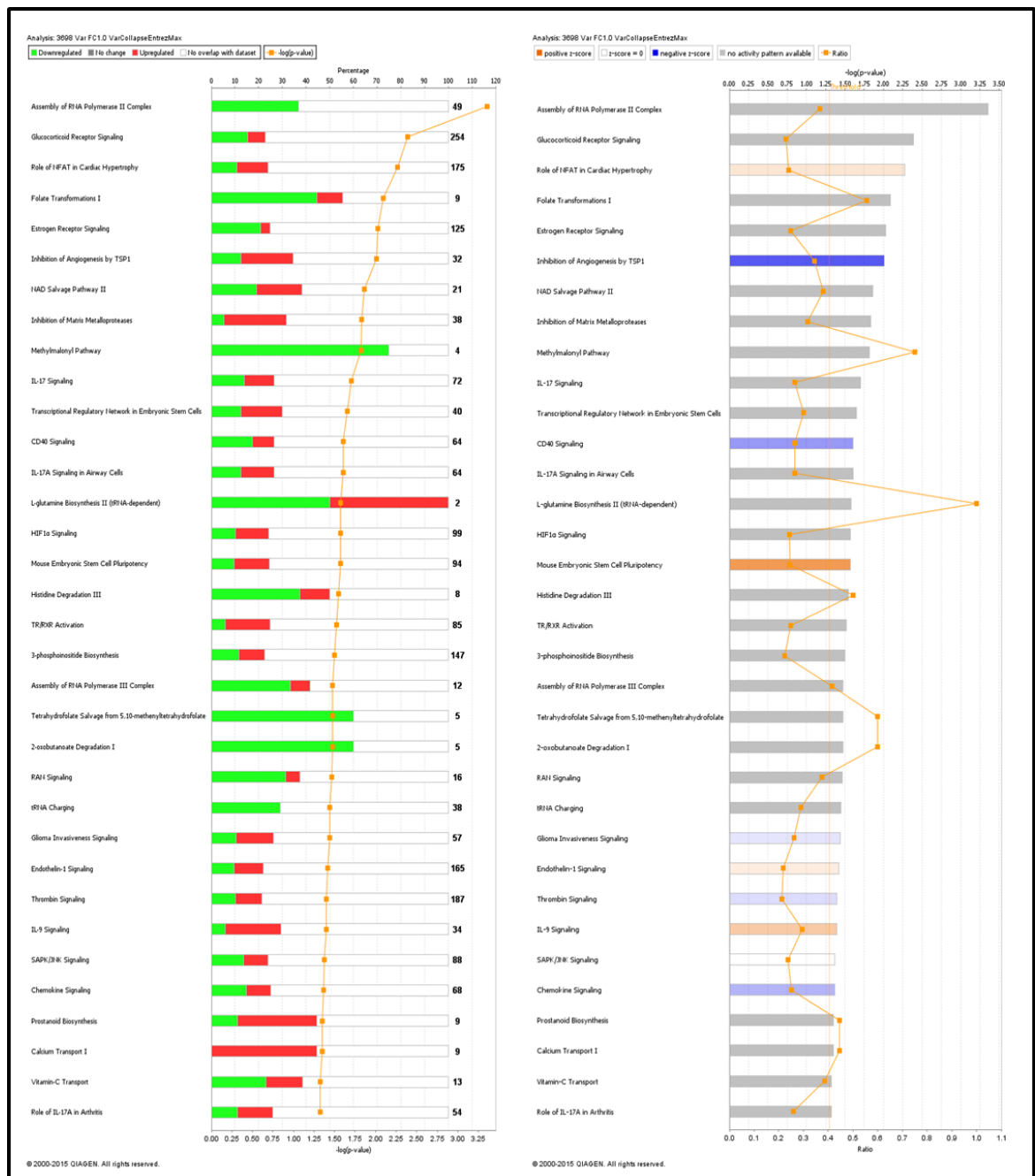


Figure 3.48 Overlap charts of IPA Core Analysis on JCV LT. **Left:** Green (down regulated); red (upregulated); white (no coverage) stacked bar chart for overlap of array data with canonical pathways. **Right:** Equivalent activity status of nine pathway modulations. Blue indicates inhibition of 5 pathways (modest decrease); orange indicate activation of 4 pathways (modest increase).

Figure 3.48 shows that no pathways with high overlap passed the Z score threshold for statistically significant activation or inhibition. Nine pathways depicted a modest modulation in their activation level. Four pathways depicted a modest increase in activity (right hand figure, orange bars) while five pathways depicted a modest decrease in activity (right hand figure, blue bars).

Table 3.6 shows that of the canonical pathways which had low overlap with the array data, six were predicted to be active and eight were predicted to be inactive.

Table 3.6 JCV LT Canonical Pathways

Activation State	IPA Rank	Ingenuity Canonical Pathways	$-\log(p\text{-value})$	Ratio	z-score
Predicted Active	153	cAMP-mediated signaling	5.71E-01	1.81E-01	2.874
Predicted Active	161	Colorectal Cancer Metastasis Signaling	5.36E-01	1.78E-01	2.874
Predicted Active	145	Neuropathic Pain Signaling In Dorsal Horn Neurons	5.94E-01	1.92E-01	2.524
Predicted Active	266	AMPK Signaling	3.36E-01	1.69E-01	2.4
Predicted Active	118	Nitric Oxide Signaling in the Cardiovascular System	7.02E-01	2.00E-01	2.357
Predicted Active	151	eNOS Signaling	5.81E-01	1.87E-01	2
Modest activation	16	Mouse Embryonic Stem Cell Pluripotency	1.57E+00	2.45E-01	1.877
Modest activation	28	IL-9 Signaling	1.40E+00	2.94E-01	1
Modest activation	3	Role of NFAT in Cardiac Hypertrophy	2.27E+00	2.40E-01	0.48
Modest inactivation	25	Glioma Invasiveness Signaling	1.44E+00	2.63E-01	-0.258
Modest inactivation	27	Thrombin Signaling	1.40E+00	2.14E-01	-0.343
Modest inactivation	30	Chemokine Signaling	1.37E+00	2.50E-01	-0.728
Modest inactivation	12	CD40 Signaling	1.60E+00	2.66E-01	-1
Modest inactivation	6	Inhibition of Angiogenesis by TSP1	2.01E+00	3.44E-01	-1.633
Predictive Inactive	222	UVC-Induced MAPK Signaling	4.24E-01	1.90E-01	-2.121
Predictive Inactive	272	Toll-like Receptor Signaling	3.23E-01	1.71E-01	-2.121
Predictive Inactive	206	LPS/IL-1 Mediated Inhibition of RXR Function	4.53E-01	1.75E-01	-2.138
Predictive Inactive	238	Ceramide Signaling	3.84E-01	1.77E-01	-2.138
Predictive Inactive	53	IL-1 Signaling	1.02E+00	2.20E-01	-2.183
Predictive Inactive	88	April Mediated Signaling	8.09E-01	2.37E-01	-2.333
Predictive Inactive	116	B Cell Activating Factor Signaling	7.11E-01	2.25E-01	-2.333
Predictive Inactive	194	NRF2-mediated Oxidative Stress Response	4.89E-01	1.78E-01	-2.53

Further analyses on ‘Upstream Regulators’ from IPA, predicted that four upstream regulators were active (TNFSF11; IL17RA; TNFRSF1B; LAMA5) and one (HOXC9) was inactive (Table 3.7).

Table 3.7 JCV LT Upstream Regulators

IPA Rank	Upstream Regulator	Molecule Type	Predicted Activation State	Activation z-score	p-value of overlap
9	TNFSF11	Cytokine	Activated	3.072	6.56E-03
18	IL17RA	Transmembrane Receptor	Activated	2.961	9.79E-03
39	TNFRSF1B	Transmembrane Receptor	Activated	2.737	2.40E-02
29	LAMA5	Other	Activated	2.4	1.68E-02
8	HOXC9	Transcription Regulator	Inhibited	-2.236	5.67E-03

In addition, IPA ‘Ingenuity Networks’ analysis revealed that four networks were associated with the array data:

1. RNA Post-Transcriptional Modification, Infectious Disease, Organismal Injury and Abnormalities.
2. DNA Replication, Recombination, and Repair, Energy Production, Nucleic Acid Metabolism.
3. Developmental Disorder, Hereditary Disorder, Metabolic Disease.
4. Post-Translational Modification, Organismal Injury and Abnormalities, Hereditary Disorder.

3.5.6.4 Two group analysis of polyclonal Vs monoclonal cells

The list from QOE analysis of clonality was parsed into ingenuity pathway and core analyses conducted. Most significantly 75% of the uploaded fold change array data was unknown by IPA’s knowledge base so currently there were very little usable findings. Due to this low coverage in IPA there was little overlap of genes between pathways and consequently none of the returned pathways passed activation Z scores.

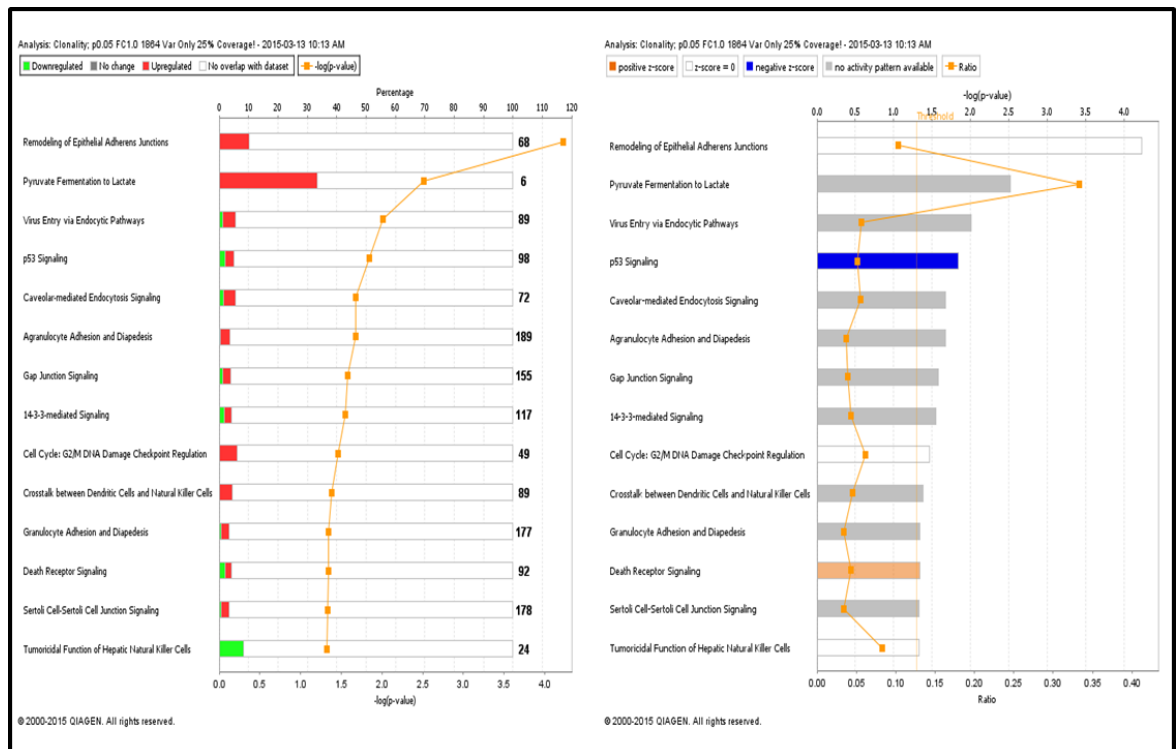


Figure 3.49 Overlap charts of IPA core analysis obtained on clonality. **Left:** Green (down regulated); red (upregulated); white (no coverage) stacked bar chart for overlap of array data with Canonical Pathways. **Right:** Equivalent activity status of pathway. Blue indicates inhibition; orange indicate activation.

Most significantly, 75% of the differentially regulated genes involved were novel with unknown functions and only 25% of the array dataset was recognised by IPA's knowledgebase. Due to the low coverage there were no predictions on neither 'Upstream Regulators' nor 'Ingenuity Networks'.

Table 3.8 Ingenuity canonical pathways modulated by clonality.

IPA Rank	Ingenuity Canonical Pathways	-log (p-value)	Ratio	Down-regulated	No change	Up-regulated	No overlap with dataset
1	Remodeling of Epithelial Adherens Junctions	4.23E+00	1.03E-01	0/68 (0%)	0/68 (0%)	7/68 (10%)	61/68 (90%)
2	Pyruvate Fermentation to Lactate	2.51E+00	3.33E-01	0/6 (0%)	0/6 (0%)	2/6 (33%)	4/6 (67%)
3	Virus Entry via Endocytic Pathways	2.01E+00	5.62E-02	1/89 (1%)	0/89 (0%)	4/89 (4%)	84/89 (94%)
4	p53 Signaling	1.84E+00	5.10E-02	2/98 (2%)	0/98 (0%)	3/98 (3%)	93/98 (95%)
5	Caveolar-mediated Endocytosis Signaling	1.68E+00	5.56E-02	1/72 (1%)	0/72 (0%)	3/72 (4%)	68/72 (94%)
6	Agranulocyte Adhesion and Diapedesis	1.67E+00	3.70E-02	1/189 (1%)	0/189 (0%)	6/189 (3%)	182/189 (96%)
7	Gap Junction Signaling	1.58E+00	3.87E-02	2/155 (1%)	0/155 (0%)	4/155 (3%)	149/155 (96%)
8	14-3-3-mediated Signaling	1.55E+00	4.27E-02	2/117 (2%)	0/117 (0%)	3/117 (3%)	112/117 (96%)
9	Cell Cycle: G2/M DNA Damage Checkpoint Regulation	1.46E+00	6.12E-02	0/49 (0%)	0/49 (0%)	3/49 (6%)	46/49 (94%)
10	Crosstalk between Dendritic Cells and NK Cells	1.38E+00	4.49E-02	0/89 (0%)	0/89 (0%)	4/89 (4%)	85/89 (96%)
11	Granulocyte Adhesion and Diapedesis	1.34E+00	3.39E-02	1/177 (1%)	0/177 (0%)	5/177 (3%)	171/177 (97%)
12	Death Receptor Signaling	1.34E+00	4.35E-02	2/92 (2%)	0/92 (0%)	2/92 (2%)	88/92 (96%)
13	Sertoli Cell-Sertoli Cell Junction Signaling	1.33E+00	3.37E-02	1/178 (1%)	0/178 (0%)	5/178 (3%)	172/178 (97%)
14	Tumoricidal Function of Hepatic NK Cells	1.32E+00	8.33E-02	2/24 (8%)	0/24 (0%)	0/24 (0%)	22/24 (92%)
15	Methylmalonyl Pathway	1.24E+00	2.50E-01	0/4 (0%)	0/4 (0%)	1/4 (25%)	3/4 (75%)
16	Epithelial Adherens Junction Signaling	1.20E+00	3.42E-02	0/146 (0%)	0/146 (0%)	5/146 (3%)	141/146 (97%)
17	CMP-N-acetylneuramate Biosynthesis I (Eukaryotes)	1.15E+00	2.00E-01	0/5 (0%)	0/5 (0%)	1/5 (20%)	4/5 (80%)
18	2-oxobutanoate Degradation I	1.15E+00	2.00E-01	0/5 (0%)	0/5 (0%)	1/5 (20%)	4/5 (80%)
19	dTMP De Novo Biosynthesis	1.15E+00	2.00E-01	0/5 (0%)	0/5 (0%)	1/5 (20%)	4/5 (80%)
20	Tyrosine Degradation I	1.15E+00	2.00E-01	1/5 (20%)	0/5 (0%)	0/5 (0%)	4/5 (80%)
21	Superpathway of Methionine Degradation	1.10E+00	6.25E-02	0/32 (0%)	0/32 (0%)	2/32 (6%)	30/32 (94%)
22	Agrin Interactions at Neuromuscular Junction	1.10E+00	4.35E-02	0/69 (0%)	0/69 (0%)	3/69 (4%)	66/69 (96%)
23	Zymosterol Biosynthesis	1.07E+00	1.67E-01	1/6 (17%)	0/6 (0%)	0/6 (0%)	5/6 (83%)
24	Germ Cell-Sertoli Cell Junction Signaling	1.07E+00	3.12E-02	0/160 (0%)	0/160 (0%)	5/160 (3%)	155/160 (97%)
25	Hereditary Breast Cancer Signaling	1.06E+00	3.48E-02	2/115 (2%)	0/115 (0%)	2/115 (2%)	111/115 (97%)

NB: pathways (in red) were junctional related, cell cycle/DNA damage related, virus related.

Of interest, in spite of low coverage, the top associated pathways were junctional signalling; p53, DNA damage & cell cycle checkpoint; and virus related as shown in the following table. Pathways either have coverage but no change, or depict only a modest change.

Chapter 4

Discussion

4. Discussion

4.1 General discussion

The primary goal of this project was to analyse any potential co-operativity between HPV and the polyomavirus family members SV40, JCV, BKV and MCV in women with pre-cancerous changes of the cervix and invasive cervical carcinomas. A secondary aim was to test if any observed co-operativity was influenced by HIV infection. Although no evidence of SV40 or MCV was seen in samples, clear evidence of BKV and JCV was demonstrated.

Initially, technical optimisation of PCR protocols for virus detection was carried using control and test clinical material. This proved challenging since approximately 8% of the human genome consists of DNA sequences that share homology with viruses [177]. Thus, sequence alignments by comparative genomics and literature mining were used extensively to optimise and develop the PCR assays used. For the purposes of primer design, the polyomavirus LT antigen was chosen as the preferred amplification target. The rationale behind this was that LT is the principal viral regulatory protein synthesised during early gene expression, it is the first part of the genome to be expressed and it has a conserved structure by virtue of its rigid functional constraints [72].

Optimisation steps involved the development and validation of PCR conditions at different annealing temperatures that could overcome the problems associated with primer-dimer accumulation and non-specific band formation. Indeed, the selection of each primer required specific optimisation for every target gene with annealing temperatures playing an essential role in the optimisation process. Multiplex procedures were evaluated that simultaneously amplified multiple target amplicons in order to increase the chances of

target detection and to reduce the chances of non-specific product amplification [178]. Furthermore, to ensure consistency, the lowest concentration of input positive control detectable was used in every assay. Moreover, specific precautions were taken during sample handling to reduce the possibility of physical transfer of DNA ‘carryover contamination’ between amplified products and test samples. For example, the positive control was aliquoted last of all after the test PCR test tubes were fastened. Using these considerations, multiplex and singleplex end-point PCR methods were successfully optimised and used to test for the presence of the indicated polyomaviruses.

What factors may be involved in the observation that no MCV or SV40 DNA was detected in cervical specimens using these methods since it was clearly demonstrated that they were able to detect reproducibly as little as 18 copies of input viral DNA? There are, however, conflicting reports in the literature showing both the presence and absence of SV40 in female genitalia. For example, in a previous study using DNA from high and low-grade pre-cancerous cervical lesions, none of 93 tested samples was positive for SV40 [179]. However, Martini et al., (2004) detected SV40 DNA in DNA isolated from 1 out of 14 normal cervical tissues which suggests that cellular tropism may not be the reason behind our negative results although contamination from urine cannot be excluded in the former study.

Previous investigations on the prevalence of SV40 in human tumours included mesothelioma, brain tumours, and non-Hodgkin lymphoma which all proved inconclusive [36, 103, 104]. This inconsistency in SV40 tissue tropism may be related to issues with either the PCR assays used or sample contamination which may occur at source or during processing. PCR contamination at source is especially significant with SV40 since millions of people were accidentally infected with SV40 in the early batches of polio vaccine.

Contamination during sample processing is an issue as cloned SV40 DNA sequences are very commonly used in laboratories throughout the world. Thus, it is possible that the aforementioned studies were conducted on individuals who received contaminated vaccine or were carried out with primers that can amplify sequences present in common laboratory contaminants [180]. It may be that future studies could include additional primer combinations that target SV40 regions that are not typically present in laboratory plasmids. Comparison of these results with those obtained from primers which do target plasmid encoded sequences would distinguish between genuine and contamination derived signals. In the current study, none of the cervical specimens from either HIV positive or HIV negative individuals, with or without HPV, tested positive for SV40 DNA which strongly suggests that the presence of SV40 in female genitalia is uncommon.

The observation that MCV DNA could not be detected in any of the cervical samples tested could be due to the fact that tumours positive for MCV do not always show positivity for all primer pairs. Therefore, it is possible that this could be related to different strains of MCV although this has yet to be determined [29]. However, in the case of MCV, PCR-based methods are also prone to subtle contamination potentially from individuals handling samples at collection as MCV, in particular, is shed from the skin. Furthermore, since DNA is extracted from cancer tissues, these may contain traces of surrounding tissues or blood which may also have viral DNA present in non-tumour rather than tumour tissue [59]. Our finding of no MCV DNA in cervical specimens suggests that this tissue does not exhibit tropism for MCV and implies that the virus does not play an aetiological role in cervical carcinogenesis. As previously discussed, MCV is the only polyomavirus with a proven role in development of a human cancer and, to our knowledge, ours is the first investigation into its prospective relationship with HPV-related cervical dysplasia and cancer.

Since the samples in this study were cervical specimens, other influences should also be considered. For example, in view of the complex nature of AIDS-related diseases, it could not be concluded whether MCV and SV40 sequences were physically absent or was this perhaps due to loss of epithelial or immune cells as a consequence of the menstrual cycle or possibly from immuno-suppression associated with HIV patients [181]. Furthermore, absence of these viruses could also result from the fact that some viruses remain latent and are not activated as a consequence of vaginal or cervical inflammation associated with genital disease [182]. However, given the high sensitivity of our methods this is not likely.

The same sample set was used to explore whether there was an association between the presence of JCV or BKV and different stages in the development of cervical cancer. Furthermore, JCV/BKV is known to establish latent infections which can be reactivated by immuno-suppression (e.g. in transplant recipients and HIV-infected patients). Moreover, previous reports have suggested that BKV and JCV are associated with multiple tumours. For example, in addition to its role in PML, JCV DNA was also detected in mesotheliomas, brain tumours, osteosarcomas, and lymphomas [168, 179] and BKV has also been found in brain tumours, adenocarcinomas, prostate cancers, and bladder carcinomas [49, 53]. Most significantly, previous studies on the presence of BKV and JCV in urogenital carcinomas have indicated that they may play a role as co-factors in the development of these malignancies [59]. Indeed, Comar et al showed that BKV was found more frequently in Italian women with high-grade squamous intraepithelial lesions in association with high-risk HPV-16 and reported that 83% (34/41) tested positive for BKV sequences, whereas 17% (7/41) were positive for JCV.

Curiously the results obtained in the current study showed that JCV DNA was present in all 24 cervical samples, whereas none contained BKV which has been previously shown to be present in female genital tumours [168]. This finding suggested that, whilst JCV and BKV are closely related, they have different geographical distributions and our study clearly demonstrates the predominance of JCV within African women. Indeed, it is well known that JCV infection rates vary depending on geographical location and ethnic origin and it has even been suggested that JCV may be a bio-anthropological marker that is useful for studying the early migration of human populations around the world [183]. Based on sequence analysis of the major capsid protein (VP1), JCV can be divided into a number of subtypes ($n > 14$) which also have distinctive geographic distributions. Thus it is possible that JCV may have co-diverged with migratory human populations over many thousands of years [184, 185] and it would be very interesting to analyse the relationship of these subtypes with respect to disease.

The work presented herein raises the obvious question what might be the reason for the finding of JCV in a sub-set of HIV positive cervical tumours but not in others? One possibility is that this could be related to HLA type as this is known to selectively influence susceptibility to infection with specific types of virus [186, 187]. In this regard, HLA typing was attempted on DNA extracted from the cervical FFPE material at the Transplantation Laboratory in Manchester Royal Infirmary. However, the HLA typing amplicon requires a fairly substantial read-length of about 750 bases and this was not possible most likely due to DNA fragmentation which occurred during paraffin embedding.

An attempt was made to find an association between the frequency of JCV virus and HPV16/18 because it was shown previously, on the same sample set, that the spectrum of

HPV types is altered by HIV infection in both cervical smears and ICCs which suggested a complex interplay between HPV and HIV during progression to cervical cancer [167]. The specific cellular interactions underlying co-infection with these viruses and how this influences cancer progression requires clarification and is not straightforward. It is possible that HIV-related immunosuppression enhances the persistence of HPV and, as a consequence, facilitates its oncogenic progression [188]. Our findings, however, would seem to be consistent with the hypothesis that co-infection with two or more different disease-causing organisms in one individual can facilitate the disease process.

Although not statistically significant, the current findings indicated that JCV was more common in HPV16/18 negative carcinomas than in HPV16/18 negative smears which implies that JCV could be involved in cervical carcinogenesis, albeit in a defined subset of this disease exemplified by HIV positive and HPV16/18 negative women. The observation of 5% JCV positivity in HPV16/18 negative smears compared to the 9% JCV positivity in HPV16/18 negative carcinomas suggested a trend whereby JCV may be more common in carcinomas that are positive for lower-risk HPV sub-types.

Comparison of the incidence of JCV in cervical smears and cervical carcinomas showed a 3-fold increase in samples from HIV positive women with cervical carcinoma ($P=0.025$) which indicated a significant association between JCV and cervical carcinoma, but only in HIV positive women. Considered collectively, it can be concluded that JCV may combine with low-risk HPV infection in women infected with HIV to influence the rate of progression to invasive cervical carcinoma. With the current data set, it could not be distinguished whether the finding of three times the rate of JCV infection was related to the aetiology of cervical cancer or alternatively was a bystander event associated with other HIV/AIDS related pathologies since reactivation of latent polyomaviruses is known to

influence AIDS-associated immunosuppression [28]. Furthermore, several studies have documented urinary excretion of JCV and BKV in HIV positive patients suggesting that polyomavirus reactivation is a feature of HIV infection [53, 54, 189]. Moreover, in association with cellular proteins, the HIV-1 Tat protein is known to bind to the JCV non-coding region to stimulate JCV transcription and replication [48]. Indeed, cross-interaction between agnoprotein of JCV and HIV-1 Tat protein is known to modulate transcription of the HIV-1 long terminal repeat in glial cells in the brains of AIDS/PML patients where astroglial cells can serve as a unique site for both viruses [190].

Our study suggests that there could be co-operativity between HPV and polyomaviruses in women infected with HIV which may influence the rate of progression to invasive cervical carcinoma. Moreover, these observations suggest there is the potential for co-operativity between polyomaviruses and other viruses in the development of human malignant disease per se. Indeed, this is supported by the fact that both HPV E6 and E7 oncoproteins and the LT antigen of polyomaviruses have been reported to significantly interfere with the tumour suppressive functions of p53 and pRb thus contributing to chromosomal instability [23]. Clearly this has the potential to affect cell cycle control and inhibit apoptosis, thereby inducing genetic instability and malignant transformation of infected target cells [21]. The findings of our study do not exclude the possibility that other co-factors could be involved in the disease process. Whether these are internal factors, such as mutation, protein mis-regulation or immunosuppression, or alternatively external factors such as radiation, chemical carcinogens or even other viruses remains to be determined [7, 45, 97, 191].

It is noteworthy that publication of the results of our study has had significant implications for medical practice since we were invited to participate in a WHO study to

assess our method as a means of detecting JCV as an International Standard Procedure. With over 23 participants from clinical and research laboratories as well as kit manufacturers, we participated in this international collaborative study to develop a method of diagnoses for JCV and, in our case, simultaneous detection of BKV. Indeed, the development of a sensitive non-invasive assay for the detection of BK/JC viruses was the second aim of this project since the current gold standard diagnostic test for BK virus related BKVN and JC virus related PML is through clinical biopsy. This is both invasive and costly as only well-equipped hospitals and laboratories with trained personnel can perform this type of procedure. Several non-invasive assays of blood and urine have been developed although none have been validated using PCR that allowed maximum sensitivity and specificity for the simultaneous detection of both BKV and JCV [136]. Indeed, our method is the subject of an invention record with The University of Manchester Intellectual Property Ltd. Commercialisation of a simple, rapid, non-invasive detection kit is believed to be of significant benefit for both clinical trials and epidemiological investigations carried out by the WHO on the prevalence of JCV/BKV related diseases especially in Africa. Furthermore, it is anticipated that improved diagnosis should lead to a better understanding of their pathogenesis and thereby contribute to the development of new treatment strategies.

In view of the previously discussed findings, it is possible that JCV may act synergistically with HPV and HIV to facilitate the transformation of the cervical epithelium. A potential limitation is that our method is based on the detection of viral genomic DNA which provides no information on the transcriptional activity of the candidate viruses. However, since JCV LT is known to promote genetic instability by targeting p53 and Rb combined with the observation that polyomavirus LT antigen dysregulates β -catenin signalling in colon cancers and medulloblastoma [74, 192], it was

decided to investigate the potential of JCV LT antigen (2067 bp ORF) to synergise with HPV E6/E7 to transform human immortalised keratinocytes *in vitro*.

The prototype E6/E7 immortalised cell lines (Keratinocytes) were chosen because SV40 LT and ST antigens were shown to trans-activate and stimulate the HPV16 and HPV18 promoter/enhancer. Co-transfection of human keratinocytes with SV40 small T antigen cDNA, together with HPV16 DNA, increased the transforming activity of HPV16 by 10-fold to 15-fold [101]. Furthermore, keratinocytes were deemed to be a suitable cell model since MCV is the only polyomavirus to demonstrate a strong correlation with the pathogenesis of human Merkel cell skin cancer [24]. The LT antigen was chosen for these investigations since, as has been discussed, it has the ability to compromise the stability of cellular tumour suppressors [193].

E6/E7 immortalised keratinocytes were stably transfected with the JCV LT expression construct and stable polyclonal and monoclonal cell lines generated. RT-PCR confirmed stable expression of LT mRNA in transfected cells and immunocytology staining, in addition to Western blotting, confirmed that the LT protein was being expressed. Immunostaining demonstrated that the LT protein was strongly expressed in many, but not all, nuclei of both polyclonal and monoclonal LT transfected cells which showed a diffuse nuclear and sometimes reticulated pattern. What factors could explain this variable staining pattern? It is possible that this could be related to cell-cycle dependent regulation of LT protein expression during the transition from one phase to another [194]. For example, p53 is known to regulate growth by holding cells at the G1/ S phase of the cell cycle long enough for DNA damage detection and repair pathways which then result in cell cycle arrest [195]. It is possible that this type of abnormal cell cycle arrest in response to DNA damage could have been the cause of the diffuse nuclear staining pattern [194-196]

although further experimentation will be needed to explore this possibility. For example, LT transfected cells could be synchronised and expression of the LT protein then analysed by flow cytometry with respect to time so that this could be directly correlated with the different phases of the cell cycle.

The cell line population doubling times showed no discernible difference in growth rate between the transfected cells and parental controls. However, although no statistical correlations were apparent between cell growth rates, there was a trend which suggested that expression of the LT protein reduced the growth rate. This is consistent with the previously hypothesised prolonged cell-cycle arrest which may occur via the detection and repair of DNA whereby cells undergo a transient arrest in response to sensing LT induced genomic instability. Indeed, the correlation between increased population doubling time associated with LT expression compared to the decrease observed in the controls suggested that the slower rate of proliferation could be explained by decreased genome stability caused by LT. This is consistent with previous studies carried out on SV40 LT which was shown to disturb the formation of nuclear DNA-double strand repair foci and it was concluded that LT has a direct effect on DNA repair [197]. Similarly, Nbs1 is another protein associated with the repair of double strand breaks which was shown to interact with SV40 LT antigen thereby disrupting the control of DNA replication [198]. Most significantly a study carried out on JCV LT showed its ability to compromise homologous recombination DNA repair was dependent on its interaction with insulin receptor substrate 1 (IRS-1) whereby this provided a link between JCV LT, insulin-like growth factor I receptor (IGF-IR) signalling and genetic instability [199]. Moreover, although the LT antigen is generally considered to augment genetic instability [57, 60, 74, 199], the molecular mechanisms underlying this effect are not well understood. In relation to our findings, it is important to consider the inherent experimental limitations such as whether

the observed changes in cell proliferation could be attributed to LT induced growth arrest at specific phase of the cell cycle, or whether they are due to other factors resulting in the reduced proliferative capacity of cells. It is clear that further experimentation will be needed to address this issue.

The ability of cells to form transformed colonies which have lost the property of cell contact growth inhibition, can be used to assess the transforming potential of any given treatment [200]. Colony formation thus provided a useful indicator of malignant transformation induced by ectopic expression of the JCV LT antigen. Other features consistent with transformation include phenotypic alterations in cellular morphology, disruption of cell-to-cell interactions, reduction of the connection of Gap junctions', and acquisition of growth factor independence [144]. As discussed, the ability of both JCV and SV40 LT to cause these effects is well established [201, 202]. However, unexpectedly in the current study, no significant difference was seen in colony formation between any of the LT transfected cells and controls. One intriguing possibility is that these results suggest that expression of JCV LT may be only one step in a series of events in the pathway toward tumorigenicity. Indeed, in the case of SV40, it has been proposed that expression of the LT antigen is not sufficient for transformation of NIH 3T3 cells [203]. Elenbaas and colleagues studied the tumorigenicity of primary human mammary epithelial cells (HMEC) cell lines after these were transfected with three oncogenes including the SV40 LT. It was found that tumourigenesis was dependent on the combined presence of all 3 oncogenes which, when expressed independently, failed to form colonies in soft agar [204]. Indeed, immortalisation per se was not sufficient to induce tumourigenesis [81, 205],

Following on from this work our observations on the morphology of JCV LT expressing cells, when compared to controls, indicated the presence of some fibroblast-

like, spindle-shaped cells in the LT expressing monoclonal cells. In light of this it was postulated that JCV LT could be enhancing a limited conversion of parental E6/E7 immortalised keratinocytes to a more migratory mesenchymal cell type (EMT). Thus it was decided to test for EMT since it has previously been demonstrated that a proportion of ovarian surface epithelial cells immortalised with SV40 LT showed an EMT phenotype associated with absence of E-cadherin, expression of vimentin, cytokeratins and type III collagen [148]. In another study, SV40 LT caused loss of epithelial differentiation in Madin-Darby canine kidney epithelial cells which showed fibroblast-like morphology and acquired invasive properties [149]. EMT was also observed in human mammary epithelial cells immortalised with SV40 LT antigen and overexpression of TGF- β , Snail, or Twist was observed [150]. Most significantly a study carried out on SV40 LT-immortalized rat liver cells showed that EMT can be reversibly observed by only switching the type of culture medium used, and the converted phenotypes can be reversed by returning them to the original culture medium [206].

It is significant in the current study that the most interesting effect on EMT markers was the difference in levels of vimentin protein which was only expressed in parent and LT polyclonal cells and not in vector or LT monoclonal cells. This may seem paradoxical although it is most likely related to the fact that the monoclonal cell lines were expanded from single cells. Vimentin is an EMT related cytoskeletal protein which is responsible for maintaining cell shape, the integrity of the cytoplasm and stabilisation of cytoskeletal interactions [156]. Our results indicate that the cloning process may have negatively influenced EMT-related changes by selecting for cells with a reduced migratory capacity. Indeed, the selection pressure encountered during the single-celled colony selection procedure is very likely to affect the reproductive success of cells growing at low cell densities. Moreover, it is well known that different culture conditions, and most notably

cell densities, can markedly influence the characteristics of derived clonal cell populations [207, 208]. Clearly, these results could have wider implications for other studies where similar cloning procedures are used and further investigation on the expression of vimentin in relation to clonality is warranted. It may be that different culture conditions could alter this effect as has been described for SV40 LT [206]. For example, growing cells on Matrigel or on irradiated feeder layers to enhance their proliferation and survival may confirm whether or not the effect on vimentin was a result of selecting for cells growing at low cell densities.

Regarding the other EMT markers, snail mRNA was actually increased in LT monoclonal cells with no concomitant up-regulation of protein suggesting that snail expression may be regulated translationally. It is known that transcriptional activation of Snail activates mesenchymal genes [157] and the observed reduction of Snail protein expression, combined with increased mRNA, suggests that snail expression may be regulated by different means other than transcription. Likely mechanisms could be altered protein stability or alternative spliced transcripts which are translated at different rates [209]. However, it is important to realise that the RT-PCR results presented were semi-quantitative and thus should not be over-interpreted since quantitative real time RT-PCR would provide a more definitive answer [210].

Neither up-regulation of N-Cadherin nor down-regulation of E-cadherin was observed in LT transfected cells demonstrating that the EMT associated phenomenon known as the 'cadherin switch' did not occur [154, 155]. Although collectively the results of analysing EMT markers did not confirm that LT could induce an EMT transition they did provide evidence of the importance of culture conditions when the intention is to evaluate these parameters in monoclonal versus polyclonal cell lines. It is perhaps

paradoxical that JCV LT might enhance genetic instability and potentially malignant transformation, but that the growth conditions used clearly had a profound effect on expression of this phenotype. For the future it would be interesting to determine whether this was a genetic or epigenetic effect.

The previously discussed results from molecular, biological, and therapeutic tests on JCV LT expressing and control cell lines indicated that this protein was not an overt oncogene in these culture systems. However, irrespective of LT expression, it was noted that there were differences in vimentin expression which were associated with cellular clonality. In light of these observations, it was decided to evaluate changes in total gene expression which occurred in these cells. The rationale underlying this was that it will identify alteration in pathways which, although not related to obvious change in cellular phenotype, may still provide new information regarding the effects of JCV LT and/or clonality.

Human transcriptome expression array analyses on the effects of ectopic expression of JCV LT proteins in E6/E7 immortalised keratinocytes did not produce any significant JCV LT related changes in cellular phenotype. JCV LT microarray analyses showed that no pathways with high overlap passed the Z score threshold for statistically significant activation or inhibition with all pathways showing only a modest change. Analysis of the data with respect to clonality showed the top scored associated pathways were junctional signalling; p53, DNA damage & cell cycle checkpoint; and virus related which are all entirely consistent with pathways which may be involved in clonal selection. Most significantly, 75% of the differentially regulated genes involved were novel with unknown functions which indicates that further analyses of the function of these genes may provide insights into their role in clonal selection.

In addition, analyses of JCV LT by IPA predicted that four upstream regulators were activated (TNFSF11; IL17RA; TNFRSF1B; LAMA5) and one (HOXC9) was inactivated with no previous work linking JCV LT to these genes. It is possible that the LT protein caused up-regulation of TNFSF11, TNFRSF1B signalling. Notably the tumour necrosis factor ligand superfamily member 11 (TNFSF11) has a role in the regulation of apoptosis [211]. Furthermore, studies on leukaemia have suggested that high expression of TNFSF11 promotes micro-environmental conditions which influence cell migration [212]. The second gene (TNFRSF1B) also belongs to the same tumour necrosis family which is also mediated within the tumour microenvironment in ovarian cancer patients [213]. Given that LT is a viral protein it is very likely it will have a pro-inflammatory role and activation of the Interleukin 17 Receptor A (IL17RA) is known to play a pathogenic role in many inflammatory and autoimmune diseases such as rheumatoid arthritis although little is known about its role cancer prognosis [214]. Laminin subunit alpha-5 (LAMA5) is a protein that is a major component of basement membranes and has been implicated in a wide variety of biological processes including cell adhesion, differentiation, migration, signalling and metastasis [215]. The observation that JCV LT caused inactivation of the function of homeobox protein Hox-C9 (HOXC9) may be especially significant. HOXC9 is a transcription factor that plays an important role in morphogenesis and it has been shown to induce neuronal differentiation in neuroblastoma cells [216]. Since JCV is known to target neuronal cells, this may have relevance to the pathogenesis of JCV induced PML lesions.

During the course of this project, it was noted that mefloquine had been reported to exert efficacy against JC virus [111] and notably Gofton et al. in 2013 reported successful treatment of PML with mefloquine in a 54-year-old woman [163]. Mefloquine has also

been reported to achieve good penetration into the CNS such that it achieved sufficient concentrations in the brain to act against JCV related PML [159-163]. Although the exact mechanism of action is uncertain, Brickelmaier et al showed that mefloquine does not block viral cell entry but inhibits viral DNA replication after viral entry [217] and a recent study has shown that mefloquine exerts anti-cancer activity in prostate cancer cells [158]. In 2014, Rodrigues et al. evaluated mefloquine activity against four cancer cell lines and concluded that mefloquine–oxazolidine derivatives are considered to be useful leads for the rational design of new anti-tumour agents [176].

Based on these observations it was decided to investigate whether mefloquine possessed any cytotoxic effects against LT transfected cells when compared to controls. It was noted that mefloquine produced a clear dose-dependent inhibition of growth in LT transfected cells at concentrations of 20 μ M and above and JCV LT M3 monoclonal cells showed the greatest susceptibility to treatment. Although not statically significant (p-value $0.06 > 0.05$), this finding inferred that mefloquine may have selective activity against the effects of JCV LT. Since the parental cells were already immortalised prior to the introduction of JCV LT, it is perhaps difficult to appreciate why they may become sensitive to a JCV targeting agent such as mefolquine. However, it is well known that cells can become addicted to ectopically expressed oncogenes which may explain this phenomenon [218].

4.2 Conclusion

The primary goal of this project was to analyse potential co-operativity that might exist between different types of tumour virus and the results suggested that JCV may

combine with low-risk HPV infection in HIV positive women to influence the rate of progression to invasive cervical carcinoma.

The secondary goal of this project was to develop a sensitive non-invasive assay for the detection of BK/JC viruses since the current gold standard diagnostic test for BKV related BKVN and JCV related PML is through clinical biopsy. The inclusion of our novel method in the standardisation of nucleic acid amplification technology in the first WHO International Standard for JCV was a notable outcome.

The third goal of the project was to address the synergistic potential between viruses to transform cells and the potential of antiviral compounds to interfere with this process. Transfection of the JCV LT antigen into the prototype E6/E7 immortalised cell lines permitted investigation of the aetiologic potential of JCV to contribute to cervical carcinogenesis. Polyomaviruses are ubiquitous worldwide [119] and we speculate they are not innocent “bystanders” since their LT antigens are known to have pleiotropic effects against tumour suppressors [42]. However, it is very clear that they are not overt carcinogens since their effects rely on immunosuppression and the presence of accessory factors [6].

4.3 Novel Findings

- JCV was more common in HIV-positive than in HIV-negative cervical carcinomas which suggested potential co-operativity between cancer viruses in the development of this disease.
- JCV was more common in HPV16/18 negative carcinomas than in HPV16/18 negative smears which suggested a trend whereby JCV may be more common in carcinomas which are positive for lower risk HPV sub-types.
- The development of a sensitive non-invasive assay for the simultaneous detection of BK/JC viruses and participation in the first WHO International Standard for JCV testing was a notable outcome of the project.
- Transformation and EMT assays indicated that JCV LT was not a potent oncogene in the cell system used which suggested mechanistically this could play an accessory role in conjunction with other factors in the transformation process.
- LT expressing cells exhibited moderately increased susceptibility to mefloquine exposure which supports further studies aimed at investigation of the antiviral properties of this compound.

4.4 Future work

4.4.1 Business potential

The development of a diagnostic kit for the detection of BK/JC viruses is a rapid, sensitive, and non-invasive method that has a commercial potential since our method is the subject of an invention record with The University of Manchester Intellectual Property Ltd. Although the formal establishment of the standard will be published by the WHO ECBS, we were informed by the NIBSC study organiser that our lab was the only one over 23 participants from clinical and research laboratories to detect co-infection with both JCV and BKV in patient A. Commercialisation of a rapid non-invasive detection kit is believed to be of a great benefit for meeting the needs of molecular diagnostics customers on ‘Large Scale Investigations’ such as the NHS clinical trials as well as the epidemiological investigations carried out by the WHO to the control of diseases especially in Africa.

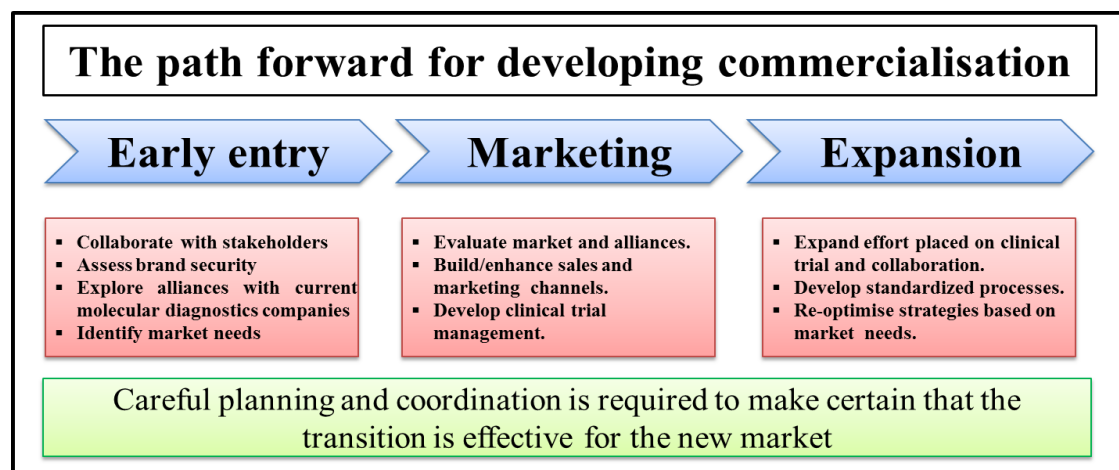


Diagram 4.1 A summary of the transitioning into the molecular diagnostics market.

Transitioning into the molecular diagnostics market will be the biggest challenge for linking research more directly to patient clinical care. The biotechnology industry has to be convinced in order to recognise the revenue and profits available in the diagnostics field. The transition strategy starts with coordinated efforts across the three parties to make sure

the resulting commercial kit would serve current and future customer needs (NHS or WHO). The biggest challenge for companies such as Roche, Affymetrix and Illumina will be to understand and manage the complexities of a different customer base each with unique needs and each influencing the purchase decision. Indeed, large scale investigations should be the key influence on customers who make the purchase decision [219]. The development of a sensitive non-invasive assay for the detection of BK/JC viruses simultaneously promises to lead to greater understanding of their pathogenesis which may, in turn, contribute to the development of new treatment strategies.

4.4.2 Further research

Expression array analyses provided novel insights into LT regulated pathways with sufficient coverage by IPA's IKB. In order to validate these LT functions, siRNA silencing could be used to test for the converse of these observations with repeat microarrays. Furthermore, LT activation of identified key points in signalling pathways could also be tested by exploring the availability of pharmacological agents which are known to target these functions. The effects of these could then be evaluated by testing for up or down regulation of specific gene targets or by repeat microarray analysis.

Mefloquine anticancer capabilities could be further investigated in human glial cell lines as model cells for CNS infection during PML in the lack of availability of purified primary human oligodendrocytes the viral target in PML.

Immunocytology showed nuclear staining variability which was thought to be attributed to an arrest of cell cycle-dependent genes during the transition from one phase to another in cell cycling and this could be further investigated by flow cytometry.

Decreased expression of vimentin indicated that the cell cloning procedure has reduced the migratory capacity of the cells, and further investigation on this property should provide new information on factors which control clonal selection. For example growing cells on Matrigel to promote proliferation or in irradiated feeder layers or 3-dimensional spheroids could enhance the survival of transformed cells.

During the course of this project, eight new polyomaviruses have been identified. Thus screening the same sample set, used in this study, for the presence of these new polyomaviruses could provide new insights into the epidemiology and pathology of these novel infectious agents.

Annotated References

1. Siegel, R., et al., *Cancer statistics, 2014*. CA Cancer J Clin, 2014. **64**(1): p. 9-29.
2. Thun, M.J., et al., *The global burden of cancer: priorities for prevention*. Carcinogenesis, 2010. **31**(1): p. 100-110.
3. Kalland, K.H., X.S. Ke, and A.M. Oyan, *Tumour virology--history, status and future challenges*. APMIS, 2009. **117**(5-6): p. 382-99.
4. Brower, V., *Connecting viruses to cancer: How research moves from association to causation*. Journal of the National Cancer Institute, 2004. **96**(4): p. 256-257.
5. Damania, B., *DNA tumor viruses and human cancer*. Trends Microbiol, 2007. **15**(1): p. 38-44.
6. McLaughlin-Drubin, M.E. and K. Munger, *Viruses associated with human cancer*. Biochim Biophys Acta, 2008. **1782**(3): p. 127-50.
7. Rwazavian, N., *Can A Virus Cause Cancer: A Look Into The History And Significance Of Oncoviruses*. Berkeley Scientific Journal, 2011. **14**(1).
8. Talbot, S.J. and D.H. Crawford, *Viruses and cancer*. Medicine, 2005. **33**(3): p. 39-42.
9. zur Hausen, H., *Viruses in human cancers*. Current Science, 2001. **81**(5): p. 523-527.
10. Sarid, R. and S.J. Gao, *Viruses and human cancer: from detection to causality*. Cancer Lett, 2011. **305**(2): p. 218-27.
11. Rickinson, A.B., *Introduction: Viruses and human cancer*. Semin Cancer Biol, 1992. **3**(5): p. 249-51.
12. Javier, R.T. and J.S. Butel, *The history of tumor virology*. Cancer Res, 2008. **68**(19): p. 7693-706.
13. Hayashi, K., *EBV-associated diseases in humans and their animal in vivo models: Part I*. Yonago Acta Medica, 2005. **48**(1): p. 1-6.
14. Liao, J.B., *Viruses and human cancer*. Yale J Biol Med, 2006. **79**(3-4): p. 115-22.
15. Butt, A.Q. and S.M. Miggin, *Cancer and viruses: A double-edged sword*. Proteomics, 2012. **12**(13): p. 2127-2138.
16. Klein, E., L.L. Kis, and G. Klein, *Epstein-Barr virus infection in humans: from harmless to life endangering virus-lymphocyte interactions*. Oncogene, 2007. **26**(9): p. 1297-1305.
17. Cooper, G., *The Cell: A Molecular Approach*. 2000, Sunderland Sinauer Associates.
18. Saha, A., et al., *Tumor viruses and cancer biology: Modulating signaling pathways for therapeutic intervention*. Cancer Biol Ther, 2010. **10**(10): p. 961-78.
19. Singh, N., *HPV and cervical cancer*. Proceedings of the American Association for Cancer Research Annual Meeting, 2008. **49**: p. 1122-1123.
20. Parkin, D.M., *The global health burden of infection-associated cancers in the year 2002*. Int J Cancer, 2006. **118**(12): p. 3030-3044.
21. Marklund, L. and L. Hammarstedt, *Impact of HPV in Oropharyngeal Cancer*. J Oncol, 2011: p. 509036.
22. Cutts, F.T., et al., *Human papillomavirus and HPV vaccines: a review*. Bull World Health Organ, 2007. **85**(9): p. 719-26.
23. Darnell, G.A., et al., *Human Papillomavirus E7 requires the protease calpain to degrade the retinoblastoma protein*. Journal of Biological Chemistry, 2007. **282**(52): p. 37492-37500.
24. Feng, H., et al., *Clonal integration of a polyomavirus in human Merkel cell carcinoma*. Science, 2008. **319**(5866): p. 1096-100.

25. Babakir-Mina, M., et al., *The novel KI, WU, MC polyomaviruses: possible human pathogens?* New Microbiologica, 2011. **34**(1): p. 1-8.
26. Bergonzini, V., et al., *View and review on viral oncology research.* Infect Agent Cancer, 2010. **5**: p. 11.
27. Wang, T.S., et al., *Merkel cell carcinoma: update and review.* Semin Cutan Med Surg, 2011. **30**(1): p. 48-56.
28. Boothpur, R. and D.C. Brennan, *Human polyoma viruses and disease with emphasis on clinical BK and JC.* Journal of Clinical Virology, 2010. **47**(4): p. 306-12.
29. Giraud, G., et al., *DNA from BK Virus and JC Virus and from KI, WU, and MC Polyomaviruses as Well as from Simian Virus 40 Is Not Detected in Non-UV-Light-Associated Primary Malignant Melanomas of Mucous Membranes (vol 46, pg 3595, 2008).* Journal of Clinical Microbiology, 2009. **47**(9): p. 3072-3072.
30. Kuwamoto, S., *Recent advances in the biology of Merkel cell carcinoma.* Human pathology, 2011. **42**(8): p. 1063-77.
31. Bartosch, B., *Hepatitis B and C Viruses and Hepatocellular Carcinoma.* Viruses-Basel, 2010. **2**(8): p. 1504-1509.
32. Bose, S., et al., *Hepatocellular carcinoma with persistent hepatitis B virus infection shows unusual downregulation of Ras expression and differential response to Ras mediated signaling.* J Gastroenterol Hepatol, 2011. **26**(1): p. 135-44.
33. Tsai, W.L. and R.T. Chung, *Viral hepatocarcinogenesis.* Oncogene, 2010. **29**(16): p. 2309-24.
34. Dash, S., et al., *HCV-hepatocellular carcinoma: new findings and hope for effective treatment.* Microsc Res Tech, 2005. **68**(3-4): p. 130-48.
35. Tabakin-Fix, Y., M. Huleihel, and M. Aboud, *Activation of simian virus 40 promoter by HTLV-I Tax protein: role of NF-kappaB and CBP.* Biochem Biophys Res Commun, 2004. **318**(4): p. 1052-6.
36. Shah, K.V., *Does SV40 infection contribute to the development of human cancers?* Reviews in Medical Virology, 2000. **10**(1): p. 31-43.
37. Reuter, S., et al., *Oxidative stress, inflammation, and cancer How are they linked?* Free Radical Biology and Medicine, 2010. **49**(11): p. 1603-1616.
38. Grivennikov, S.I., F.R. Greten, and M. Karin, *Immunity, Inflammation, and Cancer.* Cell, 2010. **140**(6): p. 883-899.
39. zur Hausen, H., *Viruses in human cancers.* Eur J Cancer, 1999. **35**(8): p. 1174-81.
40. Giordano, A., et al., *Viral infections as a cause of cancer (Review).* International Journal of Oncology, 2007. **30**(6): p. 1521-1528.
41. Houben, R., et al., *Merkel Cell Carcinoma and Merkel Cell Polyomavirus: Evidence for Hit-and-Run Oncogenesis.* Journal of Investigative Dermatology, 2012. **132**(1): p. 254-256.
42. Khalili, K., *Classic polyomaviruses: basic perspectives.* Journal of Neurovirology, 2013. **19**(3): p. 283-283.
43. Butel, J.S., *Viral carcinogenesis: revelation of molecular mechanisms and etiology of human disease.* Carcinogenesis, 2000. **21**(3): p. 405-426.
44. Dalianis, T. and H.H. Hirsch, *Human polyomaviruses in disease and cancer.* Virology, 2013. **437**(2): p. 63-72.
45. Moore, P.S. and Y.A. Chang, *Why do viruses cause cancer? Highlights of the first century of human tumour virology.* Nature Reviews Cancer, 2010. **10**(12): p. 878-889.
46. Whitty, A., *Cooperativity and biological complexity.* Nat Chem Biol, 2008. **4**(8): p. 435-9.

47. Operskalski, E.A. and A. Kovacs, *HIV/HCV co-infection: pathogenesis, clinical complications, treatment, and new therapeutic technologies*. *Curr HIV/AIDS Rep*, 2011. **8**(1): p. 12-22.
48. Wright, C.A., J.A. Nance, and E.M. Johnson, *Effects of Tat proteins and Tat mutants of different human immunodeficiency virus type 1 clades on glial JC virus early and late gene transcription*. *J Gen Virol*, 2013. **94**: p. 514-523.
49. Khalili, K., J. Gordon, and M.K. White, *The polyomavirus, JCV, and its involvement in human disease*. *Polyomaviruses and Human Diseases*, 2006. **577**: p. 274-287.
50. Pyakurel, P., et al., *KSHV/HHV-8 and HIV infection in Kaposi's sarcoma development*. *Infect Agent Cancer*, 2007. **2**: p. 4-4.
51. Casoli, C., E. Pilotti, and U. Bertazzoni, *Molecular and cellular interactions of HIV-1/HTLV coinfection and impact on AIDS progression*. *AIDS Rev*, 2007. **9**(3): p. 140-9.
52. Wood, C. and W. Harrington, *AIDS and associated malignancies*. *Cell Res*, 2005. **15**(11-12): p. 947-952.
53. Behzad-Behbahani, A., et al., *Detection of BK virus and JC virus DNA in urine samples from immunocompromised (HIV-infected) and immunocompetent (HIV-non-infected) patients using polymerase chain reaction and microplate hybridisation*. *J Clin Virol*, 2004. **29**(4): p. 224-229.
54. Knowles, W.A., *Discovery and epidemiology of the human polyomaviruses BK virus (BKV) and JC virus (JCV)*. *Adv Exp Med Biol*, 2006. **577**: p. 19-45.
55. Fraase, K., et al., *BK Virus as a Potential Co-factor for HPV in the Development of Cervical Neoplasia*. *Ann Clin Lab Sci*, 2012. **42**(2): p. 130-134.
56. M'Kacher, R., et al., *JC human polyomavirus is associated to chromosomal instability in peripheral blood lymphocytes of Hodgkin's lymphoma patients and poor clinical outcome*. *Annals of Oncology*, 2010. **21**(4): p. 826-832.
57. Atkin, S.J., B.E. Griffin, and S.M. Dilworth, *Polyoma virus and simian virus 40 as cancer models: history and perspectives*. *Seminars in Cancer Biology*, 2009. **19**(4): p. 211-7.
58. Butel, J.S., *Simian virus 40, poliovirus vaccines, and human cancer: research progress versus media and public interests*. *Bulletin of the World Health Organization*, 2001. **78**(2): p. 195-8.
59. Moens, U., M. Van Ghelue, and B. Ehlers, *Are human polyomaviruses co-factors for cancers induced by other oncoviruses?* *Reviews in Medical Virology*, 2014. **24**(5): p. 343-360.
60. Ahsan, N. and K.V. Shah, *Polyomaviruses and human diseases*. *Polyomaviruses and Human Diseases*, 2006. **577**: p. 1-18.
61. Lednicky, J.A. and J.S. Butel, *Polyomaviruses and human tumors: A brief review of current concepts and interpretations*. *Frontiers in Bioscience*, 1999. **4**(CITED FEB. 17, 1999): p. D153-164.
62. Dalianis, T., et al., *KI, WU and Merkel cell polyomaviruses: a new era for human polyomavirus research*. *Seminars in Cancer Biology*, 2009. **19**(4): p. 270-5.
63. Gjoerup, O. and Y. Chang, *Update on human polyomaviruses and cancer*. *Advances in cancer research*, 2010. **106**: p. 1-51.
64. Lee, W. and E. Langholf, *Polyomavirus in human cancer development*. *Polyomaviruses and Human Diseases*, 2006. **577**: p. 310-318.
65. Gazdar, A.F., J.S. Butel, and M. Carbone, *SV40 and human tumours: myth, association or causality?* *Nature Reviews Cancer*, 2002. **2**(12): p. 957-64.
66. Croul, S., J. Otte, and K. Khalili, *Brain tumors and polyomaviruses*. *Journal of Neurovirology*, 2003. **9**(2): p. 173-82.

67. Tolstov, Y.L., et al., *Human Merkel cell polyomavirus infection II. MCV is a common human infection that can be detected by conformational capsid epitope immunoassays*. International Journal of Cancer, 2009. **125**(6): p. 1250-1256.
68. Maginnis, M.S. and W.J. Atwood, *JC Virus: An oncogenic virus in animals and humans?* Seminars in Cancer Biology, 2009. **19**(4): p. 261-269.
69. Weinberg, G.A. and A.N. Mian, *BK virus nephropathy and other polyoma virus infections*. Pediatr Infect Dis J, 2010. **29**(3): p. 257-60.
70. Wei, G., C.K. Liu, and W.J. Atwood, *JC virus binds to primary human glial cells, tonsillar stromal cells, and B-lymphocytes, but not to T lymphocytes*. Journal of Neurovirology, 2000. **6**(2): p. 127-136.
71. Komagome, R., et al., *Oligosaccharides as receptors for JC virus*. Journal of virology, 2002. **76**(24): p. 12992-13000.
72. Eash, S., et al., *The human polyomaviruses*. Cell Mol Life Sci, 2006. **63**(7-8): p. 865-76.
73. Querbes, W., et al., *A JC virus-induced signal is required for infection of glial cells by a clathrin- and eps15-dependent pathway*. Journal of virology, 2004. **78**(1): p. 250-256.
74. White, M.K. and K. Khalili, *Polyomaviruses and human cancer: molecular mechanisms underlying patterns of tumorigenesis*. Virology, 2004. **324**(1): p. 1-16.
75. Shuda, M., et al., *Human Merkel cell polyomavirus small T antigen is an oncoprotein targeting the 4E-BP1 translation regulator*. Journal of Clinical Investigation, 2011. **121**(9): p. 3623-3634.
76. Daniels, R., D. Sadowicz, and D.N. Hebert, *A very late viral protein triggers the lytic release of SV40*. PLoS Pathogens, 2007. **3**(7): p. 928-938.
77. Ahuja, D., M.T. Saenz-Robles, and J.M. Pipas, *SV40 large T antigen targets multiple cellular pathways to elicit cellular transformation*. Oncogene, 2005. **24**(52): p. 7729-7745.
78. White, E.A., et al., *Papillomavirus e7 oncoproteins share functions with polyomavirus small T antigens*. J Virol, 2015. **89**(5): p. 2857-65.
79. Bellizzi, A., et al., *New Insights on Human Polyomavirus JC and Pathogenesis of Progressive Multifocal Leukoencephalopathy*. Clinical & Developmental Immunology, 2013.
80. Kinnaird, A.N. and G.M. Anstead, *Hemorrhagic Cystitis and Possible Neurologic Disease from BK Virus Infection in a Patient with AIDS*. Infection, 2010. **38**(2): p. 124-127.
81. Jiang, M., et al., *The role of polyomaviruses in human disease*. Virology, 2009. **384**(2): p. 266-273.
82. Ferber, D., *Virology. Monkey virus link to cancer grows stronger*. Science, 2002. **296**(5570): p. 1012-5.
83. Moens, U. and M. Johannessen, *Human polyomaviruses and cancer: expanding repertoire*. Journal Der Deutschen Dermatologischen Gesellschaft, 2008. **6**(9): p. 704-708.
84. Giuliani, L., et al., *Detection of oncogenic DNA viruses in colorectal cancer*. Anticancer Research, 2008. **28**(2B): p. 1405-1410.
85. Reiss, K. and K. Khalili, *Viruses and cancer: lessons from the human polyomavirus, JCV*. Oncogene, 2003. **22**(42): p. 6517-23.
86. Collins, D., A.M. Hogan, and D.C. Winter, *Microbial and viral pathogens in colorectal cancer*. Lancet Oncology, 2011. **12**(5): p. 504-12.
87. Allander, T., et al., *Identification of a third human polyomavirus*. Journal of Virology, 2007. **81**(8): p. 4130-4136.
88. Gaynor, A.M., et al., *Identification of a novel polyomavirus from patients with acute respiratory tract infections*. PLoS Pathogens, 2007. **3**(5): p. e64.

89. Schowalter, R.M., et al., *Merkel cell polyomavirus and two previously unknown polyomaviruses are chronically shed from human skin*. Cell Host Microbe, 2010. **7**(6): p. 509-15.
90. van der Meijden, E., et al., *Discovery of a New Human Polyomavirus Associated with Trichodysplasia Spinulosa in an Immunocompromized Patient*. PLoS Pathogens, 2010. **6**(7).
91. Scuda, N., et al., *A novel human polyomavirus closely related to the african green monkey-derived lymphotropic polyomavirus*. J Virol, 2011. **85**(9): p. 4586-90.
92. Buck, C.B., et al., *Complete genome sequence of a tenth human polyomavirus*. J Virol, 2012. **86**(19): p. 10887.
93. Siebrasse, E.A., et al., *Identification of MW polyomavirus, a novel polyomavirus in human stool*. J Virol, 2012. **86**(19): p. 10321-6.
94. Yu, G., et al., *Discovery of a novel polyomavirus in acute diarrheal samples from children*. Plos One, 2012. **7**(11): p. e49449.
95. Lim, E.S., et al., *"Discovery of STL polyomavirus, a polyomavirus of ancestral recombinant origin that encodes a unique T antigen by alternative splicing"* (vol 436, pg 295, 2013). Virology, 2013. **439**(2): p. 163-164.
96. Korup, S., et al., *Identification of a novel human polyomavirus in organs of the gastrointestinal tract*. Plos One, 2013. **8**(3): p. e58021.
97. zur Hausen, H., *The Search for Infectious Causes of Human Cancers: Where and Why (Nobel Lecture)*. Angewandte Chemie-International Edition, 2009. **48**(32): p. 5798-5808.
98. Shahzad, N., et al., *The T Antigen Locus of Merkel Cell Polyomavirus Downregulates Human Toll-Like Receptor 9 Expression*. Journal of virology, 2013. **87**(23): p. 13009-13019.
99. Spandau, D.F. and C.H. Lee, *trans-activation of viral enhancers by the hepatitis B virus X protein*. J Virol, 1988. **62**(2): p. 427-34.
100. Yeh, C.T., et al., *Characterization of a HCV NS5A protein derived from a patient with hepatoma*. Biochem Biophys Res Commun, 2005. **327**(2): p. 516-22.
101. Bernard, B.A., et al., *Modulation of HPV18 and BPV1 transcription in human keratinocytes by simian virus 40 large T antigen and adenovirus type 5 E1A antigen*. J Cell Biochem, 1990. **42**(2): p. 101-10.
102. Tannock, I.F. and R.P. Hill, *THE BASIC SCIENCE OF ONCOLOGY*. Tannock, I. F. And R. P. Hill. 1987.
103. Carbone, M., et al., *New developments about the association of SV40 with human mesothelioma*. Oncogene, 2003. **22**(33): p. 5173-80.
104. Hmeljak, J. and A. Coer, *Presence and role of Simian Virus 40 (SV40) in malignant pleural mesothelioma*. Radiology and Oncology, 2009. **43**(1): p. 9-16.
105. Krumbholz, A., et al., *Phylogenetics, evolution, and medical importance of polyomaviruses*. Infection Genetics and Evolution, 2009. **9**(5): p. 784-799.
106. Engels, E.A., et al., *Antibody responses to simian virus 40 T antigen: a case-control study of non-Hodgkin lymphoma*. Cancer Epidemiol Biomarkers Prev, 2005. **14**(2): p. 521-4.
107. Engels, E.A., et al., *Case-control study of simian virus 40 and non-Hodgkin lymphoma in the United States*. J Natl Cancer Inst, 2004. **96**(18): p. 1368-74.
108. Padgett, B.L., et al., *CULTIVATION OF PAPOVA-LIKE VIRUS FROM HUMAN BRAIN WITH PROGRESSIVE MULTIFOCAL LEUCOENCEPHALOPATHY*. Lancet, 1971. **1**(7712): p. 1257-&.
109. Kastrup, O., et al., *Progressive multifocal leukoencephalopathy of the brainstem in an immunocompetent patient--JC and BK polyoma-virus coinfection? A case report and review of the literature*. Clin Neurol Neurosurg, 2013. **115**(11): p. 2390-2.

110. Weissert, R., *Progressive multifocal leukoencephalopathy*. J Neuroimmunol, 2011. **231**(1-2): p. 73-7.
111. Young, B.E., et al., *Progressive Multifocal Leukoencephalopathy with Immune Reconstitution Inflammatory Syndrome (PML-IRIS): Two Case Reports of Successful Treatment with Mefloquine and a Review of the Literature*. Annals Academy of Medicine Singapore, 2012. **41**(12): p. 620-624.
112. Pinto, M. and S. Dobson, *BK and JC virus: a review*. J Infect, 2014. **68 Suppl 1**: p. S2-8.
113. Sweet, B.H. and M.R. Hilleman, *THE VACUOLATING VIRUS, SV40*. Proceedings of the Society for Experimental Biology and Medicine, 1960. **105**(2): p. 420-427.
114. zur Hausen, H., *Novel human polyomaviruses--re-emergence of a well known virus family as possible human carcinogens*. International Journal of Cancer, 2008. **123**(2): p. 247-50.
115. Knudson, A.G., *Mutation and Cancer - Statistical Study of Retinoblastoma*. Proceedings of the National Academy of Sciences of the United States of America, 1971. **68**(4): p. 820-&.
116. Sinagra, E., et al., *Could JC virus provoke metastasis in colon cancer?* World Journal of Gastroenterology, 2014. **20**(42): p. 15745-15749.
117. Gardner, S., et al., *New human papovavirus (B.K.) isolated from urine after renal transplantation*. The Lancet, 1971. **297**(7712): p. 1253-1257.
118. Cukuranovic, J., et al., *Viral Infection in Renal Transplant Recipients*. Scientific World Journal, 2012.
119. Dall, A. and S. Hariharan, *BK virus nephritis after renal transplantation*. Clin J Am Soc Nephrol, 2008. **3 Suppl 2**: p. S68-75.
120. Heritage, J., P.M. Chesters, and D.J. McCance, *The persistence of papovavirus BK DNA-sequences in normal human renal tissue*. J Med Virol, 1981. **8**(2): p. 143-150.
121. Fioriti, D., et al., *The human polyomavirus BK: Potential role in cancer*. J Cell Physiol, 2005. **204**(2): p. 402-6.
122. Doerries, K., *Human polyomavirus JC and BK persistent infection*. Advances in Experimental Medicine & Biology, 2006. **577**: p. 102-16.
123. Bialasiewicz, S., et al., *Detection of BK, JC, WU, or KI polyomaviruses in faecal, urine, blood, cerebrospinal fluid and respiratory samples*. J Clin Virol, 2009. **45**(3): p. 249-54.
124. Bialasiewicz, S., et al., *A newly reported human polyomavirus, KI virus, is present in the respiratory tract of Australian children*. Journal of Clinical Virology, 2007. **40**(1): p. 15-8.
125. Babakir-Mina, M., et al., *The human polyomaviruses KI and WU: virological background and clinical implications*. APMIS, 2013. **121**(8): p. 746-54.
126. Barzon, L., et al., *WU and KI polyomaviruses in the brains of HIV-positive patients with and without progressive multifocal leukoencephalopathy*. J Infect Dis, 2009. **200**(11): p. 1755-8.
127. Ren, L., et al., *WU and KI polyomavirus present in the respiratory tract of children, but not in immunocompetent adults*. J Clin Virol, 2008. **43**(3): p. 330-3.
128. Schrama, D., S. Ugurel, and J.C. Becker, *Merkel cell carcinoma: recent insights and new treatment options*. Curr Opin Oncol, 2013. **24**(2): p. 141-149.
129. Schrama, D., et al., *No Evidence for Association of HPyV6 or HPyV7 with Different Skin Cancers*. Journal of Investigative Dermatology, 2012. **132**(1): p. 239-241.
130. van der Meijden, E., et al., *Seroprevalence of Trichodysplasia Spinulosa-associated Polyomavirus*. Emerging Infectious Diseases, 2011. **17**(8): p. 1355-1363.
131. Trusch, F., et al., *Seroprevalence of human polyomavirus 9 and cross-reactivity to African green monkey-derived lymphotropic polyomavirus*. Journal of General Virology, 2012. **93**: p. 698-705.

132. Foulongne, V., et al., *Human Skin Microbiota: High Diversity of DNA Viruses Identified on the Human Skin by High Throughput Sequencing*. Plos One, 2012. **7**(6).
133. De Gascun, C.F. and M.J. Carr, *Human Polyomavirus Reactivation: Disease Pathogenesis and Treatment Approaches*. Clinical & Developmental Immunology, 2013.
134. Elfaitouri, A., A.L. Hammarin, and J. Blomberg, *Quantitative real-time PCR assay for detection of human polyomavirus infection*. Journal of Virological Methods, 2006. **135**(2): p. 207-13.
135. Randhawa, P., et al., *Correlates of quantitative measurement of BK polyomavirus (BKV) DNA with clinical course of BKV infection in renal transplant patients*. Journal of Clinical Microbiology, 2004. **42**(3): p. 1176-1180.
136. Dadhania, D., et al., *Validation of Noninvasive Diagnosis of BK Virus Nephropathy and Identification of Prognostic Biomarkers*. Transplantation, 2010. **90**(2): p. 189-197.
137. Dropulic, L.K. and R.J. Jones, *Polyomavirus BK infection in blood and marrow transplant recipients*. Bone Marrow Transplantation, 2008. **41**(1): p. 11-18.
138. Singh, H.K., et al., *Urine cytology findings of polyomavirus infections*. Polyomaviruses and Human Diseases, 2006. **577**: p. 201-212.
139. Hamilton, R.S., M. Gravell, and E.O. Major, *Comparison of antibody titers determined by hemagglutination inhibition and enzyme immunoassay for JC virus and BK virus*. J Clin Microbiol, 2000. **38**(1): p. 105-9.
140. Nilsen, I., T. Flaegstad, and T. Traavik, *Detection of specific IgA antibodies against BK virus by ELISA*. J Med Virol, 1991. **33**(2): p. 89-94.
141. Specter, S., et al., *Diagnosis of viral infections*. 2nd edn ed. Clinical virology, ed. W.R.J.H.F.G. Richman D.D. 2002, Washington: ASM Press: American Society for Microbiology. 537- 555.
142. Hogan, T.F., et al., *Rapid Detection and Identification of Jc-Virus and Bk-Virus in Human-Urine by Using Immunofluorescence Microscopy*. Journal of Clinical Microbiology, 1980. **11**(2): p. 178-183.
143. An, P., M.T.S. Robles, and J.M. Pipas, *Large T Antigens of Polyomaviruses: Amazing Molecular Machines*. Annual Review of Microbiology, Vol 66, 2012. **66**: p. 213-236.
144. Hanahan, D. and R.A. Weinberg, *Hallmarks of cancer: the next generation*. Cell, 2011. **144**(5): p. 646-74.
145. Nabarra, B., et al., *Neoplastic transformation and angiogenesis in the thymus of transgenic mice expressing SV40 T and t antigen under an L-pyruvate kinase promoter (SV12 mice)*. International Journal of Experimental Pathology, 2005. **86**(6): p. 397-413.
146. Cheng, J.C., N. Auersperg, and P.C.K. Leung, *Inhibition of p53 induces invasion of serous borderline ovarian tumor cells by accentuating PI3K/Akt-mediated suppression of E-cadherin*. Oncogene, 2011. **30**(9): p. 1020-1031.
147. Lamouille, S., J. Xu, and R. Derynck, *Molecular mechanisms of epithelial-mesenchymal transition*. Nat Rev Mol Cell Biol, 2014. **15**(3): p. 178-96.
148. Davies, B.R., et al., *Immortalisation of human ovarian surface epithelium with telomerase and temperature-sensitive SV40 large T antigen*. Exp Cell Res, 2003. **288**(2): p. 390-402.
149. Martel, C., et al., *Inactivation of retinoblastoma family proteins by SV40 T antigen results in creation of a hepatocyte growth factor/scatter factor autocrine loop associated with an epithelial-fibroblastoid conversion and invasiveness*. Cell Growth Differ, 1997. **8**(2): p. 165-78.

150. Mani, S.A., et al., *The epithelial-mesenchymal transition generates cells with properties of stem cells*. Cell, 2008. **133**(4): p. 704-15.
151. Micalizzi, D.S., S.M. Farabaugh, and H.L. Ford, *Epithelial-Mesenchymal Transition in Cancer: Parallels Between Normal Development and Tumor Progression*. Journal of Mammary Gland Biology and Neoplasia, 2010. **15**(2): p. 117-134.
152. Hirohashi, S. and Y. Kanai, *Cell adhesion system and human cancer morphogenesis*. Cancer Science, 2003. **94**(7): p. 575-581.
153. Moreno-Bueno, G., F. Portillo, and A. Cano, *Transcriptional regulation of cell polarity in EMT and cancer*. Oncogene, 2008. **27**(55): p. 6958-6969.
154. Jeanes, A., C.J. Gottardi, and A.S. Yap, *Cadherins and cancer: how does cadherin dysfunction promote tumor progression?* Oncogene, 2008. **27**(55): p. 6920-6929.
155. Schafer, G., et al., *Cadherin switching during the formation and differentiation of the Drosophila mesoderm - implications for epithelial-to-mesenchymal transitions*. J Cell Sci, 2014. **127**(Pt 7): p. 1511-22.
156. Ogrodnik, M., et al., *Dynamic JUNQ inclusion bodies are asymmetrically inherited in mammalian cell lines through the asymmetric partitioning of vimentin*. Proceedings of the National Academy of Sciences of the United States of America, 2014. **111**(22): p. 8049-8054.
157. Garg, M., *Epithelial-mesenchymal transition - activating transcription factors - multifunctional regulators in cancer*. World J Stem Cells, 2013. **5**(4): p. 188-95.
158. Yan, K.H., et al., *Mefloquine exerts anticancer activity in prostate cancer cells via ROS-mediated modulation of Akt, ERK, JNK and AMPK signaling*. Oncology Letters, 2013. **5**(5): p. 1541-1545.
159. Yoshida, H., et al., *Significant improvement following combination treatment with mefloquine and mirtazapine in a patient with progressive multifocal leukoencephalopathy after allogeneic peripheral blood stem cell transplantation*. Int J Hematol, 2014. **99**(1): p. 95-9.
160. Clifford, D.B., et al., *A study of mefloquine treatment for progressive multifocal leukoencephalopathy: results and exploration of predictors of PML outcomes*. Journal of Neurovirology, 2013. **19**(4): p. 351-8.
161. Adachi, E., et al., *Favourable outcome of progressive multifocal leukoencephalopathy with mefloquine treatment in combination with antiretroviral therapy in an HIV-infected patient*. Int J STD AIDS, 2012. **23**(8): p. 603-5.
162. Kishida, S. and K. Tanaka, *Mefloquine treatment in a patient suffering from progressive multifocal leukoencephalopathy after umbilical cord blood transplant*. Intern Med, 2010. **49**(22): p. 2509-13.
163. Gofton, T.E., et al., *Mefloquine in the treatment of progressive multifocal leukoencephalopathy*. J Neurol Neurosurg Psychiatry, 2011. **82**(4): p. 452-5.
164. Richard, C., et al., *The immortalizing and transforming ability of two common human papillomavirus 16 E6 variants with different prevalences in cervical cancer*. Oncogene, 2010. **29**(23): p. 3435-3445.
165. Smith, J.H., *Bethesda 2001*. Cytopathology, 2002. **13**(1): p. 4-10.
166. Alosaimi, B., et al., *Increased prevalence of JC polyomavirus in cervical carcinomas from women infected with HIV*. J Med Virol, 2014. **86**(4): p. 672-7.
167. Maranga, I.O., et al., *HIV Infection Alters the Spectrum of HPV Subtypes Found in Cervical Smears and Carcinomas from Kenyan Women*. Open Virol J, 2012. **6**(12): p. 121-129.
168. Martini, F., et al., *Papilloma and polyoma DNA tumor virus sequences in female genital tumors*. Cancer Invest, 2004. **22**(5): p. 697-705.

169. Batman, G., et al., *Lopinavir up-regulates expression of the antiviral protein ribonuclease L in human papillomavirus-positive cervical carcinoma cells*. *Antivir Ther*, 2011. **16**(4): p. 515-25.
170. Maniatis T, Fritsch E F, and S. J., *Molecular cloning. A laboratory manual*. 2nd ed. 1982, New York: Cold Spring Harbor Laboratory Press.
171. Jordan, N.V., G.L. Johnson, and A.N. Abell, *Tracking the intermediate stages of epithelial-mesenchymal transition in epithelial stem cells and cancer*. *Cell Cycle*, 2011. **10**(17): p. 2865-2873.
172. Findley, M.K. and M. Koval, *Regulation and Roles for Claudin-family Tight Junction Proteins*. *Iubmb Life*, 2009. **61**(4): p. 431-437.
173. Gunzel, D. and M. Fromm, *Claudins and Other Tight Junction Proteins*. *Comprehensive Physiology*, 2012. **2**(3): p. 1819-1852.
174. Vella, L.J., *The emerging role of exosomes in epithelial-mesenchymal-transition in cancer*. *Front Oncol*, 2014. **4**: p. 361.
175. Satelli, A. and S.L. Li, *Vimentin in cancer and its potential as a molecular target for cancer therapy*. *Cellular and Molecular Life Sciences*, 2011. **68**(18): p. 3033-3046.
176. Rodrigues, F.A.R., et al., *Mefloquine-Oxazolidine Derivatives: A New Class of Anticancer Agents*. *Chemical Biology & Drug Design*, 2014. **83**(1): p. 126-131.
177. Lander, E.S., et al., *Initial sequencing and analysis of the human genome*. *Nature*, 2001. **409**(6822): p. 860-921.
178. Yan, W., *Multiplex PCR primer design for simultaneous detection of multiple pathogens*. *Methods Mol Biol*, 2015. **1275**: p. 91-101.
179. Comar, M., et al., *High Prevalence of BK Polyomavirus Sequences in Human Papillomavirus-16-Positive Precancerous Cervical Lesions*. *J Med Virol*, 2011. **83**(10): p. 1770-1776.
180. Poulin and DeCaprio, *Is there a role for SV40 in human cancer? (vol 24, pg 4356, 2006)*. *Journal of Clinical Oncology*, 2006. **24**(35): p. 5620-5620.
181. Cejtin, H.E., *Gynecologic issues in the HIV-infected woman*. *Infect Dis Clin North Am*, 2008. **22**(4): p. 709-39, vii.
182. Boccardo, E., A.P. Lepique, and L.L. Villa, *The role of inflammation in HPV carcinogenesis*. *Carcinogenesis*, 2010. **31**(11): p. 1905-1912.
183. Cayres-Vallinoto, I.M.V., et al., *Human JCV Infections as a Bio-Anthropological Marker of the Formation of Brazilian Amazonian Populations*. *Plos One*, 2012. **7**(10).
184. Guo, J., et al., *Geographical distribution of the human polyomavirus JC virus types A and B and isolation of a new type from Ghana*. *J Gen Virol*, 1996. **77**: p. 919-927.
185. Shackelton, L.A., et al., *JC virus evolution and its association with human populations*. *J Virol*, 2006. **80**(20): p. 9928-9933.
186. Blackwell, J.M., S.E. Jamieson, and D. Burgner, *HLA and Infectious Diseases*. *Clinical Microbiology Reviews*, 2009. **22**(2): p. 370-+.
187. MacDonald, K.S., et al., *Influence of HLA supertypes on susceptibility and resistance to human immunodeficiency virus type 1 infection*. *Journal of Infectious Diseases*, 2000. **181**(5): p. 1581-1589.
188. Mandelblatt, J.S., et al., *Is HIV infection a cofactor for cervical squamous cell neoplasia?* *Cancer Epidemiology Biomarkers & Prevention*, 1999. **8**(1): p. 97-106.
189. Markowitz, R.B., et al., *Incidence of BK-virus and JC-virus viruria in human immunodeficiency virus-infected and virus-uninfected subjects*. *J Infect Dis*, 1993. **167**(1): p. 13-20.
190. Kaniowska, D., et al., *Cross-interaction between JC virus agnoprotein and human immunodeficiency virus type 1 (HIV-1) tat modulates transcription of the HIV-1 long terminal repeat in glial cells*. *J Virol*, 2006. **80**(18): p. 9288-9299.

191. Callaway, E., *Fighting for a Cause*. Nature, 2011. **471**(7338): p. 282-285.
192. Enam, S., et al., *Association of human polyomavirus JCV with colon cancer: Evidence for interaction of viral T-antigen and beta-catenin*. Cancer Res, 2002. **62**(23): p. 7093-7101.
193. de Oliveira, D.E., *DNA viruses in human cancer: an integrated overview on fundamental mechanisms of viral carcinogenesis*. Cancer Lett, 2007. **247**(2): p. 182-96.
194. Xiao, Y., et al., *Cell cycle-dependent gene networks relevant to cancer*. Progress in Natural Science-Materials International, 2008. **18**(8): p. 945-952.
195. Sancar, A., et al., *Molecular mechanisms of mammalian DNA repair and the DNA damage checkpoints*. Annual Review of Biochemistry, 2004. **73**: p. 39-85.
196. Curtin, N.J., *Inhibiting the DNA damage response as a therapeutic manoeuvre in cancer*. British Journal of Pharmacology, 2013. **169**(8): p. 1745-1765.
197. Digweed, M., et al., *SV40 large T-antigen disturbs the formation of nuclear DNA-repair foci containing MRE11*. Oncogene, 2002. **21**(32): p. 4873-4878.
198. Wu, X.H., et al., *SV40 T antigen interacts with Nbs1 to disrupt DNA replication control*. Genes & Development, 2004. **18**(11): p. 1305-1316.
199. Reiss, K., et al., *JC virus large T-antigen and IGF-I signaling system merge to affect DNA repair and genomic integrity*. Journal of Cellular Physiology, 2006. **206**(2): p. 295-300.
200. Franken, N.A.P., et al., *Clonogenic assay of cells in vitro*. Nature Protocols, 2006. **1**(5): p. 2315-2319.
201. Cook, J.L., B.A. Routes, and L. Sompayrac, *Experimental tumour induction by SV40 transformed cells*. Simian Virus 40 (Sv40): Possible Human Polyomavirus, 1998. **94**: p. 303-309.
202. Sariyer, I.K., et al., *Generation and characterization of JCV permissive hybrid cell lines*. Journal of Virological Methods, 2009. **159**(1): p. 122-126.
203. Cao, J., et al., *Differential effects of c-Ras upon transformation, adipocytic differentiation, and apoptosis mediated by the simian virus 40 large tumor antigen (vol 85, pg 32, 2007)*. Biochemistry and Cell Biology-Biochimie Et Biologie Cellulaire, 2008. **86**(2): p. 214-215.
204. Elenbaas, B., et al., *Human breast cancer cells generated by oncogenic transformation of primary mammary epithelial cells*. Genes & Development, 2001. **15**(1): p. 50-65.
205. Morales, C.P., et al., *Absence of cancer-associated changes in human fibroblasts immortalized with telomerase*. Nature Genetics, 1999. **21**(1): p. 115-118.
206. Takenouchi, T., et al., *Reversible conversion of epithelial and mesenchymal phenotypes in SV40 large T antigen-immortalized rat liver cell lines*. Cell Biol Int Rep (2010), 2010. **17**(1): p. e00001.
207. Rubin, H., *The role of selection in progressive neoplastic transformation*. Adv Cancer Res, 2001. **83**: p. 159-207.
208. Rubin, H., *Selected cell and selective microenvironment in neoplastic development*. Cancer Res, 2001. **61**(3): p. 799-807.
209. Snider, N.T. and M.B. Omary, *Post-translational modifications of intermediate filament proteins: mechanisms and functions*. Nature Reviews Molecular Cell Biology, 2014. **15**(3): p. 163-177.
210. Hurt, C.M., et al., *REEP1 and REEP2 proteins are preferentially expressed in neuronal and neuronal-like exocytotic tissues*. Brain Research, 2014. **1545**: p. 12-22.
211. Schmiedel, B.J., et al., *RANKL Expression, Function, and Therapeutic Targeting in Multiple Myeloma and Chronic Lymphocytic Leukemia*. Cancer Research, 2013. **73**(2): p. 683-694.

-
212. Park, H.S., et al., *Expression of Receptor Activator of Nuclear Factor Kappa-B as a Poor Prognostic Marker in Breast Cancer*. *J Surg Oncol*, 2014. **110**(7): p. 807-812.
 213. Govindaraj, C., et al., *Impaired Th1 immunity in ovarian cancer patients is mediated by TNFR2+Tregs within the tumor microenvironment*. *Clinical Immunology*, 2013. **149**(1): p. 97-110.
 214. Shi, Y.G., et al., *A novel cytokine receptor-ligand pair - Identification, molecular characterization, and in vivo immunomodulatory activity*. *Journal of Biological Chemistry*, 2000. **275**(25): p. 19167-19176.
 215. Aumailley, M., *The laminin family*. *Cell Adhesion & Migration*, 2013. **7**(1): p. 48-55.
 216. Wang, X.W., et al., *HOXC9 directly regulates distinct sets of genes to coordinate diverse cellular processes during neuronal differentiation*. *Bmc Genomics*, 2013. **14**.
 217. Brickelmaier, M., et al., *Identification and Characterization of Mefloquine Efficacy against JC Virus In Vitro*. *Antimicrobial Agents and Chemotherapy*, 2009. **53**(5): p. 1840-1849.
 218. Sharma, S.V., et al., *"Oncogenic shock": Explaining oncogene addiction through differential signal attenuation*. *Clinical Cancer Research*, 2006. **12**(14): p. 4392s-4395s.
 219. Irwin L. Goverman, Rob Jacoby, and R.G. Lester. *Bench to bedside: Formulating winning strategies in molecular diagnostics*. 2009 [cited 2015 24]; Available from: <http://www2.deloitte.com/us/en.html>.

5. Appendices

5.1 Appendix of the introduction chapter

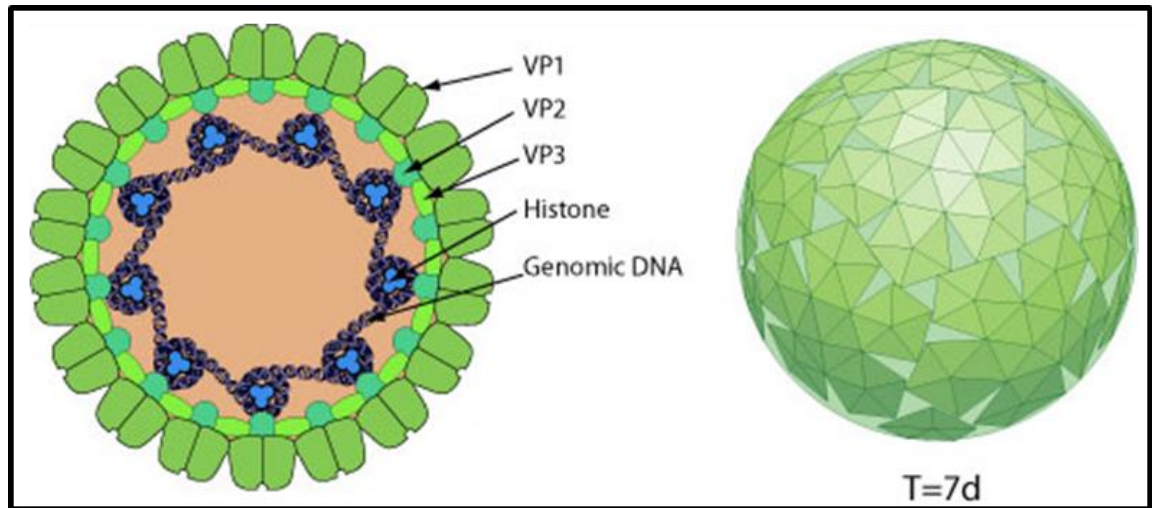


Figure 5.1.1 A schematic diagram of the virion of polyomavirus. Adapted from http://viralzone.expasy.org/all_by_species/58.html and accessed on 21/05/2011.

5.2 Appendix of the Materials & Methods chapter

5.2.1 Figures and tables

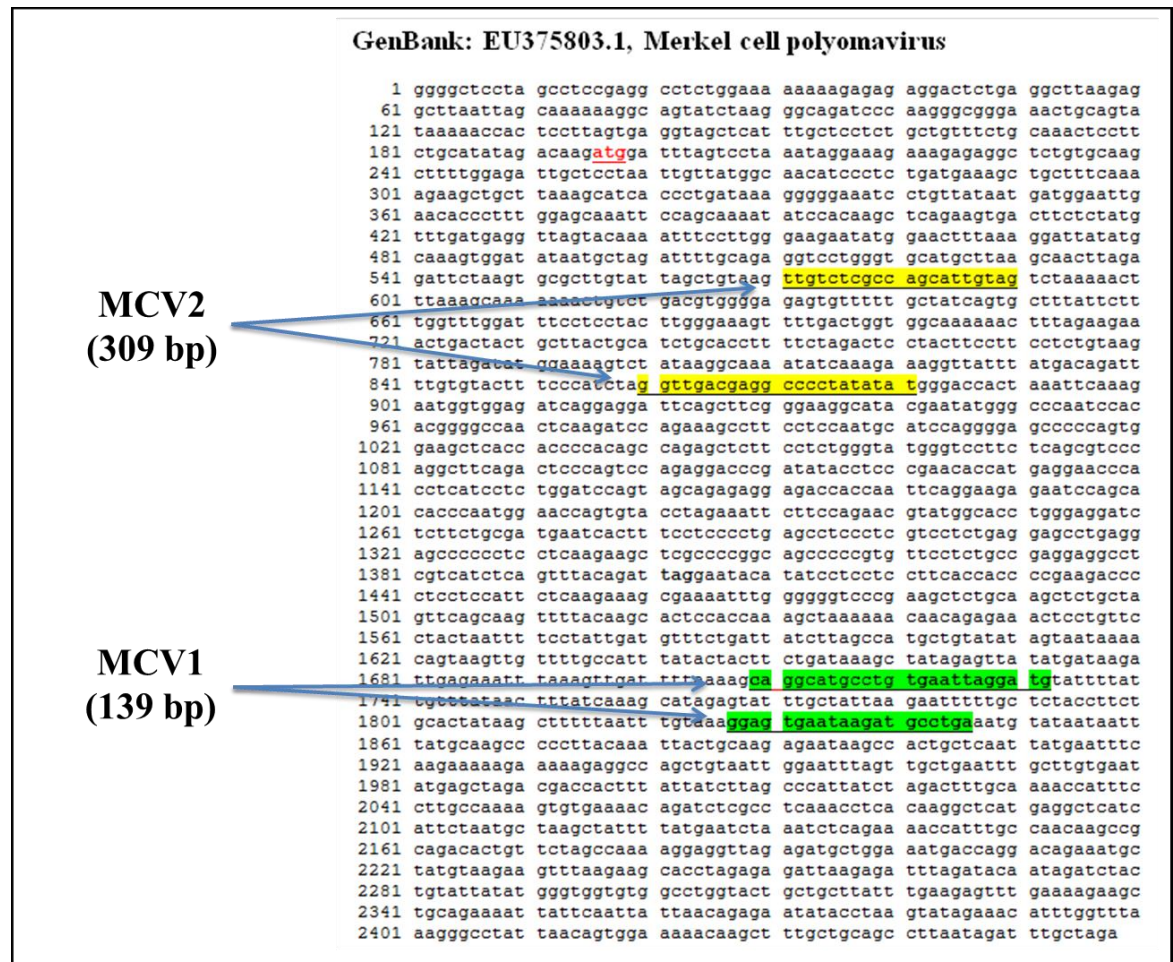


Figure 5.2.1 Whole LT sequence of Merkel cell polyomavirus isolate MCC350. A complete genome sequence was obtained from GenBank: EU375803.1 accessed on 09/08/2011 (<http://www.ncbi.nlm.nih.gov/nuccore/EU375803>). Primers are located at the LT region. Both primers were used for singleplex and multiplex PCR.

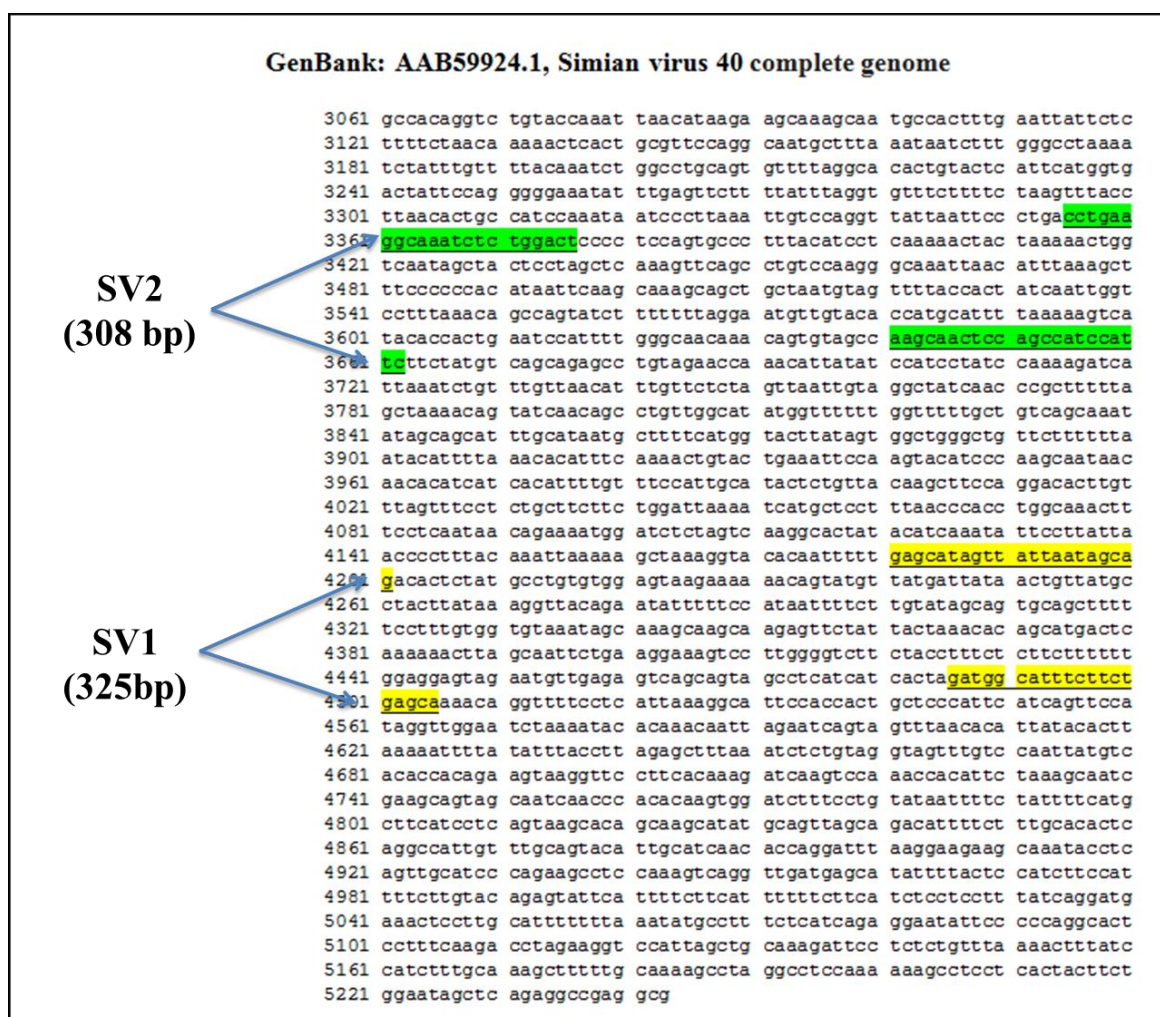


Figure 5.2.2 Whole LT sequence of SV40 isolate SV40-SP (KT). A complete genome sequence was obtained from GenBank: AAB59924.1 accessed on 03/02/2015 (<http://www.ncbi.nlm.nih.gov/nuccore/J02400.1>). Primers are located at the LT region.

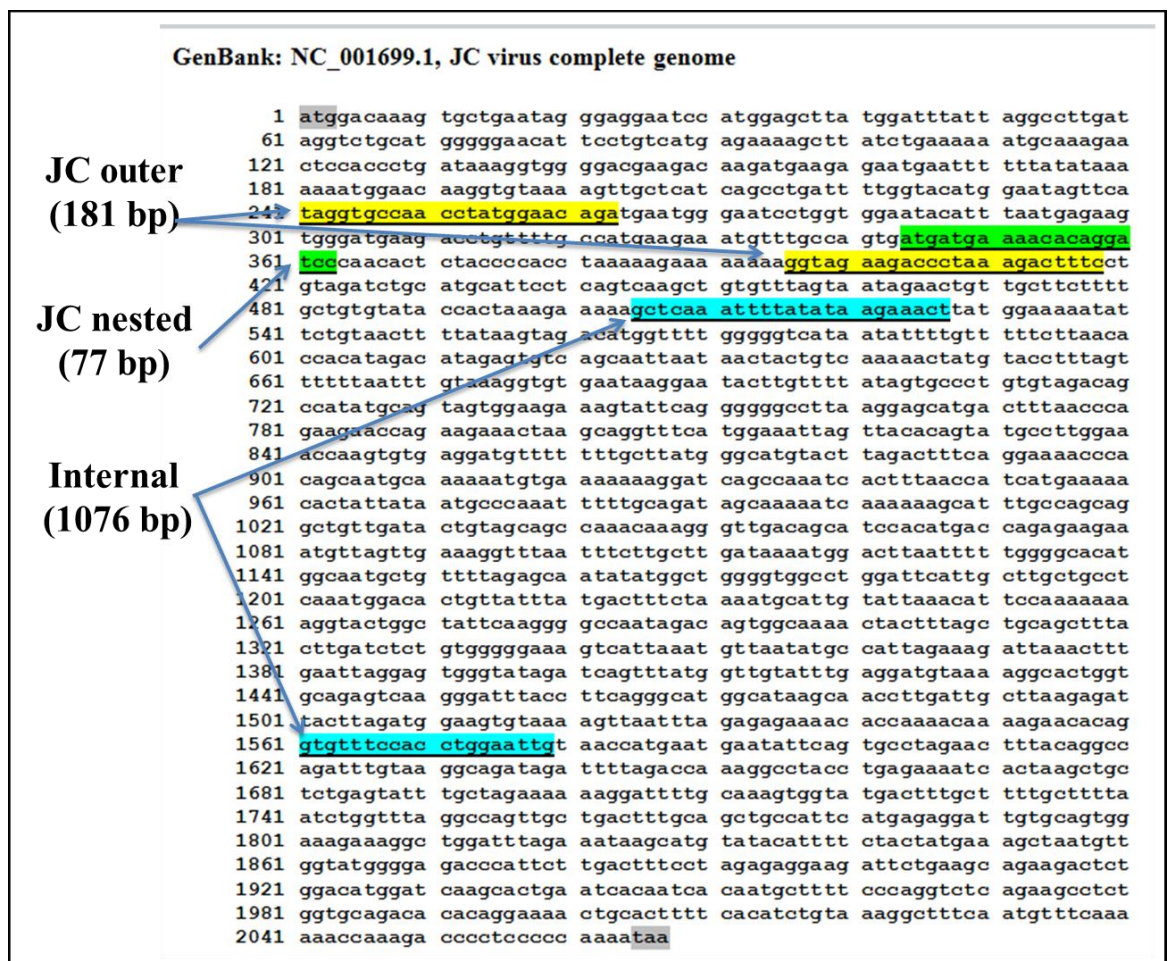


Figure 5.2.3 The complete ORF of JCV LT gene (2067 bp) obtained from GenBank: AAB59924 accessed on 03/02/2015 ([Large T gene](#)). The arrows in the left-hand side indicate the primers used for cervical screening as well as the internal primers used for nested PCR confirmation.

Table 5.2.1 list of primers used in PCR amplification of polyomaviruses in cervical cancer.

	Primer name	Sequence	Amplicon Size (bp)	
1	GAPDH-F	CATTGACCTCAACTACATGGT	130 bp	
2	GAPDH-R	TCGCTCCTGGAAGATGGTGAT		
	Primer name	Sequence	Amplicon Size (bp)	
1	MCV1.for	CAGGCATGCCTGTGAATTAGGATG	139 bp	
2	MCV1.rev	TCAGGCATCTTATTCACTCC		
	Primer name	Sequence	Amplicon Size (bp)	
1	MCV2.for	TTGTCTCGCCAGCATTGTAG	309 bp	
2	MCV2.rev	ATATAGGGGCCTCGTCAACC		
	Primer name	Sequence	Amplicon Size (bp)	
1	SV1.for	GAGCATAGTTATTAATAGCAG	325 bp	
2	SV1.rev	TGCTCAGAAGAAATGCCATC		
	Primer name	Sequence	Amplicon Size (bp)	
1	SV2.for	GAATGGATGGCTGGAGTTGCTT	308 bp	
2	SV2.rev	CCTGAAGGTAAATCTCTCGACT		
	Virus	Primer name	Sequence	Size (bp)
1	BKV & JCV outer primers	PYV.for	GAAAGTCTTTAGGGTCTTCTACC	181 bp
2		PYV.rev	TAGGTGCCAACCTATGGAACAGA	
3	BKV inner primers	BKS2.for	GAAAGTCTTTAGGGTCTTCTACC	77 bp
4		BKS2.rev	AAGAAGCAACAGCAGATTCT	
5	JCV inner primers	JCVS2.for	GAAAGTCTTTAGGGTCTTCTACC	75 bp
6		JCVS2.rev	ATGATGAAAACACAGGATCC	

Table 5.2.2 list of primers used in PCR amplification and DNA sequencing of cloning of JCV LT ORF for ectopic expression studies.

List of primers used with pCITE-4a		
	Primer name	Sequence
1	T7 (F) promoter	TAATACGACTCACTATAGGG
2	T7 (R) terminator	GCTAGTTATTGCTCAGCGG
List of primers used for nested PCR of LT gene		
	Primer name	Sequence
1	Internal forward	GCTCAAATTTTATATAAGAACT
2	Internal reverse	CAATTCCAGGTGGAAACAC
List of primers used list of primers used in TOPO cloning		
	Primer name	Sequence
1	M13 Forward	GTAAAACGACGGCCAG
2	M13 Reverse	CAGGAAACAGCTATGAC
List of primers used in PCR validation of E6/E7 gene		
	Primer name	Sequence
1	HPV 16 E6/E7 F	GTGGACCGGTCGATGTATGTCT
2	HPV 16 E6/E7 R	TCCGGTTCTGCTTGTCCAGC
List of primers used in verification of the control vector		
	Primer name	Sequence
1	T7 Promoter	TAATACGACTCACTATAGGG
2	BGH Reverse	TAGAAGGCACAGTCGAGG

Table 5.2.3 EMT markers primers sequences.

	Product Name	Primer Sequences	Size
1	β -catenin	ACAAACTGTTTTGAAAATCCA	298 bp
		CGAGTCATTGCATACTGTCC	
2	Claudin	GCGCGATATTTCTTCTTGCAGG	110 bp
		TTCGTACCTGGCATTGACTGG	
3	E-Cadherin	GTCAGTTCAGACTCCAGCCC	250 bp
		AAATTCACCTCTGCCCAGGACG	
4	Vimentin	TCTACGAGGAGGAGATGCGG	210 bp
		GGTCAAGACGTGCCAGAGAC	
5	Snail	ACCACTATGCCGCGCTCTT	94 bp
		GGTCGTAGGGCTGCTGGAA	
6	N-cadherin	GGTAGACATCATAGTAGCTA	165 bp
		TCGATTGGTTTGACCACGG	
7	GAPDH	CATTGACCTCAACTACATGGT	149 bp
		TCGCTCCTGGAAGATGGTGAT	

Table 5.2.4 list of primary antibodies used throughout western blotting of EMT.

	Primary antibody	Isotype	Mol. Wt.
1	β -catenin XP® Rabbit mAb	Rabbit IgG	92 kDa
2	Claudin XP® Rabbit mAb	Rabbit IgG	20 kDa
3	E-Cadherin Rabbit mAb	Rabbit IgG	135 kDa
4	VimentinXP® Rabbit mAb	Rabbit IgG	57 kDa
5	Snail Rabbit mAb	Rabbit IgG	29 kDa
6	Slug Rabbit mAb	Rabbit IgG	30 kDa
7	N-cadherinXP® Rabbit mAb	Rabbit IgG	140 kDa
8	Anti-rabbit IgG, HRP-linked Antibody	Goat	

Table 5.2.5 primer combinations which were excluded from the study.

	Primer name	Sequence
1	SV40-3 F	TGGCTGATTATGATCATGAAC
2	SV40-3 R	AAAGAGAGATTGGACAAAGAG
1	SV40-4 F	TGAGGCTACTGCTGACTCTCAA
2	SV40-4 R	GCATGACTCCAAAACCTTAGCAA
1	SVBKJC F	GTGCCAACCFATGGAACAGA
2	SVBKJC R	GAAAGTCTAGGGTCCTACC
1	MCV- 3 F	AAGGCCAAGAAGTCAAGTTC
2	MCV- 3 R	ACACTCACTAACTTGATTTGG
1	MCV- 4 F	GTACCACTGTCAGAAGAAAC
2	MCV- 4 R	TTCTGCCAGGCTGTAACATAC
1	BKV- 2 F	GTGCCAACCTATGGAACAGA
2	BKV- 2 R	GAAAGTCTTTAGGGTCTTCT
1	JCV- 2 F	AGTCTTTAGGGTCTTCTACC
2	JCV- 2 R	GGTGCCAACCTATGGAACA

5.2.2 Solutions

All solutions were prepared using sterile filtered water and autoclaved for 11 mins at 121°C using a Prestige Medical 2100 series bench top autoclave (Prestige Medical, Blackburn, UK):

PCR preparation		Western blotting preparation	
1x Phosphate Buffer saline (PBS)		10% Sodium dodecyl sulphate (SDS)	
PBS tablets	1 tablet	SDS	50 g
Distilled water	200 ml	Distilled water up to	500 ml
10 x TAE buffer		10% Ammonium persulfate (APS)	
Tris Base	24.2 g	APS	1.0 g
Glacial acetic acid	5.7 ml	Distilled water up to	10 ml
0.5 M EDTA (PH 8.0)	10 ml	1M Tris pH 6.8 (100 ml)	
Distilled water up to	500 ml	Tris base	12.1 g
1 x TAE buffer		Distilled water up to	100 ml
10 x TAE buffer	50 ml	pH to 6.8 with HCL	drops
Distilled water up to	500 ml	1.5 M Tris pH 8.8 (100 ml)	
DNA loading Buffer (30% FiColl)		Tris base	81.1g
FiColl	3 g	Distilled water up to	100 ml
Distilled water up to	10 ml	pH to 8.8 with HCL	drops
1.2% Agarose		Laemmli sample buffer	
Agarose	0.8 g	10% SDS	2 ml
1x TAE buffer	50 ml	Glycerol (50%)	1 ml
3M NaAc		Dithiothreitol (DTT)(0.1M)	1 ml
NaAc anhydrous	24.61 g	Tris pH 6.8 (60mM Final)	0.6 ml
Distilled water up to	100 ml	Distilled water	5.4 ml
pH to 5.2 with HCL	drops	Bromophenol Blue (0.05%)	till blue
10 x Laemmli Running Buffer		Stacking Gel	
Tris Base	15.2 g	Distilled Water	2.7 ml
Glycine	72.1 g	Acrylamide Mix	0.67 ml
Distilled water up to	500 ml	Tris (pH 6.8)	0.5 ml
1 x Running Buffer		SDS (10%)	0.04 ml
10 x running Buffer	50 ml	APS (10%)	0.04 ml
10% SDS	5 ml	TEMEDa	0.004 ml
Distilled water up to	445 ml	Separating gel (15ml of 12% Solution)	
Transfer Buffer (500 ml)		Distilled water	5ml
Tris Base	2.9 g	Acrylamide mix	6ml
Glycine	1.5 g	Tris (0.5M) pH 8.8	3.8ml
Methanol	200 ml	SDS (10%)	0.15ml
Distilled water up to	300 ml	APS (10%)	0.15ml
		TEMEDa	0.006ml

5.3 Appendix of the Results chapter

5.3.1 PCR images of all screened polyomaviruses

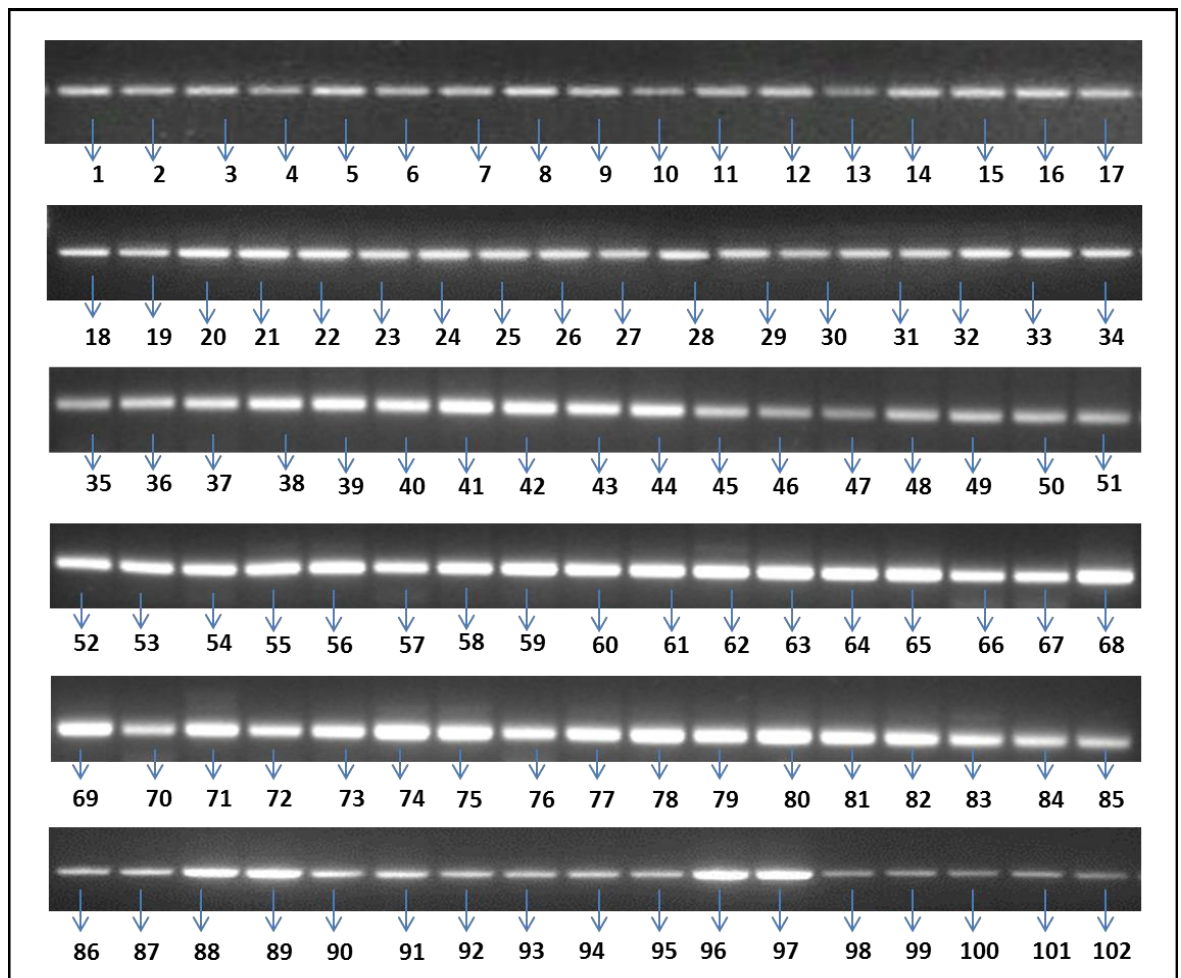


Figure 5.3.1 Agarose gel (1.5%) electrophoresis of GAPDH using GAPDH primers for 102 examined samples of the 220 cervical smears' samples. GAPDH size is 130 bp.

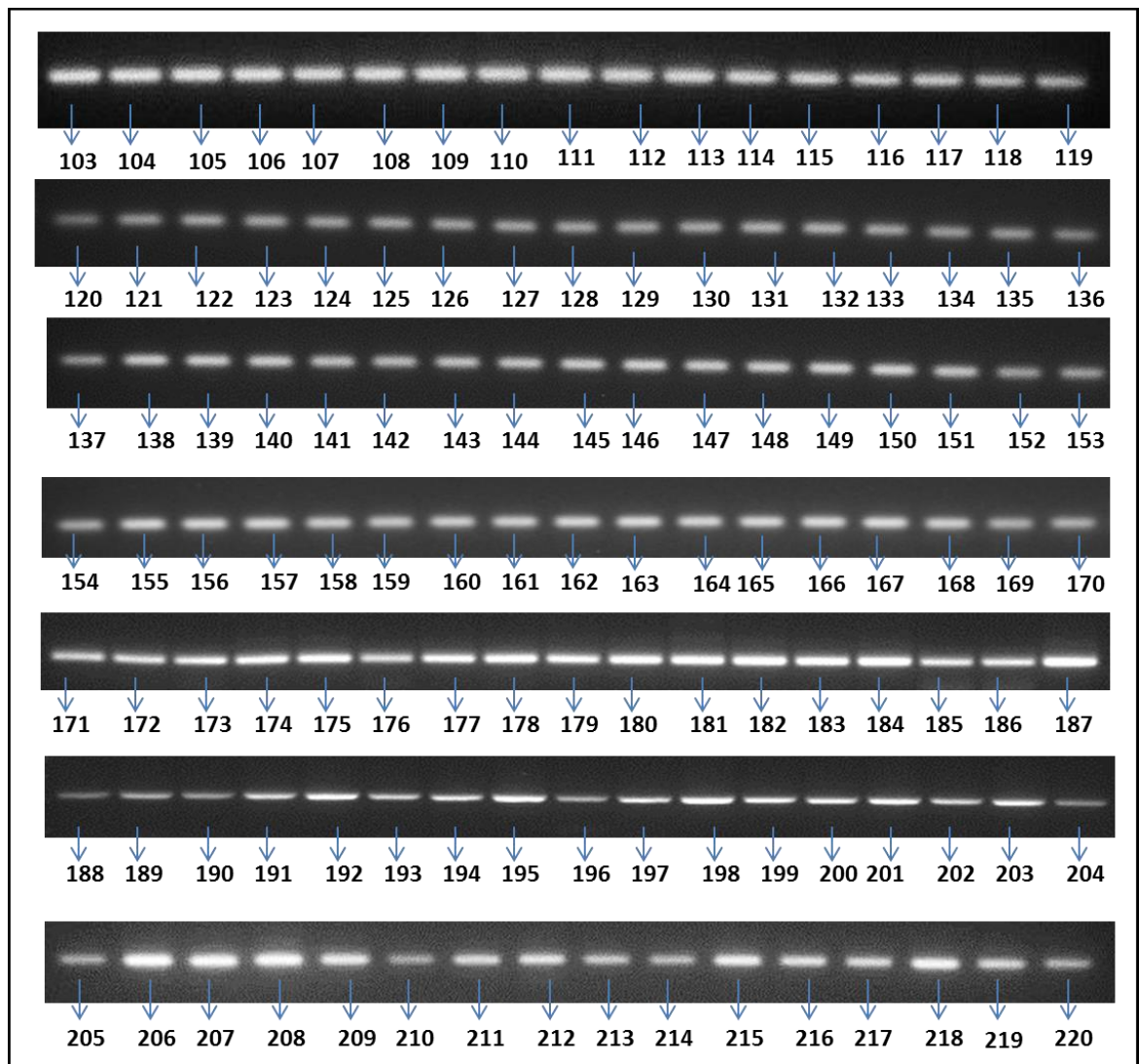


Figure 5.3.2 Agarose gel (1.5%) electrophoresis of GAPDH using GAPDH primers for 118 examined samples of the 220 cervical smears' samples. GAPDH size is 130 bp.

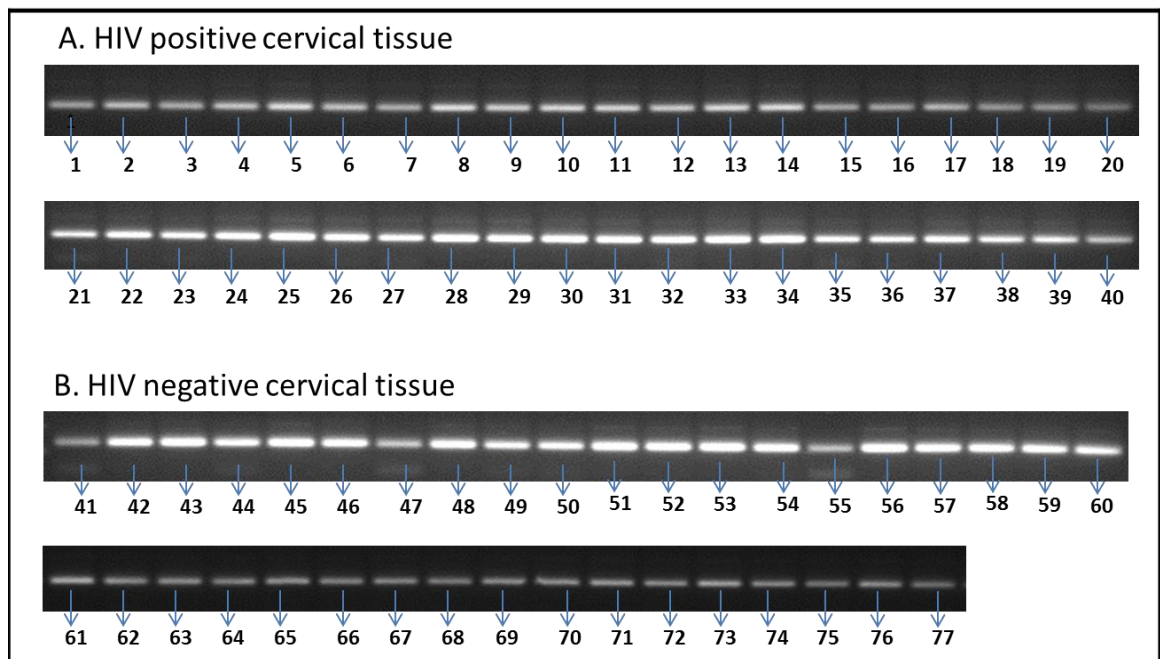
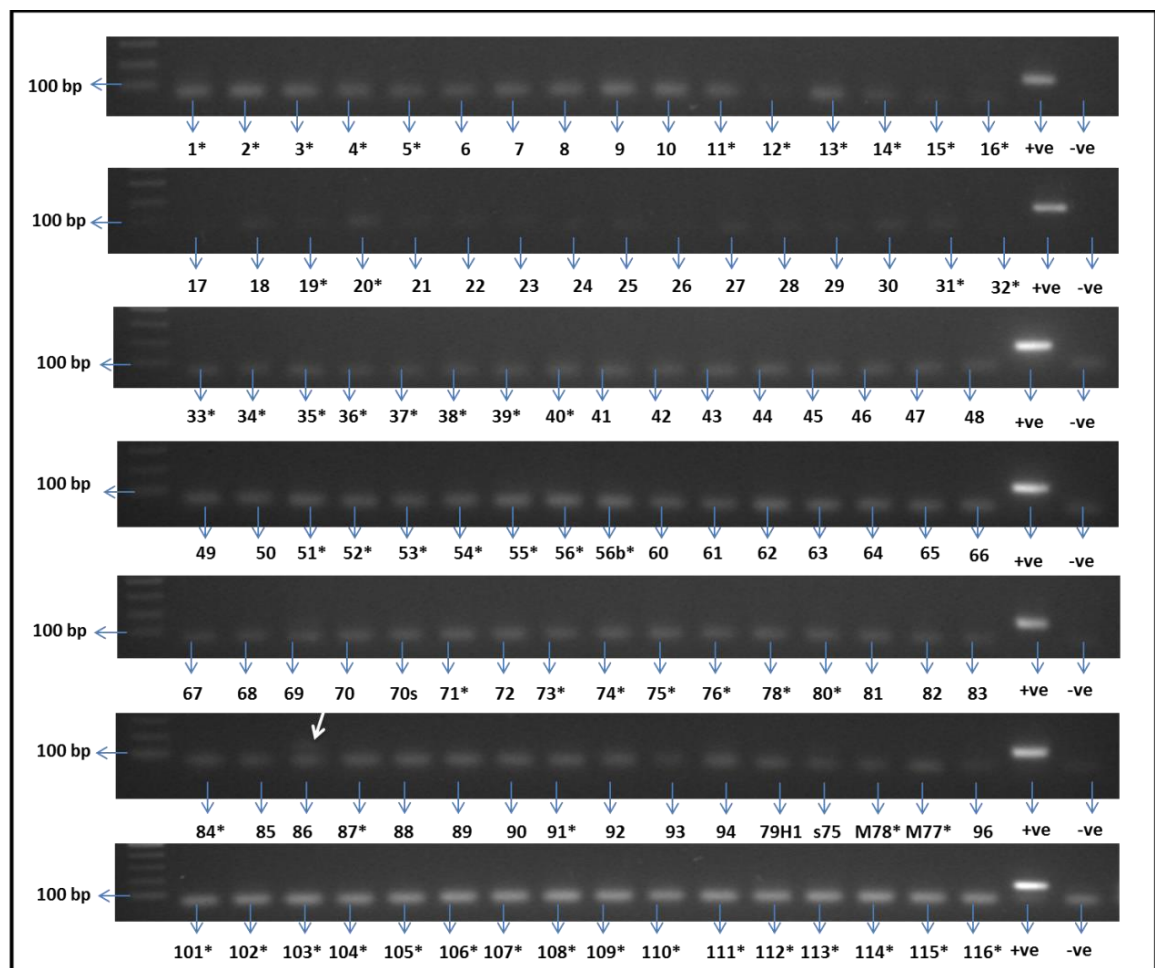
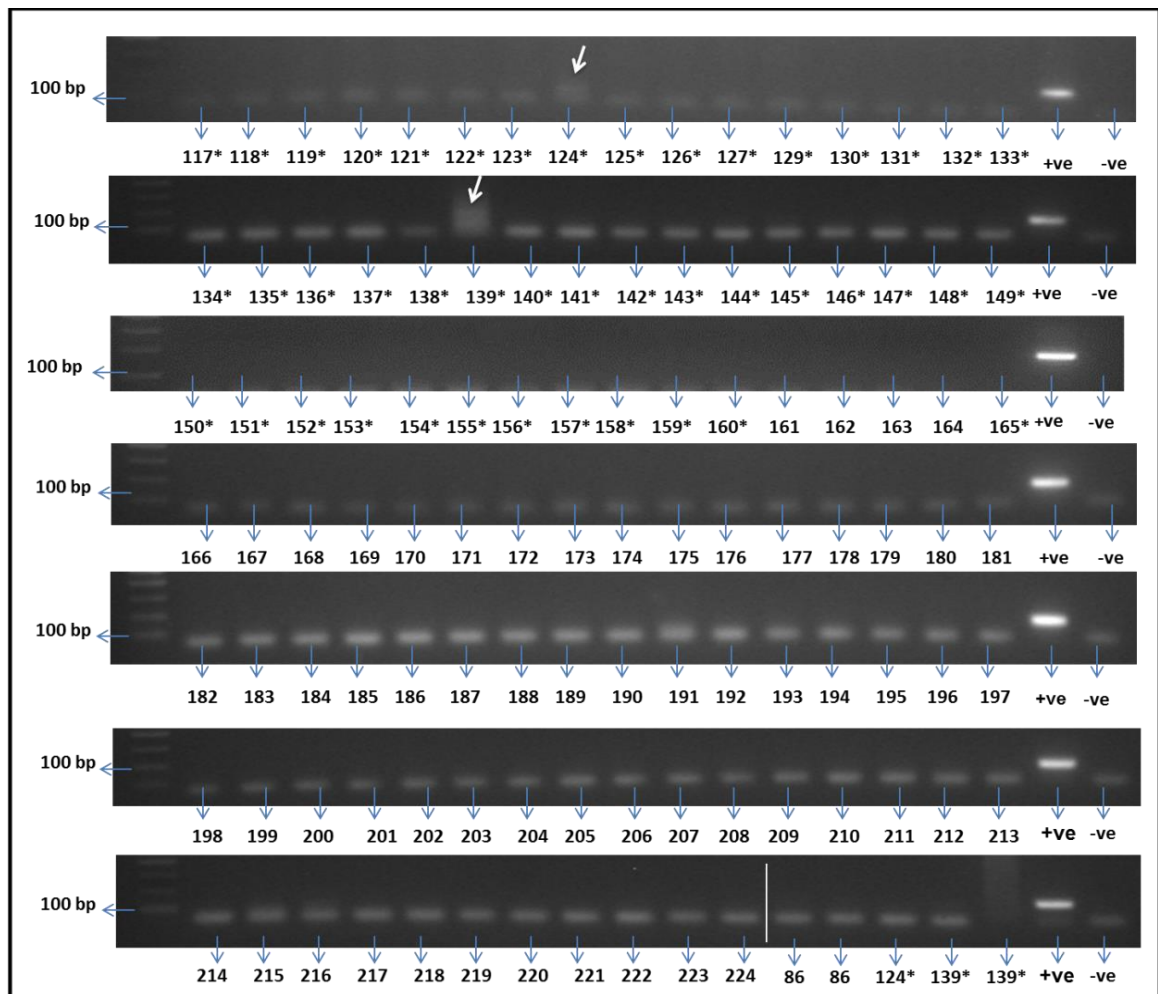


Figure 5.3.3 Agarose gel (1.5%) electrophoresis for GAPDH of HIV positive (A) and HIV negative (B) cervical cancer tissue using GAPDH primers for 77 examined samples. GAPDH amplicon size is 130 bp.



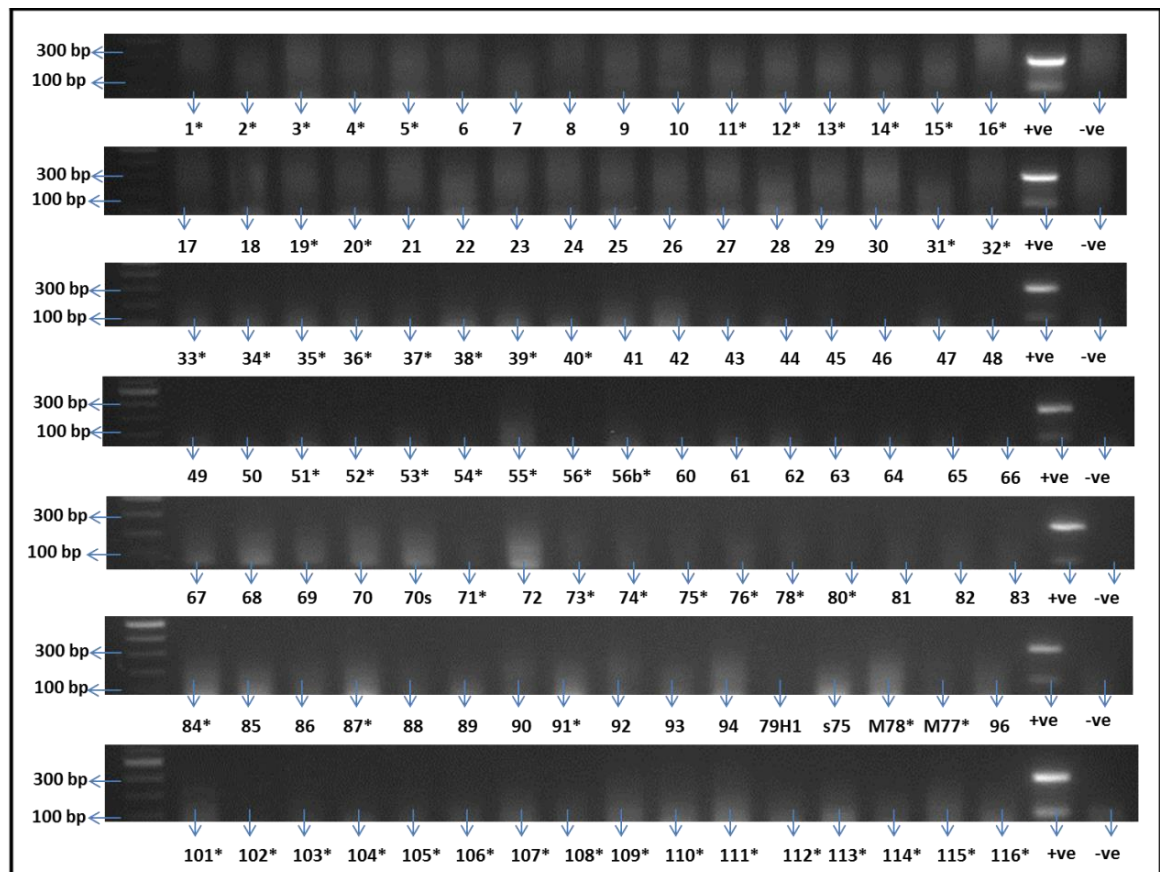
Note: HIV positive samples are marked with (*).

Figure 5.3.4 Agarose gel (1.5%) electrophoresis of MCV samples from number 1 to 116 by multiplex PCR. The expected signal size in the positive control is 139 bp and the negative control was dH₂O. The arrowed sample number 86 is a possible positive sample and re-amplified in Figure 5.3.5.



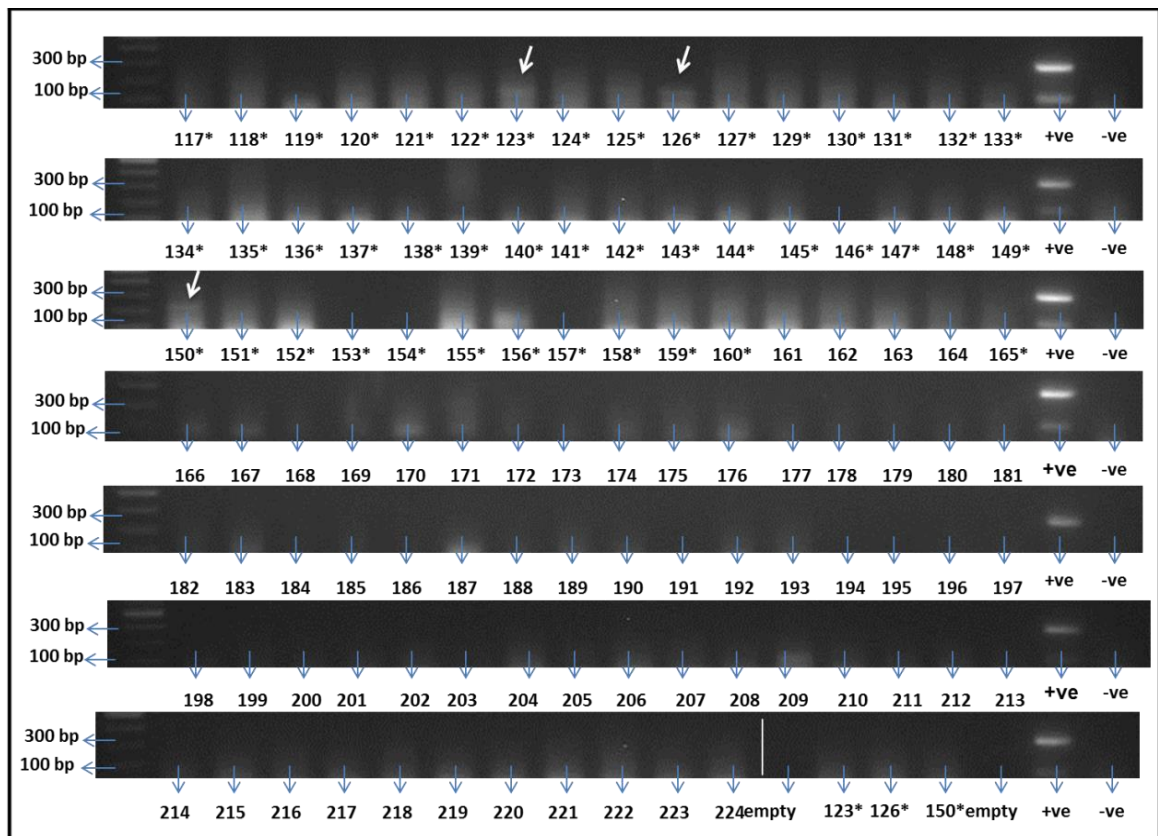
Note: HIV positive samples are marked with (*).

Figure 5.3.5 Agarose gel (1.5%) electrophoresis of MCV samples from number 117 to 224 by multiplex PCR. The expected signal size in the positive control is 139 bp and the negative control was dH₂O. The right-hand side of the last gel picture shows a repeat of 3 samples, namely: 86,124 and 139 that have shown false positivity during PCR screening.



Note: HIV positive samples are marked with (*).

Figure 5.3.6 Agarose gel (1.5%) electrophoresis of MCV second screening from number 1 to 116 by multiplex PCR, using two sets of primers as confirmation. The expected signal size in the positive control was 139 bp and 309 bp. The negative control was dH₂O.



Note: HIV positive samples are marked with (*).

Figure 5.3.7 Agarose gel (1.5%) electrophoresis of MCV second screening from samples 117 to 220 by multiplex PCR, using two sets of primers. The expected signal size in the positive control was 139 bp and 309 bp. The negative control was dH₂O. Sample number 123, 125 and 150 showed possible positivity on the lower signal (139 bp) only. However, when they were repeated on the last picture, they could not be re-amplified.

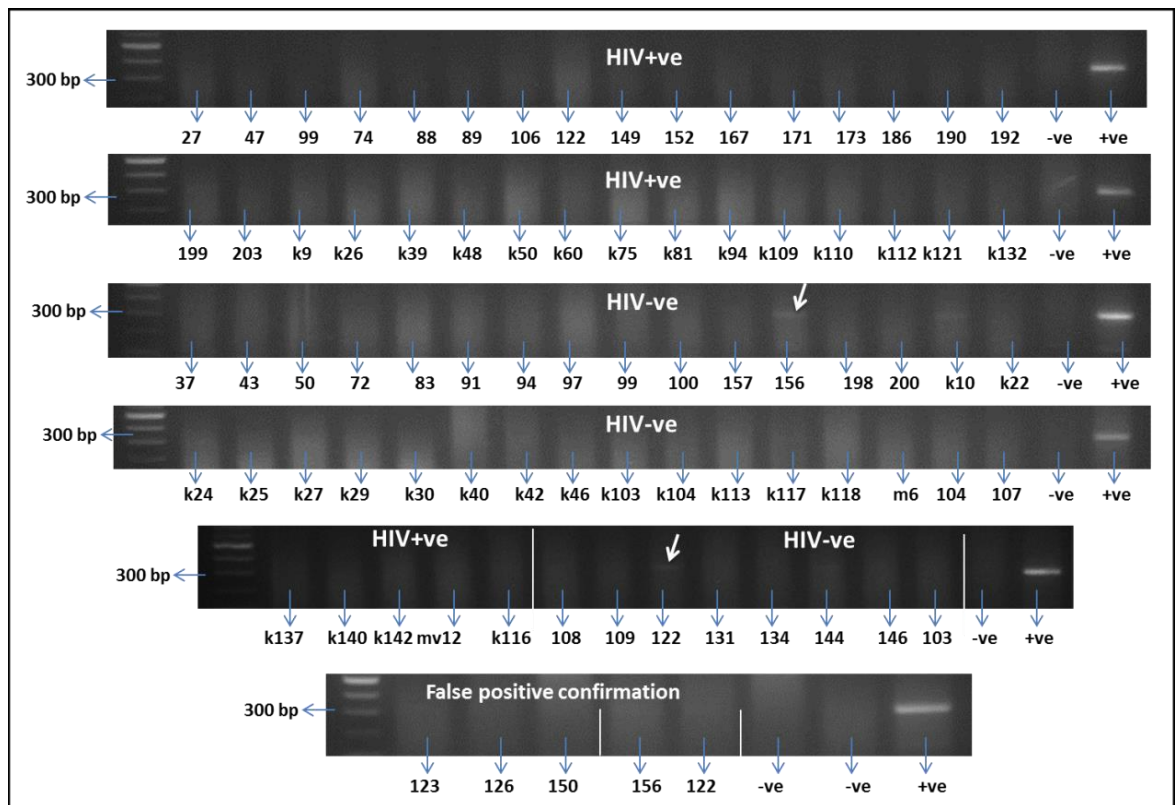
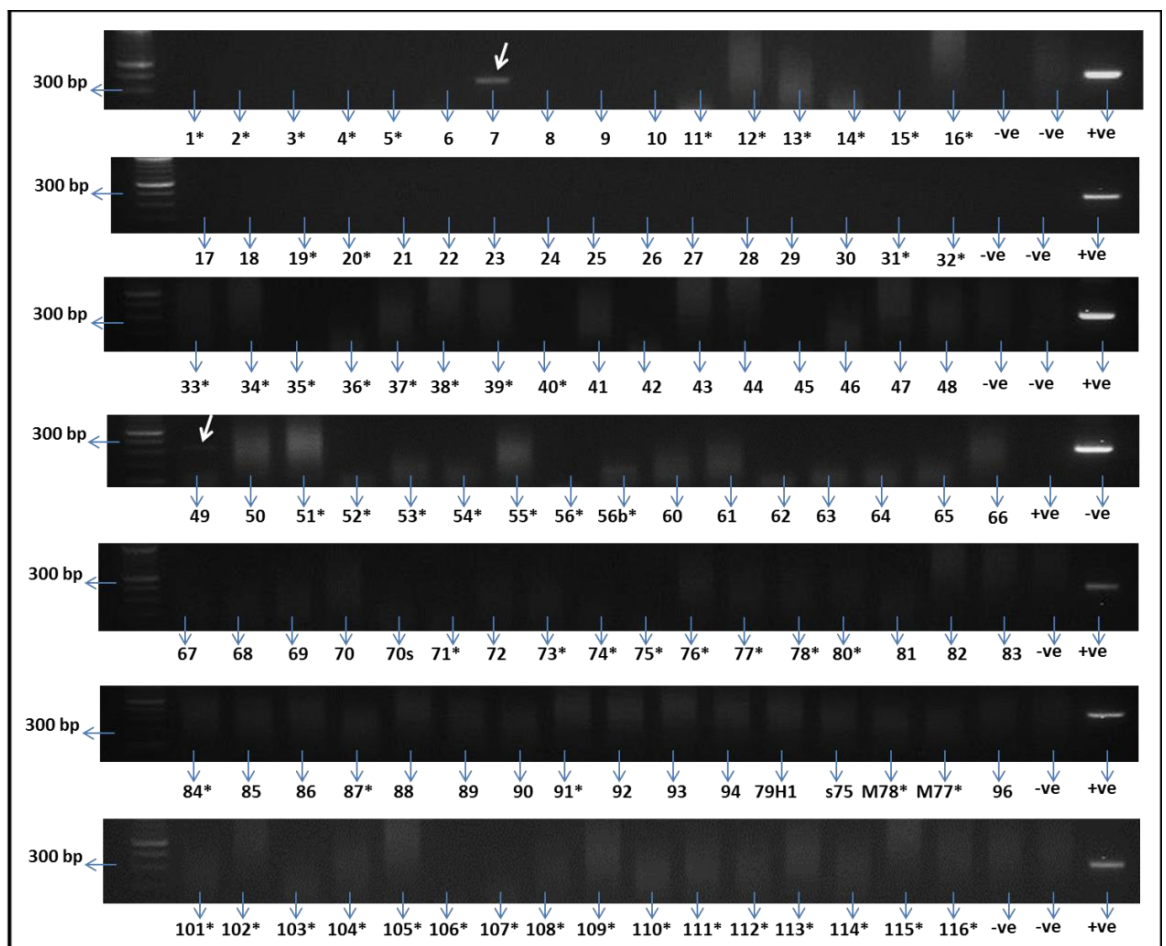
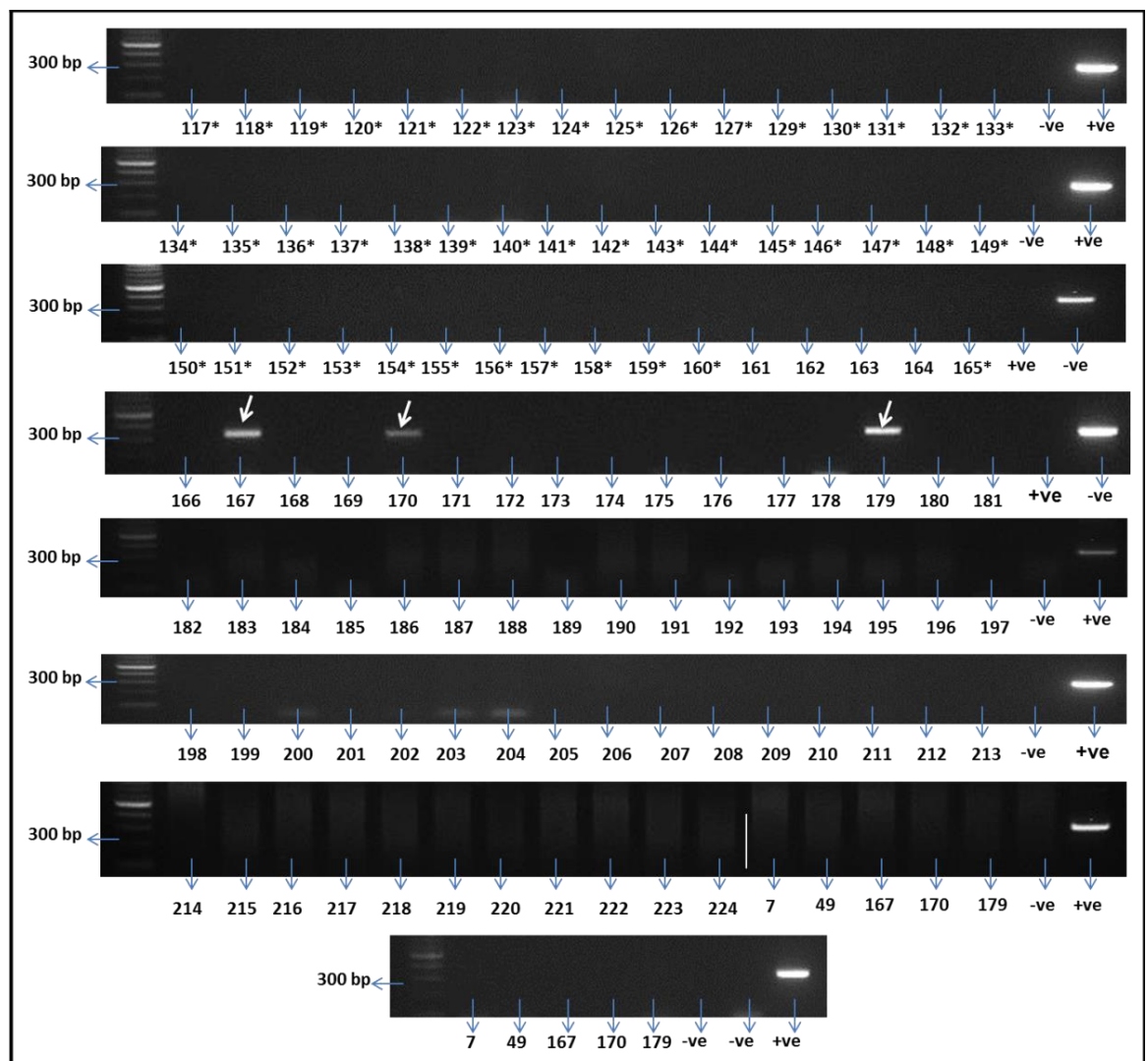


Figure 5.3.8 Agarose gel (1.5%) electrophoresis of MCV screening of 37 HIV positive and 40 HIV negative cervical tissue samples (carcinoma) using multiplex PCR. The expected signal sizes in the positive control are 309 bp as the higher signal and 139 bp product as the lower signal. dH₂O was the negative control. The arrowed signals in sample 156 and 122 are a possible positive result. However, the last gel image contains a confirmatory repeat of samples 123, 126 and 150 from the cervical smears' samples and sample 156 and 122 from the cervical tissue samples.



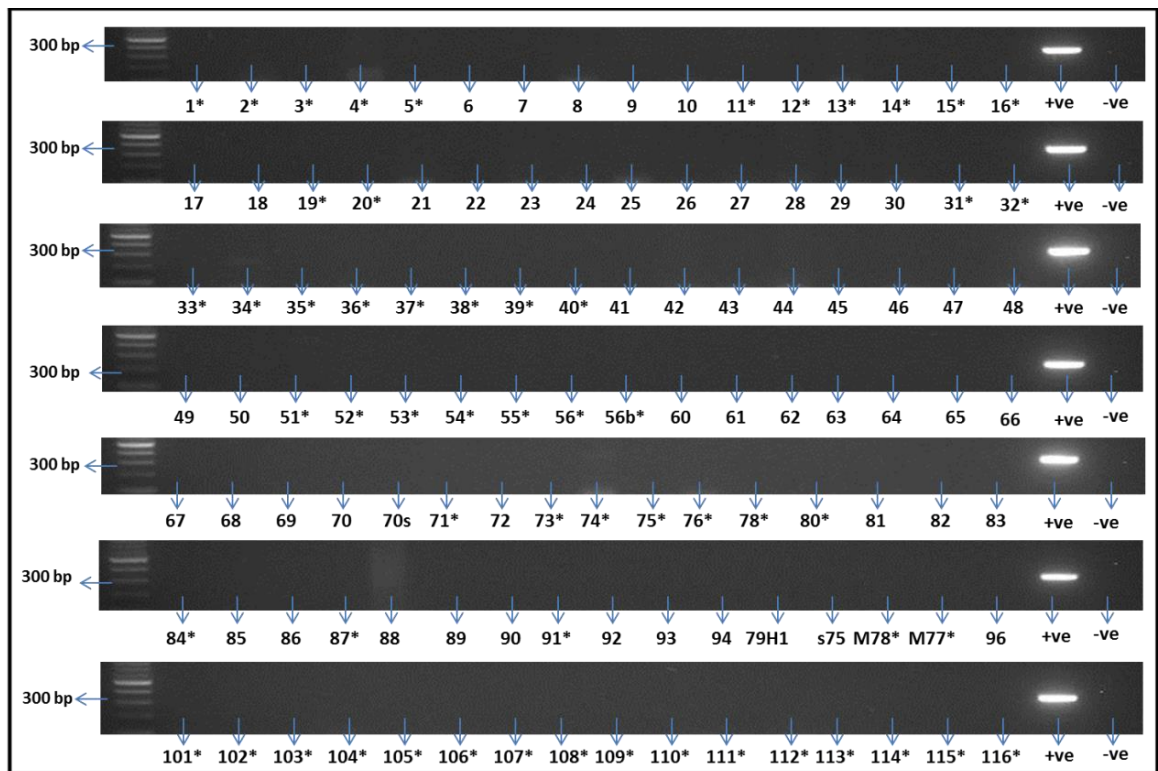
Note: HIV positive samples are marked with (*).

Figure 5.3.9 Agarose gel (1.5%) electrophoresis of SV40 samples from number 1 to 116 by singleplex PCR using Taq DNA polymerase. SV40 plasmid is the positive control and dH₂O is the negative control. The size of the expected signal of SV1 primers was 325 bp. Samples were separated alongside a 100 bp DNA ladder on the left-hand side. All screened samples show negativity to SV40 except for samples 7 and 49 in this figure and samples 167, 170 and 179 in the following figure (5.3.10).



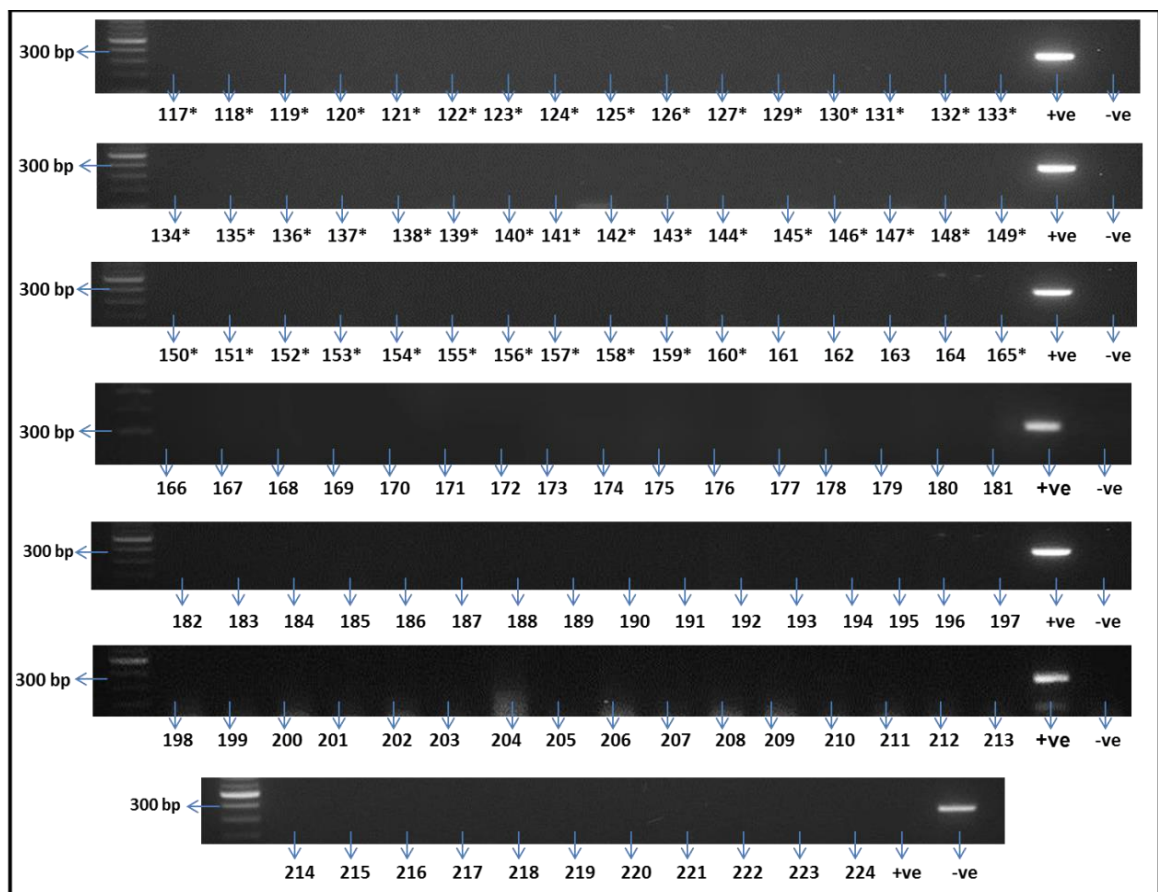
Note: HIV positive samples are marked with (*).

Figure 5.3.10 Agarose gel (1.5%) electrophoresis of SV40 samples from number 117 to 224 by singleplex PCR using Taq DNA polymerase. SV40 plasmid is the positive control and dH₂O is the negative control. The size of the expected signal of SV1 primers was 325 bp. Samples were separated alongside a 100 bp DNA ladder on the left-hand side. As can be seen in the last two PCR gels, those 5 samples were re-amplified twice but the DNA products could not be amplified again which may indicate a false positivity.



Note: HIV positive samples are marked with (*).

Figure 5.3.11 Agarose gel (1.5%) electrophoresis of SV40 second screening from number 1 to 116 by singleplex PCR. The expected signal size in the positive control was 308 bp. The negative control was dH₂O. Samples were separated alongside a 100 bp DNA ladder on the left-hand side.



Note: HIV positive samples are marked with (*).

Figure 5.3.12 Agarose gel (1.5%) electrophoresis of SV40 second screening from number 117 to 224 by singleplex PCR. The expected signal size in the positive control was 308 bp. The negative control was dH₂O. Samples were separated alongside a 100 bp DNA ladder on the left-hand side.

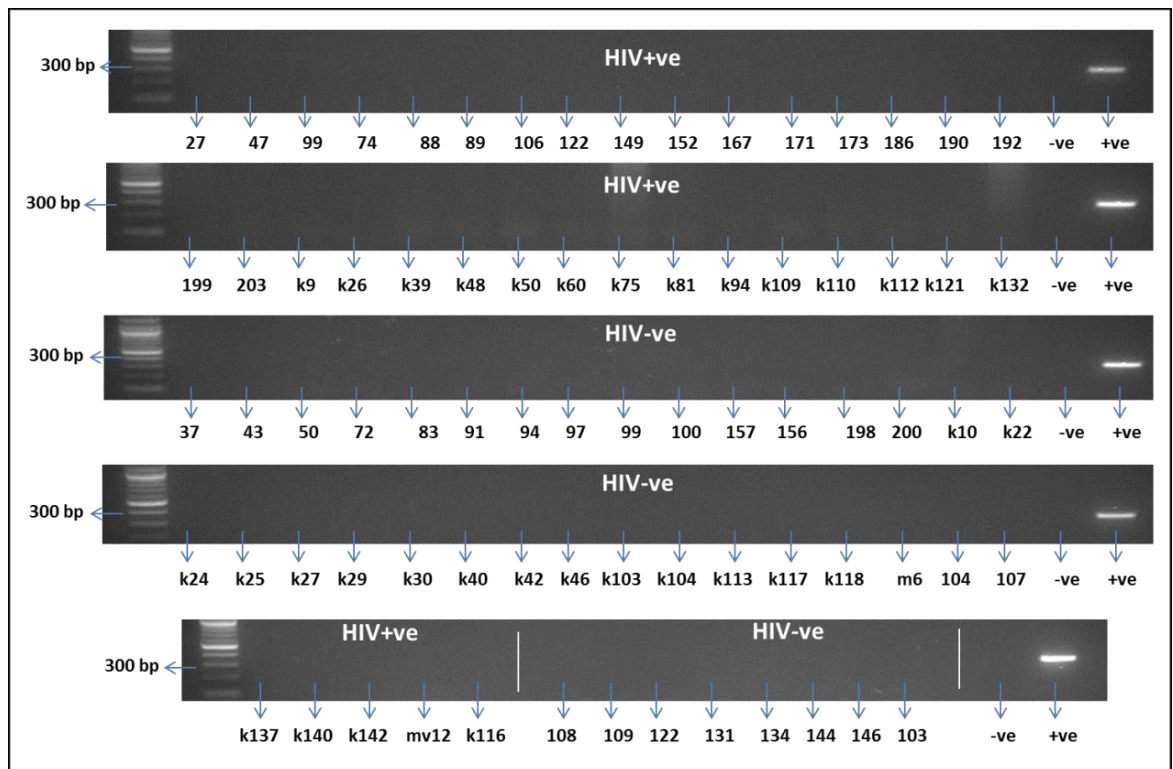
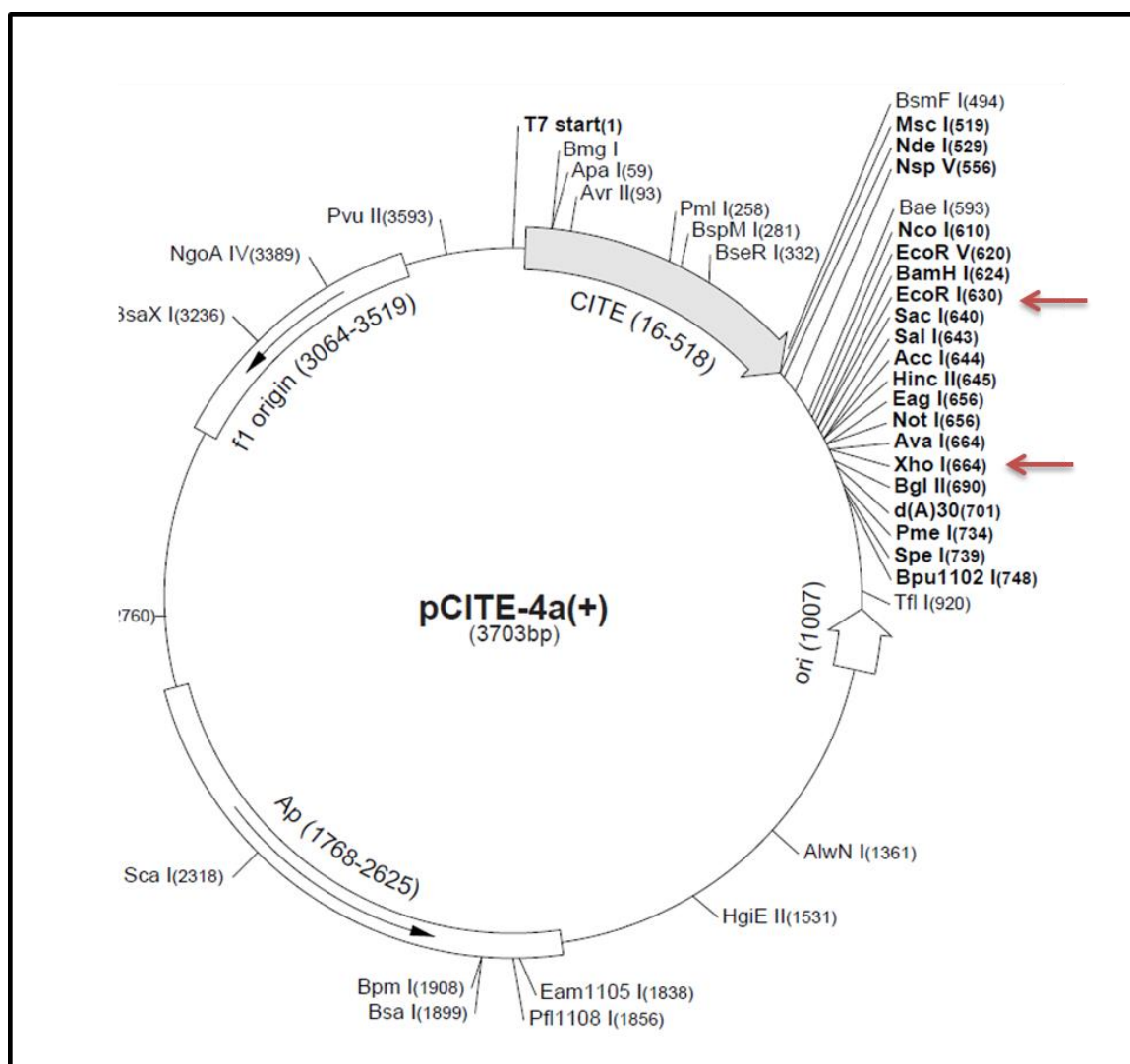


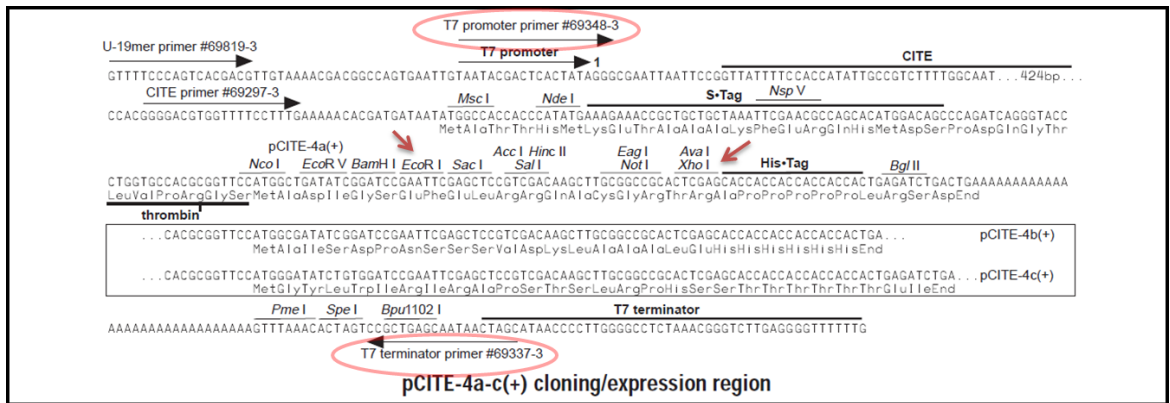
Figure 5.3.13 Agarose gel (1.5%) electrophoresis of SV40 screening of 37 HIV positive and 40 HIV negative cervical carcinomas. The expected signal size in the positive control is 308 bp. The negative control was dH₂O. The arrow on the left-hand side of the pictures indicates the anticipated product size according to a DNA ladder.

5.3.2 Appendices of cloning JCV LT ORF for ectopic expression studies



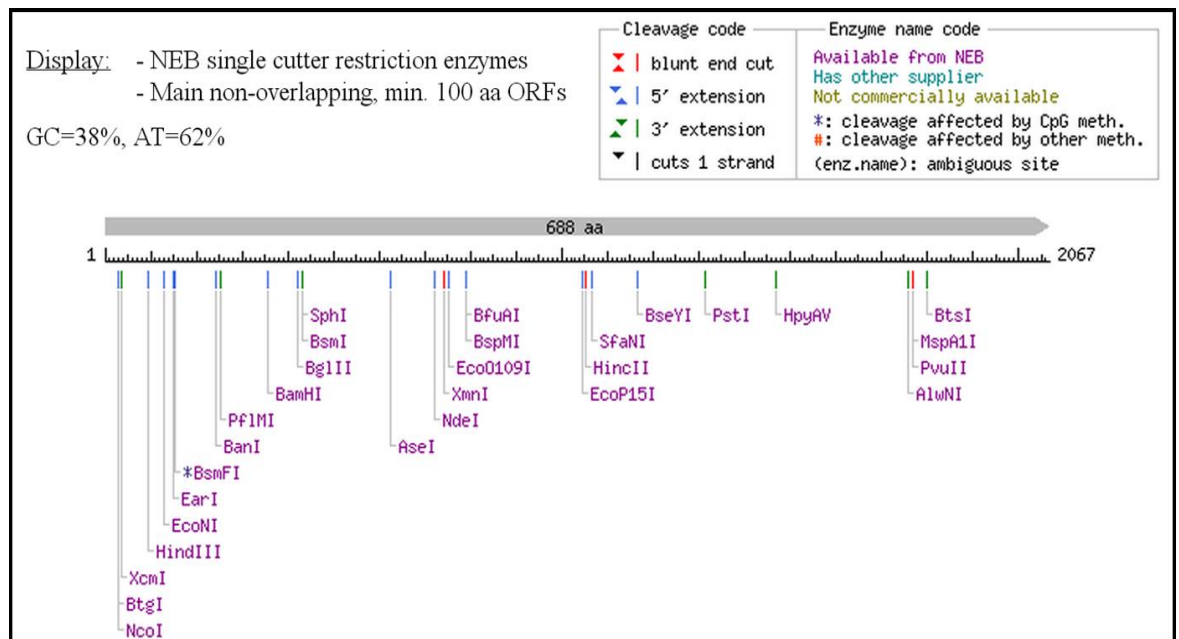
Adapted from (novagen.com)

Figure 5.3.14 pCITE-4a recombinant plasmid map. pCITE-4a is a 3703 bp plasmid, consisting of multiple cloning sites. JCV LT gene is cloned into the pCITE-4a vector at two of these restriction sites namely EcoR I and Xho I. Therefore, DNA sequencing was required to confirm LT integrity in pCITE-4a recombinant plasmid.



Adapted from (novagen.com)

Figure 5.3.15 pCITE-4a cloning/expression region. The two circled sequences include T7 promoter and terminator primers. The two arrowed restriction sites are EcoR I and Xho I which will be used for LT gene cloning.

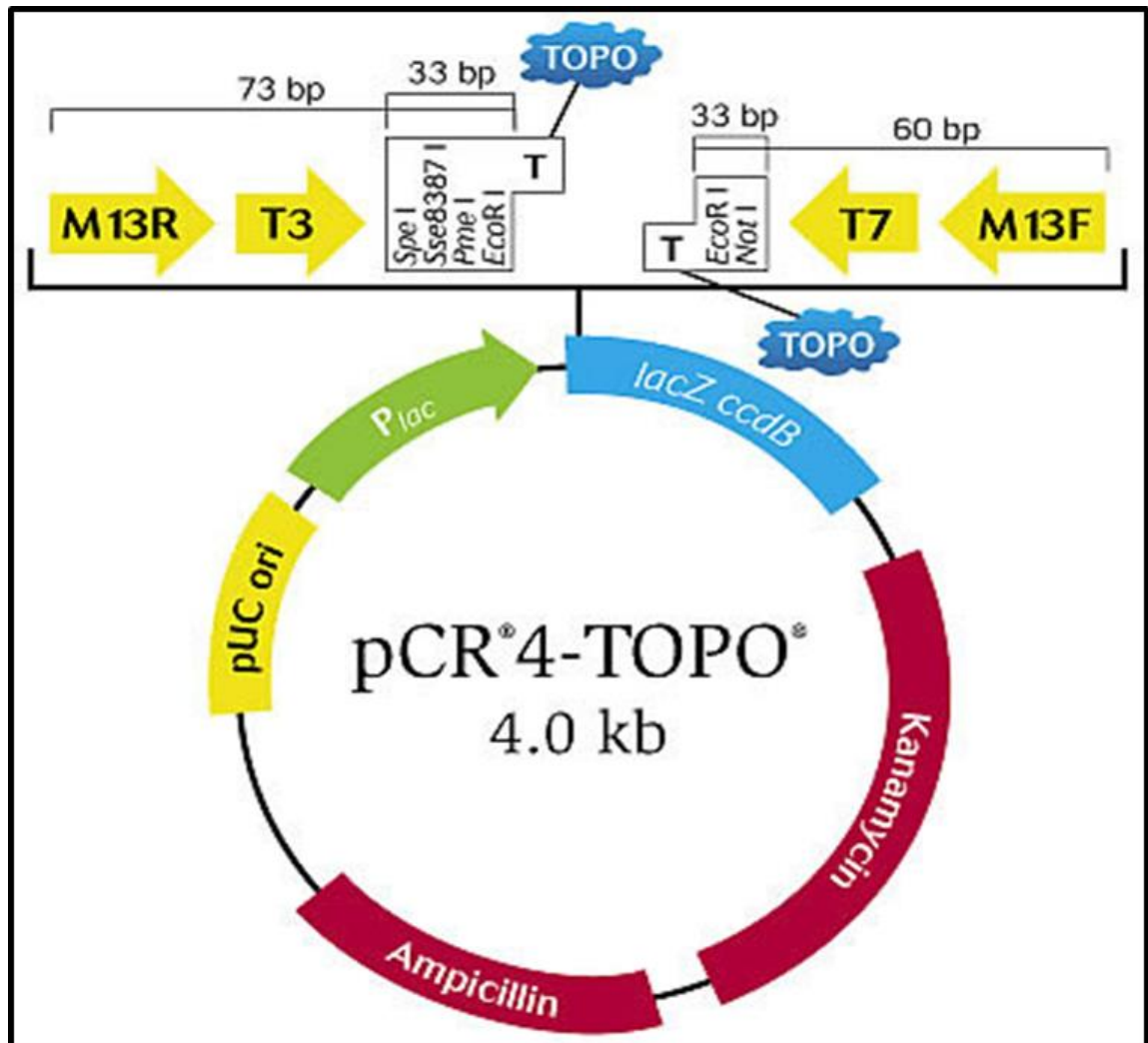


Adapted from the NEBcutter V2.0 software (NEBcutter)

Figure 5.3.16 NEBcutter result for LT gene. NEBcutter tool takes a DNA sequence and find the large, non-overlapping open reading frames of a gene and defines the restriction enzymes that cut the sequence just once. This result shows that EcoR I and Xho I could be used as restriction sites because they do not exist within the LT sequence and, therefore, the gene will be intact during the digestion steps of the cloning.

Table 5.3.1 Mismatch Primer design

Clamp	EcoR I	Start codon	LT starts
CTC	GAA TTC	ATG	GACAAAGTGCTGAATAGGGAG
Clamp	Xho I	Stop codon	LT ends
GAG	CTCGAG	TAA	TTTTGGGGGAGGGGTCTT



Adapted from Life Technologies Ltd ([TOPO[®]-TA cloning](#))

Figure 5.3.17 the PCR tube number (4) was purified and cloned into the Topo TA vector using the manufacturers' instructions (Life Technologies Ltd, UK). Kanamycin was used as a selective agent. For PCR amplification, M13 Forward and reverse primers were used.

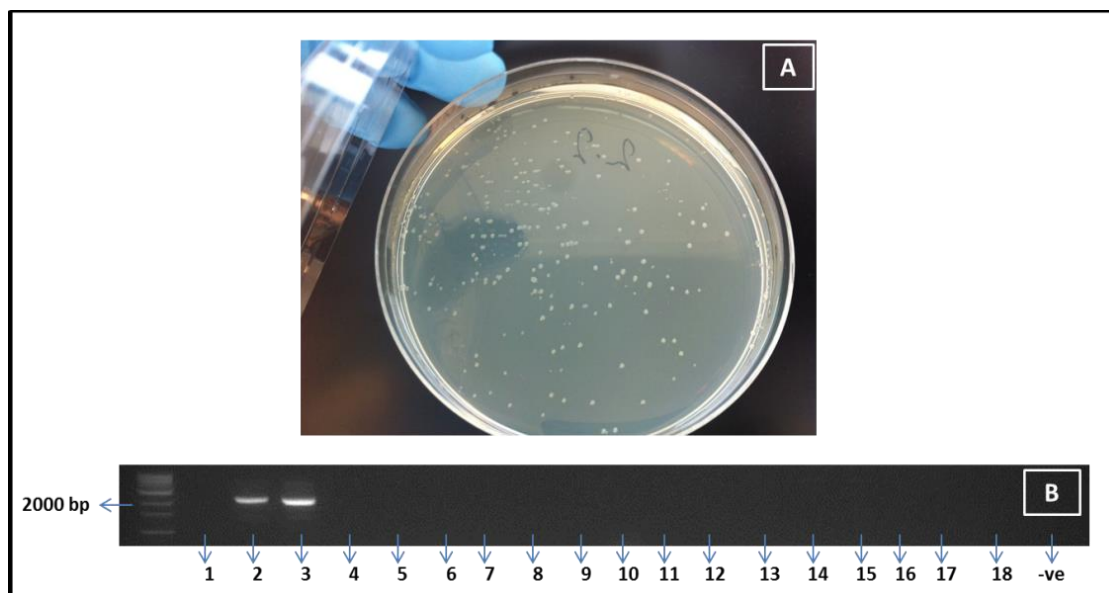


Figure 5.3.18 (A) plate picture of XL1-Blue competent cells transformed with the mismatch LT ORF product after being cloned into the Topo TA vector. (B) Agarose gel (1.5%) electrophoresis of 18 colonies. Colony numbers 2 and 3 only show an amplification of LT gene in combatant bacteria.

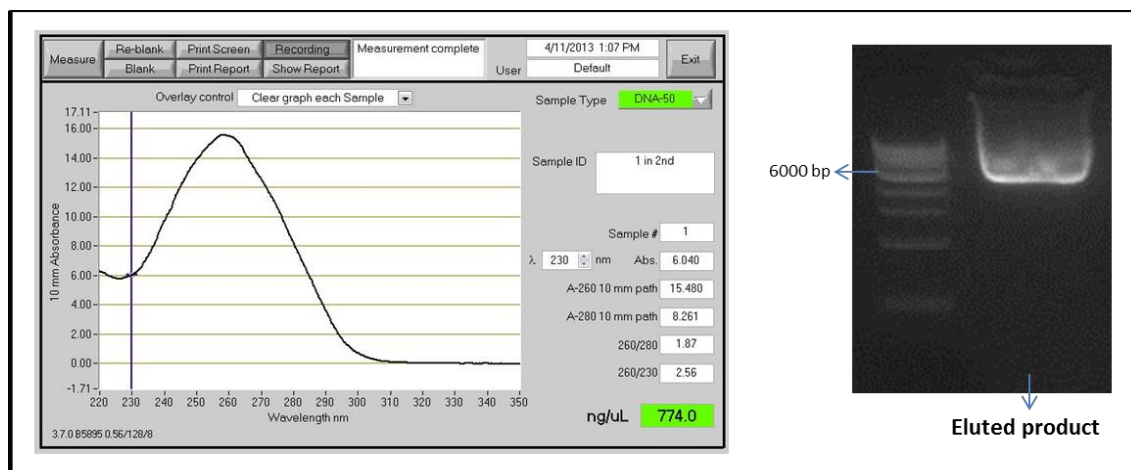


Figure 5.3.19 Agarose gel analysis of LT-Topo Mini-prep. The predicted size of this was product was 6023 bp (3956 bp TOPO + 2067 insert) and concentration of the extracted DNA was calculated by the use of a Nanodrop spectrophotometer. The combined products migrated faster than its expected size which is presumably due to the supercoiled nature of the product.



Key: LT: LT gene; RS: restriction site.

Figure 5.3.20 Sanger sequencing results of LT ORF TOPO clone. In order to cover the entire 2067 bp of the LT gene, 3 sequencing reactions were performed: M13 forward, Internal forward and M13 reverse primers. Between the first and second sequences, there were two silent mutations which have been marked by arrows.

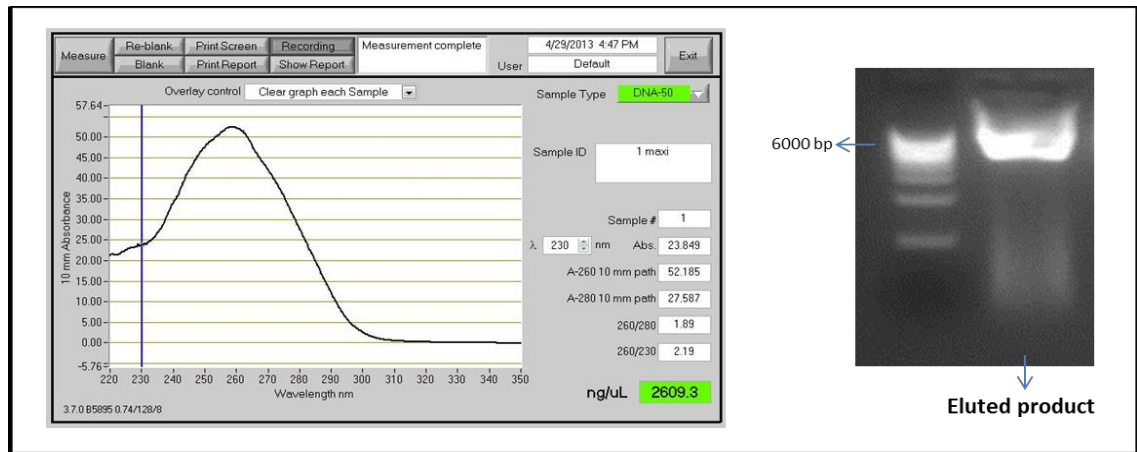
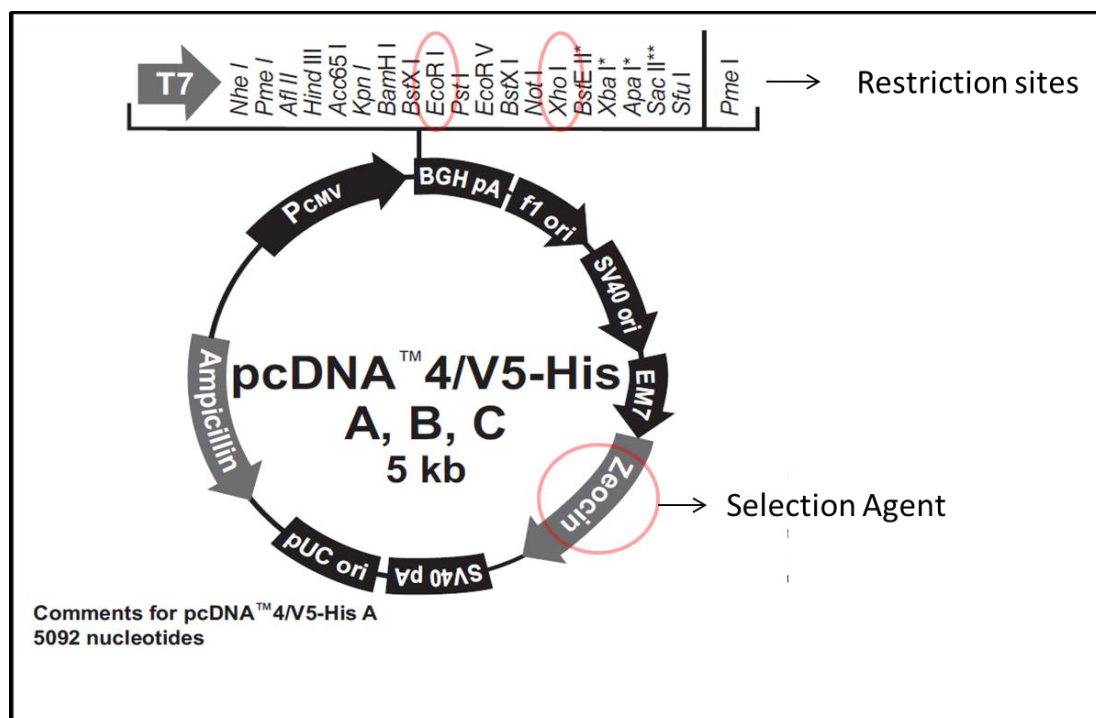


Figure 5.3.21 Agarose gel analysis of LT-Topo Maxi-prep. The predicted size of this was product was 6023 bp (3956 bp TOPO + 2067 insert) and concentration of the extracted DNA was calculated by the use of a Nanodrop spectrophotometer.



Adapted from Life Technologies Ltd ([pcDNA™4/V5-His A](#))

Figure 5.3.22 map of the target vector pcDNA™4 which LT gene was cloned into. Zeocin was used as a selective agent. For PCR amplification, T7 promoter forward and BGH reverse primers were used. Restriction sites namely EcoR I and Xho I were used in LT gene cloning. Sca I restriction site of the ampicillin resistant gene was chosen for LT linearisation.

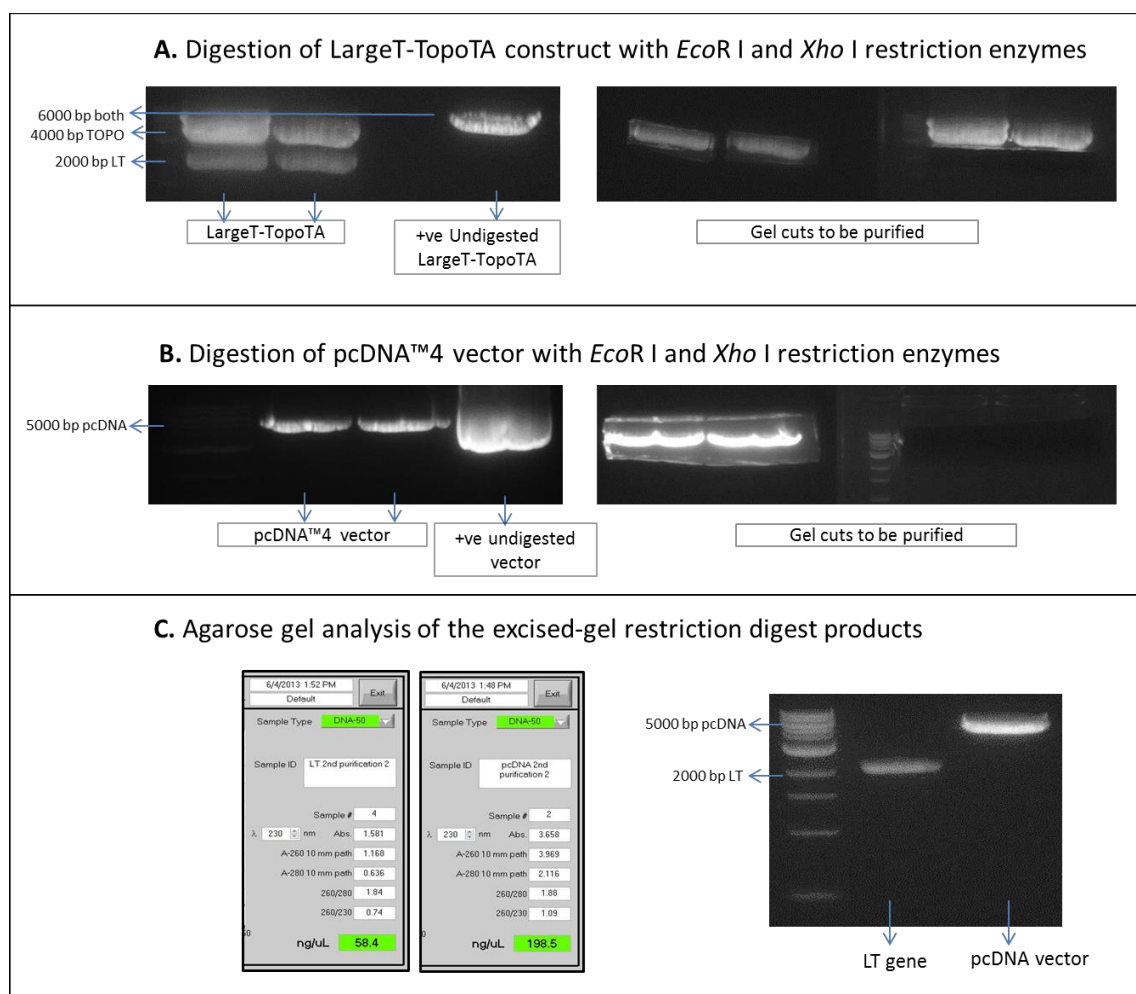


Figure 5.3.23 Agarose gel purification of *EcoR* I / *Xho* I digestion products from LT-Topo (A) and pcDNA™4 (B). Undigested controls migrated as supercoiled products whereas the digested LT insert and linearised vectors were clearly separated. The right-hand side agarose gel analysis images are of excised gel fragments prior to purification. (C) Agarose gel analysis of the excised-gel restriction digest products of LT ORF gene and pcDNA™4 vector. The 2067 bp LT insert and the linear 5068 bp pcDNA™4 target vector were successfully purified and the concentration estimated by Nanodrop spectrophotometer.

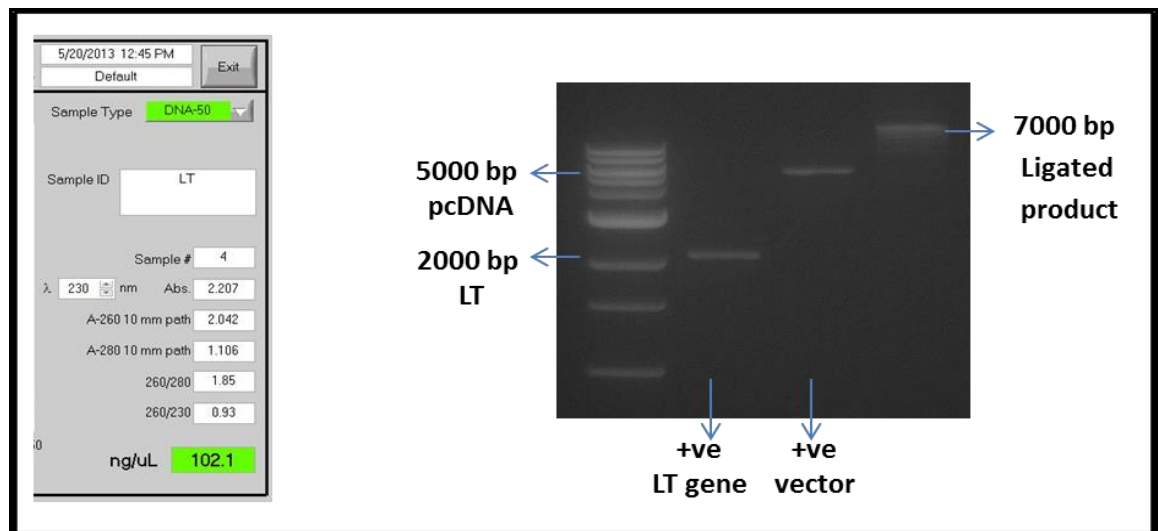


Figure 5.3.24 Agarose gel analysis of LT construct. The size of this amplicon was 7135 bp (5068 bp pcDNA^{TM4} + 2067 bp LT). Positive controls of LT gene and pcDNA^{TM4} vector were marked at around 2000 bp and 5000 bp respectively. LT full-length gene size should be 2067 bp whereas pcDNA^{TM4} vector should be 5068 bp, giving a total of 7135 bp LT construct.

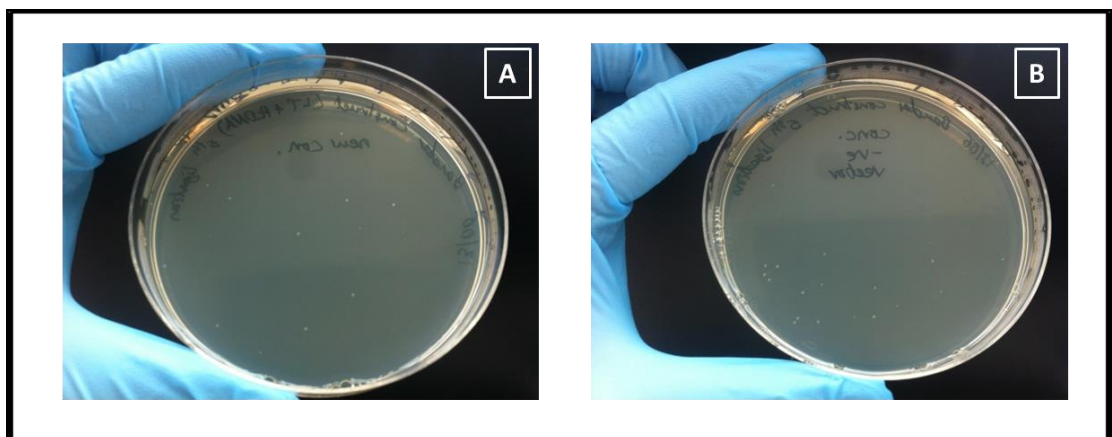


Figure 5.3.25 Plaques resulting from transforming XL1-Blue competent cells with two clones. A: LT construct. B: empty vector (pcDNA^{TM4}) encoding zeocin resistant gene. A third plate which was not inoculated with XL1-Blue acted as a negative control for the assay (plate not shown).

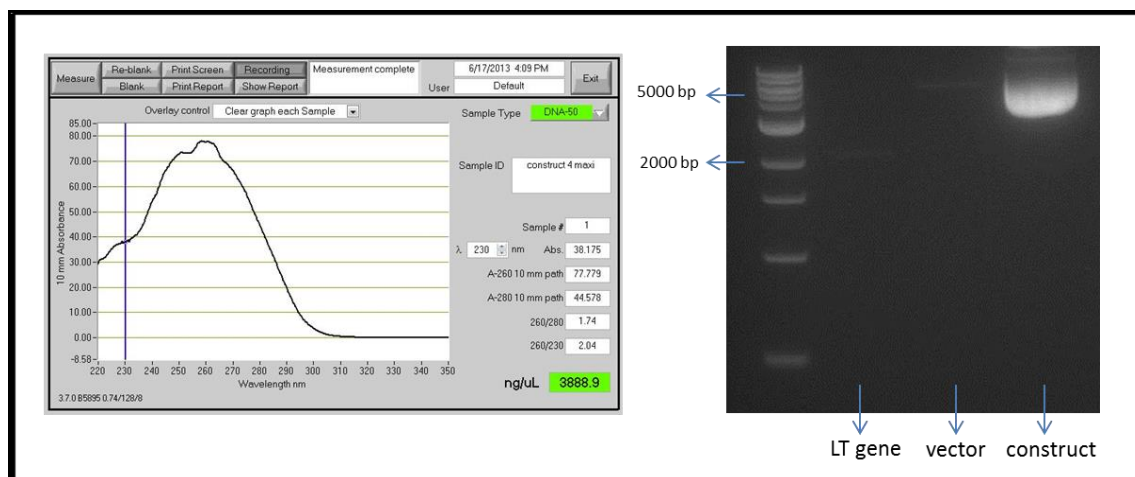


Figure 5.3.26 PCR agarose gel analysis of LT construct after Plasmid Maxi-prep was carried out for colony number (4). The size of this amplicon was 7135 bp. Positive controls of LT gene and pcDNATM4 vector are marked at around 2000 bp and 5000 bp respectively. Concentration of the extracted DNA was calculated by the use of a Nanodrop spectrophotometer.

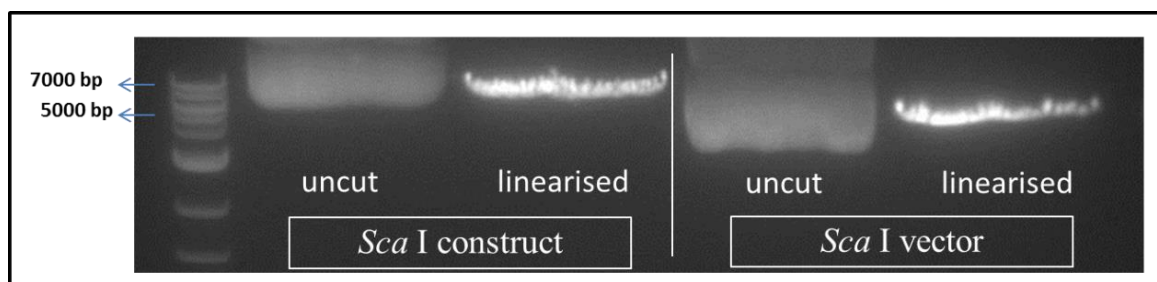


Figure 5.3.27 PCR agarose gel analysis of linearisation by restriction enzyme (*Sca* I) of LT construct and pcDNATM4 control vector. Undigested controls have amplicon sizes of 7135 bp and 5068 bp of the construct and vector respectively.

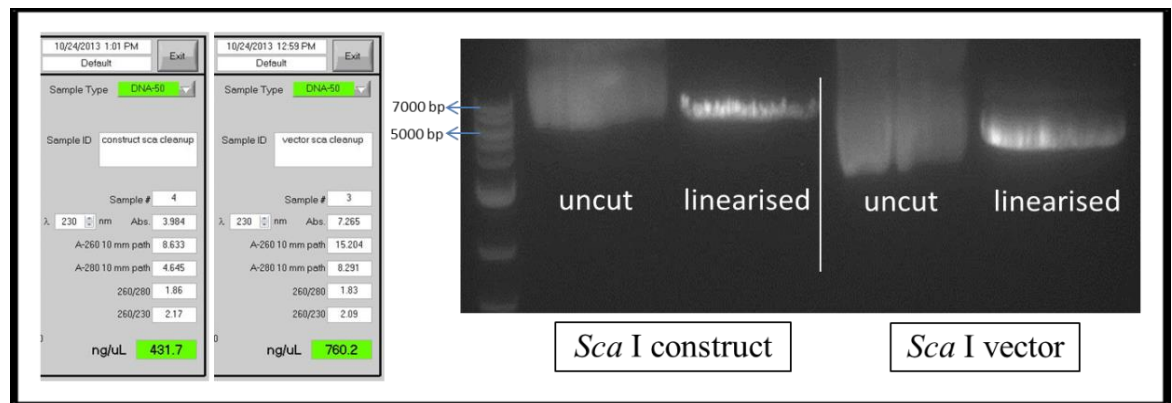


Figure 5.3.28 agarose gel analysis of the linearised products after gel purification.

The size of this amplicon was 7135 bp of the LT construct and 5068 bp of the pcDNATM4 vector. The concentration of purified DNA using a Nanodrop spectrophotometer showed the concentration of 431.7 ng/μl and 760.2 ng/μl for LT construct and empty vector respectively, which was sufficient for the transfection procedure.

Table 5.3.2 EMT markers relative intensity analysis of protein signals from western blot and genomic signals from RT-PCR compared to match GAPDH signals.

β -Catenin	WB	RT-PCR
Parent	66.46	69.40
Vector	100	100
LT 1	97.96	89.69
M 3	76.89	94.69
Claudin	WB	RT-PCR
Parent	88.16	36.27
Vector	23.18	26.42
LT 1	81.78	51.70
M 3	49.89	62.90
E-Cadherin	WB	RT-PCR
Parent	44.67	13.61
Vector	68.66	49.91
LT 1	53.48	23.75
M 3	51.80	27.94
Vimentin	WB	RT-PCR
Parent	61.43	22.42
Vector	0	2.62
LT 1	32.94	23.13
M 3	0	2.33
Slug	WB	RT-PCR
Parent	97.00	48.10
Vector	44.59	31.93
LT 1	79.35	56.69
M 3	37.77	69.44
Snail	WB	RT-PCR
Parent	53.50	20.32
Vector	34.34	3.56
LT 1	30.93	16.88
M 3	12.75	36.58
N-Cadherin	WB	RT-PCR
Parent	0	0
Vector	0	0
LT 1	0	0
M 3	0	0
control	90.32	81.92










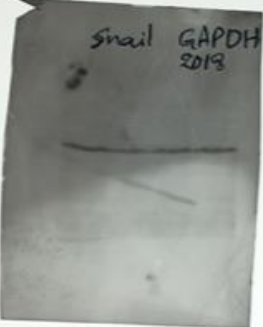


β-catenin		Claudin	
antibody	GAPDH	antibody	GAPDH
			
E-Cadherin		Vimentin	
antibody	GAPDH	antibody	GAPDH
			
Snail		N-Cadherin	
antibody	GAPDH	antibody	GAPDH
			

Figure 5.3.29 full images western blot of Parent, Vector, LT 1 and M 3 cell lines tested using 6 EMT markers.

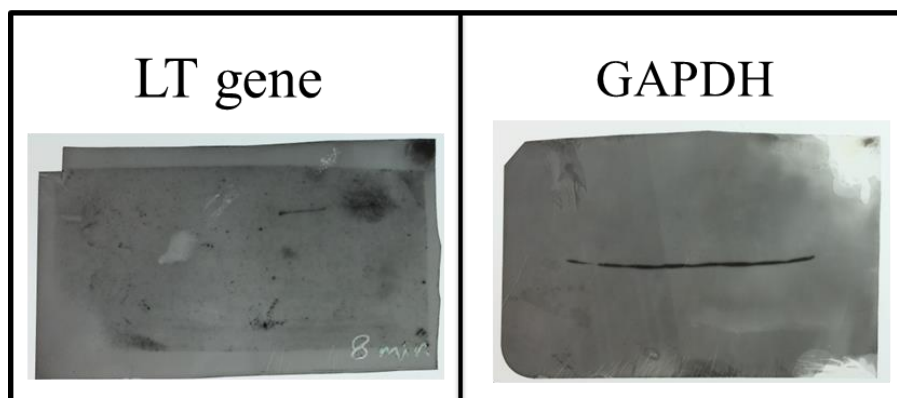


Figure 5.3.30 full image western blot of LT gene.

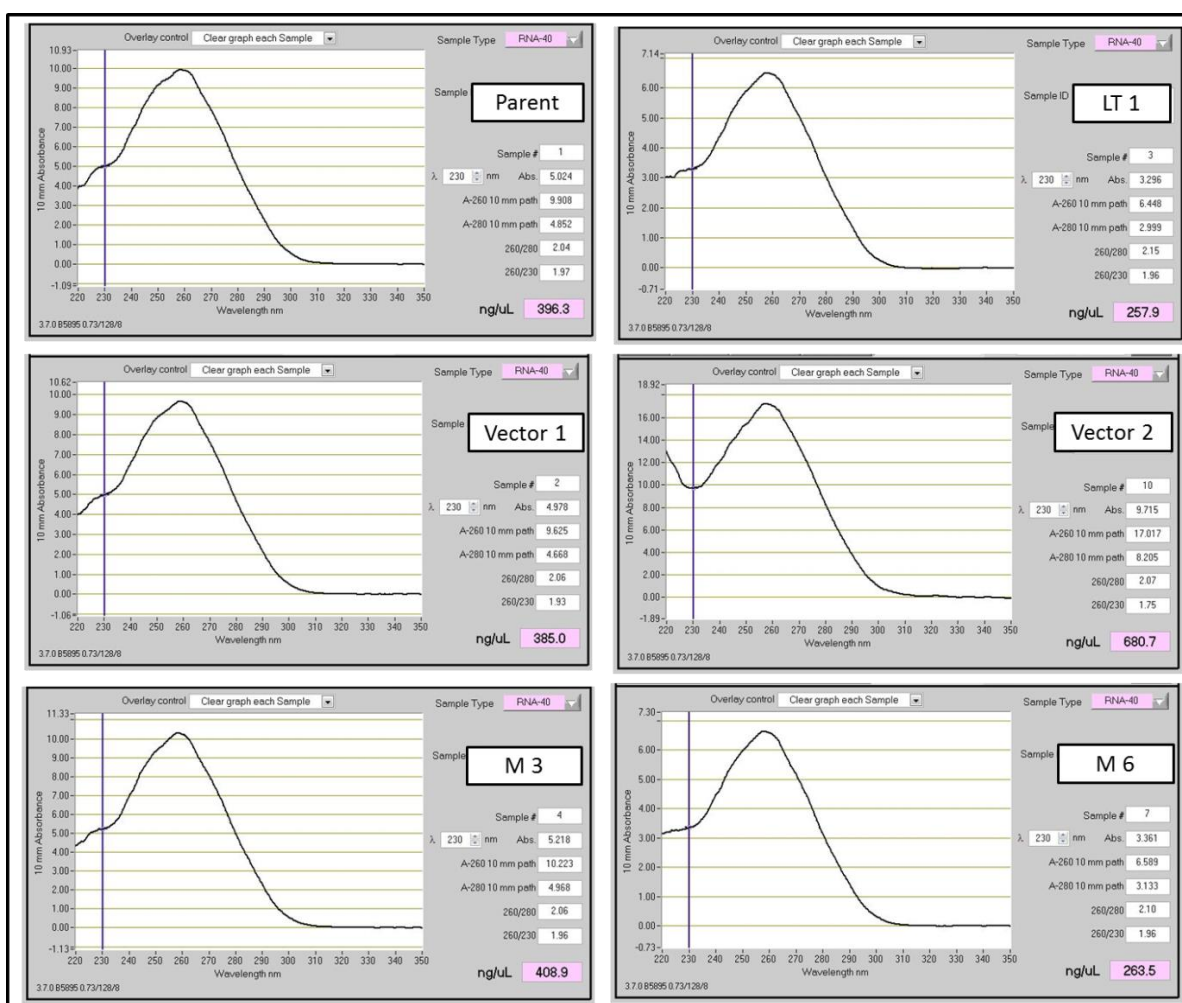


Figure 5.3.31 NanoDrop spectrophotometry RNA purity analysis for 6 tested cell lines for microarray. The images correspond to the wavelength / absorption plots. A260/A280 ratios were between 1.8 and 2.00; A260/A230 ratios were between 2.00 and 2.20.

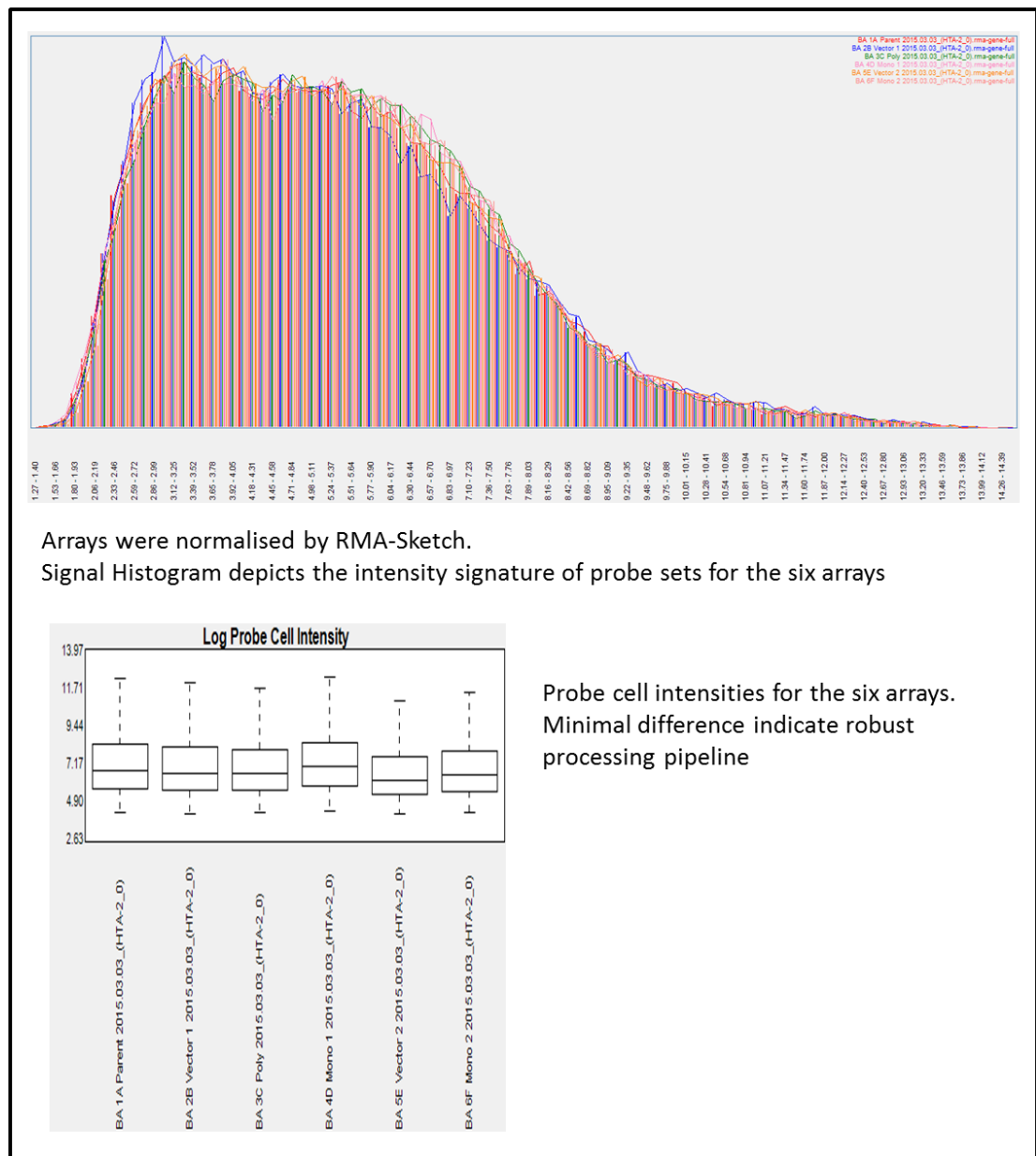


Figure 5.3.32 Resultant data from RMA-sketch were assessed by log₂ threshold test and probe cell intensity analyses (box plots of probe intensity values per array prior to summarisation / normalisation) showed minimal distribution differences indicative of a robust array generation pipeline. Relative cell intensity boxplots (distribution of probe intensities for each array compared with the median probe intensity for the array group) didn't reveal divergent probe intensity distributions. Probeset signal distributions per array (signal box plot) and the ratio compare with the median signal of the array group (relative signal box plot) showed no divergent signal distributions within the study. Signal distribution histogram depicted minimum differences across the arrays.

5.4 JCV paper & WHO correspondence

Journal of Medical Virology

Increased Prevalence of JC Polyomavirus in Cervical Carcinomas from Women Infected with HIV

Bandar Alosaimi,¹ Lynne Hampson,¹ Xiaotong He,¹ Innocent O. Maranga,² Anthony W. Oliver,¹ and Ian N. Hampson^{1*}

¹Viral Oncology Laboratories, University of Manchester Institute of Cancer Sciences, Manchester, UK

²Department of Obstetrics and Gynaecology, University of Nairobi, Kenyatta National Hospital, Nairobi, Kenya

Although subclinical persistent infections with the human polyomaviruses BKV and JCV are ubiquitous worldwide, these are known to vary in relation to diseases present and geographical location. DNAs from 220 cervical smears and 109 invasive cervical carcinomas obtained from HIV positive and HIV negative Kenyan women of known HPV status were analyzed by nested endpoint PCR for BKV and JCV. BKV–JCV DNA was detected in 5/105 (4.7%) of cervical smears and in 6/37 (16%) of cervical carcinomas from women infected with HIV whereas 9/115 (7.8%) of the cervical smears and 4/72 (5.5%) of the carcinomas were positive in HIV negative women. Nested PCR showed that all 24 samples were positive for JCV and not BKV. JCV was not more prevalent in either HPV positive ($P=0.438$) or HPV negative women ($P=0.392$). However, 37% of carcinomas and smears which were positive for JCV were also positive for a “high-risk” oncogenic HPV. Comparison of the incidence of JCV in cervical smears and cervical carcinomas showed a ~3-fold increase in samples from HIV positive women with cervical carcinoma ($P=0.025$) whereas no significant difference was found between cervical smears and cervical carcinomas from HIV negative women ($P=0.553$). These results suggest that JCV may combine with high-risk HPV infection in women infected with HIV to influence the rate of progression to invasive cervical carcinoma. *J. Med. Virol.*

© 2013 Wiley Periodicals, Inc.

KEY WORDS: HPV; BK virus; JCV; immunocompromised; cervical cancer

INTRODUCTION

The JC polyomavirus (JCV) and BK polyomavirus (BKV) are ubiquitous in human populations worldwide with a seroprevalence of 70–80% in adults

[Khalili et al., 2006; Knowles, 2006]. Primary infections are typically subclinical and probably occur early in childhood, followed by viral dissemination to sites of lifelong persistent latent infection, which are most commonly the kidney and central nervous system for both JCV and BKV [Heritage et al., 1981; Chesters et al., 1983]. Subsequent activation of these viruses can produce serious diseases including polyomavirus nephropathy and progressive multifocal leukoencephalopathy [Gardner et al., 1971; Markowitz et al., 1993]. However, the factors which control the balance between latency and disease-associated reactivation are poorly defined, although immunosuppression clearly plays a role since BKV and JCV related diseases are more common in transplant recipients and HIV-infected individuals [Behzad-Behbahani et al., 2004].

JCV is considered the etiological agent of progressive multifocal leukoencephalopathy (PML) [Wang et al., 2011]. AIDS is the most common underlying cause of immunosuppression leading to JCV reactivation, while BKV is associated with hemorrhagic cystitis in hematopoietic stem cell transplantation (HSCT) recipients and interstitial nephropathy in immunocompromised kidney transplant patients [Kinnaird and Anstead, 2010].

It has been clearly demonstrated that glial cells in the central nervous system are productively infected by both JCV and HIV-1. The striking similarity of AIDS and PML leukoencephalopathy suggests that JCV reactivation is a consequence of HIV infection, either by HIV-encoded trans-acting factors or through T4 cell depletion [Kaniowska et al., 2006]. Evidence

Grant sponsor: King Fahad Medical City, Riyadh, Saudi Arabia

*Correspondence to: Ian N. Hampson, Viral Oncology Laboratories, University of Manchester Institute of Cancer Sciences, Research Floor 5, St. Mary's Hospital, Manchester M13 9WL, UK. E-mail: ian.hampson@manchester.ac.uk

Accepted 11 December 2013

DOI 10.1002/jmv.23868

Published online in Wiley Online Library (wileyonlinelibrary.com).

© 2013 WILEY PERIODICALS, INC.

for a direct role for HIV in JCV activation has been provided by studies which showed that the JCV late promoter can be transactivated by the HIV-1 Tat protein [Del Valle et al., 2000; Qu et al., 2004].

The current study was prompted by the work of Comar et al. [2011] who showed that BKV was found more frequently in Italian women with high-grade squamous intraepithelial lesions in association with high-risk human papillomavirus type 16 (HPV-16). However, these researchers did not examine cervical carcinomas from women in the same geographical location. For the first time, the authors now report analysis of the prevalence of BK and JC polyomaviruses in cervical smears and carcinomas from HIV positive and HIV negative Kenyan women.

MATERIALS AND METHODS

Collection of Cervical Smear and Tumor Samples

Between April 2008 and February 2009 at the Specialist HIV Clinic and Family Planning Clinic at Kenyatta National Hospital (Nairobi), 220 cervical smears samples were collected with written informed consent from 105 HIV positive and 115 HIV negative Kenyan women. The women ranged in age between 21 and 52 years (median age: 35 years) and those who had prior destructive procedures for cervical disease and hysterectomies were excluded. Cervical smears were collected into PreservCyt liquid based cytology (LBC) transport solution (ThinPrep Pap Test; Hologic, Crawley, West Sussex, UK). These were analyzed together with a total of 109 formalin fixed paraffin embedded (FFPE) tissue biopsies from women with invasive cervical carcinoma recruited at the same hospital. Thirty-seven of these cervical carcinomas were from HIV positive patients while 72 were from HIV negative patients. Both LBC and invasive cervical carcinoma specimens had their DNA extracted using the methods described below.

Ethics Statement

Ethical approval was granted by both the Kenyatta National Hospital and University of Nairobi's Ethics Review Board (05.12.2007: KNH-ERC/01/4988) and the Oldham Ethics Committee UK (26.01.2009: amendment five project 07/Q1405/14).

DNA Extraction

All study patients underwent an HIV test using the Determine[®] test kit (Abbot Pharmaceuticals, Chicago, IL), and if positive, was confirmed by Uni-Gold[®] (Trinity Biotech, Bray, Ireland). Automated DNA extraction was performed on 500 μ l of all 220 PreservCyt LBC samples with the use of BioRobot[®] M48, (Qiagen, Sussex, UK) according to the manufacturer's instructions. Approximately 4 \times 10 μ l (FFPE) invasive cervical carcinomas sections were cut using

single-use disposable microtome blades and disposable forceps for section handling. DNA isolation was carried out using the Qiagen Qiacube FFPE kits (Qiagen) as described by the manufacturer.

Genomic DNA Integrity Validation

The integrity of each DNA sample was validated by detection of the housekeeping gene glyceraldehyde 3-phosphate dehydrogenase (GAPDH) (NCBI accession number: NM_002046). The forward primers sequence: CATTGACCTCAACTACATGGT; reverse primer sequence: TCGCTCCTGGAAGATGGTGAT generate amplicons of 130 bp. Standard 50 μ l reactions were prepared which comprised 2 μ l of 25 ng/ μ l template DNA, 2.5 units of Taq DNA polymerase (Qiagen), 0.2 mM dNTPs, 0.2 μ M of each primer, 5 μ l 10 \times PCR buffer, and 2.5 mM MgCl₂. Thermocycler conditions were 94°C for 5 min followed by 33 cycles of 94°C for 25 sec, 53°C for 25 sec, 72°C for 25 sec; and a final extension of 72°C for 7 min. All reactions were performed on a VerityH 96-well Fast Thermocycler.

Twenty microliters of PCR product was loaded into 2% w/v agarose gels (SeaKem LE Agarose; Lonza, Biologics, Tewkesbury, Gloucestershire, UK) and separated by agarose gel electrophoresis (Clarit-E Maxi electrophoresis tanks, Alpha Laboratories, Eastleigh, UK) at 100 V for 45 min. DNA was visualized using ethidium bromide and imaged on a UVP M-20 Gel documentation system (UVP, Cambridge, Cambs, UK).

Sensitivity of the Nested PCR

Primers (PYY) were designed to detect a conserved N-terminal region of the polyomavirus large T gene from both BK and JC viruses (Table I). The sensitivity of this assay was evaluated by using a 100–10⁻⁹ ng serial dilution of plasmid containing the JC large T open reading frame (ORF).

Nested PCR Detection of BK and JC Virus

The outer PYY primer set [Martini et al., 2004] amplifies a conserved 181 base pair (bp) long fragment from both BKV and JCV. The inner primer sets amplify a 77 bp long fragment of BKV and 75 bp of JCV, respectively. A 2 μ l aliquot of the primary PYY product diluted in 100 μ l dH₂O and used as template for the secondary internal nested PCR.

Reactions were performed in a total volume of 50 μ l containing 2 μ l of DNA template, 0.2 μ M of each primer, 0.2 mM dNTPs, 2 μ l MgCl₂, 10 μ l of 5 \times GoTaq Green buffer, and 1.25 U of Platinum Taq DNA polymerase (GoTaq[®] Hot Start Polymerase; Promega, Southampton, Hamps, UK).

PCR conditions were 95°C for 2 min HotStart activation followed by 40 cycles for primary PYY amplification and 30 cycles for the secondary nested virus specific amplification (Table I). Cycle conditions were; 94°C for 30 s, 58°C, 72°C for 30 s and a final

Prevalence of JC Polyomavirus in Cervical Carcinomas

3

TABLE I. PCR Primers Used and Their Amplicons

Primer type	Oligo name	To detect	Sequences (5'-3')	Amplicon size (bp)
Nested outer primers	PYV.for	BKV and JCV	TAGGTGCCAACCTATGGAACAGA	181
	PYV.rev	BKV and JCV	GAAAGTCTTTAGGGTCTTCTACC	
Nested inner primers	BKS2.for	BKV	AAGAAGCAACAGCAGATTC	77
	BKS2.rev	BKV	GAAAGTCTTTAGGGTCTTCTACC	
Nested inner primers	JCVS2.for	JCV	ATGATGAAAAACAGGATCC	75
	JCVS2.rev	JCV	GAAAGTCTTTAGGGTCTTCTACC	

extension at 72°C for 5 min. PCR products were performed on a VerityH 96-well Fast Thermocycler. Twenty milliliters of PCR product was loaded into 2% w/v agarose gels and separated by agarose gel electrophoresis at 90 V for 45 min. DNA was visualized using ethidium bromide and imaged on a UVP Transilluminator (Fig. 1).

Statistical Analysis

Statistical analyses were performed using the chi-square test for comparative statistical analysis between group frequencies, using IBM SPSS statistics 20 version. In order to assess the significance levels between the categorical variables, values $P < 0.05$ were regarded statistically significant.

RESULTS

Validation of JCV-BKV PCR Methods

The sensitivity limit of the assay was shown to be 10^{-7} ng of input plasmid DNA which is equivalent to an input of 18 copies of the JC/BK ORF per reaction.

BKV-JCV DNA Screening

Twenty-four out of 329 cervical specimens (7.3%) were shown to contain BKV-JCV DNA. Control plasmids containing JCV and BKV were used as positive controls for PCR amplification and dH₂O was used as a negative control.

The first Pan PYV PCR was carried out using JCV-BKV consensus primers (Table I) and in most cases a single 181-bp fragment was amplified from both the cervical smear and cervical carcinoma samples coincident with the positive control (Fig. 2A and B). The second nested PCR was performed with the JCV and BKV specific primers using the Pan PYV PCR products as input material. A single JC-specific 77-bp amplicon was produced from all 24 Pan PYV positive samples, whereas none were positive for BKV (Fig. 2C and D).

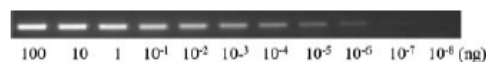
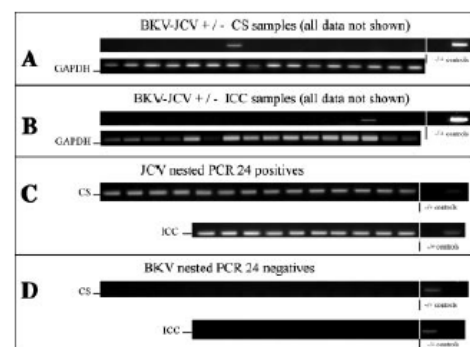


Fig. 1. Ethidium bromide stained agarose gel showing a titration of the sensitivity of the PCR amplification of the 181 bp JCV-BKV PCR product.



CS, cervical smears; ICC, invasive cervical carcinomas.

Fig. 2. PCR detection of JCV and/or BKV. A and B: The first PCR was carried out using JCV-BKV consensus primers which amplified a single 181-bp amplicon from 24 samples out of the 329 tested C: Nested PCR was performed as described on these positive samples using JCV specific primers which gave a single 77-bp amplicon from all 24 sample samples tested. D: Nested PCR on the same 181bp product with BKV specific primers gave no signal.

Presence of JCV or BKV DNA in Cervical Smears and Cervical Carcinoma Specimens

The overall prevalence of PYV DNA in cervical specimens was 24/329 (7.3%) which were all confirmed to be JCV. The overall proportion of JCV positives in cervical smears (6%) and cervical carcinomas (9%), are shown in Table II, with no significant difference in JCV infection between these two groups ($P > 0.05$).

The Association Between JCV and HPV Infection in Cervical Smears and Cervical Carcinomas

The cervical smears and cervical carcinoma samples used in this study have been previously analyzed for the presence of various HPV types using Papillocheck

TABLE II. Rate of JCV Infection Found in CS and ICC

Samples	JCV+		JCV-		Total	P-value
	No.	%	No.	%		
CS	14	6	206	94	220	>0.05
ICC	10	9	99	91	109	
Total	24	7	305	93	329	

SC, cervical smears; ICC, invasive cervical carcinomas.

HPV genotyping and dual locus multiplex PCRs respectively as described in Maranga et al. [2012]. The HPV data from this earlier study were analyzed with respect to JCV status and the results are shown in Table III. Within the HPV16/18 positives, JCV infection was found in 5 of 122 cervical smears (4%), and in 4 of 59 cervical carcinomas (6.7%); while in the HPV16/18 negatives, 9 of 115 cervical smears (6.6%) and 6 of 60 cervical carcinomas (10%) were JCV positive (Table III). Although all cervical smears and cervical carcinoma samples which were positive for JCV were also positive for a "high-risk" oncogenic HPV type, analyses of these data showed that there was no significant association between JCV and HPV16/18 in any group ($P > 0.05$). Analysis of cervical cytology showed that although there was an increase in JCV infection in HIV infected women with cervical dysplasia, this did not achieve statistical significance.

The Association Between JCV and HIV Infection in Cervical Smears and Cervical Carcinomas

As for HPV analysis, the HIV status of the women used in this study has also been previously reported [Maranga et al., 2012]. For HIV negative women, JCV DNA was detected in 9/115 (7.8%) of the cervical smears and in 4/72 (5.5%) of the cervical carcinomas, which was not statistically significant ($P > 0.05$). However, for HIV positive women, JCV DNA was detected in 5/105 (4.7%) of the cervical smears and in 6/37 (16%) of the cervical carcinomas (Fig. 3, $P < 0.05$). This suggests there may be a significant association between JCV and cervical carcinoma, but only in HIV positive women.

DISCUSSION

There is now a general acceptance that viruses play a key role in the pathogenesis of many types of human cancer [Rwazavian, 2011] and it is thought

that they promote malignant transformation by generating genetic instability in infected cells [Giuliani et al., 2008]. Polyomaviruses are capable of inducing chromosomal instability [Dolcetti et al., 2003] and although the role of polyomaviruses in carcinogenesis is still controversial, they have been linked to the etiology of various human malignancies [White et al., 2005]. The major transforming protein of polyomaviruses is the large T tumor antigen (T-Ag) which plays a key role in the deregulation of the cell cycle through interaction with the p53 and pRb tumor suppressor proteins [zur Hausen, 2008].

In the current study, it was tested whether there was an association between the polyomaviruses JC and BK and different stages in the development of cervical cancer in HIV infected and non-infected Kenyan women. Previous studies have reported on the presence of BKV and JCV in urogenital carcinomas [Monini et al., 1995; Comar et al., 2011], which suggested that these viruses may act as cofactors in the etiology of these malignancies. Indeed, Comar et al. [2011] reported that 44% (41/93) of HPV16 positive high-grade cervical intraepithelial neoplasias (HSILs) were positive for BKV in Italian women. These data are consistent with the hypothesis that co-infection with two or more different disease-causing organisms in one individual can facilitate the disease process [Operskalski and Kovacs, 2011].

JCV sequences have been detected in various tissues including kidneys, brain, liver, lung, spleen, lymph nodes, and colorectal epithelium [Easha et al., 2006; Jiang et al., 2009]. In addition to its role in PML, JCV has been previously shown to be associated with several human malignancies such as colorectal, central nervous system (CNS) lymphoma, glioblastomas, and pediatric medulloblastomas; although its role in brain tumors remains controversial [Reiss and Khalili, 2003; Khalili et al., 2006; zur Hausen, 2008; Collins et al., 2011; Rwazavian, 2011].

These data clearly show detection of JCV and not BKV sequences in samples derived from the female genitalia which is a potential latent site for polyomavirus infection [Martini et al., 2004] (see Fig. 2). This finding also suggests that, whilst closely related, JCV and BKV may hold different geographical evolutionary histories and infers the predominance of JCV within African populations. Indeed, JCV infection rates are known to vary among populations being influenced by geographical area and ethnic origin and it has been suggested that JCV may be a bio-anthropological

TABLE III. Analyses of the Association Between JCV and HPV Infections

Infections	CS		P-value	ICC		P-value
	HPV16/18+	HPV16/18-		HPV16/18+	HPV16/18-	
JCV+	5	9	>0.05	4	6	>0.05
JCV-	117	106		55	44	

SC, cervical smears; ICC, invasive cervical carcinomas.

J. Med. Virol. DOI 10.1002/jmv

Prevalence of JC Polyomavirus in Cervical Carcinomas

5

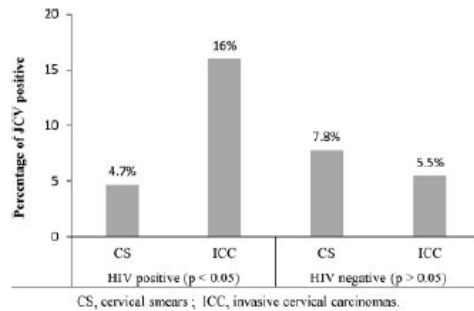


Fig. 3. Analysis of the association between JCV and HIV infection. The frequency of JCV infection in cervical carcinomas was significantly higher in HIV positive cervical carcinomas than that in any of the other groups tested irrespective of HIV status ($P < 0.05$).

marker that is useful for studying the early migration of human populations around the world [Cayres-Vallinoto et al., 2012]. Furthermore, based upon sequence analysis of the major capsid protein (VP1), JCV can be divided into a number of subtypes ($n > 14$) which also have distinctive geographic distributions. Modern *Homo sapiens* originated in Africa and it is possible that JCV may have co-diverged with migratory human populations over many thousands of years [Guo et al., 1996; Shackelton et al., 2006].

In this investigation no significant association was observed between the frequency of JCV virus and HPV16/18 (Table II). It has been shown previously that HIV infection alters the spectrum of HPV types found in both cervical smears and invasive cervical carcinomas which suggests a complex interplay between these viruses during progression to cervical cancer [Maranga et al., 2012]. The precise molecular interactions underlying co-infection with HPV in HIV positive women and how this influences progression from cervical dysplasia to invasive cervical carcinoma is not straightforward and requires clarification. For example it is generally assumed that HIV related immunosuppression will facilitate the oncogenic effects of HPV by enhancing its persistence and, as a consequence, oncogenic progression [Mandelblatt et al., 1999]. However, previous work has also suggested this may be an over simplification whereby HIV could enhance infection with some types of HPV which might actually retard progression [Maranga et al., 2012].

Clearly the present results do not support a role for JCV in the etiology of cervical cancer in HIV negative women. However, the finding of three times the rate of JCV infection in cervical carcinomas from women infected with HIV when compared to HIV negative women is intriguing. It is possible this could be causally related to the etiology of cervical carcinomas or alternatively this could be a bystander event

associated with other HIV/AIDS related pathologies. With the current data set it is not possible to distinguish between these two possibilities and this will form the basis of further work. Indeed reactivation of latent polyomaviruses is known to accompany AIDS associated immunosuppression [Boothpur and Brennan, 2010]. Furthermore, several studies have documented urinary excretion of JCV and BKV in HIV positive patients suggesting that polyomavirus reactivation is a feature of HIV infection [Markowitz et al., 1993; Behzad-Behbahani et al., 2004; Knowles, 2006] and it seems reasonable to propose JCV as a sexually transmissible viral agent. Moreover, in association with cellular proteins, the HIV-1 Tat protein is known to bind to the JCV non-coding region to stimulate JCV transcription and replication [Wright et al., 2013]. HIV is well known to increase the risk of cancers associated with other viruses best exemplified by the ability of HIV-1 tat protein to promote the growth of human herpes virus-8 (HHV-8) associated Kaposi's sarcoma [Pyakurel et al., 2007].

Martini et al. [2004] reported a simultaneous association of polyomaviruses with human genital tumors and suggested their involvement as a cofactor in the onset/progression of cervical cancer. Mechanistically, genetic instability induced by T-Ag is likely to be an important contributor to polyomavirus-induced oncogenesis. Furthermore, it has been shown that JCV T-Ag dysregulates β -catenin signaling in some colon cancers and medulloblastoma [Enam et al., 2002] and the T-Ag also binds and degrades p53 via ubiquitination thus deregulating the cell cycle and inhibiting apoptosis [White and Khalili, 2004].

In conclusion, based on the present results, it is possible that JCV may act synergistically with HPV and HIV to facilitate the transformation of cervical epithelium in some Kenyan women. However, since the majority of these HIV positive women will develop cervical carcinoma in the absence of JCV it is quite clear that more work is needed to define the potential role of this virus in the etiology of invasive cervical carcinomas in this population.

ACKNOWLEDGMENTS

We acknowledge support from the Saudi Arabian Cultural Bureau in London (to Bandar). Work in the Viral Oncology Labs was also supported by the Humane Research Trust, The Caring Cancer Trust, The Cancer Prevention Research Trust, and United in Cancer.

REFERENCES

- Behzad-Behbahani A, Klapper PE, Vallely PJ, Cleator GM, Khoo SH. 2004. Detection of BK virus and JC virus DNA in urine samples from immunocompromised (HIV-infected) and immunocompetent (HIV-non-infected) patients using polymerase chain reaction and microplate hybridisation. *J Clin Virol* 29:224-229.
- Boothpur R, Brennan DC. 2010. Human polyoma viruses and disease with emphasis on clinical BK and JC. *J Clin Virol* 47: 306-312.

J. Med. Virol. DOI 10.1002/jmv

- Cayres-Vallinoto IMV, Vallinoto ACR, Azevedo VN, Almeida Machado LF, Guimaraes Ishak MdO, Ishak R. 2012. Human JCV infections as a bio-anthropological marker of the formation of Brazilian amazonian populations. *PLoS ONE* 7.
- Chesters PM, Heritage J, McCance DJ. 1983. Persistence of DNA-sequences of BK virus and JC virus in normal human-tissues and in diseased tissues. *J Infect Dis* 147:676-684.
- Collins D, Hogan AM, Winter DC. 2011. Microbial and viral pathogens in colorectal cancer. *Lancet Oncol* 12:504-512.
- Comar M, Bonifacio D, Zanonati F, Di Napoli M, Isidoro E, Martini F, Torelli L, Tognon M. 2011. High prevalence of BK polyomavirus sequences in human papillomavirus-16-positive precancerous cervical lesions. *J Med Virol* 83:1770-1776.
- Del Valle L, Croul S, Morgello S, Amini S, Rappaport J, Khalili K. 2000. Detection of HIV-1 Tat and JCV capsid protein, VP1, in AIDS brain with progressive multifocal leukoencephalopathy. *J Neurovirol* 6:221-228.
- Doletti R, Martini F, Quaila M, Gloghini A, Vignocchi B, Cariati R, Martinelli M, Carbone A, Boiocchi M, Tognon M. 2003. Simian virus 40 sequences in human lymphoblastoid B-cell lines. *J Virol* 77:1595-1597.
- Easha S, Manley K, Gasparovic M, Querbes W, Atwood WJ. 2006. The human polyomaviruses. *Cell Mol Life Sci* 63:865-876.
- Enam S, Del Valle L, Lara C, Gan DD, Ortiz-Hidalgo C, Palazzo JP, Khalili K. 2002. Association of human polyomavirus JCV with colon cancer: Evidence for interaction of viral T-antigen and beta-catenin. *Cancer Res* 62:7093-7101.
- Gardner S, Field A, Coleman D, Hulme B. 1971. New human papovavirus (B.K.) isolated from urine after renal transplantation. *Lancet* 297:1253-1257.
- Giuliani L, Ronci C, Bonifacio D, Di Bonito L, Favalli C, Perno CF, Syrjanen K, Ciotti M. 2008. Detection of oncogenic DNA viruses in colorectal cancer. *Anticancer Res* 28:1405-1410.
- Guo J, Kitamura T, Ebiyara H, Sugimoto C, Kunitake T, Takehisa J, Na YQ, AlAhdal MN, Hallin A, Kawabe K, Taguchi F, Yogo Y. 1996. Geographical distribution of the human polyomavirus JC virus types A and B and isolation of a new type from Ghana. *J Gen Virol* 77:919-927.
- Heritage J, Chesters PM, McCance DJ. 1981. The persistence of papovavirus BK DNA-sequences in normal human renal tissue. *J Med Virol* 8:143-150.
- Jiang M, Abend JR, Johnson SF, Imperiale MJ. 2009. The role of polyomaviruses in human disease. *Virology* 384:266-273.
- Kaniowska D, Kaminski R, Amini S, Radhakrishnan S, Rappaport J, Johnson E, Khalili K, Del Valle L, Darbinyan A. 2006. Cross-interaction between JC virus agnoprotein and human immunodeficiency virus type 1 (HIV-1) tat modulates transcription of the HIV-1 long terminal repeat in glial cells. *J Virol* 80:9288-9299.
- Khalili K, Gordon J, White MK. 2006. The polyomavirus, JCV, and its involvement in human disease. *Adv Exp Med Biol* 577:274-287.
- Kinnaird AN, Anstead GM. 2010. Hemorrhagic cystitis and possible neurologic disease from BK virus infection in a patient with AIDS. *Infection* 38:124-127.
- Knowles WA. 2006. Discovery and epidemiology of the human polyomaviruses BK virus (BKV) and JC virus (JCV). *Adv Exp Med Biol* 577:19-45.
- Mandelblatt JS, Kanetsky P, Eggert L, Gold K. 1999. Is HIV infection a cofactor for cervical squamous cell neoplasia? *Cancer Epidemiol Biomarkers* 8:97-106.
- Maranga IO, Hampson L, Oliver AW, He X, Gichangi P, Rana F, Opiyo A, Hampson IN. 2012. HIV infection alters the spectrum of HPV subtypes found in cervical smears and carcinomas from Kenyan women. *Open Virol J* 6:121-129.
- Markowitz RB, Thompson HC, Mueller JF, Cohen JA, Dynam WS. 1993. Incidence of BK-virus and JC-virus viraemia in human immunodeficiency virus-infected and virus-uninfected subjects. *J Infect Dis* 167:13-20.
- Martini F, Iaccheri L, Martinelli M, Martinello R, Grandi E, Mollica G, Tognon M. 2004. Papilloma and polyoma DNA tumor virus sequences in female genital tumors. *Cancer Invest* 22:697-705.
- Monini P, Rotola A, Diluca D, Delellis L, Chiari E, Corallini A, Cassai E. 1995. DNA rearrangements impairing BK virus productive infection in urinary-tract tumors. *Virology* 214:273-279.
- Operskalski EA, Kovacs A. 2011. HIV/HCV co-infection: Pathogenesis, clinical complications, treatment, and new therapeutic technologies. *Curr HIV/AIDS Rep* 8:12-22.
- Pyakurel P, Pak F, Mwakigonja AR, Kaaya E, Biberfeld P. 2007. KSHV/HHV-8 and HIV infection in Kaposi's sarcoma development. *Infect Agent Cancer* 24.
- Qu QM, Sawa H, Suzuki T, Semba S, Henmi C, Okada Y, Tsuda M, Tanaka S, Atwood WJ, Nagashima K. 2004. Nuclear entry mechanism of the human polyomavirus JC virus-like particle—Role of importins and the nuclear pore complex. *J Biol Chem* 279:27735-27742.
- Reiss K, Khalili K. 2003. Viruses and cancer: Lessons from the human polyomavirus, JCV. *Oncogene* 22:6517-6523.
- Rwazavian N. 2011. Can a virus cause cancer: A look into the history and significance of oncoviruses. *Berk Sci J* 14.
- Shackelton LA, Rambaut A, Pybus OG, Holmes EC. 2006. JC virus evolution and its association with human populations. *J Virol* 80:9928-9933.
- Wang TS, Byrne PJ, Jacobs LK, Taube JM. 2011. Merkel cell carcinoma: Update and review. *Semin Cutan Med Surg* 30:48-56.
- White MK, Khalili K. 2004. Polyomaviruses and human cancer: Molecular mechanisms underlying patterns of tumorigenesis. *Virology* 324:1-16.
- White MK, Gordon J, Reiss K, Del Valle L, Croul S, Giordano A, Darbinyan A, Khalili K. 2005. Human polyomaviruses and brain tumors. *Brain Res Brain Res Rev* 50:69-85.
- Wright CA, Nance JA, Johnson EM. 2013. Effects of Tat proteins and Tat mutants of different human immunodeficiency virus type 1 clades on glial JC virus early and late gene transcription. *J Gen Virol* 94:514-523.
- zur Hausen H. 2008. Novel human polyomaviruses—Re-emergence of a well known virus family as possible human carcinogens. *Int J Cancer* 123:247-250.



Collaborative study to evaluate the 1st WHO International Standard candidate for JC virus (JCV) NAT-based assays.

August 2014

Dear Dr Hampson,

Study Participant # 01 (please use this number for all future correspondence)

Thank you on behalf of NIBSC for agreeing to participate in the collaborative study to evaluate the 1st WHO International Standard candidate, for JC virus (JCV) nucleic acid amplification technology (NAT) based assays.

The aim of this collaborative study is to evaluate the suitability and potency of the candidate JCV standard using a wide range of NAT-based assays represented across the 23 participating laboratories. Each participant is requested to test dilutions of the candidate standard in a matrix routinely used in their laboratory, on three separate occasions in duplicate where possible. In addition based on your reply to the participant questionnaire you will also be supplied with relevant clinical samples for testing alongside the candidate IS material. All of the samples provided should be extracted and then analyzed using either quantitative or qualitative NAT-based assays routinely performed in your laboratory. Attached you will find specific instructions for the dilution and testing of the study samples.

The results of each assay and methodology used should be recorded on the Result Reporting form. I would like to kindly request that you report your data by the 6th October 2014 by email to sheila.govind@nibsc.org.

Yours sincerely,

Sheila Govind

Division of Virology
National Institute of Biological Standards and Controls

Medicines and Healthcare
Products Regulatory Agency